

PRELIMINARY FEASIBILITY STUDIES IN TIMES OF RAPID COST ESCALATION

Earl D. Oliver and A. James Moll
Stanford Research Institute, Menlo Park, California 94025

Introduction

Costs of solid fuels conversion have risen sharply, delaying projects, prompting political investigations to determine whether cost estimates had been deliberately distorted, and startling the project sponsors themselves. In the eight years starting in 1967, the estimated cost of a daily barrel of synthetic oil capacity has increased up to tenfold.

In 1967, testimony to Congress projected a commercial shale oil plant by 1970; none has yet been built, and the earliest possible start-up year in 1979. After deferral of an application submitted in 1962, a second generation tar sand oil plant was planned in 1969 for 1976 startup; it is now under construction, with startup due in 1979.

Many factors other than regulatory delays have been responsible for this unfortunate record. They can generally be classed as inflation, other forms of escalation, process development, and increase in project scope. This paper analyzes these factors and gives perspective for estimation of future changes and avoidance of pitfalls.

Cost Escalation

Figure 1 is a plot derived from published data. It shows how cost estimates have increased for an oil shale plant using the TOSCO II process and for a tar sands plant by Syncrude Canada Ltd. (SCL). The plot also shows that the increases far exceeded the increases of the CE Plant Cost Index published by Chemical Engineering magazine, which is intended to reflect the changes in cost of process plants. The CE Index correlates with a broader index of inflation, the GNP Deflator. In fact, a plot of the GNP Deflator would be indistinguishable from the plot of the CE Index at the scale of Figure 1. How is the obvious total failure of cost indexes to be explained?

Oil shale and tar sands plants are obviously special cases in that they use unproven processes, so we should inquire whether cost indexes have successfully reflected changes in costs of routine plants. The answer is a resounding "no." For example, a 1,200 ton-per-day ammonia plant completed in 1967 cost W. R. Grace \$33.6 million, compared with a cost of \$107.4 million for a similar plant to be completed in 1978.¹ The increase is 220 percent, compared with a probable increase of about 100 percent for the CE Index. Ammonia production is well developed and relatively non-polluting, so the increase should reflect escalation more than change in design.

The year 1974 gave a particular divergence of plant costs from indexes, when an engineering contractor reported typical increases of petroleum and petrochemical plants of 30 to 40 percent in 6 months while the index rose about 14 percent. The 1974 experience is partly explained by the overheating of the economy at that time and by the derivation of the index. The CE Plant Cost Index depends on 67 Bureau of Labor Statistics (BLS) indexes, for which all of the equipment indexes depend on list prices. List prices are a fiction not reflecting contract prices in slack periods, when deep discounts are available. List prices are not likely to be raised as soon as real prices when the economy improves. This analysis was confirmed by Savay.²

Aside from details, indexes have a basic problem. Indexes attempt the impossible in trying to give a single number representative of cost of dissimilar plants when component costs are changing at greatly different rates, as shown in Table 1 for the difficult two-year period from July 1973 to 1975. The extraordinary increases for heat exchangers and centrifugal compressors reflect supply and demand. Many exchanger manufacturers left the business in earlier periods of low profitability, and many foundries shut down rather than comply with new antipollution and job safety rules.

Even the largest price increases do not explain the increases in cost estimates in boom periods because escalation clauses make the final costs uncertain, schedule stretchouts increase costs of interest, insurance, and administration, and contingency allowances are likely to be increased. A related site-specific factor, local labor shortages, requires overtime pay and causes reduced productivity and further delays.

Oil Shale Case History

The previous section showed that remarkable escalation occurred in the capital costs of perfectly conventional process plants, and that this escalation is not fully revealed by cost indexes. Three other factors have

coincided with the inflationary forces to accelerate the escalation of synthetic oil plant costs. These factors are:

- Tightening environmental controls
- Shortages of conventional fuels
- Changes in design and scope resulting from developmental programs and definitive engineering analysis.

Table 1

COST INCREASES, JULY, 1973 TO JULY, 1975

<u>BLS Code</u>	<u>Item</u>	<u>Percent Increase</u>
1072010.03	Pressure Tanks	47 %
(Nelson Index)	Heat exchangers	97
11401.03	Centrifugal compressors	92
11401.02	Industrial pumps	42
1166.04	Chemical industry machinery	67
(CE Index)	Pipes, valves, and fittings	42
CE	Plant cost index	26

Source: SRI

All the estimates for TOSCO II oil shale plants considered herein are for the same shale rate (66,000 tons per stream day), but the assumed shale assay and net yield vary. The estimates were all reported by The Oil Shale Corporation (TOSCO).

In 1967, TOSCO estimated \$130 million would buy a plant capable of producing 52,200 BPCD (barrels per calendar day) of synthetic crude. A plant for the same amount of unhydrogenated pipeline oil would cost less than \$100 million. Natural gas was to be the source of hydrogen, so no

loss in yield resulted from upgrading. Shortages later forced TOSCO and partners to abandon this desirable source of hydrogen. Ironically, the same factor that increased the need for synthetic oil also made it more costly.

Reported costs paralleled general inflation through late 1968, but by 1972 costs had increased sharply. New environmental controls, including a change of plant site from the canyon to the mesa, were required. TOSCO and partners reduced the estimated shale assay and oil yield and made plant design changes as a result of the development program. The plan to market a low-sulfur fuel oil rather than refinery feedstock may have moderated the decrease in yield. Thus an increase of about 20 percent in the CE Index, which in this period was doing a reasonable job of measuring inflation, accompanied a doubling of cost per daily barrel.

The early 1974 estimate of \$9,900 per daily barrel was based on more definitive design and energy self-sufficiency for the plant, resulting in a lower yield. From this time on, design was fixed, but hyperinflation took its toll.

A paper on the confusing subject of cost escalation should mention the inadvertent confusion caused by failure of qualifying information to get into the reports. Within the space of a few days in autumn 1974, estimates of \$630 million and \$800 million were reported. The first was in constant dollars (as used in Figure 1), and the second included estimated escalation during the construction period at about 12 percent per year.

The estimates for March 1975 and autumn 1975 are more detailed than the earlier ones, and they show the need for caution in taking total estimates at face value.^{3,4} The first included \$79 million for acquisition of oil shale reserves not in the earlier estimates. The second increases this figure to \$155 million, mainly because the plant is assumed to run for 35 years instead of 20. The references also show a large increase in contingencies for nonplant facilities.

Tar Sands Case History

We consider the SCL Athabasca plant history herein but note in passing that the earlier Great Canadian Oil Sands (GCOS) plant was finished in 1967 with only about 25 percent overrun and that the estimate increased only about 25 percent during the last year of definitive engineering.

In early 1968 SCL estimated less than half the GCOS cost per daily barrel (\$2,400 Canadian) not including a power plant or pipeline, based on "second generation" economics, a better mine site, and a larger scale. In hindsight, economy of scale can be elusive when large plants are built in remote locations because the project aggravates labor shortages and much equipment is replicated rather than increased in size.

The 1968 estimate relied on several process steps that were in the development stage. For the summer 1971 estimate, draglines and unit trains replaced scrapers and belt conveyors for handling ore. However, abandoning energy self-sufficiency and substituting natural gas as fuel and as a source of hydrogen (and perhaps the larger scale) moderated the cost increases, so they were only a little above general inflation. SCL gave a range of expected costs at that time.

By 1973, GCOS had accumulated a \$90 million loss, and SCL was emphasizing proven reliability over development processes with theoretical advantages. For the removal of water and fines from the bitumen, dilution, centrifuging, and diluent recovery replaced flash dehydration. For upgrading of bitumen, fluid coking replaced hydrovisbreaking. The estimated syncrude yield was reduced. In a year and a half, process changes increased the cost more than 100 percent, and inclusion of a power plant and pipeline added another 25 percent to the increased amount.

After the 1973 estimate, Alberta entered an investment boom accompanied by extraordinary inflation until the end of the time covered in this study. The rapid increases in cost estimates prompted a political investigation to determine whether the oil companies had deliberately distorted the estimates. The investigation found no evidence of this but attributed the increases to severe and unanticipated escalation, additional preproduction costs from delays and increased manpower, and more definitive engineering. The December 1974 estimate was \$18,600 per daily barrel in constant dollars (used on Figure 1) and \$23,100 in current dollars for the initial capacity of 104,550 BPCD.

Learning Curves

Cost estimates usually increase as processes advance from the laboratory stage to commercial use, even without the extraordinary factors of recent years. Costs may decline because of the discovery of a new catalyst or corrosion inhibitor or the like, but usually optimism prevails until dispelled by hard data. After commercialization, unit costs often

decline as larger plants are built and safety factors are reduced. Figure 2 shows these tendencies and also the hazard of comparing directly an estimate for an advanced concept with a corresponding estimate for an established process.

Amortized production costs exclusive of raw material costs, in constant dollars (also called value added), correlate well with cumulative production of an industry.⁵ Typically this cost decreases 20 percent every time cumulative production doubles. In the early stages, an industry frequently grows exponentially with time, so a linear time scale may be superimposed on a logarithmic production scale, as shown in Figure 2. For capital intensive industries, the capital cost tends to dominate the cost of value added, but raw materials are affected too much by extraneous factors to be correlatable.

Decreasing trends will probably apply to synthetic fuel costs eventually, but the time to design and build a plant is so long that benefit of experience will be slow in coming.

Implications for Cost Estimating

Table 2 lists factors that apply during the various stages of process development. This table cannot quantify cost uncertainties, but it can alert a person to omissions and unresolved questions in an estimate.

How to account for the stage of process development in an estimate is partly a matter of philosophy. On a statistical basis, less developed processes justify higher contingency allowances, but too much caution inhibits desirable research and development. Hopefully, using Table 2 as a check list will lead to better estimates in the early stages.

In summary, the cost of developmental processes may be affected by factors other than escalation as follows:

- Raw material and product specifications
- Overall process yield
- Project scope and auxiliaries
- Process variables and subprocesses
- Materials of construction--corrosion, erosion.

The following factors may affect either developmental or commercial project costs:

- Energy and raw material availability
- Environmental regulations
- Optimization versus derating.

Derating refers to loss of capacity through installation of pollution control systems, change of raw material, and the like. Potential bias may affect estimates in the form of contingencies, redundancy for reliability, and accounting practices such as capitalizing development costs and some operating costs.

As to the future, the environmental movement and energy shortage have been with us long enough that they are unlikely to cause the surprises of the past. Equipment shortages tend to attract competition, although time is required for the competition to become affective. Thus plant costs at constant scope seem likely to parallel more closely those of the general economy. Estimators may temper early over-optimism in development projects by being aware of its prevalence and by considering what questions are unresolved at the time of the estimate.

Table 2

STAGES OF PROCESS DEVELOPMENT

Scale of Development	Possible Unresolved Questions	Inaccuracies in Estimates	Estimator
Bench	All but main reaction	Only major unit may be considered. May neglect: installation cost, engineering, indirect costs, upstream, downstream, and storage costs, effect on existing equipment and capacity, cost of capital.	Perhaps inexperienced estimator, such as lab personnel or professor. Perhaps estimate is only a publicity release.
Small pilot (process development)	Materials of construction Raw material specifications Product specifications Catalyst life and cost Process materials life Effect of simulated feeds Effect of long-term recycle operations Effect of scale-up on yield structure	May have major effect. May require pretreating process. May require purification process. Sometimes major. May affect operability as well as cost. Trace components may require major process changes. May require major process changes or different materials of construction. Affects capital as well as operating cost for a given product rate. Scale-up more difficult for processing solids than fluids.	Probably a process engineer

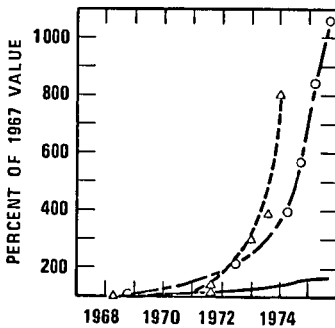
Table 2 (Concluded)

Scale of Development	Possible Unresolved Questions	Inaccuracies in Estimates	Estimator
Large pilot, prototype, or demonstration	Environmental requirements Complete integration with other processes Auxiliary unit process costs	May have a major effect. May create control problems. Historical data may not be valid because of changed requirements. Example: electrostatic precipitators.	Process engineer or engineering contractor
Commercial	Changing ground rules: unavailability of raw materials, unavailability of fuels, new environmental regulations, political opposition Remote area effects Potential bias Redundancy Capitalized development and operating costs Shortages and tight money Technological advances	Delays from changing ground rules, strikes, and bad weather are costly. Community and infrastructure development costs Licensors and promoters might tend to be low; companies seeking government support might tend to be high. Estimates based on historical costs may be high.	Engineering contractor

Source: SRI

REFERENCES

1. E. Faltermeyer, "The Hyperinflation in Plant Construction," Fortune, 102-7, 202, 204, 206 (November 1975).
2. A. C. Savay, "Effects of Inflation and Escalation on Plant Costs," Chemical Engineering 82, No. 14, 78-80 (July 7, 1975).
3. "TOSCO Proposes a Government/Industry Program to Reactivate Colony Dow West Oil Shale Project," Synthetic Fuels 12 (2), 2-1 (June 1975).
4. J. A. Whitcombe, "Oil Shale Developments: Status and Prospects," paper prepared for Soc. Pet. Engr. of AIME, 50th Annual Fall Meeting, Dallas, September 28-October 1, 1975.
5. D. M. Nathanson, "Forecasting Petrochemical Prices," Chemical Engineering Progress 68 (No. 11), pp. 89-96 (November 1972).



○ — — — TOSCO Oil Shale Plant
 △ — — — SCL Tar Sands Plant
 — — — CE Plant Cost Index

Plants based on constant dollar estimates
 in \$/BPCD of net synthetic crude.

FIGURE 1 CAPITAL COST INCREASES

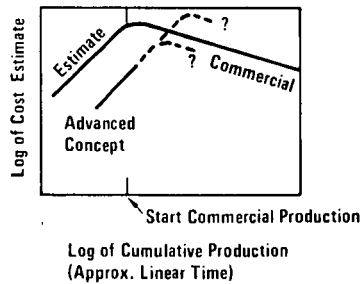


FIGURE 2 LEARNING CURVES

IN SITU OIL SHALE - RESOURCE RECOVERY

Dr. Harry E. McCarthy

Occidental Exploration and Production Company
5000 Stockdale Highway, Bakersfield, California 93309

ABSTRACT

With the completion of processing of the first large scale retort (Retort 4), Occidental is now in a position to better evaluate the potential resource recovery from a given tract of land. The results of Retort 4 will be given and then projected to a hypothetical tract of government land. Variation in retort size and geometrics will be discussed. A generalized retort layout will be presented which should allow a resource evaluation to be made on various tracts. These results will be compared with the results of alternative retorting processes.

Paraho Oil Shale Project

Harry Pforzheimer
Paraho Oil Shale Demonstration, Inc., Anvil Points, Colorado

INTRODUCTION

The Paraho Oil Shale Project is a privately financed program to prove the Paraho retorting process and hardware on oil shale at Anvil Points, Colorado, near Rifle. The project was launched in late 1973 under the sponsorship of seventeen participants*, many of whom were active in earlier oil shale research. These companies earn the right to license the Paraho Oil Shale technology on favorable terms by participating. During 1975, these participants increased the funding for the project from \$7.5 million to \$9 million and extended the term from February to May 1976.

BACKGROUND

Why is there a Paraho Oil Shale Project? Why is it being conducted at Anvil Points? The answers to these questions go all the way back to 1964 and the Colony Development programs.

The first Colony Development program was organized by Sohio Petroleum (Sohio), The Cleveland-Cliffs Iron Company (Cliffs), and The Oil Shale Corporation (Tosco) in 1964. A mine was opened and a semi-works scale Tosco type plant was built near Parachute Creek, Colorado about 23 miles from Anvil Points. Operations were commenced in 1965 and shut down in 1966.

After the shut-down of the Tosco plant in 1966, Sohio and Cliffs made an extensive survey of the world-wide technology for retorting oil shale. Among 35 different technologies which were studied in detail, a series of new inventions by John B. Jones, Jr. were selected as the most promising. They were referred to as the Paraho technology.

Before a program could be organized to test the Paraho technology on oil shale, negotiations began with Atlantic Richfield Company (Arco) to form the second Colony Development program. These were completed by Sohio, Cliffs, Tosco, and Arco in 1969. Arco became the Operator of Colony for the four companies. By early 1971 the Parachute mine and plant had been reactivated and operations attempted. In September 1971, having completed their financial commitments, Sohio and Cliffs withdrew from funding the second Colony program retaining their land interests. Arco and Tosco continued plant operations into early 1972 before shutting down.

In 1971, Sohio began providing financial assistance to John Jones to help defray certain expenses of obtaining a lease on the Oil Shale Experiment Station at Anvil Points from the Bureau of Mines. With Parachute Creek occupied, the Anvil Points site was needed so the Paraho processes could be tried on oil shale. The Anvil Points lease was approved by the President of the United States in May 1972. In 1973, organization of the Paraho Oil Shale Demonstration began. By year-end, 17 participants had joined the project.

* The seventeen Paraho participants are Atlantic Richfield, Carter Oil (Exxon), Chevron Research (Standard of California), Cleveland-Cliffs Iron, Gulf Oil, Kerr-McKee, Marathon Oil, Arthur G. McKee, Mobil Research, Phillips Petroleum, Shell Development, Sohio Petroleum, Southern California Edison, Standard Oil Company (Indiana), Sun Oil, Texaco, and the Webb-Chambers-Gary-McLoraine Group.

PROGRAM

Two new Paraho retorts, a pilot plant and a semi-works size unit, were installed at Anvil Points. The oil shale mine on the adjacent Naval Oil Shale Reserve was reactivated. The mine and new retorts were put into operation during 1974. The pilot plant is used to explore operating parameters in order to define conditions for testing in the larger semi-works size retort. The experimental operations in 1974 set the stage for the successful runs in 1975 and early 1976. The results of the Paraho operations to date have been encouraging. They demonstrate that the process works, that the equipment is durable and that both are environmentally acceptable on a pilot and a semi-works plant scale.

During 1975, the operation being conducted at Anvil Points progressed from the experimental into the operability phase. A 56-day operability run in the direct fired mode was completed on the semi-works retort in March 1975. Following this run, 10,000 barrels of the shale oil produced were refined into seven different fuels for the U. S. Navy in the largest such conversion of shale oil into military products. A nationwide product testing program by industry and government of Paraho's synthetic fuels followed. This included an operational test of Paraho JP-4 in an Air Force T-39 jet aircraft flight from Wright Patterson Air Force Base near Dayton, Ohio to Carswell Air Force Base near Fort Worth, Texas; a 7-day Great Lakes cruise on Paraho heavy fuel oil by a Cleveland-Cliffs Iron ore carrier; and a full-scale boiler burning test by Southern California Edison of Paraho crude shale oil.

Success of the Paraho Project suggested that the next logical step should be the construction and operation of a full-size Paraho retort. This would reduce industry's and government's concerns about the ability to successfully scale up proven technology to commercial size. In May 1975, Paraho announced its proposal to construct and operate a full-size Paraho module at Anvil Points. The proposal included a full-size Paraho retort, an expanded mine and all the auxiliary equipment needed to operate this full-size module. A cost of \$76 million was estimated for construction and operation.

Considerable interest and support was evidenced by industry and government in Paraho's full-size module proposal. The chairmen of the Armed Services Committees of the U. S. House of Representatives and the U. S. Senate granted the right to mine the additional shale required from the Naval Reserve. The Navy authorized proceeding when ready. Paraho's subsidiary, Development Engineering, Inc., exercised its option to extend the lease on the Anvil Points Oil Shale Experiment Station. The Bureau of Mines completed a favorable environmental assessment of the module proposal. The Solicitor's office of the Department of Interior issued Guidelines for the Federal Prototype Oil Shale Leasing Program. These Guidelines provided, among other things, that expenditures by lessees for patented or demonstrated technology, such as Paraho's, would be creditable against the fourth and fifth lease bonus payments.

In July 1975, the \$6 billion Synthetic Fuels Amendment was added to the ERDA appropriation act and was approved by the U. S. Senate. With this federal assistance in the offering, it looked like everything needed to move ahead with joint government-industry financing would be available for the full-size Paraho module.

President Ford visited Paraho's Anvil Points operation in August 1975 with Frank Zarb, Congressman Tim Wirth (Colo.-D) and Senator Gary Hart (Colo.-D). They toured the mine and plant, witnessed Paraho's ability to produce oil from oil shale and were impressed. President Ford reported favorably to the media about the size, productivity and environmental acceptability of Paraho's operation and stated that oil shale must have a bigger part in this country's energy program. This was before the Energy Research and Development Administration reacted to a legal threat by an environmentalist.

In October 1975, ERDA decided that a new Environmental Impact Statement would have to be prepared before Paraho could build its full-size module at Anvil Points. This would require at least a year and was commenced immediately.

In November 1975, Paraho conducted a 26-day direct fired run on the semi-works retort. This run, designed to confirm the results of the earlier 56-day run and subsequent variable studies, was an outstanding success. A very stable operation at essentially 100% on-stream time with high thermal efficiency (87%) and excellent liquid yield (97% by volume of Fischer Assay C₅+ oil) confirmed that the Paraho direct fired process was ready for scale-up to the full-size module. This mode will produce more than enough low Btu gas to provide fuel for the process and to generate all the electricity required to power and light a commercial plant.

Two federal actions adverse to oil shale occurred in December 1975. One was the defeat of the \$6 billion Synthetic Fuels Amendment in the House of Representatives. The other was the passage of the compromise 1975 Energy Policy and Conservation Act which rolled-back the price of domestic crude oil. Unfortunately, these actions occurred at a time when incentives, rather than restraints were and still are needed to encourage energy production and conservation.

On February 10, 1976, Paraho completed a 32-day run in the indirect heated mode. Operation in this mode, which offered the potential of higher liquid yields and the production of a high Btu gas, was one of the original objectives of the Paraho Oil Shale Project. Selected conditions from the run indicated a high liquid yield of 98% and gas production of 850 standard cubic feet per ton containing 865 Btu per cubic foot (dry basis).

It was not anticipated when the objective of testing the indirect mode was set that the liquid yield on the direct mode would be as high as the 97% actually obtained. All of this oil is useful product because the large amount of low Btu gas produced in the direct mode can be used to fuel the process. In the indirect heated mode it would be necessary to burn as fuel either the high Btu gas or some of the oil produced. A potential benefit of the indirect heated mode is the production of a higher quality, lower pour point crude shale oil. This oil may be suitable for pipeline transmission without local upgrading or prerefining. If so, the savings in investment and operating cost of prerefining would more than off-set the higher costs of indirect mode retorting. Eliminating local prerefining also would eliminate a major water consumer.

A confirming indirect heated run was commenced in March 1976. During this run, a series of evolutionary changes in operating conditions were made which reduced the heat input required per ton of shale thereby increasing thermal efficiency.

OBSERVATIONS

Paraho's retort performance exemplifies simplicity in process and mechanical design:

1. It has few moving parts and low construction and operating costs.
2. It utilizes counter-current flow and gravity transport without requiring a separate circuit for solid, heat carrying bodies.
3. The Paraho retort consumes no water.
4. The lumps of retorted shale it produces do not create serious dust problems.
5. Retorted shale management experiments demonstrate the ability to easily compact this material to a condition which is impermeable to water. Very little water is required in retorted shale management. This is primarily

- for vegetating the surface of the retorted shale.
6. Emissions of sulfur and nitrogen oxide and particulates have been found acceptable under the strict Colorado standards.
 7. High thermal efficiencies are attained. Rather than discard the residual carbon on the retorted shale, the Paraho direct heated process consumes much of it to fuel and power the process. On the other hand, the indirect mode produces a high Btu gas and a better quality oil. A combination of the direct and indirect mode may be the ultimate solution. It should be possible to fuel the combination mode by burning carbon on the retorted shale. This would liberate both the oil and the high Btu gas as useful products.

In anticipation of the May 31, 1976 Paraho Project completion date, the Anvil Points mine was closed in December 1975 as sufficient rock was on hand to carry out the privately funded retorting program. The retorts are scheduled to shut down on March 31, 1976 unless additional funding is obtained. The equipment will be put in stand-by condition and the plant secured by April 30, 1976. All final reports will be issued by May 31, 1976 except for the Commercial Evaluation Study which will be ready for distribution by June 30, 1976. After analysis of the results of the retorting program, a mode or modes of operation will be selected for the Commercial Evaluation Study. The advantages of the Paraho process will be reflected in the economic results obtained in this study. However, construction of a full-size Paraho module at Anvil Points or at some other location would still be the next logical step toward commercialization.

WHAT NEEDS TO BE DONE NOW

It is almost inconceivable, during this time of critical need for synthetic fuel development, that the only operating, large scale, successful oil shale retorting project in the United States will be compelled to shut down upon completion of its privately funded program. Continued operation of the Anvil Points facilities would offer important benefits. Additional variable studies need to be performed to improve efficiency and optimize operating conditions. A second generation retort could result from additional work on the combination mode. Significant volumes of shale oil could be produced. This crude shale oil would be extremely desirable for large scale refining and synthetic product testing programs over an extended period of time.

Paraho is a small privately owned company which appears to have the answer for oil shale commercialization. It is operating at Anvil Points under a lease from the federal government in the presence of ERDA observers. It has been successful in accomplishing its initial objectives. Paraho does not fit into ERDA's highly structured methodology for developing and demonstrating technologies by making requests for ERDA's conceived specific proposals. What is wrong with accepting progress already made? Paraho has established by its accomplishments what should be an acceptable basis for initiating government financial support for continued operation.

Our national alternative to supplementing our domestic crude oil supply with shale oil production is to purchase more and more imported crude oil. Such purchases would be made at higher and higher prices exporting both dollars and U. S. jobs. Under this alternate we will become more and more vulnerable to another oil embargo and less and less capable of maintaining a prosperous economy or of mustering an effective national defense.

This nation must recognize that we have an energy shortage and that all acceptable forms of domestic energy development will fall short of meeting our needs, particularly for transportation fuels. New legislation must be passed to correct the adverse federal actions of December 1975. Federal non-recourse, guaranteed loans should be made available to help fund the building of full-size modules for oil shale. They are the best way to eliminate uncertainties relating to the production and economic acceptability of shale oil. Technologies already demonstrated by industry on a semi-works scale should qualify for such funding.

After the module phase is completed, one or more retorting technologies may be successfully demonstrated and be ready for commercial plant construction. Ten to twenty full-size retorts might be required for such a commercial plant. To justify moving into commercial mining, retorting, and upgrading, involving very high capital investments, an exception to the administered oil prices under the "Energy Bill" will be required. Industry needs to know now that a free market will exist in which crude shale oil and refined synthetic products can compete price-wise with imports.

Conceding that our government needs to take a long look down the road to energy independence and help in developing technologies toward commercialization, it is still in this nation's best interest to encourage private industry to move through the profit system into the new technologies as they reach feasibility. The future conditions actually required to encourage commercialization by private competitive enterprise cannot be determined at this time. When such conditions do occur, if federal funding assistance is required, it should be available. Non-recourse guaranteed loans may be needed to encourage the construction of the first group of commercial plants by industry and for socio-economic projects by the communities to be impacted by such commercial plants for which actual private commitments to build are made.

H. Pforzheimer
Program Director

sam
August 1976

DOD SYNTHETIC FUELS R&D PROGRAM

Lt. L. A. Lukens

U.S. Navy Energy and Natural Resources R&D Office
Navy Department, Washington, DC 20360

ABSTRACT

The DOD is now, and will remain so over the foreseeable future, extremely dependent upon an adequate supply of petroleum products. This dependency, when coupled with the politico-economic and source availability uncertainties of conventional petroleum supplies, has led the DOD to seek alternative sources of liquid hydrocarbon fuels. The DOD Synthetic Fuels R&D Program is primarily directed towards optimizing the production of military specification fuels from domestic sources of coal, oil shale, and tar sands, and assessing the suitability of these fuels for service use. To date, several synthetic fuels derived from coal, oil shale, and tar sands have been examined. Over the next several years, the DOD, in cooperation with other federal agencies, plans to continue programs directed towards the production and utilization of synthetic military fuels. Only through this effort will the military departments be able to keep pace as an informed customer with the development of national synthetic fuels industry-an industry which will provide a viable alternative to our present and ever increasing dependence upon imported oil.

Net Energy Analysis of Oil Shale Systems

By Dr. Kenneth P. Maddox

Colorado School of Mines Research Institute
P. O. Box 112, Golden, Colorado 80401

Introduction

Net energy analyses of three shale-oil-producing systems have been conducted. The presentation of these analyses is divided into several parts. First the methodology is outlined, next process descriptions are given, and after that results are listed and comparisons are made with conventional energy-producing systems. Then a discussion of the results follows, and conclusions are drawn. The final section describes some uses of net energy analysis in decision-making.

Methodology

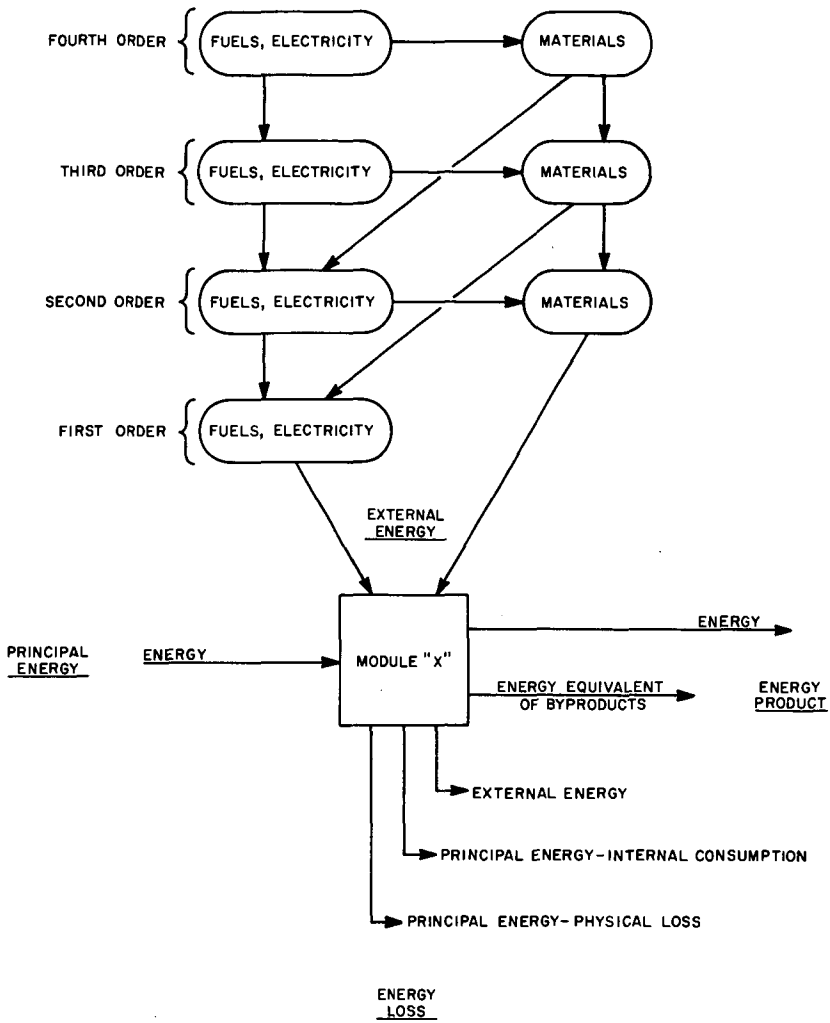
Fuel systems generally can be divided into steps. For the purpose of this analysis seven steps, or modules, were chosen. The seven steps are: (1) Extraction, (2) Transport I, (3) Process, (4) Transport II, (5) Conversion I, (6) Conversion II, and (7) Distribution. All systems follow the same general sequence although there may be minor variations of format from one system to another.

An analysis of a multi-step fuel system reduces to the combination of analyses of individual modules. The diagram of one module of a fuel system (Fig. 1) displays the important features of modular analysis. The first law of thermodynamics is observed-- $E_{in}=E_{out}$. Also, energy derived from and used within the system is always internal to the module. These precautions reduce one problem associated with energy analyses, construction of system boundaries.

Energy input consists of two parts, Principal Energy and External Energy. Principal Energy is the primary energy input. External Energy is the sum of fuels, electricity, and of the energy embodied in materials which are purchased or "imported" from energy systems other than the one being analyzed.

The energy "backup" needed to deliver External Energy must be considered to fully account for energy drain from other energy systems. This is diagrammed as ascending higher orders of External Energy. Two different methods have been used to compute the higher-order energy inputs. Conversion factors developed from economic input-output data ⁽¹⁾ were applied to material dollar costs, after appropriate deflation to the base year of 1967. This method is the best available for each material input without employing tedious calculations. However, for fuels and electricity the alternative of iteration combined with empirically derived approximations at or above order three is used. This alternative is more precise, and flexible, than the application of conversion factors similar to those used for material energy equivalents.

Energy Product and Energy Loss comprise E_{out} . Energy Product is defined as the major energy form produced by the module, plus other energy produced for outside distribution, plus the energy equivalent of salable byproducts. Energy Loss has been divided into three parts. Physical Loss is the sum of losses of the Principa



Energy input due to spillage, leakage, disposal of waste materials, etc. Internal Consumption is the energy required from Principal Energy to provide heat or power for the process. The third loss category is External Loss. Normally this is the sum of the external energy inputs. In some circumstances, however, an external energy input will be incorporated in the Energy Product, e.g. additives to petroleum products.

Modules are combined simply by adjusting the Energy Product of one module to equal the Principal Energy of the following module, and so on. This automatically requires a corresponding change in the External Energy, the Energy Loss, and the Principal Energy of the modules in the fuel system. Finally, totals for the fuel system, a sequential combination of seven modules, are: (1) Principal Energy--the initial Principal Energy input to the system, (2) External Energy--the sum of External Energy inputs of each normalized module, (3) Energy Loss--the sum of Energy Loss outputs of each module, and (4) Energy Product--the final Energy Product output plus the sum of byproduct energies of each module.

Process Description

One difficulty with analyses of synthetic fuel processes is the absence of commercial data. In this analysis, the best available data is used. However, information presented here should be viewed as probable, not actual, characterization of oil shale processes.

The three oil shale retorting systems studied are the Bureau of Mines Gas Combustion Retort, the TOSCO II Retort, and the Union B Retort. Because the data for each process are calculated averages, and because it is not realistic to draw fine distinctions among oil shale processes without further information, the results will not be specifically identified with each process. Rather, the letters A, B, and C (not corresponding to the order listed above) will be used to identify results.

Bureau of Mines Gas Combustion Retort

The Bureau of Mines Gas Combustion Retort features direct heating of shale by hot combustion gases from partial burning within the retort. A schematic diagram is shown in figure 2. The flow of shale and gas is countercurrent. Consequently, incoming shale is first preheated and then retorted, while air entering the retort is heated prior to combustion by hot spent shale as it exits.

The Gas Combustion Retort has, from an energy efficiency standpoint, advantages and disadvantages. It makes use of carbon remaining on the spent shale after kerogen is pyrolyzed, and the sensible heat of both spent shale and combustion gases is well utilized. However, the Fischer Assay oil yields (82-87%) are lower than for other types of retorts; and the Gas Combustion Retort cannot handle finely crushed material without briquetting, which adds to capital and operating costs (and therefore to energy use).

TOSCO II Retort

The TOSCO II Retort (Fig. 2) transfers heat from hot (1200°F) ceramic balls to finely crushed raw oil shale. Sensible heat is recovered from the spent shale (950°F); and the ceramic balls are recycled and heated by gas recovered from the

retort, as is the incoming raw shale.

Advantages of the TOSCO II Retort are: high oil and gas yields (as high as 108 percent of Fischer Assay); high-Btu gas, since there is no dilution from combustion within the retort; direct retorting of fine shale, even dust.

Disadvantages are: chemical potential of residual carbon is not recovered; the retort is mechanically complex, with many moving parts; shale must be finely crushed, which adds to processing.

Union B Retort

The Union B Retort (Fig. 2) uses externally heated recycled gas to pyrolyze oil shale. The product gas from the retort is split; and one part of the gas is burned to heat the other, which is then returned to the retort. A rock pump is used to move shale from bottom to top of the retort. There is no combustion in the retort. The Union B retort yields up to 100 percent of Fischer Assay and produces a high-Btu gas. It is rather simple mechanically. However, the residual carbon on the spent shale is not utilized; and there is little sensible heat recovery, either.

The fuel systems studied in these analyses produce two different final energy forms--gasoline and electricity. The oil shale gasoline systems produce gasoline from oil shale extracted by underground mining, crushed and retorted aboveground, refined at or near the plant site, pipelined 300 miles, and distributed by truck 70 miles. The transportation mileages and refinery type are characteristic of the Rocky Mountain region. Oil shale electric systems are based on underground extraction, aboveground crushing and retortion, generation at or near the plant site, and 150-mile transmission. Conventional petroleum systems correspond to the oil shale systems in refining, product type, and transport distances.

Results and Discussion

Tables 1 and 2 display results for the net energy analysis of three oil shale systems. It can be seen from Table 1 that (with current technology) more external energy is required to produce 100 energy units of gasoline from oil shale processes than from conventional petroleum systems. Furthermore, the process losses for oil shale are higher than for petroleum. However, the initial recovery of petroleum is low, i.e. unrecovered resource is high; and consequently the sum of losses and unrecovered resource for oil shale is comparable to that for petroleum. Similarly, external losses and process losses for oil shale converted to electricity are higher than for petroleum electricity; but the sums of losses and unrecovered resource are comparable.

The analyses of oil shale systems (and of conventional petroleum) are based on commercial or near-commercial current technology. No attempt has been made to estimate the potential of tertiary oil recovery, of subsequent extraction of shale mine pillars, or of improvements in retorting efficiency. Comparisons incorporating such changes require additional studies.

Three questions which appropriately concern the public and their representatives in business and in government are:

TABLE 1

Net Energy Analysis
Summary of Oil Shale Systems

Product: Gasoline Final Output: 100					
Process	Initial Principal Resource Required	Initial Process Input	Total External Losses	Total Process Losses	Total Losses and Unrecovered Resource
Oil Shale A	320	160	16	84	250
Oil Shale B	330	160	12	80	250
Oil Shale C	310	150	14	76	240
Conventional Petroleum	330	110	10	24	250

TABLE 2

Net Energy Analysis
Summary of Oil Shale Systems

Product: Electricity Final Output: 100					
Process	Initial Principal Resource Required	Initial Process Input	Total External Losses	Total Process Losses	Total Losses and Unrecovered Resource
Oil Shale A	980	490	26	440	940
Oil Shale B	1000	500	16	420	930
Oil Shale C	940	470	21	420	910
Conventional Petroleum	1000	330	10	260	970

How much energy is produced by oil shale systems compared to the amount necessary to operate the system?

How efficient are the processes of oil shale systems?

How well do oil shale systems use natural resources?

These basic questions require many modifications, additions, and explanations to respond fully to all the concerns voiced by interested parties. Nevertheless, they are valid, and can be answered generally in the following ways. First, oil shale systems deliver much more energy than they require from other sources. Gasoline-producing systems provide 6-8 times the amount they use, while shale-electric systems deliver 4-6 times as much energy as they consume. Second, process efficiencies for an oil shale system are typically 50-60%, considerably less than the efficiency of a petroleum system (approximately 80%). Process losses to produce 100 units of output are more than three times as much for shale as for petroleum. Process losses are primarily due to retorting, and at the present time different retorting methods vary little in overall efficiency. Third, oil shale systems make as good use of natural resources as do present-day petroleum systems; but neither oil shale recovery nor petroleum recovery is high; and it appears that efforts more fully to extract our finite fossil fuels are essential.

Conclusion

Net energy analyses offer valuable information on energy-producing systems and can be helpful in focusing attention on concerns about use of finite natural fuel resources. Net energy analysis supplements other planning and decision-making tools - e.g. economic analysis, technical feasibility, environmental study, social impact planning. Potential applications include selection of priorities for research and development, aid to energy policy planning, identification of conservation goals for end use consumption, determination of potential improvements in the energy processing and delivery system, and contribution to decisions about resource management and environmental effects.

One example may illustrate the use of net energy analysis. Suppose that it is necessary to provide space heating on a large scale (perhaps to replace dwindling sources of natural gas). Assume the available resources are oil shale and coal. Either resource may be surface or underground mined. Oil shale may be liquefied or further converted to electricity. Coal may be burned directly for space heating (highly unlikely), liquefied, gasified, burned in a steam-electric power plant, or perhaps converted via magnetohydrodynamics. At end use the fuels may be burned in forced-air or water-radiant systems, while electricity may be used for direct-radiant heating or to power heat pumps. Is there a best option or a best set of options among these many possibilities? Which ones produce least resource impact? Which require least "energy support" from existing energy systems? Which are most process efficient (and thus perhaps least likely to produce unfavorable impacts)? Where can improvements in each system be made, and how large are the potential effects of improvements? These are all questions which can be answered using net energy analysis.

Net energy analysis can be employed at the micro level or at the macro level; i.e. the importance of an analysis may be its detail of an energy system, or the

central question may be a large-scale comparison of alternatives. A comprehensive analysis will provide both process specifics and summary aggregations.

Many assumptions concerning energy system processes and resource-related variables largely affect net energy analyses. However, difficulties comparing one analysis with another or applying results to different questions can be overcome if investigators are careful to list their assumptions, to explain their methodologies, and to define their scopes of study. Net energy analysis should be presented so that the reader can determine for himself how appropriate a study is to his needs.

Net energy analysis is a useful tool which can and should be used to aid those involved in questions of energy supply and demand. It does not supplant, but rather supplements, other planning inputs. New problems often require new ways of looking at things. Net energy analysis is one new way of looking at energy supply and demand. It is a good addition to the decision-making process.

1/ Herendeen and Bullard 1974

MECHANISMS HELPING TO HEAT OIL-SHALE BLOCKS

John Ward Smith and Donald R. Johnson

U.S. Energy Research and Development Administration
Laramie Energy Research Center, Laramie, Wyoming 82071

INTRODUCTION

Oil shale rubble piles, like those created in the vertical modified in-situ combustion process pioneered by Occidental Oil Shale, Inc., or those postulated in Project Bronco, consist of oil-shale blocks of assorted sizes. Heating these blocks through to produce their oil seemed a formidable problem until work in the Laramie Energy Research Center's large scale batch combustion retorts showed that temperatures high enough to evolve shale oil were attained completely through blocks weighing several tons (1-3)¹. Although some anomalously high rates of temperature increase in shale blocks during combustion retorting have been reported (2,3) and explanations for these high rates attempted (5,9), the high rates appear too rapid for ready explanation. However, some mechanisms do operate to help heat oil-shale blocks and evolve their shale oil. Three separate mechanisms are identified: (1) thermal exfoliation of the shale; (2) gas evolution assisting and augmenting the exfoliation; and (3) combustion of light decomposition products from the organic matter in the oil shale. Existence of each of these is demonstrated and their combined effects are evaluated.

EXPERIMENTAL

Thermal Expansion and Exfoliation

ERDA's Laramie Energy Research Center developed apparatus to measure the thermal expansion and exfoliation effects on oil shale in relation to temperatures. The apparatus, to be described in detail elsewhere, consists of a position transducer suspended from one end of a beam and a stainless steel pad suspended from the other. The beam, supported on a knife edge at its center like a balance beam, is free to move. In operation the stainless steel pad rests on the flattened face of an oil-shale specimen prepared as a cylindrical core about 1/2-inch in diameter and 1-1/2 inches long. The pad contains a thermocouple for measuring the sample temperature. Weight on the beam is adjusted to place a small load (0.5 to 1 gm) on the core to maintain contact between the core and the pad. As the sample length changes during heating, the pad is moved which moves the position transducer to generate a corresponding electrical signal.

The sample rests on the bottom of a platinum tube equipped with a gas exit tube running up its side from the lower corner. A gas inlet is attached at the top of the sample chamber, permitting controlled flow of a selected gas around the sample. A bell jar over the beam closes the system and provides the complete atmosphere control so vitally necessary to oil-shale

1 Underlined numbers in parentheses refer to items in the list of references at the end of this report.

thermal studies (7). The sample chamber is surrounded by a furnace that provides rapid and uniform heat transfer to the sample. The heating rate of the furnace is programmable. This arrangement is very similar to the simultaneous DTA-TG-EGA apparatus developed for oil-shale study at the Laramie Energy Research Center (4).

Thermal expansion plotted with temperature is shown in Figure 1 for an oil-shale specimen cored perpendicular to the bedding planes from a 1-foot Mahogany zone sample yielding 35 gallons per ton. The sample was run in a nitrogen atmosphere and was heated at the rate of 10° C. per minute.

Several expansion events are recorded in Figure 1. The sample apparently began to increase in length as heating began. The initial lengthening probably expresses the linear expansion of the organic matter in the oil shale, undoubtedly many times (~20) larger than the mineral expansion. In 35 gallon per ton oil shale the organic matter represents about 40 volume percent of the rock (6). If the length increase between 50° and 100° C. is due to expansion of the organic matter, the organic matter's expansion coefficient is about 3.4×10^{-4} length per unit length per °C. This rather large linear expansion is on the order of but somewhat smaller than values in the same temperature range reported for asphalt and paraffin. Consequently it is not an unreasonable value. Its validity is limited, however, by possible inclusion of effects from the thermal event which occurs next.

The thermal expansion trace (Figure 1) shows that very rapid lengthening occurs through the temperature interval 190° to 225° C. By the time this sample had reached 225° C. it had increased its length by about 8 percent. This elongation is accompanied by sharp irregularities in the trace. These irregularities are real, expressing equipment response to sudden events, the development of fissures. Visual examination of a core sample heated through this temperature interval and then cooled reveals numerous fissures approximately parallel to the bedding planes.

Two factors contribute to development of these fissures in the temperature range from 190° to 225° C. The primary mechanism is failure due to thermal stress. This requires some explanation. Oil-shale cores perpendicular to the bedding planes cut many individual beds. Some contain relatively large amounts of organic matter and some contain relatively small amounts. Organic-rich layers will elongate much more rapidly than organic-poor layers. If these layers happen to be adjacent in the sample, a stress is developed. Weak planes fail suddenly, popping the shale apart. The partings are rarely completely across the specimen because the stress is relieved by partial failure. The second factor, the release of combustible gases, is treated later. However, it definitely contributes to the lengthening and to the uneven length trace.

Above 225° C. a period of little length increase appears, almost as if all the significant stress had been released. Above 300° C. a steady and gradual length increase again occurs.

At about 400° C. the organic matter begins to decompose rapidly. From 400° C. until about 485° C. the sample again shows rapid, irregular length increase. By the time it reached 485° C. this core had lengthened by almost 14 percent. Gas development is the predominant force producing this lengthening. In this temperature range the organic matter loses much of its physical competence, so evolving gases push some organic-tied layers apart.

When decomposition of the organic matter is completed at about 485° C. (Figure 1) additional heating produces little length increase. Between 485° C. and 1000° C. this sample increased in length by only 1.1 percent. Decomposition of dolomite and calcite, which occurred in this temperature range, produced no significant length change, either increase or decrease.

GAS EVOLUTION AND COMBUSTION

Oil shale is very sensitive to the presence of oxygen during heating. Smith and Johnson (7) used thermal analysis to evaluate this effect. Figures 2, 3, and 4 are extracted from that paper which gives a detailed discussion of applying thermal analysis to study of oil shale and other solid fuels. Description of the apparatus and the conditions of these runs are given there (7). Figure 2 shows the DTA (differential thermal analysis) and TG (thermogravimetry) behavior of oil shale heated in an inert atmosphere. The sample begins to lose weight at about 200° C., but its reactions are all endothermic. In Figure 3 oil shale is heated in air. Sensitivity was cut by a factor of 5 and the sample size was reduced to about 1/3 to keep the two exotherms on the chart. The two exotherms peaking at about 330° C. and 430° C. are due to combustion of the organic matter in two separate phases, the second of which is burning of carbon coke. Combustion of light ends to evolve heat definitely occurred by the time the programmed heating curve reached 200° C.

Oil shale heated in an atmosphere containing only 1 percent air (0.2 percent oxygen) shows significant heat production from oxidation of organic matter. Figure 4 shows DTA and TG traces for such a run. Sensitivity and sample size are back to those used in Figure 2. Heat from combustion of light organic fractions is being produced below the 200° C. point of the temperature program even though the oxygen supply is very small. Two exotherms are generated by oil shale heated in atmospheres containing 20 percent or 0.2 percent oxygen, although their intensities decrease with smaller oxygen concentrations. The important point is that the oil shale produces significant heat by oxidation even at very low oxygen levels.

DISCUSSION

Oil-shale specimens not only expand during heating but show two separate temperature zones of fracturing. Although the behavior of only one sample is shown (Figure 1), other oil shales exhibit similar behavior. This fracturing, occurring under no load in these experiments, will also occur in an oil-shale rubble pile. In a rubble pile the shales are subjected to

point loads. At other locations on a block the shale is free to expand and fracture into surrounding void space under essentially no load.

The two separate zones of rapid expansion with fracturing are particularly important to heating of oil shale. This is graphically demonstrated by comparing the temperature locations of the oxidation exotherms in Figures 3 and 4 with the temperature locations of the rapid expansion. Expansions (which occur in any atmosphere) coincide with combustion exotherms in an oxygen-bearing atmosphere. In addition the expansion trace in Figure 2 shows that in these zones of rapid expansion the core both expands and contracts. During expansion the surrounding atmosphere, oxygen-bearing in combustion-based processes, is sucked into the core, then expelled with the contractions. This automatically provides oxygen and expels combustion products. The combustion itself may provide some atmosphere exchange. By burning rapidly the gases may be unable to transfer heat rapidly to the surrounding oil shale. Gas pressure capable of expelling the remaining combustion products would build. The remaining gas would then cool by gradually heating the surrounding rock. This would draw in additional oxygen-bearing gas.

In addition to the heat effects inside the block, the combustible gases evolving from the shale will travel out from the block. They have been observed evolving and burning along fissures in oil-shale blocks. Such combustion at the block surface provides heat to the block and its immediate atmosphere.

After retorting is completed, the carbon residue is distributed throughout the shale block. Because the original organic volume fraction has shrunk by 90 percent (8), the spent shale is now porous. The carbon residue is available for burning if oxygen can reach it. The fissuring produced by heating the oil shale provides access routes which help oxygen diffuse into the spent shale.

REFERENCES

- (1) Carpenter, H. C. and H. W. Sohns, Colo. School Mines Quart., 63 (4), 71 (Oct. 1968).
- (2) Harak, A. E., L. Dockter, and H. C. Carpenter, BuMines TPR-30, 14 (1971).
- (3) Harak, A. E., L. Dockter, A. Long, and H. W. Sohns, BuMines RI-7995, 31 (1974).
- (4) Johnson, D. R. and J. W. Smith, BuMines RI-7429, 17 (1970).
- (5) Mallon, R. G. and W. C. Miller, Colo. School Mines Quart., 70 (3), 221 (July 1975).
- (6) Smith, J. W., BuMines RI-7248, 14 (1969).
- (7) Smith, J. W. and D. R. Johnson, "Proceedings Second Toronto Symposium on Thermal Analysis," H. G. McAdie, ed., Toronto Sect., Chem. Inst. of Canada, 1967, pp 96-116.
- (8) Smith, J. W. and N. B. Young, Colo. School Mines Quart., 70 (3), 69 (July 1975).
- (9) Tyler, A. L., ibid., 207 (July 1975).

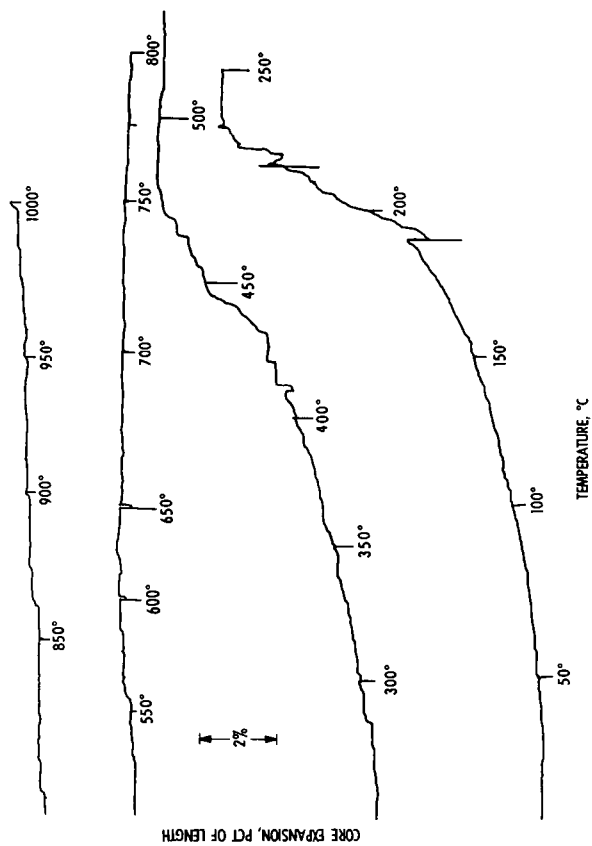


Figure 1. Thermal expansion of oil-shale core cut perpendicular to bedding planes.

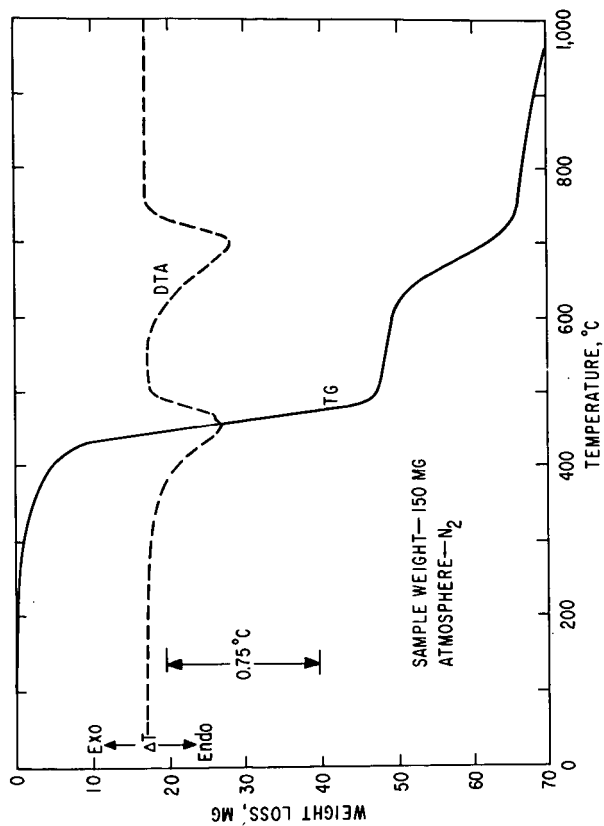


Figure 2. Thermal analysis (DTA-TG) of oil shale in an inert atmosphere.

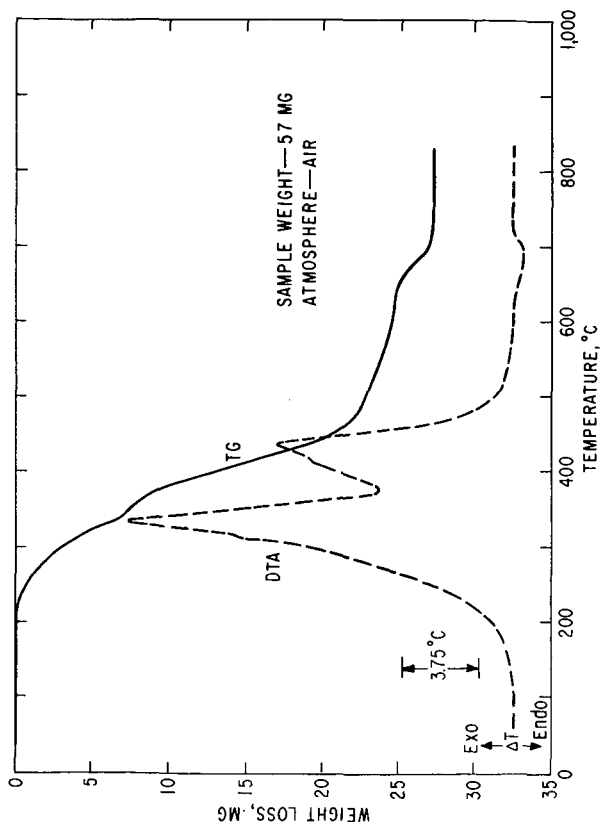


Figure 3. Thermal analysis (DTA-TG) of oil shale in air.

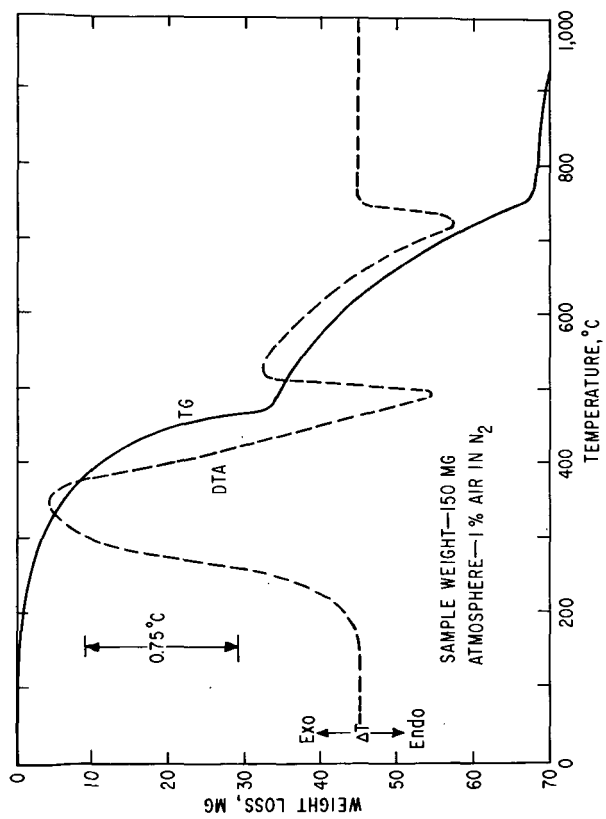


Figure 4. Thermal analysis (DTA-TG) of oil shale in 1 percent air in inert atmosphere.

Explosive Rubblization of *In Situ* Oil Shale Retort Beds

William J. Carter

University of California, Los Alamos Scientific Laboratory
Los Alamos, New Mexico 87545

Introduction:

A number of technical, environmental, economic and political problems remain to be solved before *in situ* extraction of hydrocarbons from oil shale deposits becomes a practical reality (1). Of all the technical problems, perhaps the most challenging is that of preparing the resource bed on the massive scale and with the control and precision required for commercial exploitation. Although the requirements are not yet fully defined, it is generally agreed that a properly-prepared *in situ* oil shale retort would have the following characteristics:

- a) The particle size distribution achieved by the process should peak in the range of that required for maximum extraction efficiency. Current chemical kinetics and process studies places this range as roughly 5-50 cm, with the peak around 10 cm.
- b) Void distributions in both the horizontal and vertical sense must be uniform in order to achieve a stable flame front and avoid channeling.
- c) The permeability of the resultant rubble pile must be sufficient to support pyrolysis and allow removal of retorted products.
- d) Fines produced in the rubblization process must be minimal, both to avoid plugging the pores through which the gases and other products must move and to maximize the efficiency of the rubblization event.
- e) The rubblized volume must be well defined, with maximum residual wall and roof integrity in order to provide retort stability, containment of combustion products, safety for workers in adjacent areas, and maximum utilization of the resource.
- f) The economics of the process must be favorable.

Obviously, the final result must be a compromise between the ideal and that which is achievable. At present, chemical explosives appear to be the most feasible method for achieving these goals, but present blasting technology is certainly not sufficiently well-advanced to guarantee any success of the event, much less technical and economic optimization.

For this reason, the Los Alamos Scientific Laboratory and Sandia Laboratories have jointly undertaken a basic research program, under the auspices of the Energy Research and Development Administration, aimed at producing a controlled, predictable, and optimized breakage pattern in western, or Green River, oil shale. The work of Los Alamos is presently directed primarily toward the modified *in situ* technology, in which void space and free faces can be created by conventional mining operations, although the results will be applicable to design of true *in situ* operations as well. This is a long-term and continuing program which will involve a considerable effort both in the laboratory and the field. This report is therefore intended only to indicate the direction of the program and the long-term goals. However, the importance of the program to the eventual success of *in situ* technology makes it desirable for chemical and process engineers to be aware of the difficulties, possibilities, and achievements of research on the bed preparation problem.

Program Outline:

The laboratory phase of the program falls into three clearly defined but closely related categories:

a) Measurement of material properties of oil shale. The Los Alamos effort is concentrated on measurement of properties of the shale subjected to high strain rate loading such as is encountered in an explosive event. Wave propagation characteristics, such as Hugoniot and wave profiles on shock and release, are measured in order to determine the stress field. This stress field must then be related to the dynamic failure surfaces and the kinetics of the fracture process. Measurement of these dynamic materials properties is a program which is well advanced.

b) Measurement of non-ideal explosive behavior. Detailed knowledge of the detonation characteristics of ANFO and other commercial explosives is required in order to define the initial conditions of the expanding stress waves into the oil shale. Tailoring of the explosive impulse to the response of the rock is also an eventual goal which should result in reduced fines around the borehole and enhanced energy transfer to the far-field region. The effect of expanding explosive gases in propagating radial cracks is also a subject of interest. This work is presently underway.

c) Computer modeling. Lagrangian and Eulerian hydrodynamic computer codes are being used to synthesize the materials and explosive properties into a coherent picture of the event. Ideally, the codes could be used both as a design tool for shot layout and as a predictive tool for shot optimization. A series of field tests specifically designed for testing the predictive capability of the codes are required before the codes can be used with confidence. These tests constitute a major part of the latter stages of the program.

Results to Date:

In the first few months of the program, attention has been directed primarily toward propagation characteristics of the stress waves rather than the dynamic fracture properties of the material. At low pressures, this is a particularly complex problem because of the anisotropic nature of the material and its non-linear response to dynamic stresses. Figure 1 shows the u_s - u_p Hugoniot in the pressure region of 50-200 kb of oil shales of varying density obtained from explosive experiments on small samples. This pressure range is that which would be experienced in the near-field region around a borehole, and lies just below the sluggish but large-volume phase transformation identified in dolomite. The Hugoniot of a material is the locus of thermodynamic equilibrium states attainable by a single shock along which the energy is known, although not constant, and is fundamental to the science of shock wave physics (2). Here, u_s is the velocity of propagation of the shock front, and u_p is the associated material, or particle, velocity. The shock velocities were measured by high-speed smear cameras which recorded the transit times through small samples, and the particle velocities were determined by impedance matching against an aluminum alloy standard. The family of Hugoniot shows a well-defined sequence from the low density, or high kerogen content, samples to the high density samples. Figure 2 shows these kinematic data transformed from the shock velocity-particle velocity plane to the pressure-relative volume plane by use of the Rankine-Hugoniot conservation relations, which require equilibrium for their validity. The solid lines on these plots are not fits to the data, but rather calculations based on a simple mixing theory known to be generally valid for mixtures of non-reacting components. The Hugoniot and thermodynamic parameters for the end members of pure kerogen and the lean rock matrix must be known. These have been obtained from the work on dolomite by Grady, et al. (3) and from extensive shock wave work on rocks and minerals and on polymers performed at Los Alamos in the past (4,5). It is

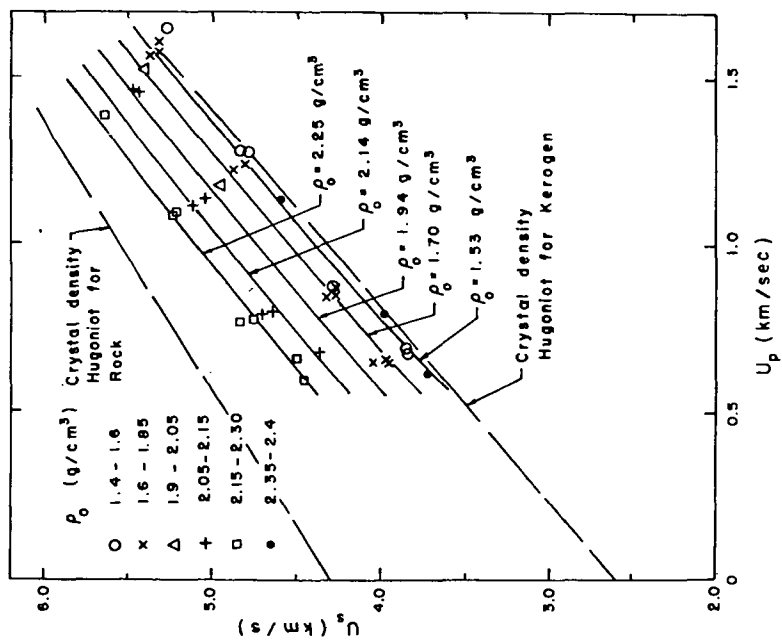


Figure 1. High pressure u_s - u_p Hugoniot data for oil shales of varying densities. The solid lines are theoretical calculations.

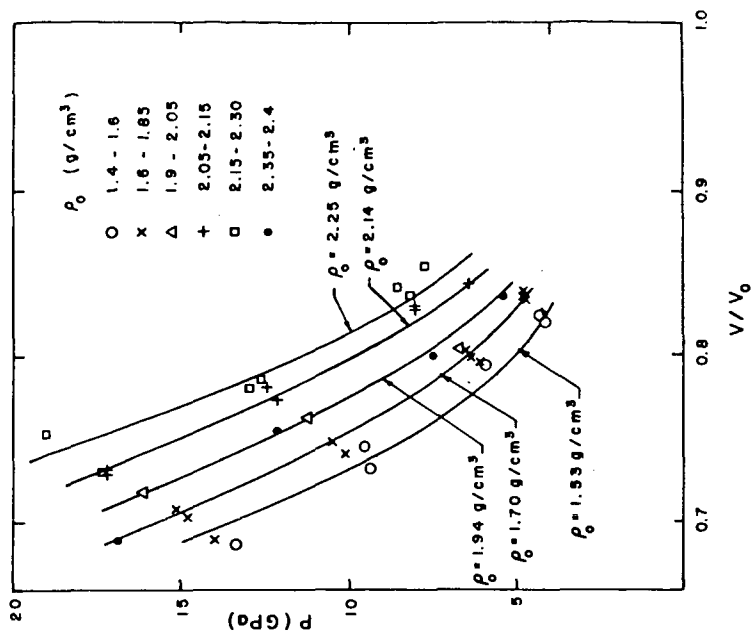


Figure 2. P - V/V_0 Hugoniot data and calculations for oil shale. The Rankine-Hugoniot conservation relations were used to transform these data from Figure 1.

evident that the theoretical Hugoniot are quite adequate to reproduce the data, and that Hugoniot of oil shale with arbitrary kerogen content can now be calculated with confidence. These Hugoniot include the effect of shock heating, and theories such as that of Mie-Grüneisen must be used to calculate the equation of state $E(P,V)$ off the Hugoniot, such as along an isentrope or isotherm. Samples were also fired with varying orientation of the shock wave to the bedding planes, and no significant orientation effects have been found at these high pressures. Experiments are underway to determine wave anisotropy at lower pressures, where those effects should be larger.

In order to establish the initial low pressure response of oil shale to both static and dynamic stresses, a program to determine the elastic constants at zero pressure as a function of kerogen content has been undertaken (6). The shale has been treated with the model of a transversely isotropic material, a reasonable assumption in view of the bedded nature of the material. Pulse-echo techniques were used to determine transverse and longitudinal sound velocities as functions of orientation in small, carefully prepared samples. The results are shown in Figure 3, where V_1 , V_3 , and V_5 are longitudinal velocities parallel, perpendicular, and 45° to the bedding planes and V_4 and V_6 are shear velocities parallel to the bedding with particle motions perpendicular and parallel to the bedding respectively. From these five quantities, the various mechanical properties of oil shale such as elastic moduli, bulk modulus, and Poisson's ratio are readily obtainable as functions of density or kerogen content. The discontinuity in slope observed for all the sound velocities at a density slightly above 2.0 g/cm^3 is tentatively attributed to the fact that below this density the rock particles float more or less discretely in a matrix of kerogen and the properties of the kerogen largely determine the elastic properties of the shale. At higher densities, the rock properties play a more important role. We intend to continue such measurements under a hydrostatic environment up to pressures of about 10 kb.

Gas guns, with bores ranging in diameter from 2" to 6", are being used for detailed study of low-pressure wave profiles both on loading and release with the expectation that these profiles will have an important effect on fracture kinetics. There is good reason to believe that the high explosive properties can be tuned to take advantage of the dynamic response of the shale in this pressure range, as evidenced by these profiles, and thereby promote desirable fracture characteristics (7). Pressure gages, magnetic probes, pins, and free-surface capacitor gages are typical diagnostics used in these experiments. Other quantities amenable to measurement using these techniques include attenuation parameters, low pressure Hugoniot and dynamic spall strengths. Many of these experiments have already been performed, although discussion of them is as yet premature. As an example of the kind of experiment which can be useful in defining the fracture characteristics of oil shale, Figure 4 shows the velocity of the free surface of an oil shale sample as a function of time when the material is subjected to a plane impact stress of about 5 kb. This record was obtained using the dc capacitor technique, in which a thin metallic coating is placed on the free surface and the time rate of change of capacitance between the free surface and a charged parallel plate is monitored. Internal tension due to the rarefactions sends a signal which will decrease the free surface velocity and which can be directly related to the tensile stress necessary to cause spall fracture. In this experiment, the bedding planes were aligned along the direction of shock propagation. Other experiments include detonation of spherical charges in meter-size blocks of oil shale with pressure and particle velocity gages to monitor wave propagation and flash x radiography to view cavity formation and near-field behavior. The logical extension of these experiments, of course, is to small-scale field events which will test our ability to predict the breakage pattern resulting from any given explosive configuration, a prerequisite to optimization.

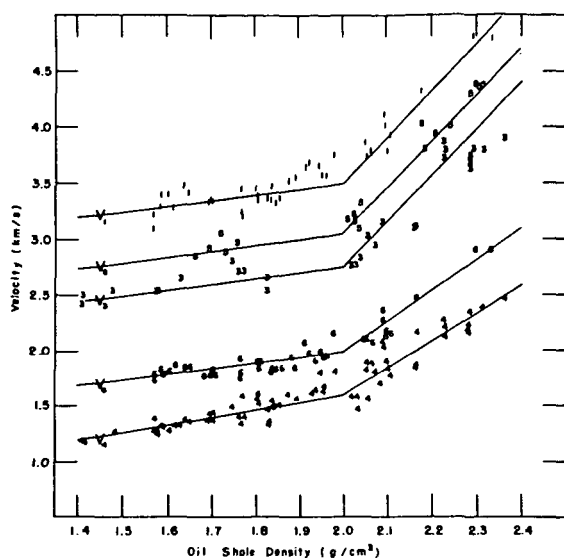


Figure 3. Zero-pressure sound velocities for oil shale as a function of density, or kerogen content. These data allow calculation of zero-pressure elastic moduli, assuming transverse isotropy.

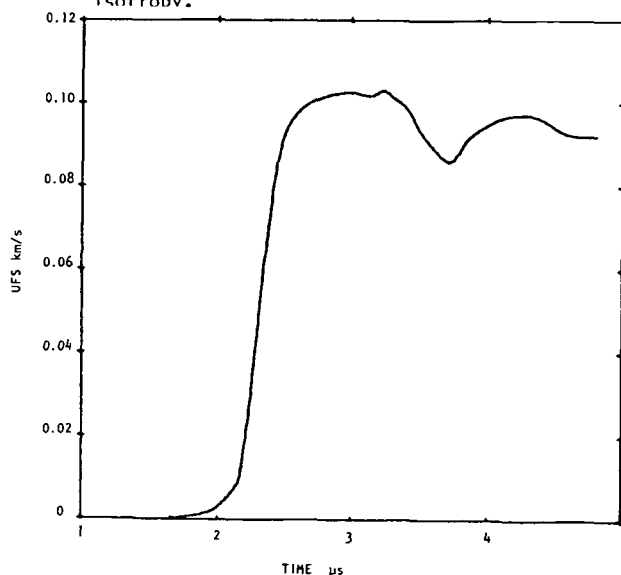


Figure 4. Typical capacitor free-surface record showing spallation of oil shale subjected to a 5-kb shock.

In order to demonstrate a quantitative understanding of the material response obtained by experiment, efforts are underway to model the results of the one-dimensional experiments described above. Large-two dimensional Lagrangian and Eulerian hydrodynamic codes originally used for weapons effects calculations have been modified to allow for plastic anisotropy, again assuming transverse isotropy. These codes are also being used for design and analysis of the large-block experiments mentioned earlier. This work is well underway, but detailed discussion of the results would be premature. Success of the codes in predicting the results of a large-scale rubbleization effort in the field will be the test of our quantitative understanding of the physical processes involved in blasting.

Summary:

Since the program is still in its infancy, useful results to date are very preliminary and this paper is intended only as a program review. Eventually, there must be closer collaboration between those concerned with extraction efficiency and those who can set the attainable limits on the properties of the re-tort bed. It is hoped that the results of this study will have a favorable influence on decisions affecting the future utilization of the oil shale resource.

References:

- (1) S. Rattien and David Eaton, "Oil Shale: The Prospects and Problems of an Emerging Energy Industry," in Annual Review of Energy 1 (1976), J. M. Hollander and M. K. Simmons, eds. (Annual Reviews, Inc., Palo Alto, 1976).
- (2) R. G. McQueen, S. P. Marsh, J. W. Taylor, J. N. Fritz, and W. J. Carter, "The Equation of State of Solids from Shock Wave Studies," in High Velocity Impact Phenomena, R. Kinslow, Ed. (Academic Press, New York, 1970).
- (3) D. E. Grady, W. J. Murri, and K. D. Mahren, J. Geophys. Res. 81, 889 (1976).
- (4) W. J. Carter, S. P. Marsh, and R. G. McQueen, "Hugoniot Equation of State of Polymers," (to be published).
- (5) R. G. McQueen, S. P. Marsh, and J. N. Fritz, J. Geophys. Res. 72, 4999 (1967).
- (6) B. Olinger, Los Alamos Scientific Laboratory (private communication).
- (7) J. Hershkowitz and I. Akst, "Improvement of Metal Acceleration Properties of Non-Ideal Explosives Containing AN," PA Technical Report 4789 (1975).

THE FISCHER ASSAY, A STANDARD METHOD?

Robert N. Heistand

Development Engineering, Inc.
P.O. Box A, Anvil Points
Rifle, Colorado 81650

Mr. Heistand, on loan from Sun Oil Company, is the chief chemist for the Paraho Oil Shale Demonstration. D.E.I. is the operator of the demonstration being conducted at ERDA's Anvil Points Experimental Station. The facility is located on the U.S. Naval Oil Shale Reserve near Rifle, Colorado.

INTRODUCTION

The Fischer assay is not a standard analytical procedure. It does not produce quantitative values such as the weight percent nickel in a stainless steel or the ppm mercury in water. Rather, the Fischer assay is a performance test such as the octane number of motor fuels or the tensile strength of fibers. Because it is an assay -- a performance test -- the data obtained are quite dependent upon the test procedure. Variances in the test procedures, permitted in the widely accepted USBM Fischer assay method, do cause significant differences in the data obtained.

HISTORY OF THE FISCHER ASSAY

The Fischer assay had its origins in the early low-temperature coal retorting research of Franz Fischer and Hans Schrader⁽¹⁾. However, our present concern is with the USBM procedure as described in detail by Stanfield and Frost and Hubbard in Bureau of Mines Reports of Investigations 4477 and 6676 (2,3). The main details of the USBM procedure are shown in Figure 1. Many of the details are no longer followed by laboratories doing Fischer assays (some are no longer followed by the USBM (4)!).

The USBM Fischer assay presents many problems to analysts attempting to use this procedure. The suggested apparatus, particularly the cast-aluminum retort, is the major source of problems. The softening point of the aluminum alloy is quite close to the suggested retorting temperature and the seal of the plug and retort is not perfect. A diagram of the USBM apparatus is shown in Figure 2. We use these U.S.B.M. retorts in our laboratory. By carefully controlling the retort temperature through the use of continuous control and proportional heat (5), the problem of the retort melting has been lessened. Two retorts have been developed to obviate the softening and leakage problems. The TOSCO retort (6) shown in Figure 3, is constructed of steel. The head is fastened with four steel studs. Thermocouples are placed both in the retort and adjacent to the retort as shown. The overall configuration of the TOSCO retort is similar to the USBM retort. The Core Laboratories retort (7), shown in Figure 4, is also constructed of steel. The cap is threaded on. The Core retort represents a drastic change from the USBM system. Ten of these retorts are placed in an oven with a single temperature controller. The Core Laboratories retort systems require much less space than the TOSCO or USBM. Both modifications, TOSCO, and Core, are designed to duplicate data

obtained by the USBM procedure. Because of problems with the USBM apparatus, a standardized modification is clearly needed.

Fischer assay results, obtained from various laboratories, do indeed differ. This difference is illustrated in Table I. A sample of raw shale was carefully blended and riffle-split into 2 1/2 lb. packages for use as a standard in our laboratory. The mean results from ten replicates of this standard are shown. The four laboratories are not necessarily those mentioned previously. These data, I feel, show that the Fischer assay is not a standard method.

VARIANCE OF FISCHER ASSAY DATA

Without studying each laboratory's procedures in detail, it is impossible to determine the causes of variability shown in Table I. However, studies made in our laboratory show that modifications in the Fischer assay, many permitted in the USBM procedure, do have an effect on the data.

Mesh Size. The particle size of the sample has two different effects on the oil yield. First, it seems that oil shale richer in organics is more resistant to crushing than leaner shales. Thus, as shown in Table II, the oil yield tends to increase with increasing particle size (decreasing mesh size). Thus, neither lumps nor fines may be discarded. Careful splitting (without loss of dust) must always be used to obtain a valid sample. Grab samples, such as needed to obtain the 100.0 grams recommended in the USBM procedure, may not be representative.

The other effect that particle size has on oil yield as shown in Table III. Here the same original samples were reduced by grinding to smaller particle size. Again, the yield decreases with decreasing particle size. In this case, the cause is not clear. No apparent degradation, or partial retorting, seemed to occur with grinding.

In order to obviate effects of mesh size of Fischer assay data, the following are recommended:

- (1) Neither large pieces nor fine dust may be discarded.
- (2) Mass reduction should be by riffle splitting.
- (3) Samples should be ground to uniform, standard mesh size.

Temperature. In the USBM procedure, the temperatures of three components are defined. These components are the receiver, the condenser, and, of course, the retort.

Since temperature is the controlling factor of the Fischer assay in defining the gas-liquid split (the condensation of gaseous vapors into liquids) the temperature of the receiver has a pronounced effect on oil yields. This is shown in Table IV where the temperature of the receiver ranged from 20°F to 100°F. Changing from the prescribed 32°F to the permissible 100°F does affect the oil yield. An ice bath, recommended by Atwood (6) seems best suited for controlling the receiver temperature.

The temperature of the condenser is listed as 32 ± 9°F in the USBM procedure. Yet, the condenser has no effect on the oil yield data; any oil escaping the receiver and condensed in the condenser will not be measured. Because of the low pour point of crude shale oil, this material will remain on the condenser walls and not be weighed with the receiver and adapter. Studies in our laboratory have shown that removing the condenser from the

system has had no effect on the Fischer assay data. Perhaps the condenser can be eliminated.

The suggested time-temperature profile of the retort is shown in Figure 5. This is a strip-chart recording from our 12-position bench. Failure to reach the 932°F prescribed in the USBM procedure produced low results as shown in Table V. Increased time does not appear to increase the oil yield. The effect of increased temperature cannot be studied using the aluminum USBM retort. It has been suggested (8) that the location of the thermocouple well (beneath the spout) is poor. Truer readings and better control can be achieved if the thermocouple is located at the bottom center or rear of the retort. This position would be similar to that suggested by Atwood (6).

In order to obviate errors in Fischer assay data caused by various temperature fluctuations, the following are recommended:

- (1) The temperature of the receiver be controlled by an ice bath.
- (2) The condenser be eliminated.
- (3) The temperature of the retort be carefully controlled with the suggested relocation of the thermocouples to the rear of the retort.

FISCHER ASSAY ALTERNATES

With the uncertainties in the Fischer assay data, the capital costs in fabricating a Fischer assay bench, the larger laboratory space required, and the long time needed to complete the test, it is no wonder that several alternatives for the Fischer assay have been proposed in recent years. Some of these alternatives are listed in Table VI. Pulsed NMR (9) is used to measure the organic hydrogen content of shale. Direct organic carbon, by controlled combustion, eliminates effects of the inorganic carbonates (10). Thermal chromatography (11) and laser-chromatography (12) relate oil yields to the concentration of certain hydrocarbon released by heating. Although each of these alternatives has certain advantages, most suffer from the following disadvantages:

- (1) They offer little or no improvement in precision.
- (2) Instrument costs are similar to those of a Fischer bench.
- (3) Sample size are small. This requires additional sample preparation time and trouble.
- (4) They are used to measure only oil yields whereas the normal Fischer assay measures oil yield (gal/ton), water yield (gal/ton), gas + Loss (wt%), specific gravity of the oil, and coking tendency of the shale.

STANDARD FISCHER ASSAY

In spite of the differences in procedures and the variations in the data obtained, the Fischer assay seems destined to be the standard for the oil shale industry. No alternative procedure offered to date is completely satisfactory. With this in mind, the ASTM Committee D-2 on Petroleum Products and Lubricants has formed a subcommittee to solve the aforementioned inconsistencies and create a standard Fischer assay. In our laboratory, we await the results -- a standard Fischer assay test procedure!

ACKNOWLEDGEMENT

The author would like to acknowledge the many Fischer assay run by Mr. D. Yoder to obtain the data for this paper.

REFERENCES:

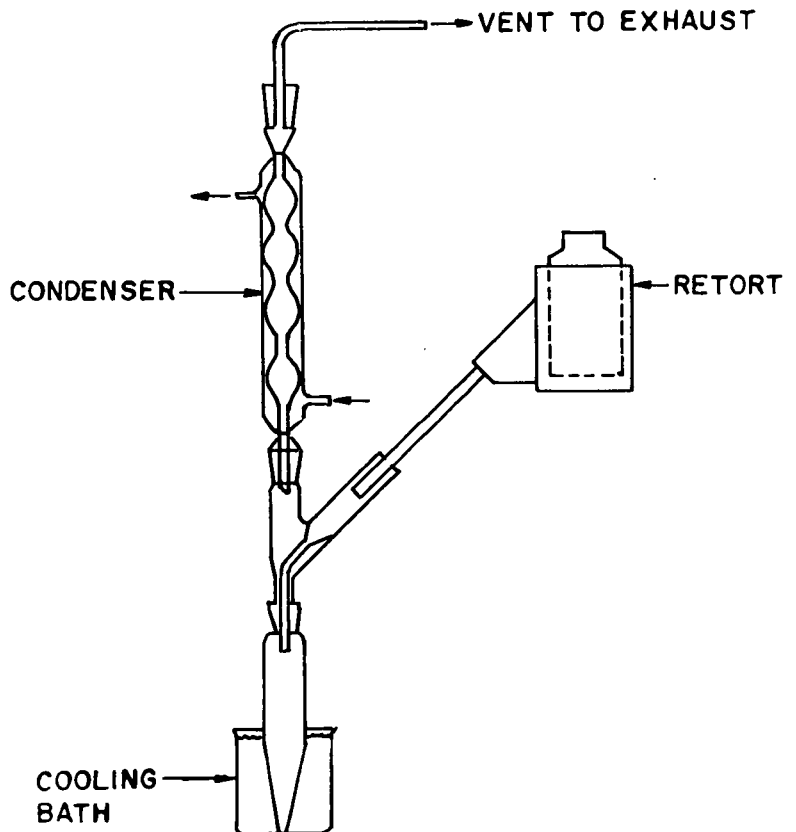
- (1) F. Fischer and H. Schrader, Zeit. an. Chem., 33, 172-75 (1920)
- (2) K. E. Stanfield and I. C. Frost, Bureau of Mines Report of Investigation 4477 (1949)
- (3) A. B. Hubbard, Bureau of Mines Report of Investigation 6676 (1965)
- (4) Laramie Energy Research Center personnel, private communication (1974-75)
- (5) R. N. Heistand, Energy Sources, 4, (1976)
- (6) M. T. Atwood, "Oil Shale Developments - Current Status," pp. 29-58, report of the conference-workshop "Analytical Chemistry Pertaining to Oil Shale and Shale Oil," NSF, Wash. D.C., June 24-25, 1974.
- (7) E. H. Koepf, Core Laboratories, Inc., Dallas, Texas, Private Communication (1976)
- (8) R. G. Guthru, Electric Power Equipment Company, Commerce City, Colorado - Private Communication (1975)
- (9) F. P. Miknis, A. W. Decora, and G. L. Cook, Bureau of Mines Report of Investigation 7984 (1974)
- (10) R. N. Heistand and H. B. Humphries, Anal. Chem., 48 (1976)
- (11) D. A. Scrima, T. F. Yen, and P. W. Warren, Energy Sources, 1, 321-34 (1975)
- (12) R. L. Hanson, N. E. Vanderbough, and D. G. Brookins Anal. Chem., 47 335-38 (1975)

USBM FISHER ASSAY PROCEDURE

SAMPLE	100.0 GRAM -8 MESH
RETORT	CAST ALUMINUM WITH TAPERED PLUG
HEAT	AMBIENT TO 932°F IN 40 MINUTES HOLD AT 932°F FOR 20 MINUTES
COOLANT	ETHYLENE GLYCOL - WATER AT 32°F
CONDENSERS	32 ± 9°F
RECEIVER	23 TO 100°F

Figure 1

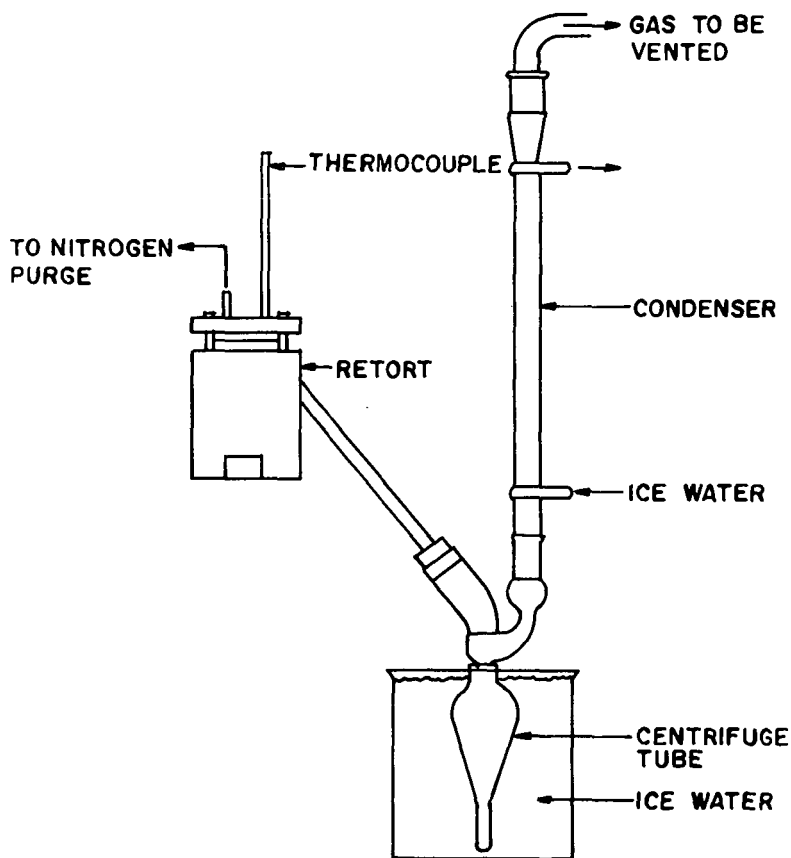
USBM RETORT



USBM RI 6676 (1965)

Figure 2

TOSCO RETORT



"ANALYTICAL CHEMISTRY PERTAINING TO OIL SHALE AND
SHALE OIL " JUNE 24-25, 1974

Figure 3

**CL-7000 RETORT CUP
120 GRAM CUP**

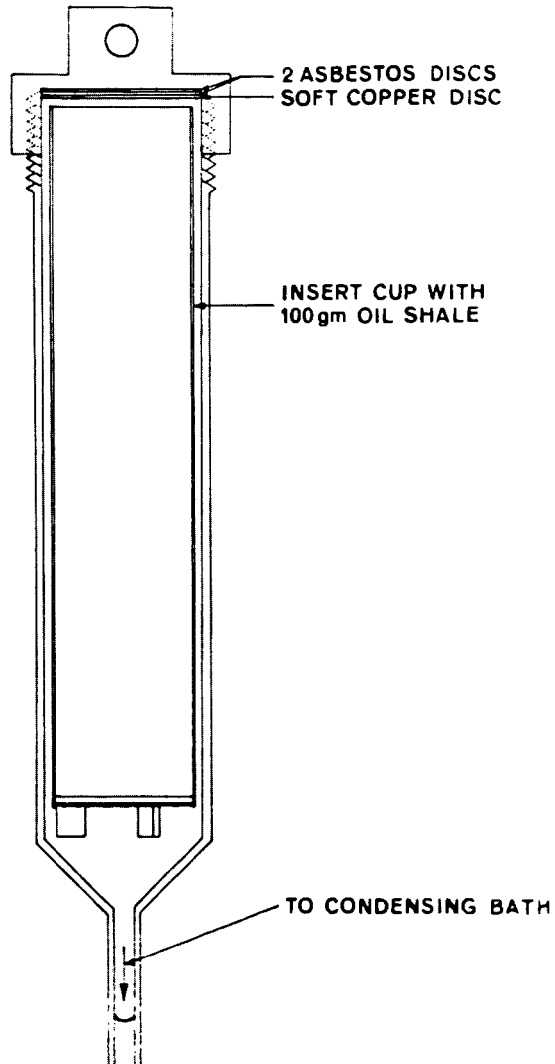


Figure 4

FISHER ASSAY DATA

LABORATORY	A	B	C	D
OIL, GAL / TON	24.94 ± 0.17	25.35 ± 0.33	26.16 ± 0.71	24.07 ± 0.26
WATER, GAL / TON	3.28 ± 0.10	3.47 ± 0.16	3.86 ± 0.36	3.20 ± 0.11
OIL, SP. GR	0.9133 ± 0.0028	0.9014 ± 0.0020	0.8997 ± 0.0040	0.9162 ± 0.0012
GAS + LOSS WT. %	2.32 ± 0.24	1.98 ± 0.12	2.81 ± 0.21	2.37 ± 0.13

Figure 5

SIZE DISTRIBUTION AND FISCHER ASSAY

MESH SIZE (MESH TO IN.)	DISTRIBUTION (WT %)	FISCHER ASSAY (OIL, GAL / TON)
+ 2 1/2	0.4	
-2 1/2 + 4	3.9	30.6
+ 6	8.3	31.7
-6 + 8	12.1	30.9
+ 14	31.5	29.8
-14 + 28	19.9	27.2
+ 48	10.9	25.6
-48 + 100	3.9	24.3
-100 + 200	2.1	22.1
-200	4.4	14.5

Figure 6

FISHER ASSAY VS. GRINDING

	-8 MESH	-20 MESH	-65 MESH
XI-A	28.6	28.3	28.0
B	29.8		28.8
C	18.3		17.8
D	43.2		42.6
E	29.5		28.0

Figure 7

FISHER ASSAY VS. RECEIVER TEMPERATURE

TEMPERATURE °F	OIL YIELD GAL / TON
19-24	28.8±0.7
32	29.1±0.5
35-45	28.1±1.1
65-100	27.5±0.8

Figure 8

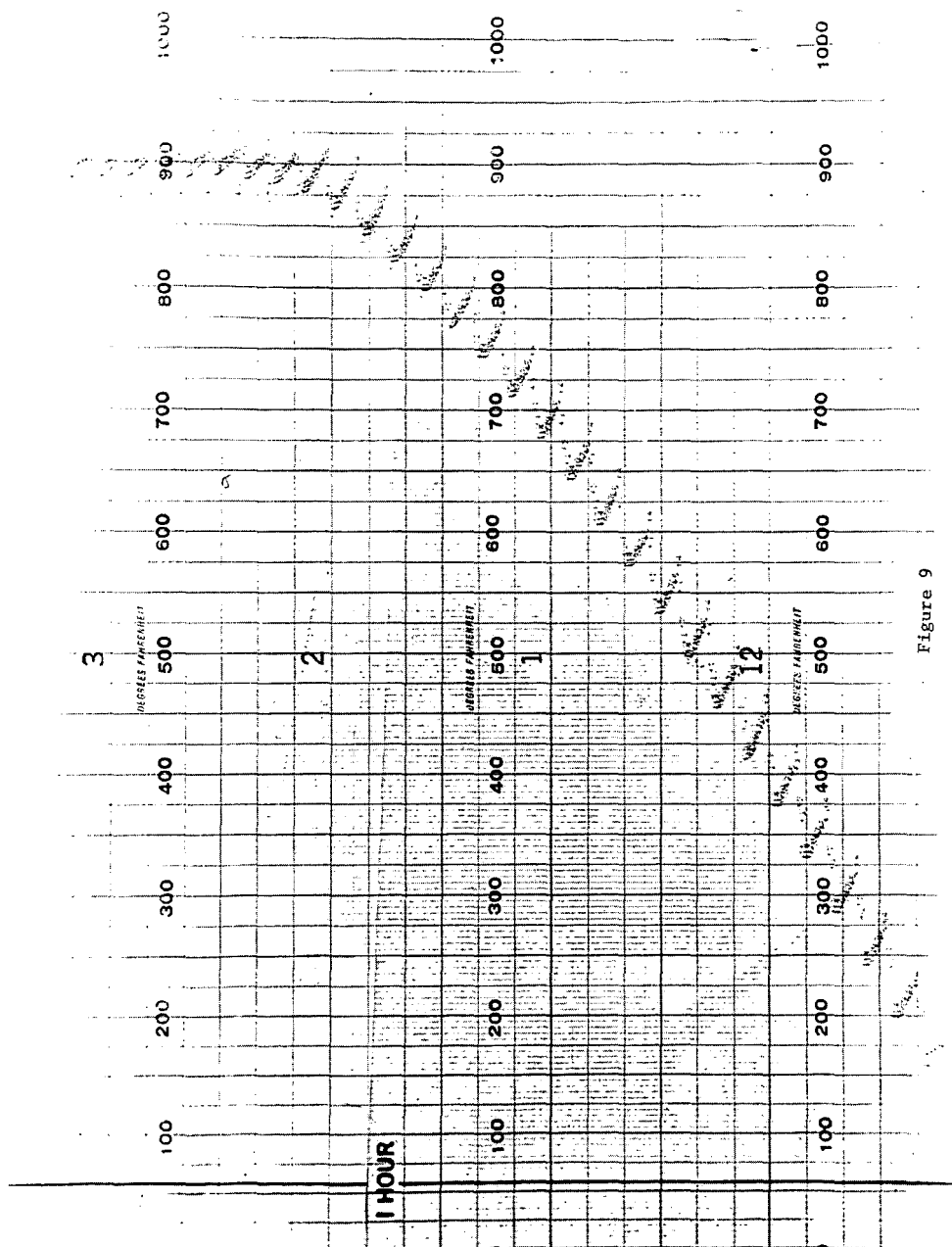


Figure 9

FISHER ASSAY VS. RETORT HEATING

TIME (MIN)	TEMP (°F)	OIL YIELD (GAL / TON)
5	932	27.6 ± 1.0
20	932	29.1 ± 0.5
35	932	28.8 ± 0.7
20	825	27.8 ± 1.5
20	750	10.0 ± 4.1

Figure 10

FISHER ASSAY ALTERNATIVES

THERMAL CHROMATOGRAPHY

ORGANIC CARBON

LASER - CHROMATOGRAPHY

PULSED NMR

Figure 11



COMPOSITIONAL DIAGRAMS: A METHOD
FOR INTERPRETATION OF FISCHER ASSAY DATA

V. Dean Allred

Denver Research Center, Marathon Oil Company
Littleton, Colorado 80120

BACKGROUND

Oil shale can be broadly classified as a mixture of two major components, that is organic and inorganic derived matter. In the Green River oil shales the organic portion is usually the minor constituent, but may be present in quantities varying from about zero to as great as 50 weight percent within very small vertical intravals, i.e., the varves which define the bedding planes in the deposit. Obviously because of such variations, sampling and sample preparation are extremely important if representative assay data are obtained. However, a major point to be made in connection with this paper is that within any given assay sample the organic concentration probably varies quite widely for the individual shale particles. Statistically this probably accounts for the observation that as a broad general rule, the pyrolytic decomposition seems to take place to form volatile products and organic residue on the pyrolyzed shale in constant proportions and independent of the inorganic matter concentration.

The commonly accepted technique for characterizing oil shale in the U. S. is the Modified Fischer Assay (MFA)(1). Assay data from this technique are usually reported in terms of the volatile components as: oil yield, water yield, and gas plus loss. The retorted shale (often called spent shale) is often omitted. However, it can be accurately reestablished since it is the difference between 100 weight percent and the volatiles. Interestingly the weight fraction of retorted shale is possibly the most accurately determined assay quantity since it is done gravimetrically and does not involve condensation, separation, and density determinations as do the liquid products. For this reason the retorted shale (or its analog, the total volatiles) should be of great value in making correlations with MFA data. In this paper these types of data are used to establish relationships between the oil yield, the total organic matter, and the organic residue remaining on the retorted shale.

COMPOSITIONAL DIAGRAMS

The "compositional diagram" (CD) is a useful tool for visually evaluating oil shale assay data -- particularly the relationship of oil yield to the total organic matter and the organic residue left on retorted shales. The basic concepts used in the development of the CD plot involves only simple material balances, and straight forward assumptions that inorganic decomposition is small and the ratio of the products to total organic matter is not concentration dependent and remains constant for a given assay procedure as follows:

1. Material Balances:

a. Raw shale:

$$\text{organic } (X_t) + \text{inorganic } (Y_i) = 100 \text{ wt } \% \quad 1)$$

b. Retorted shale:

$$\text{volatiles } (X_v) + \text{retorted shale } (Y_s) = 100 \text{ wt } \% \quad 2)$$

2. Pyrolysis Mechanism:

a. Organic matter

$$\text{Organic } (x_t) \stackrel{A}{=} \text{Volatiles } (x_v) + \text{Organic Residue } (x_r) \quad 3)$$

b. Volatile matter:

$$\text{volatiles } (x_v) + \text{gas } (x_g) + \text{water } (x_w) + \text{oil } (x_o) \quad 4)$$

3. Assumptions:

a. Inorganic decomposition negligible.

$$\text{Inorganic} \stackrel{A}{=} \text{Inorganic} + \text{H}_2\text{O} + \text{CO}_2$$

b. Pyrolysis product distribution constant:

$$\frac{x_o}{x_t} = K_1, \frac{x_w}{x_t} = K_2, \frac{x_g}{x_t} = K_3, \frac{x_v}{x_t} = K_4 \quad 5)$$

Obviously, neither the organic residue on the retorted shale, nor the total organic are obtained directly from the MFA. However, if one of these quantities is known then the other is easily calculated by equation 3 and these values can be rather uniquely determined from the MFA data if the assumption of constant product ratios holds. The development of a coordinate system showing these relationships is given as figure 1. In this figure line \overline{AB} is representative of equation 1 and gives the relationship between the total organic and the inorganic matter in the raw shale. A line \overline{AD} can also be drawn which represents the weight percent of the organic matter which will pyrolyze to oil during assay. Another line \overline{AE} can also be drawn which represents the total volatiles evolved during the pyrolysis. Obviously the difference between line \overline{AB} (total organic) and line \overline{AE} (total volatiles) must be the organic residue (\overline{BE}) which will be found with the retorted shale.

Line \overline{AE} also has a unique relationship to the retorted shale value (y_s) since the volatile organic must always simultaneously be represented by a point 'G' on the line \overline{AB} in order to fill the requirement of equation 2. By simple geometry it follows that the line \overline{JG} can be established with a point 'H' on the line \overline{AE} , giving the following relationships:

1. for the organic residue,

$$\overline{GE} = \overline{HD} = \overline{EB} \quad 6)$$

2. the gas and water (plus loss):

$$\overline{HG} = \overline{DE} \quad 7)$$

3. and the oil:

$$\overline{CD} = \overline{JH} \quad 8)$$

Figure 1 therefore becomes a diagram on which the relationship of the known values (oil, volatiles, or residual shale) from a MFA can be plotted and the value of the other unknowns (inorganic, total organic, and organic residue) can be determined directly, provided the position of the lines \overline{AE} and \overline{AD} can be reliably established. The position of these lines can be determined from literature data by noting that --- the line \overline{AH} in figure 1 bears the same relationship between the oil and the retorted shale as the line \overline{AG} does to the total volatiles and the retorted shale. Therefore

a plot of oil yield data (in weight percent)* versus the retorted shale (or its analog the total volatiles) should give a straight line which will be line AH. Such a plot for a wide range of organic content is given in figure 2. A least square evaluation of these data using the constraint that the 'y' intercept equals 100 weight percent leads to an equation:

$$y_s = -1.282x_o + 100 \quad (9)$$

The intercept with the x axis gives a value of 78.0 weight percent for the volatiles, a value of 22.0 weight percent for the organic residue, and a value of 60.8 weight percent for the oil as a percent of the total organic.

Mathematically the relationships developed in figures 1 and 2 give some interesting correlations where 'M' is the slope of the line AE and x_o is the oil yield in weight percent, as follows:

$$1. \text{ Total organic content: } x_t \cong M^2 x_o \cong 1.644x_o \quad (10)$$

$$2. \text{ Organic Residue: } x_r \cong (M^2 - M)x_o \cong 0.361x_o \quad (11)$$

$$3. \text{ Gas and water: } (x_g + x_w) \cong -(1+M)x_o \cong 0.282x_o \quad (12)$$

$$4. \text{ Product Distribution: a. Oil: } \frac{x_o}{x_t} = 1/M^2 \cong 0.608; \text{ b. Residue: } \frac{x_r}{x_t} \cong (1 - \frac{1}{M}) \cong 0.220;$$

$$\text{c. Gas, Water, and Loss: } \left\{ \frac{x_g + x_w}{x_t} \right\} \cong \left(\frac{1+M}{M^2} \right) \cong 0.172 \quad (13)$$

It is also possible to independently check the assumption that the product ratios to total organic are constant from literature references. Table 1 summarizes these data.

Table 1. Distribution of Organic Matter

Data Source	Shale Assay (g/t)	Product to Organic Ratios			
		Oil	Gas + Water	Volatiles	Residue
Smith ⁽⁵⁾	25.2 ^a	0.543	0.243	0.785	0.215
Goodfellow ⁽⁴⁾	33.2 ^b	0.569	0.212	0.781	0.220
Stanfield ⁽²⁾	18-52 ^c	0.614	0.159	0.773	0.228
Stanfield ⁽²⁾	27.7 ^d	0.607	0.161	0.768	0.233
Hubbard ⁽³⁾	78 ^e	0.67	msg	msg	msg
(Figure 2)	f	0.61	0.17	0.78	0.22

a. Data from 8 replicate samples; b. Data from 42 replicate samples; c. Averaged data from 9 samples; d. Compositied sample of above 9 samples; e. Data for kerogen enriched shales (see Table 2 RI4872); f. Data cover multiple samples ranging from 5 to 93 gal/ton.

As can be seen from Table 1, the ratios for total organic to volatiles and the organic residue are essentially constant with values of about 0.78 and 0.22 respectively -- as had been predicted from the data used in obtaining figure 2. The data of Hubbard covers assay data obtained for kerogen enriched shales and covers a wide range of

*Oil yields are commonly reported as (gal/ton). In the absence of density data, they can be converted to an approximate weight percent using the equation (gal/ton) $\cong 2.61$ (weight percent).

concentration. Although it is not possible to make a material balance from these data they do show that the ratios of oil to kerogen (also for water to kerogen) are constant over a wide concentration range.

DEVIATIONS FROM THE IDEALIZED CASE

In the preceding section it was shown that a plot of assay oil yield from the Green River oil shales as a function of the retorted shale yield statistically defined a line represented by equation 9. Interestingly, figure 3 shows that much of the more recent MFA data do not fit the relationship -- an observation which is particularly true of some of the better statistical data, i.e., that of Goodfellow⁴, Smith⁵, and Hubbard⁶, as well as that from commercial laboratories. (As noted in Table 1 - Goodfellow's analysis involved 42 replicate determinations.)

It is apparent from figure 3 that the deviation from ideal shows a consistently low retorted shale yield (or high volatile content). Therefore, it could be easily argued that the problem is associated with the decomposition of the inorganic portion of the shale and that the assumption of a 'y' axis intercept of 100 wt percent is not valid. Further, decomposition of the inorganic portion is not entirely unexpected since it is known that a small amount of carbonate decomposition takes place during the MFA procedure, e.g., Smith⁵ reports 0.6 weight percent for a typical 25 gal/ton oil shale. However, carbonate decomposition will not account for the magnitude of observed deviation, particularly for low assay oil shales.

The latter is shown by examination of the large quantity of assay data from the cores obtained in drilling exploratory core holes which can be readily obtained by request from the Laramie Energy Research Center of ERDA. MFA data from core holes has the advantage of covering the assay of barren or lean shale in addition to the very rich shales -- something that is not normally done in routine investigation of oil shales.

Figures 4, 5, and 6 show characteristic CD plots for selected intervals of typical cores taken from the oil shales in the Green River Formation for Colorado, Utah, and Wyoming, respectively. As might be anticipated these data show that the retorted shale recovery from samples with zero or negligible oil yield are typically only 98-99 weight percent. The interesting observation is that the dominate volatile loss is associated with water -- not gas as would be the case with carbonate decomposition.

This latter observation suggests that sample preparation, particularly drying, needs to be reevaluated in making the MFA, (or at least determining and reporting the 'as received' or total moisture content of the sample). In discussing the drying procedures used by various individuals one finds considerable variation between laboratories and more importantly from the procedure initially set up by Stanfield and Frost⁽¹⁾. Whereas the latter carefully dried their samples and often reported MFA data on a 'moisture corrected' basis -- one now finds that assays are almost universally being done on an 'air dried' or as received basis.

Failure to correct for moisture not only leads to small inaccuracies in the MFA data as is shown in table 2. It also has a considerable effect on the data points of a CD plot, as shown in figure 3, where the data is also plotted on a moisture-free basis and more nearly fits the derived relationship.

Table 2. Effect of Using Moisture-free Basis
On Modified Fischer Assay Data

Assay Item (wt %)	Data Source					
	Goodfellow ⁽⁴⁾		Smith ⁽⁵⁾		Hubbard ⁽⁷⁾	
	A	B	A	B	A	B
Retorted Shale	82.40	83.36	86.28	87.45	86.12	87.23
Oil	12.60	12.75	9.51	9.63	10.06	10.19
Gas (+ loss)	3.85	3.89	2.87	2.91	2.55	2.58
Water	1.15	-	1.38	-	1.27	-
Total	100	100	100	100	100	100
Change in Oil Assay (gal/ton) [†]		+0.4		+0.3		+0.3

A As reported

B Moisture-free

† Calculated using 2.61 times difference in oil present.

Caution must be used in arbitrarily applying a moisture-free basis to MFA data since 'water of pyrolysis' is derived from the pyrolytic decomposition of the organic matter. The quantity of 'pyrolysis water' (x_w) will be proportional to the total organic content; (the author uses the relationship $(x_w) \approx 0.077 (x_o)$ to estimate its value) whereas, the moisture in the shale decreases with increasing organic content (i.e., refer to figures 4, 5, 6). Therefore, it is not uncommon for assay data to show little or no change in MFA water yield as a function of oil yield.

It is therefore suggested that those involved in evaluating or standardizing the MFA procedure take note of this problem. Certainly the relationship between drying technique and water yield needs to be evaluated -- and perhaps a much more detailed study should be made determining the relationship between water yield and retorting temperatures.

INTERPRETATION OF TGA DATA

Figure 7 shows a typical TGA trace for the pyrolysis of a sample of Colorado oil shale in a CO₂ atmosphere. TGA does not give oil yield, and unless the volatiles are recovered and analyzed it is difficult to get such data directly. On the other hand, the data does readily lend itself to analyses on a CD plot since the volatile content is determined rather precisely by TGA. Therefore, if the position of the oil yield line (AE in figure 1) is known for the particular shale in question the oil yield can be estimated from the 'x' intercept of that line.

In the event the relationship of the oil yield to the total volatiles is not known for the TGA sample a second data point can be obtained by oxidizing the residual organic matter (Figure 8) at the pyrolysis temperature (to minimize carbonate decomposition). The total volatile data can then be used to establish a point on the oil versus inorganic boundary line (AD in figure 1) and the yield estimated again from the 'x' intercept of that line. These data are shown plotted on a compositional diagram as figure 9. The Fischer assay oil yield predicted from the data from figure 7 would be 34.5 gal/ton. That, based on data from figure 8, is 33.4 gal/ton (assuming G/T \approx 2.61 wt %). Fischer assay of four samples of this material averaged 33.38 gal/ton.

CORRELATIONS WITH TOTAL ORGANIC MATTER

Figure 10 shows data for the total organic matter as a function of the oil yield as reported in the literature (3,4,5,8,9) together with the correlation curve derived

to fit these data by the investigators of the USBM³. Obviously these latter data do not fit the relationship suggested by equation 10, nor do they seem to fit the more precise determinations of Smith⁵ and Goodfellow⁴. For this reason care should be used in using the older literature data for total organic content and its correlation particularly as they might apply to making energy balance calculations.

SUMMARY

A compositional diagram has been developed which provides a visual means of evaluating oil shale assay data for the Green River oil shales. Of particular value is the ability to estimate the total organic and organic residue in the pyrolyzed shale from Modified Fischer Assay data. For approximate purposes these relationships are as follows:

1. Total Organic = $1.644 \times (\text{MFA oil yield})$
2. Organic Residue = $0.361 \times (\text{MFA oil yield})$
3. (Gas + Water + Losses) = $0.282 \times (\text{MFA oil yield})$
4. Water (from pyrolysis) = $0.077 \times (\text{MFA oil yield})$

The compositional diagram can also be used to evaluate TGA (Thermogravimetric Analysis) data for oil shales in order to estimate the oil yield. It is also recommended as a tool for evaluating experimental retorting data, particularly for bench scale and pilot plant retorts where material balance data on the feed and retorted shales can be accurately ascertained.

LITERATURE CITED

1. Stanfield, K. E. & Frost, I. C. 'Method of Assaying Oil Shale by a Modified Fischer Retort,' RI4477 USBM (1949).
2. Stanfield, K. E., et al, 'Properties of Colorado Oil Shale' RI4825 USBM (1951).
3. Hubbard, A. B., et al, 'Method of Concentrating Kerogen in Colorado Oil Shale,' RI4872 USBM (1952).
4. Goodfellow, L., et al, 'Modified Fischer Assay-Equipment, Procedures, and Product Balance Determinations,' Proceedings - Petroleum Chemistry Division, American Chemical Society Meeting - San Francisco April 2-8, (1968).
5. Smith, J. W. 'Analytical Method for Study of Thermal Degradation of Oil Shale,' RI5932 USBM (1962).
6. Hubbard, A. B., 'Automated Modified Fischer Retorts for Assaying Oil Shale and Bituminous Materials,' RI6676 USBM (1965).
7. Hubbard, A. B., 'Oil Shale Assay Method for Product Balance Studies,' Fuel, Vol. 41, (1962) pp 49-54.
8. Private communications.
9. ----- 'Synthetic Liquid Fuels - Oil from Shale,' Annual Report for 1948. RI4457 USBM (1949).
10. Hendricksen, T. A. 'Synthetic Fuels Data Handbook,' Cameron Engineers, Inc., (1975) p. 48.

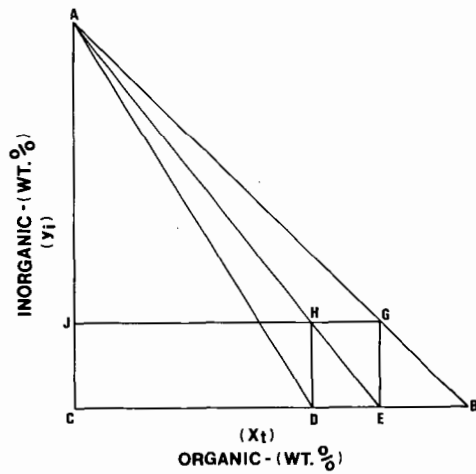


Figure 1. Development of the Compositional Diagram

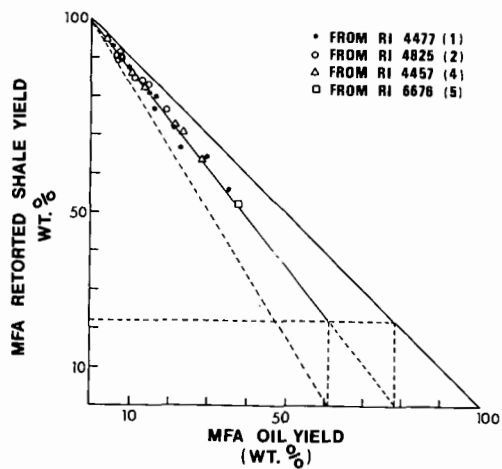


Figure 2. Relationship between Oil Yield and Retorted Shale Yield

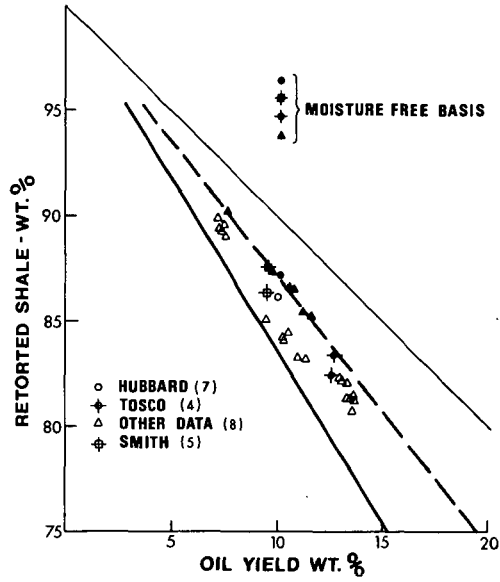


Figure 3. Compositional Diagram Showing Deviation From Ideal Case

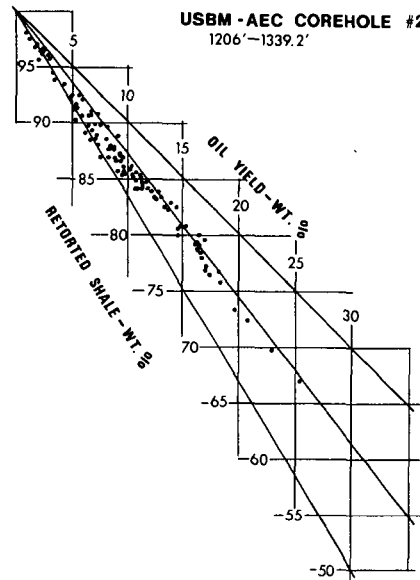


Figure 4. CD Plot for USBM-AEC Corehole #2

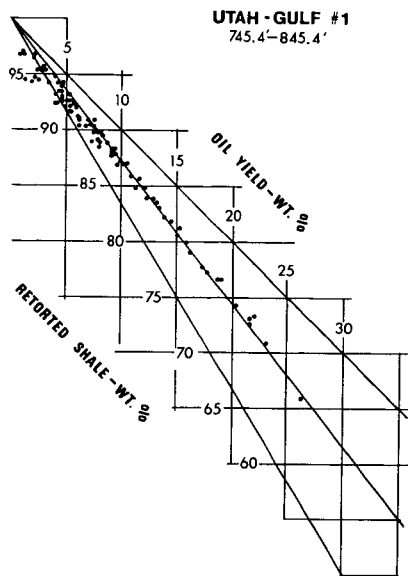


Figure 5. CD Plot of Utah-Gulf Evacuation #1

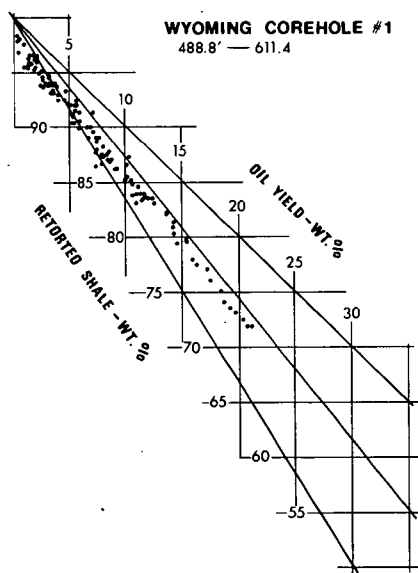


Figure 6. CD Plot of Wyoming Corehole #1

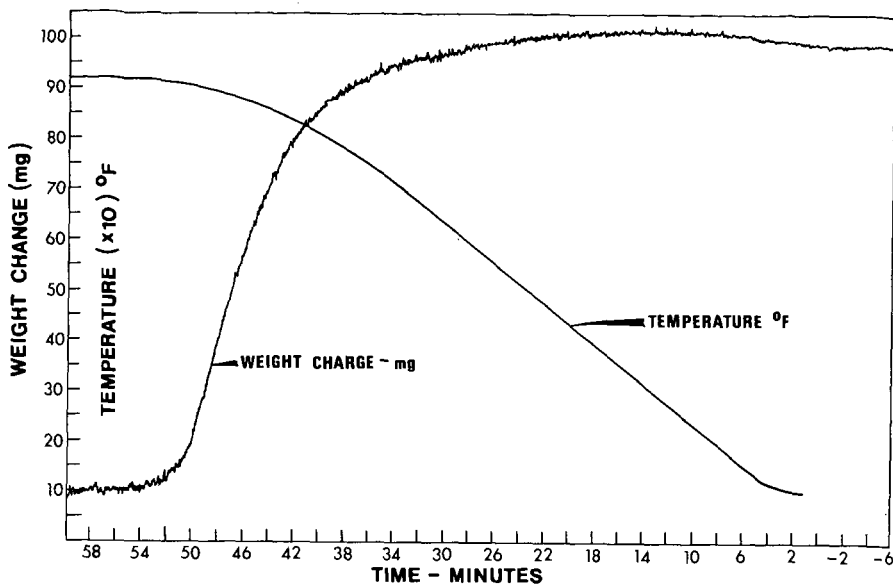


Figure 7. Typical TGA Trace for Colorado Oil Shale

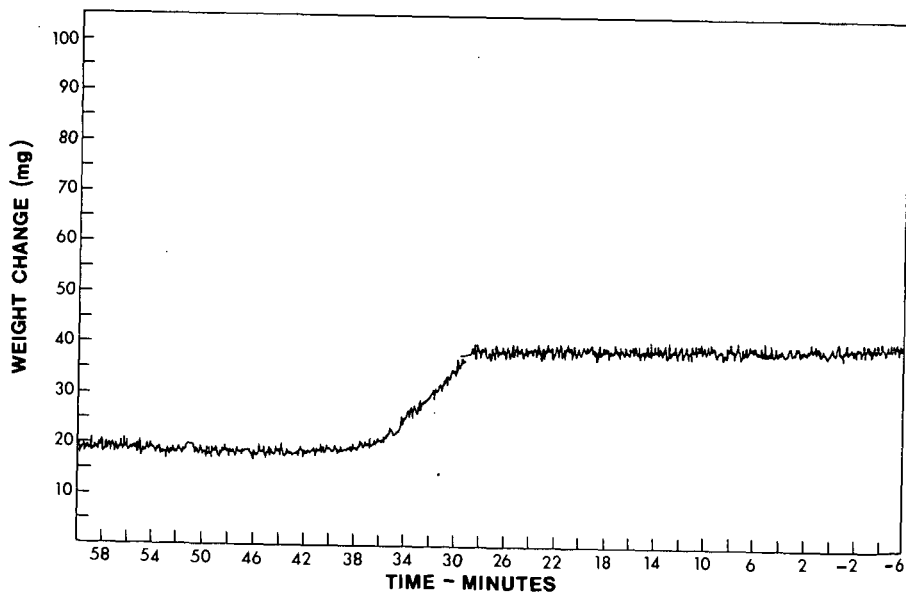


Figure 8. TGA Trace for Oxidation of Residual Organic Matter at 920°F in Air

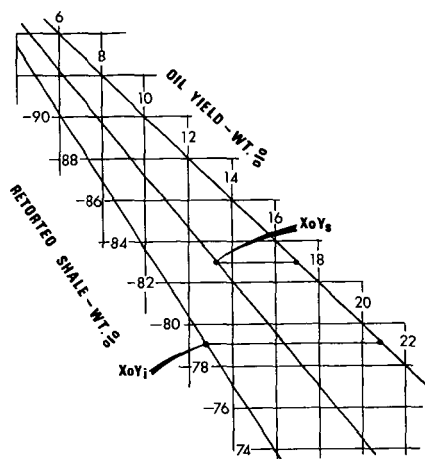


Figure 9. Typical CD Plot for TGA Data of Colorado Oil Shale

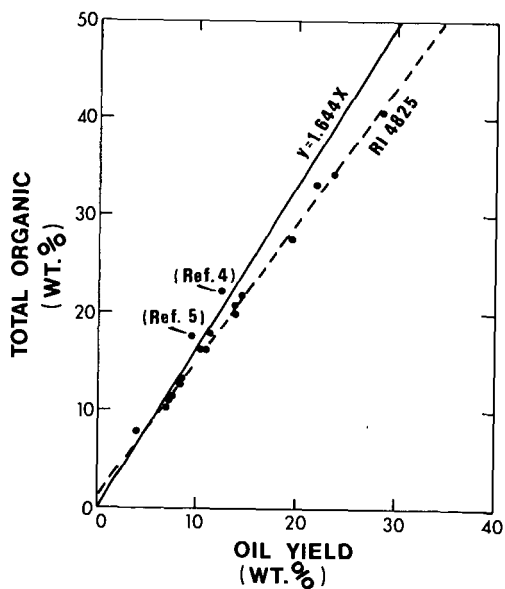


Figure 10. Relationships between Oil Yield and Total Organic Matter

SIMULATED GROUND WATER LEACHING OF IN SITU RETORTED OR BURNED OIL SHALE

H. W. Parker, R. M. Bethea, N. Güven, M. N. Gazdar, and J. K. Owusu

Department of Chemical Engineering and Department of Geosciences
Texas Tech University, Lubbock, Texas 79409

INTRODUCTION

Many social, political, ecological and economic factors combine to make predictions regarding the date of significant commercial shale oil production very uncertain. Although the actual date for commercial shale oil utilization is unknown, scientists and engineers have a responsibility to develop factual information regarding oil shale utilization in order that technical information will not be the delaying factor in utilization of oil shale when required by our nation. This paper is one addition to the technical data base needed for sound utilization of oil shale.

After oil shale has been retorted in situ, the long term hazard to the surface environment will be the possibility of ground water movement through the oil shale to leach various soluble salts from the spent shale. The possible environmental hazard divides itself into two major aspects. One aspect regards the geological details of the particular in situ retorting site, in particular the amounts and quality of ground water which might flow into the previously retorted zone and subsequently have an opportunity to reach the surface. These site dependent factors can be evaluated best by hydrologists, if they have available information regarding interactions between previously retorted oil shale and the invading ground water.

The present research is aimed at a systematic development of information describing the leaching of soluble salts from retorted oil shale by ground water. The total study includes determining the amounts of material made available for leaching by the retorting process, and also the rates at which leaching may occur. The present paper primarily considers the amounts of material made available for leaching as a result of retorting oil shale under varied conditions. Work now in progress is evaluating the rates at which leaching may occur.

EXPERIMENTAL PROCEDURES

One sample of oil shale was employed in this investigation so that the total data set regarding quantities of materials to be leached from the oil shale, and leaching rate studies to be conducted in future work will be on a consistent basis. The slab of oil shale was first drilled to remove cores for future leaching rate studies, and the remainder of the slab was crushed for use in the tests reported here. The slab was from the Rifle, Colorado, mine, but it was not identified further. Data regarding the shale sample are given in Table I.

The shale was retorted in a randomized experiment with factorial treatment combinations. The factors were temperature (4 levels: 430, 483, 630, and 780°C) and retorting time (2 levels: 15 and 30 hours). Two replications were made. These retorting temperatures represent a range of temperatures from a low temperature at which kerogen begins to decompose at a reasonable rate to high temperatures at which carbonates decompose and other reactions in the mineral matter may occur. Actual in situ retorting may employ very long retorting times; however, experimental

expediency necessitated rather short retorting times in this initial set of experiments.

Two extremes of gaseous environment were employed. One sequence of tests as described above was conducted with a slow purge of air through the oil shale to burn carbon from the spent shale and provide an oxidizing environment. In addition, the air flow purged carbon dioxide from the oil shale as carbonates decomposed to facilitate further carbonate decomposition. This test partially simulated the portions of oil shale which might have been burned by air to energize the in situ retorting process. In a second series of tests, no gas purge was used during retorting of the shale which resulted in residual carbon on the spent shale, and reducing atmosphere about the spent shale during retorting. These two series of tests are distinguished as Air-Yes and Air-No in the tabular data.

Retorting of the shale was accomplished in a vertical stainless steel tube 43 cm long and 1.4 cm ID. The central portion of this tube contained 50 g of oil shale. A 1/16 inch swaged magnesia Type K thermocouple was centered inside the tube. A horizontal screen attached to the thermocouple supported the shale in the central portion of the retorting apparatus. For one series of experiments, air was purged into the top of the apparatus at a rate of 0.25 l/hr. Gases and oil were produced from the bottom of the tube into a container with a water leg seal so air could never contact the shale in those tests conducted in the absence of air. A close-fitting electric furnace was placed around the tube. Power input to the furnace was adjusted by a PID type controller actuated by the internal thermocouple. Approximately 0.5 hours was required to heat the apparatus to the desired operating temperature.

After retorting, the shale was allowed to cool to room temperature, then transferred to a 250 ml polyethylene bottle and 200 ml of demineralized and deionized water added. The retorted shale and water were mixed together for 15 hours by revolving the bottle at 160 RPM while tilted at a 45 degree angle. The samples were allowed to settle for 5 hours and the clear water decanted from the shale. Prior to analysis by atomic absorption spectroscopy the samples were filtered through Whatman No. 42 filter paper, and measurements made of the pH and conductivity. These results are reported in Table III.

The 15 hour time used for extraction of the oil shale with water was thought to be generous for extraction of the oil shale fragments which were less than 2 mm in diameter. To confirm this assumption, oil shale was retorted in the absence of air for 15 hours at 483°C and extracted by the previously stated procedure except the pH and conductivity were measured as a function of time. These results are shown in Figure 1. Most of the solids were extracted prior to the first observation after one hour of leaching. Additional solids were extracted during the 24 hour period of the test. The rapid extraction of solids followed by a slow increase in dissolved solids indicated the complexity of the total problem which is being addressed in the leaching rate studies now in progress. The additional variable of extraction time was not considered further in this paper.

The raw shale was analyzed for several elements by colormetric procedures in those cases when atomic adsorption was not effective. These data are given in Table I. V, Be, Sn, and Sb were determined by the methods described in Reference 1. As, B, and Se were determined by methods described in References 2, 3, and 4, respectively. Prior to analysis the shale was digested in HF.

EXPERIMENTAL RESULTS

Data for the 32 retorting and extraction experiments are reported in Table III.

These results were analyzed by standard analysis of variance procedures, AOV. A significance level of $\alpha = 0.05$ was selected for interpretation of the AOV results. Significant variations in the results are indicated in the left column in regard to retorting time, T_m , retorting temperature, T_p , and the time temperature interaction, TT .

For the two retorting times examined, 15 and 30 hours, little effect of retorting time was shown on the amounts of each element leached from the oil shale. The total amount of dissolved solids was not influenced by retorted time as determined by the AOV analysis. The results in Table III indicate that the amounts of several elements dissolved were dependent on retorting time by the AOV technique, K, Mg, Sr, Zn, and Cd when retorted in the presence of air. Standard analysis of covariance procedures, ANCOVA were applied to the experiments conducted in the presence of air. When leachate pH was used as the covariant, the apparent dependency on retorting time regarding the amounts of Mg dissolved was eliminated. This set of data indicated that the only significant influence on the amount of magnesium dissolved was pH of the extract. The ANCOVA examination of the data also indicated that pH of the leachate influenced the amounts of Fe and Al extracted, and perhaps the amounts of Zn, as might be expected. The ANCOVA tests indicated that only the amount of K leached was clearly dependent on retorting time.

Retorting temperature was the major variable influencing the amounts of material extracted. The difference in the amounts extracted after retorting at the two highest temperatures was not great. In some cases, retorting at the highest temperature, 780°C for the longest period of time, 30 hours, resulted in less of a particular element being leached from the oil shale, for example Sr and Zn.

The relative amounts of material leached in the absence or presence of air were not examined by statistical methods, but it appears obvious that less material was leached after retorting in the absence of air at the two lower retorting temperatures employed. This effect is not just a function of pH as shown in Figure 2, since the samples retorted in the presence of air had a lower pH, but a larger amount of solids were dissolved. The X-ray diffraction studies shown in Table II show no major alteration of the crystalline material due to retorting at the lower temperatures either in the presence or absence of air. The X-ray diffraction data shown in Table II show the production of a new mineral phase, hydrotalcite, $Mg_6Al_2CO_3(OH)_{16} \cdot 4H_2O$, at the most severe retorting conditions.

DISCUSSION OF RESULTS

These results show the influence of selected retorting conditions on the amounts of material leached from oil shale by pure water. Much of the ground water associated with oil shale deposits already contains large amounts of dissolved salts, up to 40,000 ppm (5), contrasted to the maximum of 1800 ppm observed in these tests. The interactions of these real ground waters with oil shale will be considerably different than observed in these tests with pure water; however, the tests with pure water provide more reproducible and readily interpretable results. Tests are now in progress using ground water.

ACKNOWLEDGMENT

Work reported in the paper is a portion of a research grant from ERDA through its laboratory in Laramie, Wyoming, to the Chemical Engineering Department of Texas

Tech University to investigate ground water leaching of in situ retorted oil shale. The enthusiastic support of the Contracting Officers, Harry C. Carpenter and Richard E. Poulson is appreciated by the authors.

REFERENCES

1. Owusu, J. K. and R. M. Bethea, "Screening Techniques for Hazardous Metallic Compounds in Particulate Stack Effluents", Paper 75-33.1, 68th Annual Air Pollution Control Association Meeting, Boston (1975).
2. Gomez, C. A. and M. T. Lopez, "Determination of Arsenic in Copper and Iron Alloys", *Revista de Metalurgica* (Madrid) 9(5): 382-384 (1973).
3. Hayes, M. R. and J. Metcalfe, "The Boron-Curcumin Complex in the Determination of Trace Amounts of Boron", *Analyst* 87: 926-929 (1962).
4. West, P. W. and T. V. Ramakrishna, "A Catalytic Method for Determining Traces of Selenium", *Chem.* 40: 966-968 (1968).
5. Jackson, L. P., R. E. Poulson, T. J. Spedding, T. E. Phillips and H. B. Jensen, "Characteristics and Possible Roles of Various Waters Significant to In Situ Shale Processing", Symposium on the Environmental Aspects of Oil-Shale Development, Colorado School of Mines, Golden, Colorado, October 9-10, (1975).

TABLE I

Properties of the Oil Shale Investigated

Fischer Assay Yield (gal/ton)

19.1

Principal mineral species present

(Please see Table II)

Analysis for Selected Metals

Metal	Method	Amount Present PPM in Shale	Detection Limit in Shale PPM
Be	Colorimetric	Trace	0.2
V	Colorimetric	Absent	0.5
Cr	AAS	Absent	0.005
Fe	AAS	3.68	0.1
Ni	AAS	Trace	0.01
Cu	AAS	0.16	0.003
Ag	AAS	Absent	0.005
Cd	AAS	Trace	0.003
Hg	AAS	Absent	1.00
B	Colorimetric		2.00
Pb	AAS	0.49	0.04
As	Colorimetric	Absent	8.00
Sb	Colorimetric	Absent	0.05
Se	Colorimetric	Absent	0.04

Screen Analysis of Crushed Oil Shale

Screen Mesh (US Std.)	Wt% Retained	Screen Mesh (US Std.)	Wt% Retained
+16	32.0	60	10.8
24	13.9	115	10.8
32	14.1	250	4.0
42	12.2	Pan	2.5

TABLE II. Mineralogical Phases in Raw and Retorted Oil Shale by X-ray Diffraction

Retorting Conditions			Minerals and their relative percentages						
Air	time (hrs)	temperature (°C)	Quartz	Dolomite	Calcite	Analcite	Hydrotalcite	Illite	Feldspars
(Raw Shale)			25	30	10	15	-	10	10
Yes	15	430	30	30	+	20	-	10	10
Yes	30	430	25	30	+	20	-	10	10
Yes	15	483	30	30	+	20	-	10	10
Yes	30	483	30	35	+	15	-	10	10
Yes	15	630	25	10	20	20	10	+	10
Yes	30	630	20	10	20	10	10	10	5
Yes	15	780	30	15	10	5	10	-	30
Yes	30	780	40	10	10	10	5	-	25
No	15	430	20	30	5	20	-	10	10
No	30	430	20	30	5	20	-	10	10
No	15	483	20	30	5	20	-	10	10
No	30	483	20	30	5	20	-	10	10
No	15	630	25	15	25	15	5	5	10
No	30	630	25	25	20	20	+	+	10
No	15	780	35	10	20	10	5	+	20
No	30	780	35	10	10	10	10	+	25

+ indicates trace quantity; - indicates not detectable

TABLE III Equilibrium Extraction Study-Miscellaneous Data

Retort Temp °C		430		483		483		630		630		780		780	
Retort Time hours		15		30		15		30		15		30		15	
Air Replicate		A ₁		A ₂		B ₁		B ₂		C ₁		C ₂		D ₁	
%weight loss after retorting	NO	I	7.21	10.3	11.3	11.3	11.3	11.3	11.3	19.2	18.7	18.7	27.4	27.4	27.0
		II	7.74	10.1	11.5	11.5	11.6	11.6	11.6	19.0	18.9	18.9	27.1	27.1	26.9
		Av	7.48	10.2	11.4	11.4	11.4	11.4	11.4	19.1	18.8	18.8	27.2	27.2	26.9
YES		I	12.1	11.4	13.6	13.6	15.2	15.2	15.2	21.6	24.5	24.5	28.6	28.6	29.0
		II	12.4	11.6	13.8	13.8	14.3	14.3	14.3	22.0	24.6	24.6	28.4	28.4	29.2
		Av	12.2	11.5	13.7	13.7	14.7	14.7	14.7	21.8	24.5	24.5	28.5	28.5	29.1
pH when analyzed (Tp)*	NO	I	9.02	10.28	10.34	10.34	9.39	9.39	11.84	11.91	11.82	11.82	11.82	11.82	11.51
		II	8.74	9.17	10.76	10.76	10.67	10.67	12.20	12.11	12.21	12.21	12.21	12.21	11.75
		Av	8.88	9.73	10.55	10.55	10.03	10.03	12.02	12.01	12.02	12.02	12.02	12.02	11.63
(Tp)*	YES	I	7.48	7.83	11.72	11.72	11.96	11.96	12.17	12.72	12.72	12.72	12.16	12.16	11.98
		II	8.04	8.93	11.53	11.53	12.07	12.07	12.49	12.70	12.70	12.70	12.27	12.27	12.00
		Av	7.76	8.38	11.63	11.63	12.02	12.02	12.33	12.71	12.71	12.71	12.22	12.22	11.99
Total Dissolved Solids via Conductivity in Extract (Tp)*	NO	I	305	195	185	185	150	150	1410	1645	1645	1645	1575	1575	945
		II	195	160	245	245	235	235	2140	2250	2250	2250	>2500	>2500	1275
		Av	250	178	215	215	193	193	1775	1948	1948	1948			1110
(Tp, TT)*	YES	I	860	810	1125	1125	1410	1410	1215	1750	1750	1750	1615	1615	1395
		II	915	905	1000	1000	1060	1060	1270	1700	1700	1700	1760	1760	1520
		Av	888	898	1063	1063	1235	1235	1243	1725	1725	1725	1688	1688	1458

*See note at end of Table III.

TABLE III (cont.) Equilibrium Extraction Study--Group I-A Elements
(ppm extracted from oil shale after retorting)

Retort Temp °C		430	430	483	483	630	630	780	780
Retort Time hours		15	30	15	30	15	30	15	30
Element	Air Replicate	A ₁	A ₂	B ₁	B ₂	C ₁	C ₂	D ₁	D ₂
Mg	NO	I	16.80	0.88	1.25	1.09	0.37	0.32	0.37
	II	0.80	11.40	0.61	13.38	0.40	0.38	0.43	0.40
	Av	8.80	6.14	0.93	7.23	0.38	0.35	0.40	0.34
Mg (Tp, Tm, TT)*	YES	I	94.1	36.4	0.16	0.12	0.08	0.014	0.08
	II	66.0	22.0	0.16	0.14	0.08	0.016	0.08	0.08
	Av	80.0	29.2	0.16	0.13	0.08	0.015	0.08	0.08
Ca *Tp)*	NO	I	105	92	80	596	869	659	370
	II	168	25	105	59	995	693	1113	504
	Av	137	59	92	61	796	781	886	437
Ca	YES	I	924	1008	1680	1722	1814	2100	764
	II	1008	939	1327	1424	1147	2058	706	596
	Av	966	974	1504	1573	1481	2079	752	680
Sr (Tp)*	NO	I	0.088	0.056	0.104	0.064	19.6	9.0	4.40
	II	0.040	0.024	0.088	0.056	30.2	25.0	28.4	7.60
	Av	0.064	0.040	0.096	0.060	27.6	22.3	18.71	6.00
Sr (Tp, Tm, TT)*	YES	I	14.0	14.2	19.8	24.2	34.4	23.6	14.2
	II	14.1	15.8	19.6	24.0	60.0	90.0	24.0	15.8
	Av	14.0	15.0	19.7	24.1	47.2	87.0	23.8	15.0

* See note at end of Table III

TABLE III (cont.) Equilibrium Extraction Study--Group II-B Elements
(ppm extracted from oil shale after retorting)

Retort Temp °C		430		483		483		630		630		780		780	
Retort Time hours		15		30		15		30		15		30		15	
Element	Air Replicate	A ₁		A ₂		B ₁		B ₂		C ₁		C ₂		D ₁	
Zn	NO	I	0.220	0.022	0.005	0.032	0.160	0.096	0.040						
		II	0.005	0.008	0.008	0.008	0.149	0.400	0.080						
		Av	0.112	0.015	0.006	0.020	0.154	0.248	0.060						
Zn (Tp, Tm, TT)I	YES	I	0.190	0.160	0.110	0.120	0.220	0.170	0.080						
		II	0.200	0.160	0.100	0.120	0.208	0.160	0.080						
		Av	0.195	0.160	0.105	0.120	0.214	0.165	0.080						
Cd	NO	I	X	X	X	X	X	X	X						
		II	X	X	X	X	X	X	X						
Cd (Tm)*	YES	I	X	X	X	X	T	X	X						
		II	X	X	X	T	T	X	X						
Hg	NO	I	X	X	X	X	T	X	X						
		II	X	X	X	X	T	T	T						
YES	I	X	X	X	X	X	X	X	X						
	II	X	X	X	X	X	T	T	T						

*

See note at end of Table III.

TABLE III (cont.) Equilibrium Retorting Study--Transition Elements
(ppm extracted from oil shale after retorting)

Retort Temp °C		430	430	483	483	483	630	630	780	780
Retort Time hours		15	30	15	15	30	15	30	15	30
Element	Air Replicate	A ₁	A ₂	B ₁	B ₂	C ₁	C ₂	D ₁	D ₂	D ₂
Cr	NO	I II	X X	X X	X X	X X	X X	X X	X 0.04	X 0.02
Cr	YES	I II Av	0.400 0.600 0.500	0.360 0.040 0.200	1.20 1.20 1.20	0.80 1.80 1.30	2.40 0.04 1.22	T X	7.20 4.00 5.60	19.2 16.0 17.6
Fe	NO	I II Av	0.004 0.003 0.004	0.005 0.004 0.004	0.004 0.004 0.004	0.005 0.005 0.005	0.006 0.005 0.005	0.006 0.005 0.006	0.008 0.005 0.006	0.006 0.005 0.005
Fe (Tp)*	YES	I II Av	0.400 0.400 0.400	0.360 0.480 0.420	0.080 0.200 0.140	0.032 0.040 0.030	0.036 0.040 0.038	0.200 0.080 0.140	0.036 0.040 0.038	0.032 0.036 0.034
Mo	NO	I II	T T	T T	T T	T T	T T	T T	T T	T T
Mo	YES	I II	0.120 T	0.100 T	0.140 T	0.120 T	0.120 T	0.120 T	0.120 T	T T

*See note at end of Table III.

TABLE III (cont.) Equilibrium Retorting Study--Group III-A and IV-A
(ppm extracted from oil shale after retorting)

Retort Temp °C		430	430	483	483	630	630	780	780
Retort Time hours		15	30	15	30	15	30	15	30
Element	Air Replicate	A ₁	A ₂	B ₁	B ₂	C ₁	C ₂	D ₁	D ₂
Al	N0	I 4.40	4.00	10.0	14.0	18.0	18.4	28.0	32.0
	II	3.60	3.60	8.8	14.0	14.0	18.0	3.8	24.0
	Av	4.00	3.80	9.4	14.0	16.0	18.2	15.9	28.0
Al (Tp)*	YES	I 15.0	1.10	X	X	X	X	X	X
	II	12.0	0.80	X	X	X	X	X	X
	Av	13.5	0.95						
Pb	N0	I X	X	X	X	0.152	0.192	X	X
	II	X	X	X	T	0.120	0.144	X	X
	Av					0.136	0.168		
Pb	YES	I X	X	X	X	X	X	X	X
	II	X	X	X	X	X	X	X	X

* The symbols enclosed in parentheses indicate that the factor made a significant contribution to observed result at the 95% confidence level over the range of variables investigated by standard AOV techniques.
Tm=Time, Tp=temperature, TI=time-temperature interaction

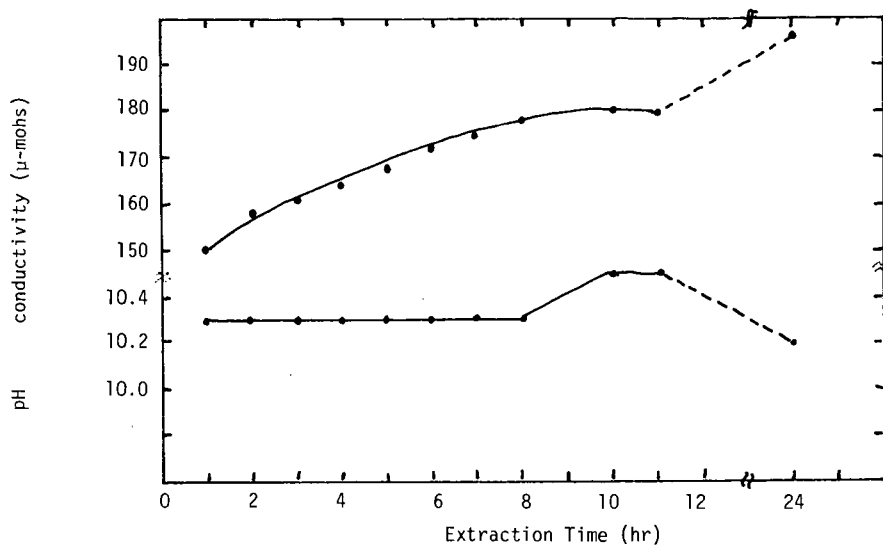


Figure 1. Conductivity and pH of Leachate As A Function Of Extraction Time

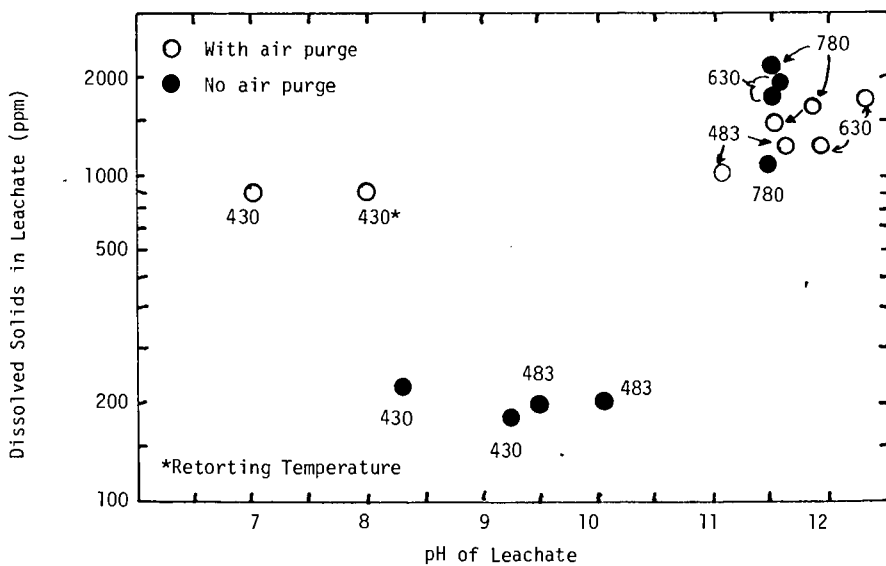


Figure 2. Dissolved Solids Concentration Versus Leachate pH

THERMAL AND ELECTRICAL CONDUCTIVITIES OF GREEN RIVER OIL SHALES*

J. DuBow, R. Nottenburg, and G. Collins

Department of Electrical Engineering
Colorado State University
Fort Collins, Colorado 80523

INTRODUCTION

Oil-shale retorting is a thermal process, yet the thermal conductivity of oil shale is incompletely known.⁽¹⁾ A detailed knowledge of the thermal conductivity is necessary before the temperature distributions in oil-shale rocks, in oil-shale beds, and in the rock surrounding in situ oil-shale retorts may be accurately determined. The limited experimental data and limited theoretical understanding of the thermal conductivity of oil shale to date hinders control of in situ retorting processes and limits the accuracy of mathematical simulations of oil-shale retorting.

Previous studies^(2,3) of the thermal conductivity of oil shale recognized that thermal conductivity could vary with temperature, kerogen content, and varve geometry. However, other aspects of the thermal conductivity were never extensively studied. For example, Prats and O'Brien⁽²⁾ report chemical analyses of oil-shale samples of nearly equal Fischer assay, but which exhibit substantially different mineral matrix compositions. It is unreasonable to expect two oil-shale samples of equal grade but different mineral composition would exhibit identical thermal and electrical conductivities during retorting. Cook⁽⁴⁾ noted that carbonate minerals, such as nahcolite and dawsonite, decomposed over the temperature range used in their experiments and are therefore the most likely minerals to affect the thermal and electrical properties of oil shale. These studies^(2,3) utilized the transient line probe technique to measure thermal conductivity. This technique relies on a diffusional heat flow model and utilizes a thermal history sample treatment which masks the effects of chemical reactions.⁽⁵⁾ However, these chemical reactions significantly effect the temperature distribution in an oil-shale retort⁽⁶⁾ and form a key to understanding the behavior of thermal conductivity.

A key to unravelling some of the complexities in the thermal conductivity of oil shale lies in simultaneous parameter measurements. In this investigation thermal conductivity and electrical conductivity were measured simultaneously as a function of organic content, temperature and under stress levels simulating field conditions. These parameters were correlated and, as such, yielded much more useful results than thermal conductivity data alone. Some deviations from the major trends of previous work were observed.

SAMPLE PREPARATION

Mine-fresh rocks were obtained from the Paraho Oil Shale Development Corporation, Rifle, Colorado. Other samples were obtained from the Laramie Energy Research Center (LERC), Laramie, Wyoming. The five samples selected were analyzed by LERC using nuclear magnetic resonance. Their oil yield and sample number are given in table 1. Test specimens, cut perpendicular to the bedding plane, were carefully selected to insure that both the organic and the mineral matter were fairly evenly distributed and that the specimens contained no visible fractures. The polished specimens measured 2 inches in diameter and 3/4 inch thick. A groove, 0.100 inch deep, as shown in Fig. 7, was cut on each face of the specimen. Thermocouples in double bore ceramic tubes were inserted in the grooves, with the junction placed in direct contact with the shale. The thermocouples were fixed in place with Saureisen Cement.

* Supported under contract from the Laramie Energy Research Center of the U.S. ERDA.

EXPERIMENTAL PROCEDURE

Measurements were taken in a modified Dynatech⁽⁷⁾ TCFCM thermal conductivity apparatus. This apparatus is shown in Fig. 1a. The thermal conductivity measurement technique used is the "Comparative Method."⁽⁸⁾ This technique does not require (1) a diffusional model of heat flow, as does the transient line probe method; (2) it does not require drilling an extra thermocouple insertion hole into the oil shale sample; and (3) it does not require thermal history techniques to be utilized. The comparative method is similar to the standard Guarded Hotplate Technique,⁽⁸⁾ but is much faster and results in only a small sacrifice in accuracy. The modified apparatus was calibrated by measuring the thermal conductivity of Pyrex 7740 a number of times. The results showed a maximum deviation of 4 percent from published NBS results.

The oil-shale sample was sandwiched between two copper discs and the unit was sandwiched between two Pyrex 7740 reference samples as shown in Fig. 1b. The initial pressure was set using a Morehouse Ring Force gauge and power-screw apparatus shown in Fig. 1a. The pressure variation was determined by the variation on a ring force gauge dial indicator. The electrical resistance was determined by measuring the relative voltage drop across the shale between the two copper discs as compared to a reference resistor. A microvoltmeter was used to determine these voltages.

Complete runs were made on each sample at four average initial pressures shown in table 2. These runs were done in an air atmosphere at an approximate average heating rate of 65° F per hour. Experiments were started at ambient temperature and continued until the oil shales lost structural integrity--that is, to the temperature where the shale underwent complete structural collapse. Each specimen was heated in 45° F to 90° F increments per hour with a stack temperature gradient of 36° F to 54° F maintained across the test stack. When thermal steady state was attained, which required about 45 minutes per increment, stack temperatures, pressure, electrical resistivity, and time were recorded. The heaters were turned off during the pressure and electrical resistivity measurements to eliminate artifacts caused by heating and stray magnetic fields.

DATA ANALYSES

Experimental data were analyzed with a HP 2100 minicomputer. Thermal conductivity was computed according to equation

$$K_s = \frac{\lambda_s}{2\Delta T_s} \left\{ K_{TR} \frac{\Delta T_{TR}}{\lambda_{TR}} + K_{BR} \frac{\Delta T_{BR}}{\lambda_{BR}} \right\} \quad (1)$$

where the subscript "s" denotes the oil shale, "TR" the top reference, and "BR" the bottom reference. K is the thermal conductivity, ΔT the temperature drop, and λ the thermocouple to thermocouple spacing.

Electrical conductivity, stack temperatures, and pressure were also stored in a computer memory. These three sets of experimental data permitted us to compute three derived parameters as shown in Fig. 6: (1) one parameter coefficient of thermal expansion was computed using Equation 2

$$\beta = \frac{1}{\lambda_0} \frac{\Delta \lambda}{\Delta T} \quad (2)$$

where λ_0 is the original sample length, $\Delta \lambda$ the change in sample length over the temperature interval ΔT ; (2) the second derived parameter is the resistance ratio as it was computed according to Equation 3

$$R = \frac{V(T+\Delta T)}{V(T)} ; \quad (3)$$

(3) the third derived parameter, energy balance, is computed according to Equation 4. This parameter equals the ratio of the heat flowing into the top of the oil shale (Q_T) to the heat flowing out of the bottom of the oil-shale sample (Q_B).

$$\frac{Q_T}{Q_B} = \frac{k_{TR} \frac{\Delta T_{TR}}{L_{TR}}}{k_{BR} \frac{\Delta T_{BR}}{L_{BR}}} \quad (4)$$

The energy balance ratio (Q_T/Q_B) should equal unity at equilibrium, but deviates significantly from unity, as shown in Fig. 6, when heat is generated or absorbed during chemical reactions or physical transformations within the sample. The presence of carbonate minerals in an air ambient atmosphere caused chemical reactions to occur which seriously effected energy balance and temperature distributions. The thermal conductivity is not usually defined under nonequilibrium conditions such as those encountered over much of the temperature range we observed. What was measured was an effective thermal conductivity. Moreover, it can be shown that Equation 1 holds in the presence of heat generation within the sample as well as under equilibrium conditions.⁽⁹⁾ The effective thermal conductivity included the effect of the carbonate and kerogen decompositions, as well as the varve boundaries, cracks, and pores.

DISCUSSION OF EXPERIMENTAL DATA

The thermal conductivity versus temperature for four grades of oil shale at four different initial pressures, is shown in Fig. 2. The effect of pressure on the thermal conductivity becomes significant only at high temperatures. The pressures exerted by the oil shales on the press bar as a function of temperature are shown in Fig. 3. Even at low temperatures, these pressures were seen to increase. The pressures continued to increase until the specimens reached the structural transition temperature, at which point the specimens failed to sustain any stress and collapsed. The rapid decrease in pressure and eventual loss of structural integrity over a narrow temperature range was first reported by Tisot.⁽¹⁰⁾

The structural transition temperature also marks a significant change in the electrical and thermal transport parameters. Fig. 4 indicates that, just prior to the onset of structural yield, there is a change in the mechanism of the electrical conductivity. A measure of the nature of the electrical conduction mechanisms is the activation energy for electronic conduction, which is the slope of the electrical conductivity versus inverse temperature ($1/KT$) curve. The activation energy for electronic conduction may be obtained from Equation 5

$$E_a = \frac{T_2 - T_1}{KT_1 T_2} \ln \frac{\sigma_2}{\sigma_1} \quad (5)$$

where σ_2 and σ_1 are the conductivities measured at temperatures T_1 and T_2 . The electrical conductivity is plotted as a function of inverse temperature in Fig. 4. Electrical conductivity exhibits considerable variance at low temperatures, but all curves tend to coincide at temperatures approaching the structural transition temperature and above (Fig. 5). A least-squares fit to the data yields an activation energy for electrical conductivity of 1.8 eV at temperatures above the structural transition temperature. After the transition temperature, conductivity activation energy is reduced by a factor of almost two. The rapid rise in electrical conductivity is accompanied by a marked increase in the thermal conductivity. However, just prior to the structural transition temperature, the thermal conductivities attained a minimum (Fig. 2). After the transition temperature, the thermal conductivities increase. These increases in thermal conductivity are accompanied by a more rapid rise in the electrical conductivity, suggesting a possible electronic origin of the increase in thermal conductivity above the structural transition temperature.

One possible mechanism for the increase in the thermal conductivity at high temperature is a fundamental change in the heat conduction mechanism at the structural transition temperature. At low temperatures the shale is nonporous and conduction is mainly through solid-solid contact. The onset of chemical reactions in the oil shale, such as the decomposition of carbonates, alters the manner in which heat flows through the oil shale. Thus, in contrast to other workers,^(2,3) the experimental data show that the thermal conductivity often remains steady or increases with increasing temperature. Near the structural transition temperature, the oil shale, which was under uniaxial compression, began to consolidate. However, the oil shale could expand radially, and radially directed cracks and fissures could form. These structural flaws fill with air and gas, which have very low thermal conductivity, and therefore reduce the thermal conductivity of the oil shale. Above the structural transition temperature, oil shale begins to undergo structural failure along with chemical decomposition. Large numbers of pores which become increasingly filled with shale oil are formed (Fig. 7). This shale oil originates in those portions of the oil shale that begin to retort. As oil shale approaches retorting temperature, the relative contributions of solid-fluid and fluid-fluid heat transfer mechanisms increase and, at relatively low porosities, can dominate the thermal transport properties.⁽¹¹⁾

The increase of electrical and thermal conductivities at high temperatures, possibly caused by oil-filled pores, is supported by previous work which demonstrated that, for porous rocks, the electrical and thermal conductivities can be related to one another through a common parameter--porosity.⁽¹²⁾ In addition, shale oil at high temperatures appears to be highly electrically conductive. During one experiment, some shale oil seeped into a heater winding and caused a short circuit which damaged the heater. The high electrical conductivity of hot shale oil could cause difficulty in measuring oil-shale behavior at high temperatures since the shale oil could short-circuit thermocouples or other electrical transducers, unless they are properly insulated. It was also observed that the gray, retorted sections of the oil-shale samples used exhibited much higher resistivity than the unretorted sections.

The raw data exhibited considerable variations at particular temperatures. These variations are accentuated, and interparameter correlations highlighted, when the resistivity ratio, thermal expansion coefficient and energy balance at the temperature measurement data points are plotted for the various grades. A typical curve is shown in Fig. 6. The energy balance should be unity in equilibrium, but it begins to deviate substantially from unity as the shale undergoes decomposition reactions. These samples were heated in air and, hence, were subject to a number of carbonate decompositions beginning at about 195 F. Significant changes in the energy balance are accompanied by resistivity changes. The structural transition temperature is marked by rapid rises in the electrical and thermal conductivities.

SUMMARY AND CONCLUSIONS

The results from this investigation show that when oil shale is heated in air:

- (1) The thermal conductivity remains relatively constant up to the structural transition temperature (0.5 ± 0.15 Btu/ft²-°F).
- (2) In a narrow temperature range around the structural transition temperature, thermal conductivity attains a minimum and then increases.
- (3) At temperatures above the structural transition temperature, all grades of shale exhibit the same activation energy for electronic conduction (1.8 eV).
- (4) The values of the electrical conductivity tend to coincide at temperatures above the structural transition temperature.
- (5) Below the structural transition temperature, the electrical conductivity is low and exhibits a spread in activation energies centered around 3.5 eV.

- (6) Simultaneous measurement of electrical conductivity, thermal conductivity, and pressure permits the computation of three derived parameters--the coefficient of thermal expansion, the energy balance ratio, and the resistance ratio.
- (7) The experimental data point to a common mechanism for the increase in thermal and electrical conductivities at temperatures above the structural transition temperature. This mechanism is the filling of pores with conductive shale oil.

The data reported here can be used to develop an improved mathematical model of oil-shale retorting. The electrical and pressure data can be used to develop sensors which predict the onset of structural failure and kerogen decomposition.

ACKNOWLEDGMENTS

The authors acknowledge the helpful criticism, friendly advice and experimental intuition provided by P. R. Tisot who did much to assist in experimental design, sample selection and data analysis. The authors thank Howard Jensen and John Duvall of the Laramie Energy Research Center, Laramie, Wyoming, for furnishing guidance during the course of the work. The authors thank Tom Meals, Philip Milling and Robert Wiff for support in various phases of this work.

BIBLIOGRAPHY

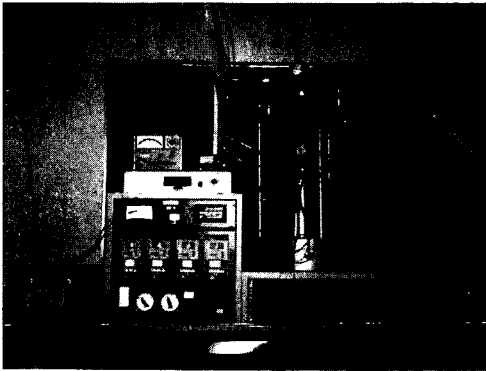
1. Cameron Engineers, "Synthetic Fuels Data Book," June 1975.
2. Prats, M. and O'Brien, S., "Thermal Conductivity and Diffusivity of Green River Oil Shale," JPT, Jan. 1975, pp. 97-106.
3. Tihen, S., Carpenter, H., and Sohns, H., "Thermal Conductivity and Thermal Diffusivity of Green River Oil Shale," NBS Special Publication, 1968.
4. Cook, E. W., "Thermal Analysis of Oil Shales," Quarterly of Colorado School of Mines, vol. 65, No. 4, Oct. 1970, p. 133.
5. Woodside, W., and Messmer, J., "Thermal Conductivity of Porous Media II Consolidated Rocks," J. Appl. Phys., 32, 9, 1961, p. 1699.
6. Fausett, D., "A Mathematical Model of an Oil Shale Retort," Quarterly of Colorado School of Mines, July 1975.
7. Reference to a brand name does not imply endorsement of the product by the investigators or the Laramie Energy Research Center of the U.S. ERDA.
8. Powell, R., "Thermal Comparator Methods," in Thermal Conductivity, vol. 2, R. Tye, ed., Academic Press, 1968.
9. DuBow, J., Nottenburg, R., and Collins, G., "Thermal and Electrical Conductivity of Green River Oil Shale," Final Report, June 1976.
10. Tisot, P. R., "Alterations in Structure and Physical Properties of Green River Oil Shale by Thermal Treatment," J. Chem. Eng. Data, v. 12, No. 3, 1967, p. 405.
11. Huang, J. N., "Effective Thermal Conductivity of Porous Rocks," J. Geophys. Res., vol. 76, No. 26, p. 6420, 1971.
12. Hust, J. and Berg, J., "Thermal and Electrical Conductivities of Sandstone Rocks and Ocean Sediments," Geophys., vol. 33, No. 3, 1968.

<u>Sample</u>	<u>Grade (gpt)</u>
AAII top	21.6
AAII bottom	25.1
AA2 top	29.6
AA2 bottom	32.2
AA8 top	47.9

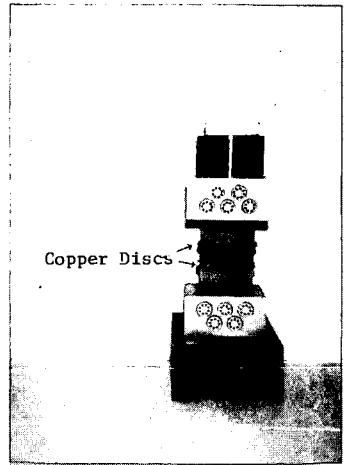
Table 1 Notation For Oil Shale Grades Reported in Subsequent Figures

<u>Condition</u>	<u>Uniaxial Pressure Applied to Sample (psi)</u>
1	120
2	310
3	460
4	600

Table 2 Notation used in Figures To Designate the Four Conditions of Pressure applied to the Sample



a



b

Fig. 1: a) Apparatus b) Test Stack

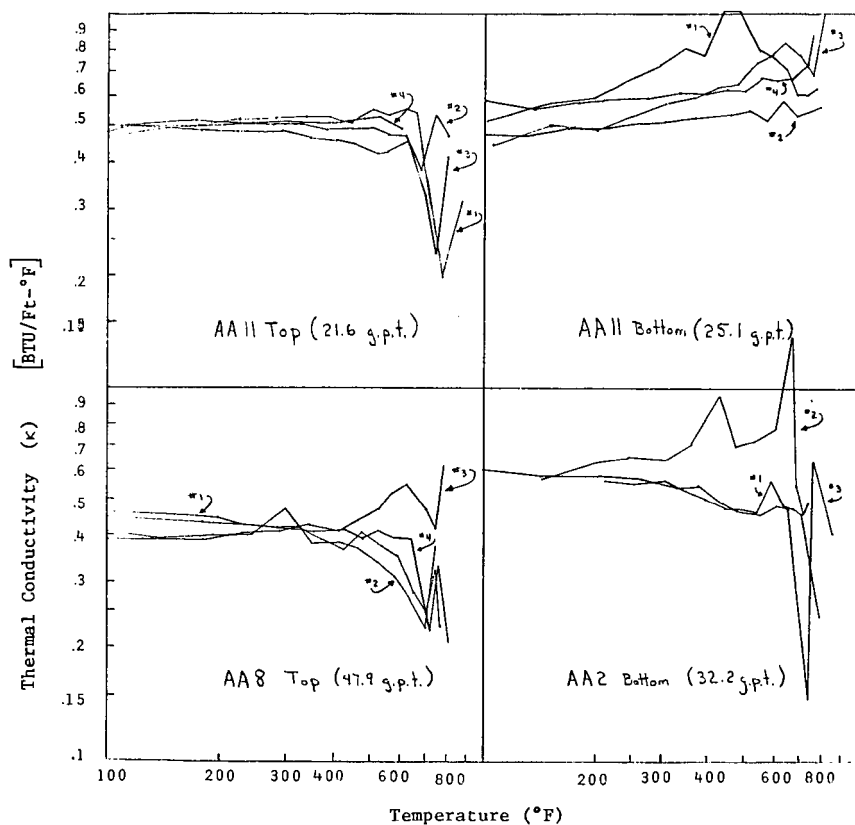


Fig 2: Thermal Conductivity versus Temperature for four selected grades of oil shale at four different pressures

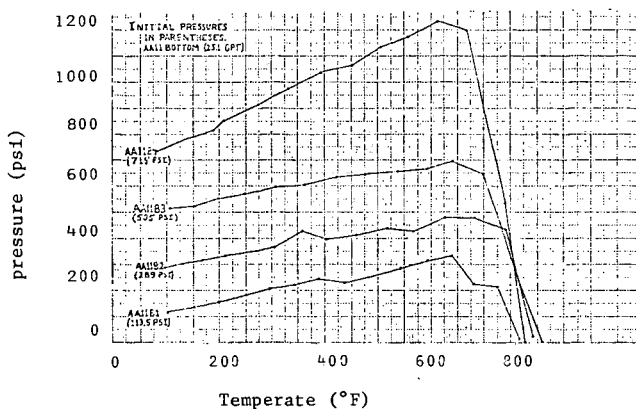


Fig. 3. Variation of Pressure with Temperature for Samples
AA 11 B (25.1 g. p. t.)

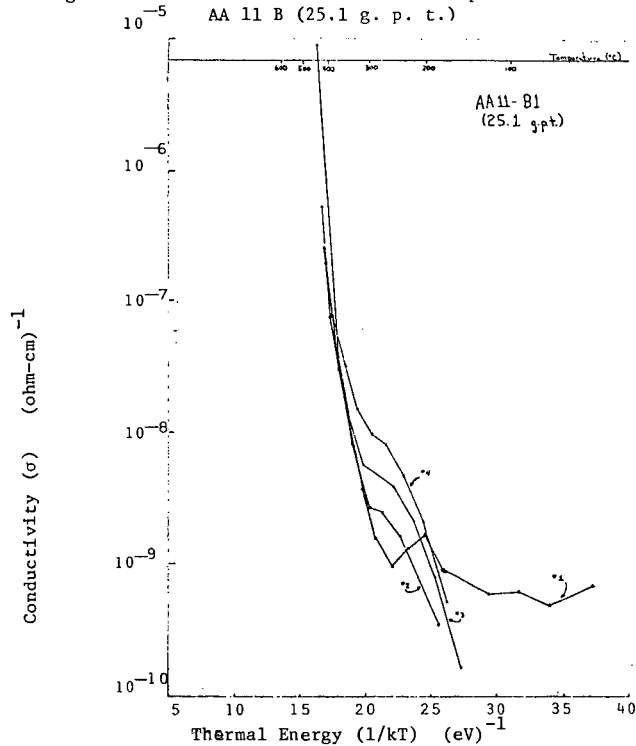


Fig. 4: Electrical Conductivity versus temperature with pressure as a parameter

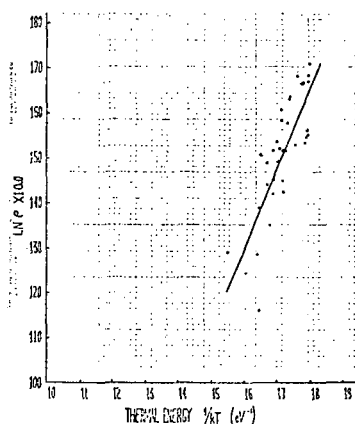


Fig. 5. Plot of least squares fit of resistivity vs. temperature for many oil shale samples which exhibit an activation energy of 1.8 eV.

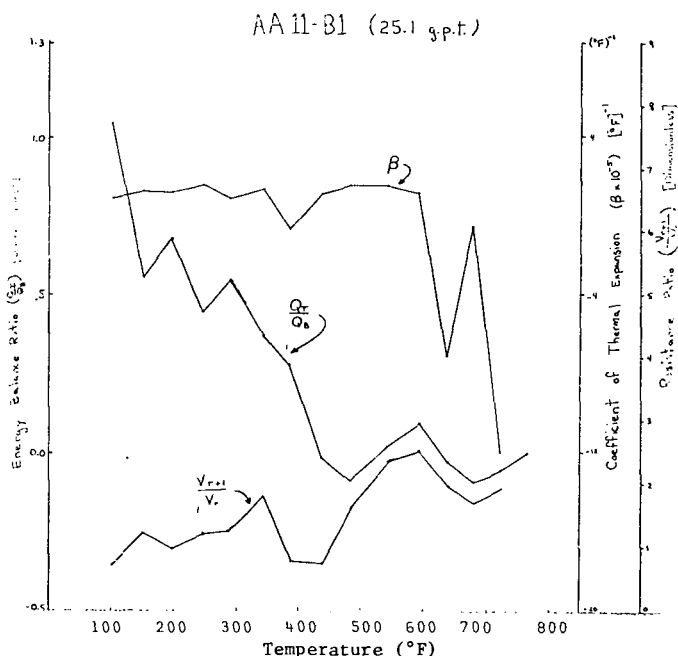


Fig. 6 Derived parameters: energy balance ratio, resistance ratio, and coefficient of thermal expansion versus temperature (°F)

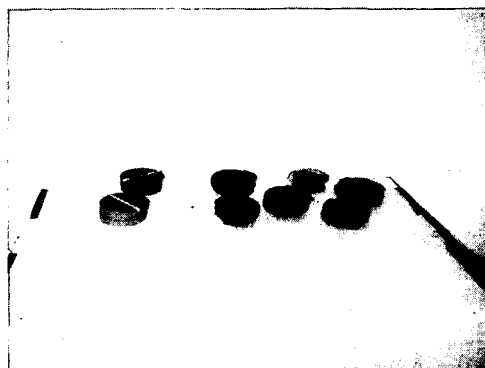


Fig. 7 Samples before and after experiment

A LABORATORY STUDY OF GREEN RIVER OIL SHALE
RETORTING UNDER PRESSURE IN A NITROGEN ATMOSPHERE

R. L. Wise, R. C. Miller and J. H. George

Laramie Energy Research Center of ERDA,
and The University of Wyoming
P.O. Box 3395, University Station
Laramie, Wyoming 82071

INTRODUCTION

In situ retorting of oil shale is being considered as a possible means of energy recovery. Currently proposed in situ processes would involve creation of adequate permeability in the shale beds followed by combustion or gas injection at high temperature. Pressure will increase with depth of the shale for these operations. Retorting data to provide information relative to in situ processes is meagre for the effects of pressure and retorting atmosphere on shale oil production and quality.

In a previous study, Bae (1) investigated effects of retorting atmosphere (N_2 , CO_2 , H_2O , NH_3 , and H_2), pressure and sweep gas rate on oil shale retorting. The retort was vertical, with upward gas flow, and there was no mechanism for removal of produced oil except with the exit gas. Bae (1) found little effect of interchanging the sweep gas or the sweep gas rate. However, there was a large reduction in oil yield with increased pressure, accompanied by greater gas production and coke deposits. Oil yields dropped dramatically with increased pressure, even when hydrogen was used as the sweep gas, in contradiction to typical oil hydrotreating results.

Some proposed in situ recovery methods would allow segregation of produced oil by drainage from the regions where it originated by pyrolysis. Thus it was decided to study the effects of sweep gas identity, sweep gas rate, gas pressure and heating rate on the retorting process in a downflow vertical oil shale retort. This paper summarizes the important results with nitrogen as the sweep gas. In addition, the results now available with hydrogen as sweep gas are included and discussed. This portion of the study is still in progress.

EXPERIMENTAL WORK

Retorting System and Procedure

A flow diagram of the pressure retorting system is shown in Figure 1. Sweep gas was taken from high pressure cylinders and regulated to a desired system inlet pressure. The nitrogen and hydrogen sweep gases were used as obtained commercially. No detectable impurities were found in either gas by chromatographic analysis. For atmospheric pressure experiments, the cylinder gas was regulated to about 50 psig, and flow rate was controlled with a metering valve, the compressor being bypassed. To obtain the desired flow rate for the higher pressure experiments, the cylinder gas was regulated to appropriate pressure for inlet to the reciprocating diaphragm compressor. The gas pressure in the retort vessel was fixed by a back-pressure regulator for these high pressure experiments. The sweep gas entered the pressure retort at the top, flowed down through the packed shale bed and exited from the retort bottom.

The pressure retort was a stainless steel commercial high-pressure cylindrical reaction vessel of 2-9/16-inch-inside diameter by 32-inch-inside depth. Vessel access was at the upper end with an outside cap-type compression closure on a flat copper gasket. The top plug was provided with three holes: a sweep gas inlet port, a pressure measurement port and a port for a thermocouple well. The inside bottom

of the vessel was hemispherical in shape and was provided with an exit line for gas and oil. A stainless steel screen conforming to the vessel bottom was used to support the shale charge.

The retort vessel below the upper head was surrounded by a cylindrical electrical heater composed of five elements along the length of the retort. A thermocouple was placed between each element and the outside retort wall. Current to each element was proportionally controlled to maintain the corresponding thermocouple reading in line with the desired heat-up rate. The actual heat-up rate of the vessel contents would be somewhat different from the desired rate and was monitored by four internal bed thermocouples spaced vertically in a 1/4-inch thermocouple well.

Shale for all runs came from the Anvil Points Facility of ERDA near Rifle, Colorado. It was crushed and screened (minus 3/4-inch and plus 1/4-inch) and mixed to form a single uniform batch from which portions were taken for each run. The shale analyzed 31.1 gallons of oil per ton by modified Fischer assay. Analysis of the raw shale is shown in Table 1.

The retort vessel was loaded with 2240 grams of crushed raw oil shale for each run. Sweep gas flow and retort pressure were adjusted to the desired values and then the heating initiated. The heat-up was continued until a predetermined final bed temperature was indicated on the external controller thermocouples, after which the heaters were controlled to keep the retort temperature at this fixed value for a period of several hours. At the termination of a run the heaters were turned off and the sweep gas allowed to flow until the bed returned to near ambient temperature.

Oil and gas exiting from the retort bottom entered an oil collection system. This collection system consisted of two knock-out traps in series. Oil collected in the first of these traps could be monitored with time. A differential-pressure cell continuously measured the hydrostatic pressure of the oil in this trap. Since most of the produced oil was collected at this point, a good estimate could be made of total oil produced with time. Total oil produced was determined by draining the various collection points and weighing.

Downstream of the oil collection system and backpressure regulator, the exit gases were filtered, and a small portion bled off to a gas chromatograph for analysis. Analysis was accomplished with a three-column system using a thermal conductivity detector.

Experiments and Calculations

Using nitrogen as the sweep gas, the raw shale was retorted at pressures of 0, 750, and 1500 psig (barometric pressure approximately 11 psia). Uniform heating rates of 14, 25, 75, and 125° F per hour were employed at each pressure. At fixed pressure and heat-up rate, a number of sweep gas space velocities were studied, with a maximum of about 120 SCF per hour per square foot of bed cross section.

Hydrogen sweep gas experiments have been performed in the same ranges of pressure, heat-up rate, and space velocity. These experiments are not yet complete.

Actual heat-up rates were determined from the steady-state portion of average bed temperature versus time plots. Actual nitrogen space velocities were calculated from the measured exit gas flow rates and nitrogen content. Hydrogen feed rates were measured with the wet-test meter prior to the heat-up period.

Material balances for each run were made on total mass, ash, carbon and hydrogen. On some of the early nitrogen runs at atmospheric pressure the oil collection system then in use did not trap all of the oil produced. The collection system was subsequently modified to minimize this loss. On these early nitrogen runs the carbon

Table 1. Analyses of raw and retorted shales

		<u>Retorted shales</u>		
		<u>Raw shale</u>	<u>Atmospheric pressure run¹</u>	<u>1500 psig run²</u>
Total weight	g	2240	1861	1911
Organic carbon	wt-pct	13.7	4.4	5.5
Hydrogen	do	2.01	0.22	0.40
Nitrogen	do	0.46	0.29	0.30
Sulfur	do	0.77	0.67	0.61
Water	do	1.2	0.2	0.1
Mineral CO ₂	do	16.4	19.0	18.0
Ash	do	66.9	77.6	75.8

¹ Run number 9 of table 2 in Reference (2).² Run number 52 of table 2 in Reference (2).

Table 2. Pressure retort results for two example runs

		<u>Atmospheric pressure run</u>	<u>1500 psig run</u>
Heat-up rate	° F/hr	34.4	21.6
Space velocity	SCF/hr-ft ²	117	116
Max bed temp,	° F	951	921
Organic carbon distribution			
Retorted shale	wt-pct	26.4	33.8
Oil (C ₄ +) wt-pct		66.1	56.5
Gas (C ₃ -) wt-pct		5.1	9.5
CO ₂ -free gas (C ₃ -)	g	29.8	40.8
Oil yield	vol-pct	84.6	77.2
Oil yield (C ₄ +) vol-pct		88.7	82.9

Table 3. Oil properties for example runs

	<u>Atmospheric pressure run</u>	<u>1500 psig run</u>
Specific gravity	0.920	0.873
Analysis, weight-percent:		
H ₂	11.7	12.1
N ₂	2.0	1.9
S	0.8	0.5
C	84.7	84.3
Distillation fractions, weight-percent:		
72-400° F	7	14
400-600	25	34
600-800	34	29
800 +	34	23
Pour point, ° F	86	15
Viscosity, cp:		
at 100° F	24	4
at 130° F	13	3

balances were not good. It was assumed that any initial carbon unaccounted for in the products was due to lost oil. The oil yield figures were adjusted for lost oil. No such corrections have been made for any of the hydrogen experiments.

Two types of oil yields as volume percent recovery of the raw shale modified Fischer assay were calculated. One oil yield was based on liquid product only and the other on liquid product plus all C_4 and heavier hydrocarbons analyzed in the exit gases.

The final distributions of the organic carbon in the raw shale were also calculated. Organic carbon in the raw shale, retorted shale, oil and gas were all independently determined. For presentation, the carbon in the C_4 gases was added to the carbon in the oil. Any carbon as CO_2 in the exit gases was assumed to have come from mineral decomposition and was not included as organic carbon.

RESULTS

Nitrogen Sweep Gas Experiments

For the nitrogen runs, there was a definite decrease of oil yield with increase of pressure. The average oil yield (including C_4 gases) for 22 atmospheric pressure runs was 93%, with a standard deviation of 5%. At 750 psig, the average C_4 oil yield for 21 runs dropped to 82%, with a standard deviation of 8%. At 1500 psig, the average C_4 oil yield for 18 runs was only 78%, with a standard deviation of 6%. Within the scatter in the data, no dependence of the oil yield on either heat-up rate or sweep gas space velocity could be detected.

Accompanying the decrease in average oil yield with increasing pressure for the nitrogen experiments, there was an increase in both the average amount of gas produced and the average percentage of the initial organic carbon left on the retorted shale as coke. Other effects of increasing pressure included a decrease in oil specific gravity and viscosity, and an increase in amounts of lighter distillation fractions for the oil.

Detailed results of the nitrogen sweep gas experiments are available in another source (2). Results for only two example runs, one at 0 psig and one at 1500 psig, are included here for illustrative purposes. These are runs 9 and 52 from Table 2 of Reference (2). Retorted shale properties are included in Table 1. Retorting conditions, distribution of organic carbon in the products, gas production and oil yields are given in Table 2. Oil properties are shown in Table 3. Increased coking with increase of pressure is shown by the increase in organic carbon on the retorted shale for the 1500 psig experiment when compared with the 0 psig run (See Tables 1 and 2). This is also confirmed by the increase in gas produced in the high pressure run. The oil properties in Table 3 indicate that the oil from the high pressure run was lighter with lower pour point and viscosity than the oil from the low pressure run. No appreciable differences could be detected in the C/H ratio for oils produced at the various pressures. The increased gas production for the 1500 psig run over the 0 psig run was primarily due to an increase in the light normal alkanes.

Hydrogen Sweep Gas Experiments

The preliminary data for experiments employing hydrogen as sweep gas indicate an increase in oil yield with increase of pressure and also with increase of sweep gas space velocity. Oil yields (including C_4 gases) of 100 to 125 volume percent of the raw shale modified Fischer assay have been consistently obtained at pressures of 750 to 1500 psig and hydrogen space velocities in excess of 50 SCF per hour per square foot of bed. The effect of heating rate variations at constant pressure and space velocity does not seem to be pronounced. There appears to be little difference in oil yield between nitrogen and hydrogen sweep gas for runs at atmospheric pressure

Comparison With Previous Work

The present nitrogen results are compared with those of Bae (1) in Figure 2. Oil yields from the present study are in reasonable agreement with the previous work for constant gas residence times in the retort. In no cases did we observe the dramatic reduction in oil yields found in the previous work for constant gas feed rate. In the previous study (1), oil yields were found to decrease with increase of pressure when hydrogen was used as the sweep gas. The present results indicate just the opposite trend, that is, an increase in oil production with increase of hydrogen pressure.

The discrepancies between the present work and the former study are probably due to differences in the way the retorting was conducted. In the previous work the sweep gas entered below the shale bed and exited from near the top of the bed. There was no provision for oil produced at the lower temperatures to be removed from the retort until it was volatilized and carried out with the sweep gas. On the average, the oil was subjected to higher temperatures and a longer retort residence time than in the present work. With increased pressure this effect would be even more pronounced, accounting for the large drops in oil yield noted in the former work.

Mathematical Model

Experimental oil shale pyrolysis data of Hubbard and Robinson (3) were used to develop a simple kinetic model for oil plus gas production versus time. This model will be described in more detail elsewhere (4). Since the Hubbard and Robinson work was with a raw shale of different Fischer assay, the model was adapted to give ultimate amounts of C₄+ oil in line with the average nitrogen sweep gas results of the present study.

The basic model is embodied in the equation

$$\frac{dx}{dt} = K_1 \times \left(1 - \frac{x}{K_2 F} \right) \quad 1)$$

where x is the weight percent of the initial available oil in the raw shale (by modified Fischer assay) which has been produced as C₄+ oil and t is the time. The parameters K₁, K₂ and F are given by

$$\begin{aligned} K_1 &= 0 & \text{for } T < 700^\circ \text{ F} \\ K_1 &= \exp(.03476T - 29.5994) & \text{for } 700^\circ \text{ F} < T < 825^\circ \text{ F} \end{aligned} \quad 2)$$

$$K_1 = \exp(.00645T - 6.0633) \quad \text{for } T > 825^\circ \text{ F}$$

$$K_2 = 0.0006911T + 0.1766 \quad 3)$$

$$F = 1 + 0.004647P^{\frac{1}{2}} \quad 4)$$

where T is the temperature in ° F and P is the pressure in psig. The heating rate (h) is incorporated by letting the temperature at any time be given by

$$T = T_0 + ht \quad 5)$$

where T₀ is the initial bed temperature.

In a kinetic expression of the form of Equation 1, some mechanism is necessary to initiate a non-zero rate. In this work, this was achieved by setting x = 0.125 at T = 700° F.

The above model has been utilized to predict C₄+ oil yield as a function of

time for the nitrogen sweep gas experiments. Good agreement was found between model and experimental oil yield - time curves.

REFERENCES

1. Bae, J. H., "Some Effects of Pressure on Oil-Shale Retorting," Soc. Petrol. Eng. J., September 1969, pp. 287-292.
2. Wise, R. L., Miller, R. C., and George, J. H., "A Laboratory Study of Green River Oil Shale Retorting Under Pressure in a Nitrogen Atmosphere," BuMines LERC TPR 76/1, 1976, 23 pp.
3. Hubbard, A. B., and Robinson, W. E., "A Thermal Decomposition Study of Colorado Oil Shale," BuMines RI 4744, 1950, 24 pp.
4. George, J. H., and Finucane, D., "A Simplified Model for Oil Shale Kinetics," In preparation.

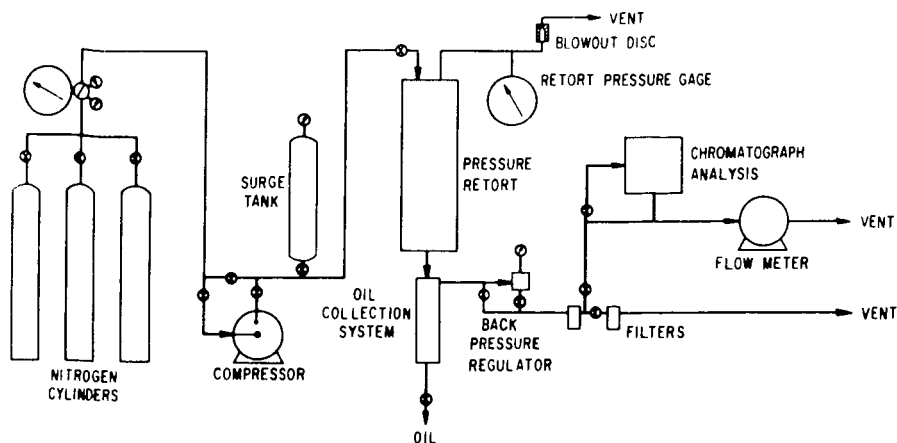


FIGURE 1.- SCHEMATIC DIAGRAM OF PRESSURE RETORT SYSTEM.

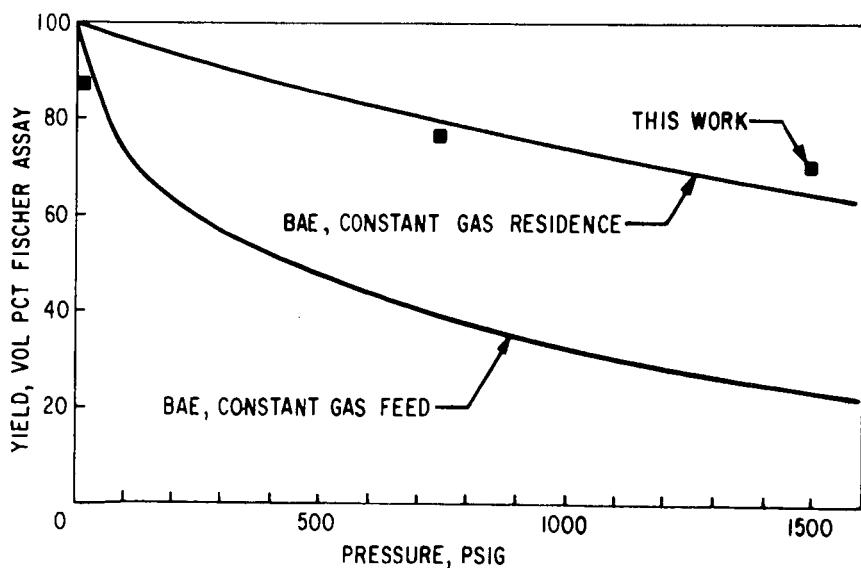


FIGURE 2.-OIL YIELD VERSUS PRESSURE NITROGEN SWEEP GAS.

THERMAL CONVERSION OF OIL-SHALE KEROGEN IN THE PRESENCE OF CARBON MONOXIDE AND WATER

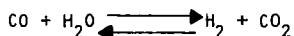
J. J. Cummins and W. E. Robinson

U.S. Energy Research and Development Administration
Laramie Energy Research Center, Laramie, Wyoming 82071

INTRODUCTION

The decrease in the world's oil supply must be supplemented by alternate energy resources. One of these alternate energy resources is oil shale. Oil shale is composed of insoluble organic material (kerogen), soluble organic material (bitumen), and inorganic minerals. Although oil shale contains no oil, the insoluble organic kerogen can be converted to oil by heat.

Both aboveground and underground retorting techniques (7, 11, 12, 16,)¹ have been used to process oil-shale kerogen. Some of these processes utilize solvent, hydrogen, and steam (3, 6, 8, 9, 14); however, present technology can be improved relative to increased yields of products with less environmental impact (13). The CO-H₂O reaction to be discussed in this report is a method by which oil-shale kerogen is converted to gaseous and soluble products in the presence of molecular or reactive hydrogen formed during the water shift reaction shown below:



The converted products can be recovered along with water-soluble minerals. The major advantage of this reaction is that more of the insoluble kerogen is converted to gaseous and soluble products in the presence of CO and H₂O than is converted by conventional methods at the same temperature. Also removal of the water-soluble minerals would make the shale residue inert to water leaching on disposal and the water-soluble minerals would be available for commercial use.

In recent years the CO-H₂O reaction has been used to convert organic wastes to oil (1), to hydrogenate coal (2, 4, 10), to liquify coal or lignite (5, 7, 17) and to degrade oil-shale kerogen (13). Since high yields of soluble products are obtained from carbonaceous materials at low-temperatures, study of the CO-H₂O reaction and its application to oil-shale kerogen conversion to soluble products is continuing at the Laramie Energy Research Center.

The present paper describes the effects of seven variables on the CO and water reaction. The seven variables are temperature, heating time, CO pressure charged, presence and absence of carbonates, shale particle size, shale grade, and water to shale ratio. In addition, the conversion of kerogen in the presence of water only, the composition of some soluble products and the effect of the CO-H₂O reaction on some oil-shale minerals will be described. Other processes utilize steam or steam and recycle gas but none have duplicated the conditions of this study. For this reason only limited comparisons with other kerogen conversion methods will be discussed.

EXPERIMENTAL

All of the oil-shale samples came from the Piceance Creek Basin of the Green River Formation. Most of these samples for this research were ground to

¹ Underlined numbers in parentheses refer to items in the list of references at the end of this report.

pass through a minus 100 mesh screen. To determine the effect of different grades of oil shale on kerogen conversion, four grades namely 8, 18, 23, and 65 gallons of oil per ton of shale were selected for this investigation. To determine the effect of shale particle size on kerogen conversion, some large pieces of 65 gallon per ton shale were crushed and screened to the following sizes: 0.01, 0.015, 0.029, 0.125, 0.25, and 0.50 inches. In addition, some 1-1/4" cube shale blocks were cut from a 35 gallon per ton piece of oil shale to determine if the kerogen in a block of shale of this size could be converted by the CO-H₂O reaction.

Some minus 100 mesh 65 gallon per ton oil-shale sample was leached with 10 percent hydrochloric acid to remove the natural carbonates. The sample was then washed free of acid and dried under reduced pressure at 60° C. This sample was used to study the effect of the presence and absence of mineral carbonates on kerogen conversion in the presence of CO-H₂O.

An American Instrument Company² 1-liter reaction vessel constructed of inconel - 600 metal and mounted in a rocking assembly was used for all reactions. The reaction vessel was externally heated with electrical heaters enclosed in a metal jacket. The heating elements were controlled by a Love Controls Corporation model 49 proportioning controller.

Prior to each test a weighted amount of oil-shale sample and a selected amount of water were placed in the pressure vessel. When sodium carbonate was used, it was added at this time. The pressure vessel was then sealed and charged to the selected CO pressure. The oil-shale samples were then heated in the presence of CO and H₂O at the predetermined conditions. On completion of each test the pressure vessel was allowed to cool to room temperature after which a gas sample was taken for mass spectral analysis. The reaction vessel was opened and the heated residue and water were recovered.

The heated oil-shale residue was separated from the water by filtration. The water was extracted in a separatory funnel with diethyl ether. The heated oil-shale residue was air-dried at room temperature and then extracted with a methyl alcohol-benzene mixture overnight to recover the soluble product from the oil-shale residue. The ether-soluble product and methyl alcohol-benzene soluble products were combined to represent the total soluble product.

All gas analyses were performed on a CEC 21-620 mass spectrometer capable of analyzing low-molecular-weight polar and hydrocarbon materials. All soluble products, all oil-shale residues and the original oil-shale sample were analyzed for carbon, hydrogen, nitrogen, and sulfur by the standard methods used at this Center for oil shale and oil-shale products. Mineral carbonate contents were determined for the oil-shale sample and all heated residues. The organic carbon contents of the oil-shale sample and the heated residues equalled the total carbon content minus the mineral carbon content. Kerogen conversion was calculated from the amount of organic carbon present in the oil-shale sample before and after heating.

² Reference to specific trade names or manufacturers does not imply endorsement by the Energy Research and Development Administration.

RESULTS AND DISCUSSION

Effects of Variables

Time and temperature series

The conversion of oil-shale kerogen in the presence of $\text{CO-H}_2\text{O}$ at temperatures from 300° to 450° C for heating times from 0.25 to 6 hours was investigated. The kerogen conversions relative to time are plotted in figure 1. Kerogen conversion increases 3.7 times from about 26 to 98 percent with increased temperatures. Kerogen conversion does not increase consistently with increased heating time and only at 400° C does the conversion increase with increase in heating time. Heating time has a minor effect on kerogen conversions at the heating time selected for study. Kerogen conversion results obtained at 350° C and 400° C by Hubbard and Robinson (11) using dry heat and no hydrogen at atmospheric pressure are included for comparison with the $\text{CO-H}_2\text{O}$ reaction results. Generally, conversions using the $\text{CO-H}_2\text{O}$ reaction at the same temperature show little increase in conversion with increase in heating time. In contrast, data presented by Hubbard and Robinson (11) at 350° and atmospheric pressure show a gradual increase in conversion with increase in heating time. Also, kerogen conversions at 350° and 400° C using the $\text{CO-H}_2\text{O}$ reaction exceed the conversion obtained by Hubbard and Robinson (11) by 200 and 125 percent respectively with 98 percent of the kerogen being converted to either a soluble or gaseous product at 450° C.

Effect of varying pressure of CO charged

The effect of varying pressure of CO charged on oil-shale kerogen conversion while being heated at 375° C for 2 hour was investigated and the results appear in figure 2. The five charge pressures appear at the bottom of the figure and approximate operating pressures appear at the top of the figure. Oil-shale conversion decreases from about 80 to 60 percent as the CO charge pressure increases from 200 to 1000 psig and the operating pressure increases from 3000 to 6000 psig. These results suggest that no benefit in conversions results from increasing charged CO pressure above 200 psig and an adverse effect on conversion does result at higher CO charged pressures. Some additional tests at varying pressures will be made in a bench scale reactor at a later date to confirm these results.

Effect of varying mineral carbon content

The effect on oil-shale kerogen conversion of the absence of natural oil-shale carbonates and the addition of sodium carbonate to shale samples prior to the tests was investigated and the results appear in figure 3. Kerogen conversion increased with increase temperature in the presence or absence of carbonates. Almost the same amount of kerogen was converted in the presence and absence of added sodium carbonate when raw shale was heated in the presence of $\text{CO-H}_2\text{O}$. A decrease in kerogen conversion was obtained when the oil-shale natural carbonates were removed at each temperature except at 375° C. Addition of sodium carbonate did not increase the yield equal to that obtained with the natural carbonates present in the raw oil shale.

In general, the results show that more kerogen is converted in the presence of the oil-shale carbonates (raw oil shale over HCl leached shale) and that the addition of sodium carbonate does not benefit kerogen conversion during $\text{CO-H}_2\text{O}$ reaction.

Effect of varying particle size of oil shale

The effect of oil-shale particle size on kerogen conversion during the $\text{CO-H}_2\text{O}$ reaction was studied and the results appear in figure 4. About 70 to 80 percent of the kerogen is converted when less than 0.1 inch shale particle sizes are reacted. Kerogen conversion decreases to about 50 percent as the particle size increases to .5 inches and increases to 60 percent as the particle size increases to the 1.25 inch cubes. The cubes became pliable, soft, and even spongy as the result of the reaction. Generally these results show that the $\text{CO-H}_2\text{O}$ process will be more useful in converting finely ground oil shales to soluble products; however, particle sizes up to at least 1.25 inches can be satisfactorily converted.

Effect of varying grade of oil shale

The effect of varying grade of oil shale on kerogen conversion was studied and the results appear in figure 5. Oil-shale kerogen conversion, increases from 50 to more than 70 percent as the grade of oil shale increases from less than 10 to more than 60 gallon of oil per ton of shale. These results suggest that all grades of oil shale could be satisfactorily converted, but the conversion tends to increase with increase in the richness of the oil shale. Very rich oil shales, which cause considerable problems with some retorting operations, would be converted very successfully with the $\text{CO-H}_2\text{O}$ reaction.

Effect of varying amount of water

The effect of the amount of water on kerogen conversion was investigated. The amount of water was varied from .25 to 3 milliliters water per gram of oil shale. Kerogen conversions varied some but at 350°C and water to shale ratios greater than 0.25 kerogen conversion appears to be independent of the amount of H_2O present. These results show that only small amounts of water are needed to convert kerogen using the $\text{CO-H}_2\text{O}$ process as the 0.25 water to shale ratio represents only the amount of water needed to wet the oil shale.

Conversion in Presence of Water Only

Kerogen was converted in the presence of water only to determine the amount of kerogen converted at temperatures from 350° to 450°C for heating times from .25 to 6 hours. The conversion results are compared with some of the results obtained in the presence of $\text{CO-H}_2\text{O}$ and appear in table 1. The operating

TABLE 1. - Effect of varying the temperature and heating time on oil-shale kerogen conversion in the presence of $\text{CO-H}_2\text{O}$ and H_2O only

Heating time, hrs	Temperature $^\circ\text{C}$	Kerogen converted, wt percent			
		$\text{CO-H}_2\text{O}$		H_2O	
		Gas product	Soluble product	Gas product	Soluble product
2.0	350	1.1	39.7	4.5	36.4
6.0	350	0.1	39.0	6.5	46.4
0.25	400	2.0	66.3	12.7	57.6
1.0	400	1.9	75.0	19.5	69.3
1.0	450	18.7	79.2	63.4	22.7

pressures ranged from 2400 psig to 3600 psig in the presence of H_2O only and from 4800 psig to 6000 psig in the presence of $CO-H_2O$. About 3 to 9 times more gas is formed when water alone was used over that obtained with water and carbon monoxide. Some carbon residue was evident in the sample heated at the highest temperatures when water alone was used.

Relative to results obtained using CO and H_2O more kerogen is converted to the soluble product at the lower temperatures and less kerogen is converted to soluble products at the higher temperatures in the presence of H_2O alone. Conversely, significantly greater amounts of gaseous products are produced in the presence of H_2O only. The composition of the residual gases generated at $450^\circ C$ in the presence of water only consists of about 29 percent saturate and 10 percent unsaturate C_1 to C_6 hydrocarbons and in the presence of $CO-H_2O$ consists of about 19 percent methane. Hydrogen content of the gas from the test using water only was 29 percent and the gas from $CO-H_2O$ test was 44 percent. These results show that 3 to 9 times more kerogen is converted to gas in the presence of water only than in the presence of water and carbon monoxide.

Composition of Soluble Products

The average atomic ratios calculated from the elemental analysis of the soluble products appear in figure 7. In all cases the atomic hydrogen-to-carbon ratio (X 10) for the soluble extracts exceeded the 154 ratio obtained for kerogen. All of the O/C, N/C, and S/C ratios are less than the O/C of 5.40, the N/C of 2.56, and the S/C of 0.47 ratios obtained for the kerogen. Using Stanfield's (15) elemental analyses of composite Fischer Assay oils, the following atomic ratios were calculated for a representative retorted shale oil: H/C ratio of 164, O/C of 1=0, N/C of 2.0, and S/C of 0.3. With the exception of oxygen amounts, the soluble extracts from the $CO-H_2O$ reaction appear to have average compositions similar to that of a representative Fischer Assay oil. The presence of more oxygen in the extracts indicates a less severe thermal history than the usual retorted oil.

Generally the results show that some hydrogen is probably added to the soluble products during the $CO-H_2O$ process. Also the elemental composition of the soluble products is similar to the elemental composition of the Fischer Assay oils except the oxygen content which is 3 to 5 times more. This higher oxygen content (14) occurs because the soluble products are formed 50° to $200^\circ C$ below the normal $500^\circ C$ retorting temperature at which Fischer Assay oil is formed. These oxygen values (17) do not exceed the amount of oxygen present in the kerogen. The soluble products should be suitable feedstock for hydrocracking and refining operations.

During the $CO-H_2O$ reaction numerous changes occur to the oil-shale minerals. If sufficient water is present the water-soluble minerals, which are mainly alkali carbonates, are solubilized. In addition, the crystalline forms of the quartz minerals are altered and if dawsonite (an aluminum containing mineral) is present it is converted to another mineral form. The removal of the readily water-soluble minerals could prove to be an environmental advantage because these materials may contaminate surface and ground waters when stored with the remainder of the oil-shale residue as is commonly done with other conversion processes.

Effect on Mineral Compositions

A dawsonitic oil shale and the dawsonitic shale residue heated at $400^\circ C$ in the presence of $CO-H_2O$ were X-rayed. The peak intensities of five minerals

(dolomite, feldspar, quartz, analcime, and dawsonite before and after heating at 400° C in the presence of CO-H₂O) are plotted in figure 8. Three minerals (dolomite, quartz, and dawsonite) present in the original oil-shale sample are not detected in the shale residue after heating at 400° C. Apparently the dolomite decomposes into calcium and magnesium carbonate with the formation of calcite. The dawsonite probably reacts to form analcime and carbon dioxide in the presence of CO-H₂O at 400° C. All the quartz loses its crystalline structure upon being heated at 400° C and is converted to an amorphous form not detectable by X-ray. Feldspar appears to be fairly stable in the presence of CO-H₂O at 400° C. Unfortunately the aluminum present in dawsonite is converted to a more insoluble form during the CO-H₂O reaction. To remove the aluminum for commercial use, it would be necessary to degrade the dawsonite to a soluble form prior to the CO-H₂O reaction or devise a technique which would prevent the formation of analcime during the reaction. An environmental advantage is gained with the removal of the water-soluble minerals because the oil-shale residue would become essentially inert to leaching of the salts by atmospheric or ground water moisture. However, more research needs to be done in this area.

SUMMARY

Using the CO-H₂O reaction more kerogen is converted to soluble products and and gas at lower temperatures than is obtained by dry retorting at near atmospheric pressure.

Pressure does not appear to be a significant variable for kerogen conversion in the CO-H₂O reaction

Natural carbonates present in the oil shale are adequate to promote kerogen conversions and additional sodium carbonate does not increase kerogen conversion.

The CO-H₂O reaction is suitable for use with either finely ground or extremely rich oil shales, materials that create difficulties for some oil-shale conversion processes.

Only small amounts of water are needed to convert oil-shale kerogen to a soluble product during the CO-H₂O reaction.

More kerogen is converted to gaseous products in the presence of water alone than in the presence of both carbon monoxide and water.

Soluble products formed in the presence of carbon monoxide and water should be satisfactory materials for refining to needed energy fuels.

Some of the oil-shale minerals undergo major changes during the CO-H₂O reaction for example dawsonite being converted to analcime.

REFERENCES

1. Appell, H. R., Y. C. Fu, S. Friedman, P. M. Yavorsky, and I. Wender. Converting Organic Wastes to Oil. A Replenished Energy Source. BuMines RI 7560, 1971, 20 pp.
2. Appell, H. R., and I. Wender. The Hydrogenation of Coal with Carbon Monoxide and Water. Preprints, Div. Fuel Chem., ACS, v. 12, No. 3, 1968, p. 220.
3. Burwell, E. L., and I. A. Jacobson, Jr. Concurrent Gasification and Retorting of Oil Shale - A Dual Energy Source. Preprints, Rocky Mt. Regional Meeting, Soc. Petr. Eng., Paper number SPE 5335, 8 pp.
4. Fisher, F., and H. Schrader. Hydrogenation of Coal with Carbon Monoxide. Brennstoff-Chem., v. 2, 1921, pp. 257-261.
5. Handwerk, J. G., R. M. Baldwin, J. O. Golden, and J. H. Gary. Co-Steam Coal Liquefaction in a Batch Reactor. Preprints, Div. Fuel Chem., ACS v. 20, No. 1, 1975, pp. 26-46.
6. Hartley, F. L. High Recovery Proves Out for Shale-Oil Process. Chem. Eng. News, July 1, 1974, pp. 15-16.
7. Henderson, T. A. Oil-Shale Processing Methods. Quart. Colo. School Mines, v. 69, No. 3, 1974, pp. 45-69.
8. Hendrickson, T. A. Oil-Shale Processing Methods. Quart. Colo. School Mines, v. 69, No. 2, 1974, pp. 45-69.
9. Jensen, H. B., W. I. Barnet, and W. I. R. Murphy. Thermal Solution and Hydrogenation of Green River Oil Shale. BuMines Bulletin 533, 1953, 42 pp.
10. Nguyen, D. Reduction of Subbituminous Coal with Carbon Monoxide and Water. Ph.D. Thesis, Montana State University, 1973, 83 pp.
11. Hubbard, A. B., and W. E. Robinson. A Thermal Decomposition Study of Colorado Oil Shale. BuMines RI 4744, 1950, 24 pp.
12. Ridley, R. D. In Situ Processing of Oil Shale. Quart. Colo. School Mines, v. 6, No. 2, 1974, pp. 21-24.
13. Robinson, W. E., and J. J. Cummins. An Oil-Shale Conversion Process Using Carbon Monoxide and Water. E.R.D.A. Technical Progress Report 75/1, 1975, 14 pp.
14. Robinson, W. E., and J. J. Cummins. Composition of Low-Temperature Thermal Extracts from Colorado Oil Shale. J. Chem. Eng. Data, v. 5, No. 1, 1960, pp. 74-80.
15. Stanfield, K. E., I. C. Frost, W. S. McAuley, and H. N. Smith. Properties of Colorado Oil Shale. BuMines RI 4825, 1951, 27 pp.
16. Weichman, B. The Superior Process for Development of Oil Shale and Associated Minerals. Quart. Colo. School Mines, v. 69, No. 2, 1974, pp. 25-43.

17. Smith, J. W. Ultimate Composition of Organic Material in Green River Oil Shale. BuMines RI 5725, 1961, 16 pp.
18. York, W. J. Reduction of Subbituminous Coals and Lignite Using Carbon Monoxide. Ph.D. Thesis, Montana State University, 1971, 83 pp.

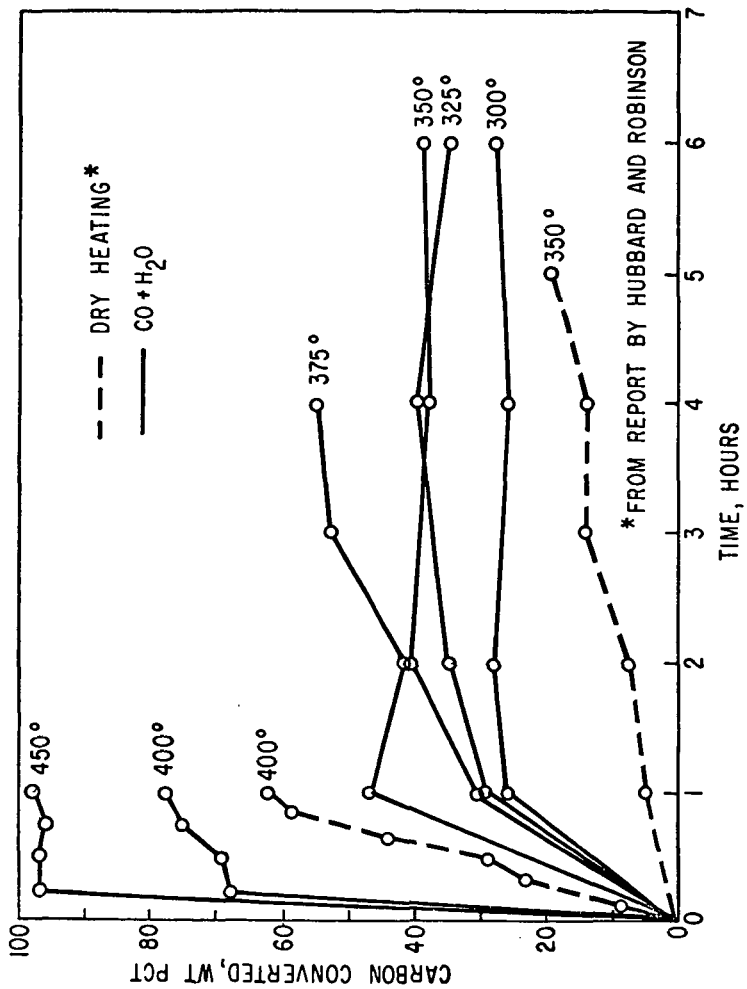


FIGURE I.-KEROGEN CONVERTED TO SOLUBLE PRODUCTS & GAS AT
300 TO 450 °C IN THE PRESENCE OF CO AND H₂O.

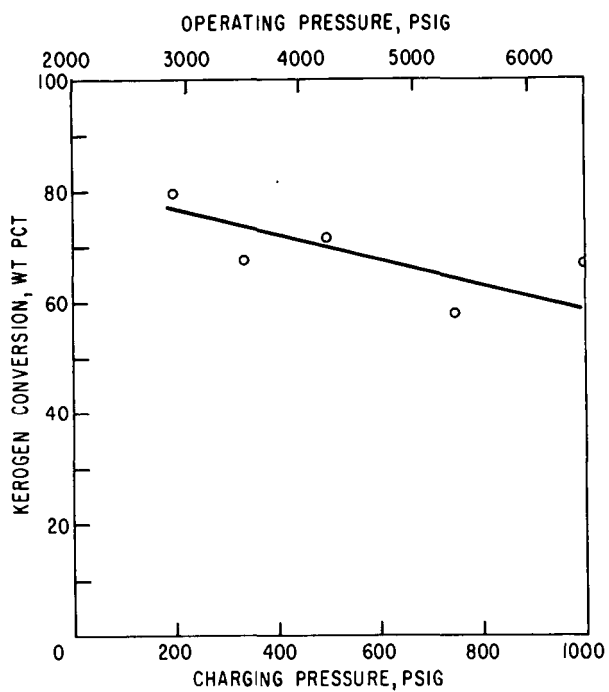


FIGURE 2.-EFFECT OF VARYING PRESSURE
ON KEROGEN CONVERSION AT
375°C FOR TWO HOURS.

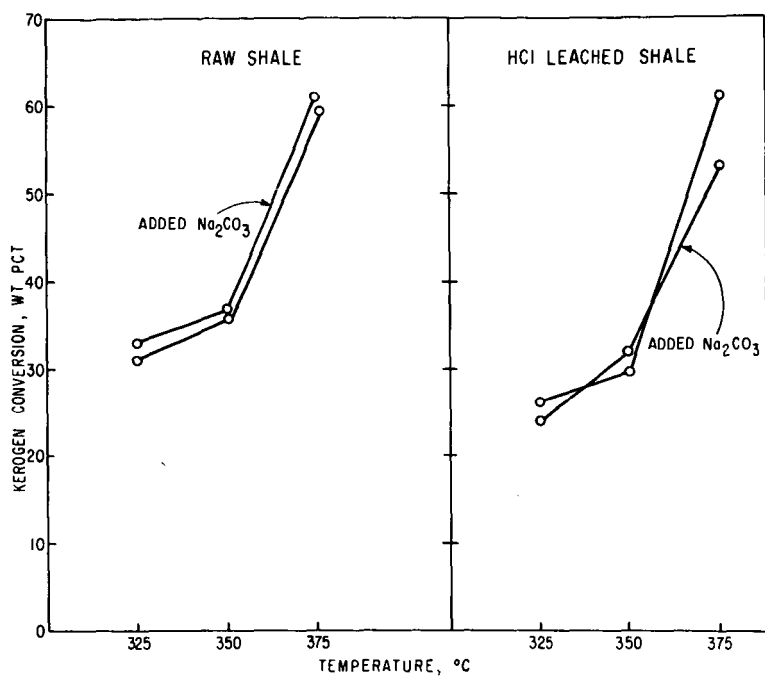


FIGURE 3-EFFECT OF PRESENCE OR ABSENCE OF CARBONATE ON KEROGEN CONVERSION AT 325 TO 375 °C FOR TWO HOURS IN THE PRESENCE OF CO AND H₂O.

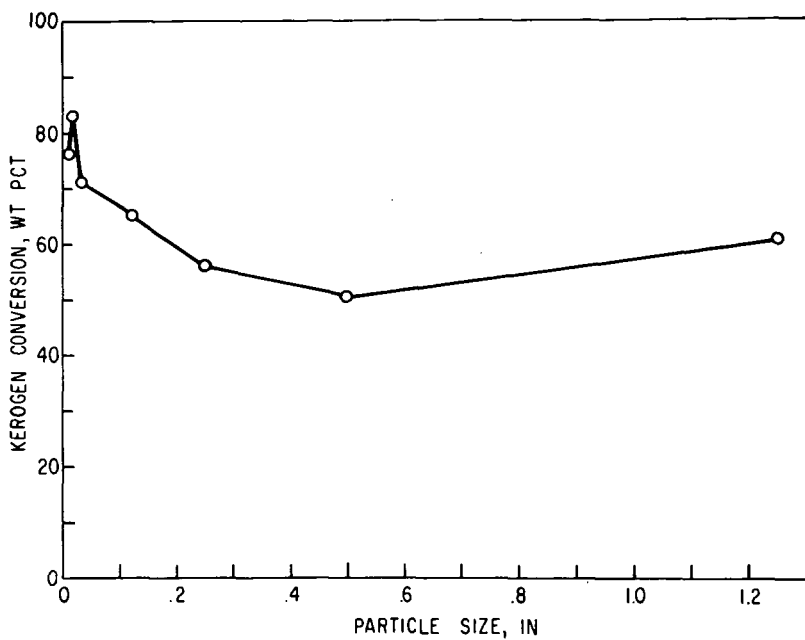


FIGURE 4.-EFFECT OF VARYING OIL SHALE PARTICLE SIZE ON KEROGEN CONVERSION AT 400 °C FOR ONE HOUR.

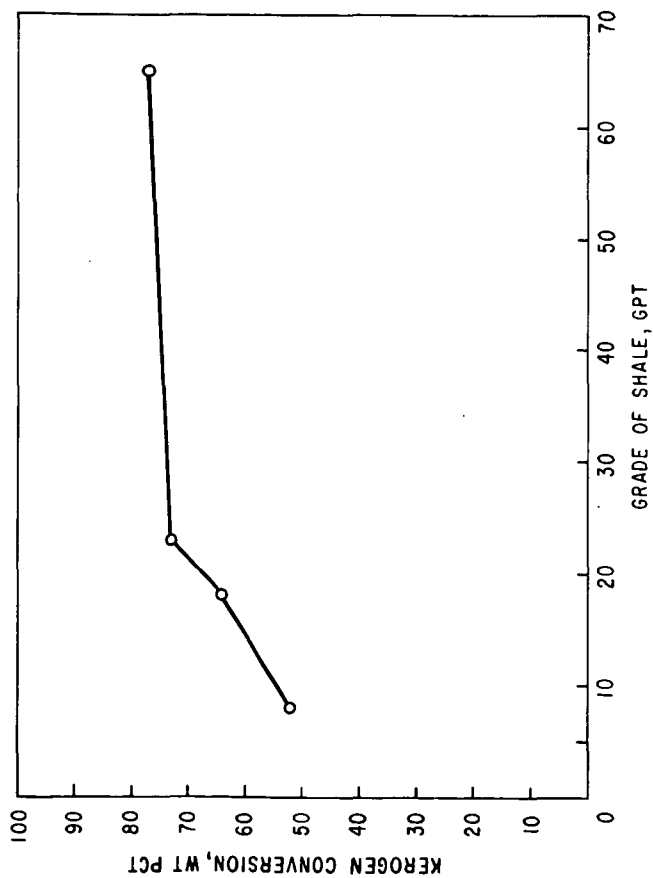


FIGURE 5.-EFFECT OF VARYING THE GRADE OF SHALE ON
KEROGEN CONVERSION AT 400°C FOR ONE HOUR.

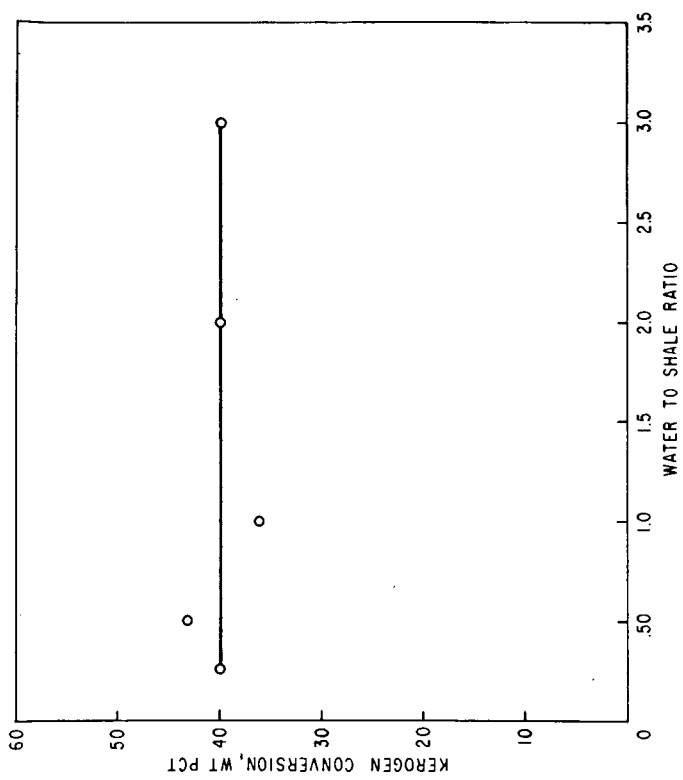


FIGURE 6.-EFFECT OF VARYING THE AMOUNT OF WATER ON
KEROGEN CONVERSION AT 350°C FOR TWO HOURS.

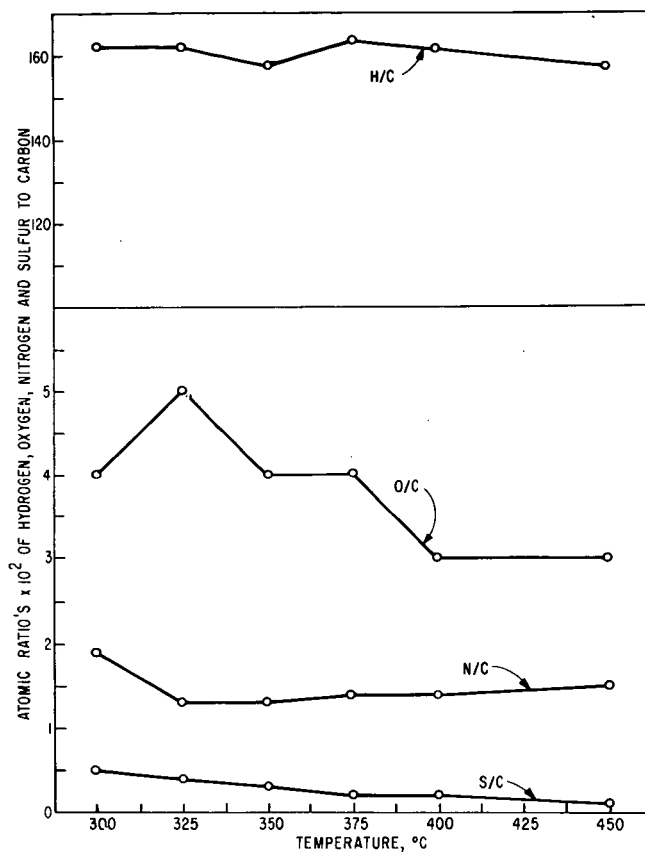


FIGURE 7.-AVERAGE ATOMIC RATIO'S OF THE SOLUBLE PRODUCTS FORMED IN PRESENCE OF CO-H₂O AT VARIOUS TEMPERATURES.

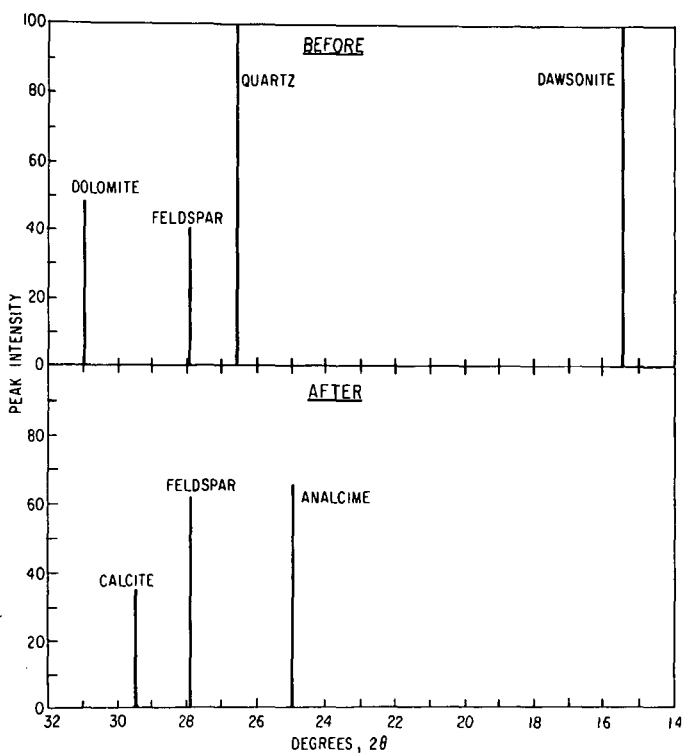


FIGURE 8.-EFFECT OF CO-H₂O ON MINERALS IN DAWSONITE CONTAINING OIL SHALE AT 400 °C.

HOT WATER EXTRACTION OF BITUMEN FROM UTAH TAR SANDS

by J.E. Sepulveda, J.D. Miller and A.G. Oblad

Department of Mining, Metallurgical and Fuels Engineering

University of Utah, Salt Lake City, Utah 84112

INTRODUCTION

The dramatic projections for the energy market in the next few years have forced applied researchers and process designers to consider energy sources other than petroleum; such as tar sands, oil shale and coal. Physically tar sands consist of sand grains surrounded by a bituminous film (Figure 1). This bituminous coating, if properly separated from the sands, may certainly be used as feedstock for the production of fuels and petrochemicals.

Utah has 51 deposits of tar sands containing an estimated 25 billion barrels of bitumen in place, which is about 95% of the total mapped resources in the United States(1). Although the extent of Utah tar sands is small in comparison to the large bitumen potential of Canadian tar sands, which amounts to approximately 900 billion barrels, Utah deposits do represent an appreciable potential when compared to the United States domestic petroleum and condensate production of 3.2 billion barrels of equivalent oil in 1974 and the United States crude oil imports of 1.3 billion barrels during the same year. In spite of its significance, extraction and processing technology of Utah tar sands has not yet been developed. Since noticeable differences in the chemical and physical properties between Canadian and Utah bitumens have been observed, the technology acquired over the last fifty years in Canada can not be applied to Utah tar sands directly; rather, a detailed investigation on Utah tar sands is required.

Currently, at the University of Utah, an ambitious research program on Utah tar sands is being conducted in order to obtain basic information concerning products characterization and process development. Different aspects of interest such as mining, extraction, upgrading and characterization of the products are being studied. The purpose of this paper is to summarize some of the advancements in the hot water extraction of bitumen from Utah tar sands and the characterization of this bitumen, specifically its viscosity.

FUNDAMENTALS OF THE HOT WATER PROCESS

The Hot Water Process (HWP) was first described by Dr. K.A. Clark in 1923 (2,3) and it is currently being used on a commercial scale by Great Canadian Oil Sands Limited in Athabasca, Province of Alberta, Canada (4,5). In this process, the displacement of the bitumen from the sands is achieved by wetting the surface of the sand grains with

an aqueous solution (Figure 2). The aqueous solution contains a caustic wetting agent, such as sodium hydroxide, sodium carbonate or sodium silicate. The resulting strong surface hydration forces operative at the surface of the sand particles give rise to the displacement of the bitumen by the aqueous phase. The name of the process comes from the fact that the system is operated at temperatures near the boiling point of water. Once the bitumen has been displaced and the sand grains are free, the phases can be separated by froth flotation based on the natural hydrophobicity exhibited by the free bituminous droplets at moderate pH values.

The mechanism of bitumen displacement from the solid surface is not yet well understood and, as a result, a useful theoretical framework does not exist. Most approaches have been based on an energy balance for the system postulating that, in order for the bitumen to be displaced, the total free energy of the system must decrease. Thermodynamically, this can be expressed as (6,7):

$$dF = \sum \mu dn + \sum \phi dq + \sum \gamma dA < 0, \quad 1)$$

at constant temperature and volume

where

dF = Helmholtz free energy change

$\sum \mu dn$ = change in free energy due to chemical reaction

$\sum \phi dq$ = change in free energy due to a change in surface charge

$\sum \gamma dA$ = change in free energy due to a change in surface energy

Summations include all the phases and interfaces present in the system. In the past, the term corresponding to chemical reaction and the one corresponding to surface charge have been neglected. In addition, changes in interfacial area have often been neglected, which may be acceptable in mineral flotation systems but not in oil displacement where the variations in interfacial areas are significant. Further, as pointed out by Leja and Bowman (6), the magnitude of the electrical work term in aqueous systems may be of the same order as that of the surface work. Consequently, it seems that neither the surface energy term nor the surface charge term should be neglected in Equation 1.

There are several objections to this fundamental approach. The first one is related to the difficulties in obtaining reliable information on solid-liquid interfacial tensions and also, the complexities appearing from the estimation of the surface charge term in Equation 1. The second objection is that, even if the above information is available, the model only provides a qualitative description of the process which cannot be successfully used for process control or design. Finally, the highly viscous nature of the bitumen in Utah tar sands may give rise to kinetic barriers, in such a way that the equilibrium condition predicted by Equation 1 may be unattainable in a reasonable period of time. Also, electrostatic barriers could be expected (6).

Consequently, a radically different approach is needed. The application of new concepts in the modeling of particulate processes, such as Population Balance Models, which are phenomenological in nature, may result in a better description of the system.

EXPERIMENTAL

Hot Water Extraction Tests

As stated before, due to the difference in physicochemical properties between Canadian and Utah tar sands, the optimum operating conditions and the phase disengagement mechanism itself would be expected to be different. Because of the high viscosity of the Utah bitumen, a high shear, stirred tank reactor was selected for digestion of the tar sand samples, and wetting agents were added to assist the phase disengagement process.

A flowsheet of the process is presented in Figure 3. Mined tar sand feed is extruded down to smaller pieces (3/8") and fed to a 1-gallon, model 1-E-150-SFTN, stirred tank reactor, manufactured by Bench Scale Equipment Co. The impeller for this reactor consists of two pitched blade turbines, 4" OD, which can be easily exchanged with several other types of turbines or propellers. Additional features of this reactor are a torquemeter, a reflux/takeoff condenser, a temperature control and heating system, a SCR speed controller and a tachometer. In the reactor, the feed is contacted with the hot aqueous solution and stirred, at constant temperature, for a specified digestion time. Ideally, at the end of the digestion stage, the bitumen has been displaced from the sand surface and can be separated from the dispersed sand in a standard bench scale Denver flotation machine where bitumen is floated with air. At this point in the research program, no frothers or collectors have been added in the flotation stage. The hydrophobic bitumen concentrate removed from the top of the flotation cell would be sent to a refining plant. On the other hand, the hydrophilic free sand grains sink to the bottom of the cell for discharge, thickening and disposal. On occasions, relatively large lumps of non-floatable bitumen are found with the sand tails. This material can be recovered from the tails, simply by screening on a vibratory screen (14 mesh). The scavenger concentrate so produced has a grade sufficiently high to either be recycled or refined as is. In any event, a scavenger is not obtained when digestion has been done efficiently.

Analytical Techniques

Samples of the feed, concentrates and tailings obtained during experimentation are analyzed to determine their composition with respect to bitumen, sand and water. For this purpose, three Dean and Stark assemblies (Figure 4) were set up according to the procedure reported by the U.S. Bureau of Mines (8).

A weighed sample, contained in a double thickness cellulose extraction thimble, is placed in the neck of a specially designed receiver flask, held by four indentations. About 200 ml of reagent grade toluene are added to the flask and heated to boiling. Toluene vapors dissolve the bituminous materials in the sample and also, remove any trace of water present. The vapors of the toluene - water mixture are trapped by the condenser. Due to its higher specific gravity, water separates from the condensate and is collected in the capillary tube, while the toluene is refluxed. After a few hours (4-6), extraction reaches completion and the volume of water in the sample can be read from the graduated capillary. The thimble is dried and weighed to determine the amount of solids left, and the bitumen is calculated by difference, assuming the density of the water is equal to unity. This analytical technique has proved to have very good reproducibility, $\pm 0.1\%$.

Bitumen Characterization

The most appropriate way to characterize the raw bitumen for hot water processing is by its viscosity. The viscosity is an important property of the bitumen and the determination of its dependence on temperature and system composition will help to establish the optimum conditions for the separation. Furthermore, this fundamental property is of primary importance to insitu mining, recovery, upgrading and material handling processes. Process design will strongly depend upon the viscosity of the feed and products.

Samples of pure bitumen were prepared by dissolving the flotation concentrates obtained from HWP experiments with an excess of benzene, allowing the sand remaining in the concentrate to settle, transferring part of the liquid to another vessel, and finally, evaporating the benzene by heating the solution on a hot plate, for an extended period of time (10-15 hours).

The viscosity of Athabasca and Utah bitumens were determined with a rotational viscometer, Rotovisco. This instrument allows the operator to set the temperature of the sample as desired, adjust the angular velocity of the rotating bob and measure the torque necessary to maintain that velocity; so that, a flow curve (shear stress versus shear rate) can be obtained, based on 3 easily determined calibration constants.

RESULTS AND DISCUSSION

Hot Water Extraction

Preliminary extraction experiments were performed in order to establish the range of conditions under which the separation could be made. The main variables being considered in the Digestion and Flotation stages are listed in Table I.

TABLE I. OPERATION VARIABLES CONTROLLING
THE PERFORMANCE OF THE HWP

DIGESTION:	Discrete	Feed Source
		Wetting Agents
		Impeller and reactor design
	Continuous	Temperature
		Percentage solids in the vessel
		Digestion time
		Wetting agents additions
		Feed size distribution
FLOTATION:	Discrete:	Intensity of agitation (RPM)
		Cell Design
	Continuous	Flotation Reagents
		Percentage Solids
		Intensity of Agitation
		Temperature
		Solution pH
		Flotation reagents additions

Owing to the large number of variables and the lack of background information on the subject, the effect of each individual variable on the overall performance could not be studied separately as this would require a very large number of experiments. Rather, experimental design

techniques in which the number of experiments is reduced to a minimum are being considered for application in combination with several optimization algorithms. With this approach, the main objectives are to determine the optimum experimental conditions for separation and to formulate a mathematical description of the system response in the region of the optimum. This sort of information, if obtained, will provide a solid basis for the development of theoretical and semi-theoretical models.

The excellence of the separation is quantified not only by the grades of the concentrates and the recovery of the different components but also by the coefficient of separation (CS), which is defined as the fraction of the feed material which undergoes a perfect separation, while the rest of the feed is distributed unchanged into the respective product streams(9). In terms of recoveries, it can be shown that the CS is equal to the difference between the recovery of bitumen in the concentrate and the recovery of sand in the same concentrate.

So far, HWP extraction tests have been performed with samples from three different Utah tar sand deposits: Asphalt Ridge, P.R. Spring and Sunnyside. Scanning electron photomicrographs of these samples are shown in Figure 1. Satisfactory results were obtained only with the first two samples, namely, Asphalt Ridge and P.R. Spring which exhibited a fairly similar behavior. Typical results are presented in Table II. Unexpectedly high coefficients of separation and recoveries of bitumen in the concentrate were obtained under these conditions. These high coefficients of separation are indicative of an excellent separation and suggest that development of a HWP for Utah tar sands may be possible.

TABLE II. HOT WATER EXTRACTION TESTS FOR ASPHALT RIDGE AND P.R. SPRING SAMPLES

EXPERIMENTAL CONDITIONS

Digestion: Wetting Agent addition: 0.2 (g sodium silicate/g tar sands)
 Temperature: 200°F
 Percentage Solids: 67%, by weight tar sands
 Digestion time: 15 min; RPM = 1000
 Flotation: Percentage Solids: 20%, by weight tar sands
 RPM = 1200
 Temperature = 15°C

ASPHALT RIDGE

	Weights %	Grade, %		Recoveries, %	
		Tar	Sand	Tar	Sand
Conc.	14.68	83.74	16.26	97.15	2.72
Tail	85.83	.42	99.58	2.85	97.28
Feed	100.00	12.65	87.86	100.00	100.00

P.R. SPRING

	Weights %	Grade, %		Recoveries, %	
		Tar	Sand	Tar	Sand
Conc.	20.38	70.50	29.50	99.12	7.03
Tail	79.62	.16	99.84	.88	92.97
Feed	100.00	14.50	85.50	100.00	100.00

However, there is a negative aspect related to the results presented in Table II in that, an excessive amount of sodium silicate (20% by weight of the tar sand feed) was added as a wetting agent. When the sodium silicate addition was reduced to 5%, the digested bitumen became very sticky and a much lower concentrate grade of 53.5% tar was obtained. Under these conditions the recovery was 89%. The inferior response at low sodium silicate additions may be related to the pH of the digested pulp, whose critical role in bitumen displacement has been recognized elsewhere (4,6,10).

Tar sands in general are slightly acidic so that they will consume base when contacted with a caustic solution. Consequently, titration curves of Utah tar sands with sodium silicate and other caustic solutions ought to be determined in order to be able to predict the pulp pH during digestion. Equilibrium pH values ranging from 8.0 to 8.5 proved to be successful in processing Athabasca tar sands (4), but corresponding evidence for Utah tar sands has not been reported.

Samples from Sunnyside do not seem to be amenable for Hot Water extraction. These results can be explained based on the low bitumen content of these samples (less than 8%, by weight) which gives a brittle nature to the feed material. In fact, the samples obtained could be easily ground to -65 mesh or finer in a conventional tumbling mill. Such was not the case with samples from Asphalt Ridge and P.R. Spring which could only be reduced in size to a limited extent by extrusion. Also, as can be observed in Figure 1, there is a remarkable constitutional difference between low and high grade tar sands. Unlike the Sunnyside sample (Figure 1c), Asphalt Ridge and P.R. Spring samples (Figure 1a and 1b, respectively) exhibit a continuous bituminous matrix surrounding the sand grains. With such samples shear forces can be transferred to the bitumen-solid interface through the continuous matrix. As a result, deformations occur at the interface which allow for the aqueous solution to advance to the interface and wet the sand grains. In other words, a high shear stress field helps to destroy kinetic barriers such as those mentioned before at the end of the section on Fundamentals. On the other hand, the bitumen content of Sunnyside samples is low and is not present as a continuous matrix; hence the tar sand particles are free flowing inside the reaction vessel. In such cases, it appears that shear stress cannot be transferred to the bitumen-solid interface for phase disengagement. Alternative processes such as thermocracking in fluidized bed reactors seem to be more appropriate to process the low grade tar sands.

In most of the experiments, the digestion time was 15 min. Separation was not significantly improved by increased digestion times indicating that residence times shorter than 15 minutes may be acceptable.

Bitumen Characterization

The flow properties of a fluid are completely described by the relationship between the shear stress applied to a fluid element and the rate at which the element is deformed as a result of the applied stress (shear rate). This relationship is characteristic of the fluid and is referred as its flow curve. Usually, flow curves are determined experimentally and the collected information is then correlated on the basis of some semi-theoretical models, such as the well known Newton's law of viscosity. A Newtonian fluid is such that its viscosity, defined as the proportionality constant between the

applied shear stress and the resulting shear rate, is constant, equal to the slope of the flow curve.

Flow curves for Athabasca and Asphalt Ridge bitumens are shown in Figures 5 and 6 for various temperatures. The essentially linear response for both samples indicates that both bitumens behave as Newtonian fluids, i.e. the viscosity is independent of the rate of shear and can be calculated from the slope of the lines, at a given temperature. Perhaps of more practical significance is the fact that the viscosity of the Utah bitumen is about two orders of magnitude greater than the viscosity of the Canadian bitumen in the temperature range studied, as shown by the plots presented in Figure 7. This accounts for the fact that the Athabasca tar sands can be digested in a simple tumbling mill, while the Utah tar sands seem to require intense shear conditions. The measured temperature dependence of both bitumens follows very closely a functional relationship of the type:

$$\mu = Ae^{B/T}$$

where

μ = viscosity, poises

T = temperature, $^{\circ}\text{K}$

A, B = empirical constants

In general, this type of temperature dependence is obtained for Newtonian fluids. Further, viscosity measurements of Athabasca bitumen agree well with data reported in the literature (4).

An apparent activation energy on the order of 27 (kcal/mole) was calculated for Utah bitumen from the data in Figure 7a, indicative of the fact that momentum transfer is accompanied by rather significant structural transformations.

Future studies on the effect of organic solvents on the viscosity of bitumen is contemplated as a part of this research program.

SUMMARY AND CONCLUSIONS

Preliminary results indicate that effective disengagement and separation of bitumen from high grade Utah tar sands (12% by weight bitumen) can be achieved by a hot water process, involving the addition of wetting agents, digestion under high shear conditions, and final separation by froth flotation. Coefficients of separation as high as 0.95 have been realized for these high grade systems. On the contrary, effective separation of low grade Utah tar sands (less than 8% by weight bitumen) has not been achieved.

The processing technique described in this article differs significantly from the one used in processing Canadian tar sands, mainly because of a considerable difference in the viscosity of the two bitumens. Experimental data have established that Utah bitumen, which is shown to behave as a Newtonian fluid, is at least two orders of magnitude more viscous than Athabasca bitumen.

Thus far in the research program, the following preliminary conclusions have been obtained:

1. Effective separations by HWP can be attained for high grade tar sands.

2. Rather large additions of alkaline wetting agents are required for effective separation.
3. For the experimental conditions reported, satisfactory phase disengagement is achievable with digestion times of 15 min or less.

ACKNOWLEDGEMENTS

The authors wish to acknowledge financial support of the Department of Development Services of the State of Utah, Mobil Foundation, and NSF Grant AER 74-21867.

REFERENCES

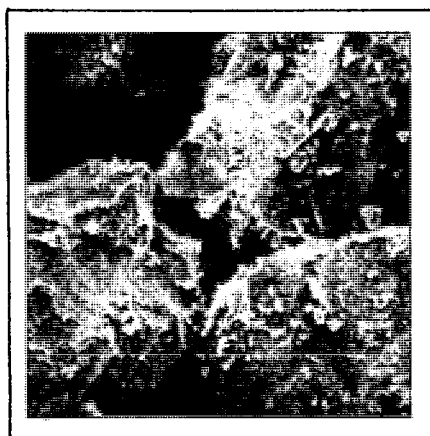
1. Ritzma, H.R., "Oil Impregnated Rock Deposits of Utah", Utah Geological and Mineralogical Survey, Map 33 (1973).
2. Clark, K.A. and Pasternack, D.S., "Hot Water Separation of Bitumen from Alberta Bituminous Sand", Ind. and Eng. Chem., Vol. 24, No. 12, 1932, p. 1410.
3. Clark, K.A., Research Council of Alberta, Report 8, Annual Report 1922, Edmonton, Alberta, Canada, 1923, p. 42-58.
4. Camp, F.W., "The Tar Sands of Alberta, Canada", Second Edition, Cameron Engineers, Inc., Denver, Colorado (1974).
5. Innes, E.D. and Fear, J.V.D., "Canada's First Commercial Tar Sand Development", p. 633 of "Proceedings of the 7th World Petroleum Congress", Vol. 3, Elsevier Publishing Co., 1967.
6. Leja, J. and Bowman, C.W., "Application of Thermodynamics to the Athabasca Tar Sands", Canadian Journal of Chem. Eng., Vol. 46, December, 1968, p. 479.
7. Bowman, C.W., "Molecular and Interfacial Properties of Athabasca Tar Sands", p. 583-640 of "Proceedings of the 7th World Petroleum Congress", Volume 3, Elsevier Publishing Co., 1967.
8. U.S. Bureau of Mines, Report of Investigations No. 4004.
9. Schulz, N.F., "Separation Efficiency", Trans. SME/AIME, Vol. 247, 1970, pp. 81-87.
10. Seitzer, W.H., "Hot Water Processing of Athabasca Oil Sands: I. Oil Flotation in a Stirred Reactor", Am. Chem. Soc., Div. of Petroleum Chemistry, Preprints 13 (2), p. F18-F24 (1968).



a. ASPHALT RIDGE
Bitumen Content: 13%, by weight



b. P.R. SPRING
Bitumen Content: 12%, by weight



c. SUNNYSIDE
Bitumen Content: 8%, by weight

Figure 1. Scanning Electron Photomicrographs of Utah
Tar Sand Samples. Magnification: 200X.

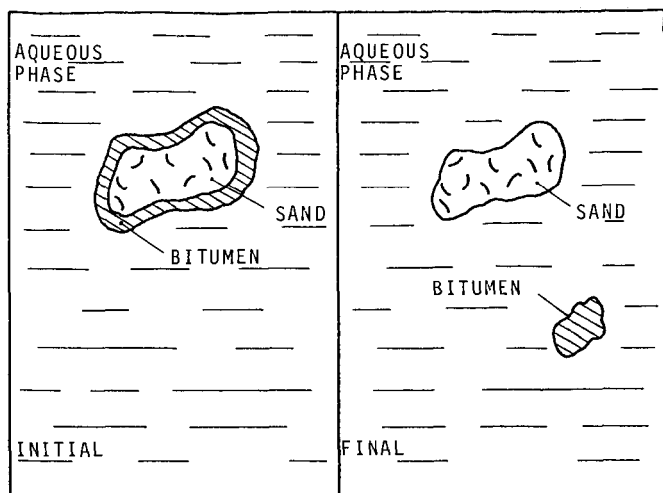


Figure 2. HOT WATER PROCESS. Bitumen Displacement.

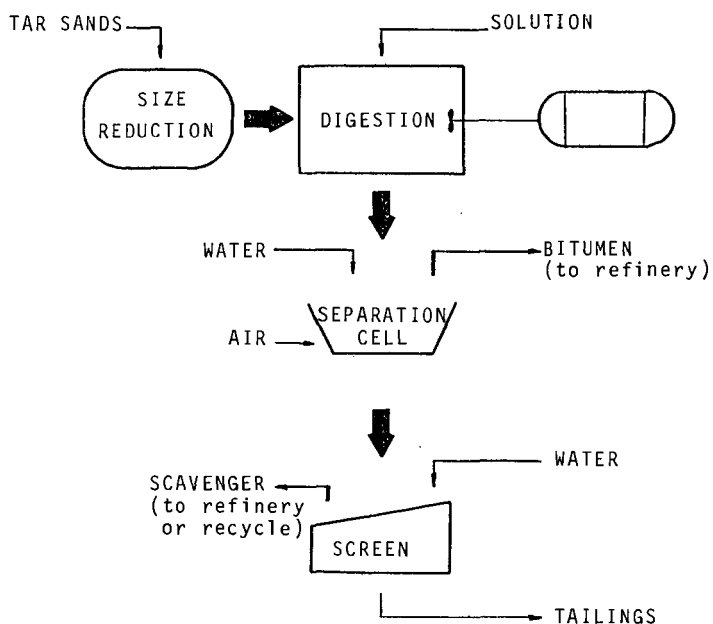


Figure 3. HOT WATER EXTRACTION PROCESS. Flowsheet.

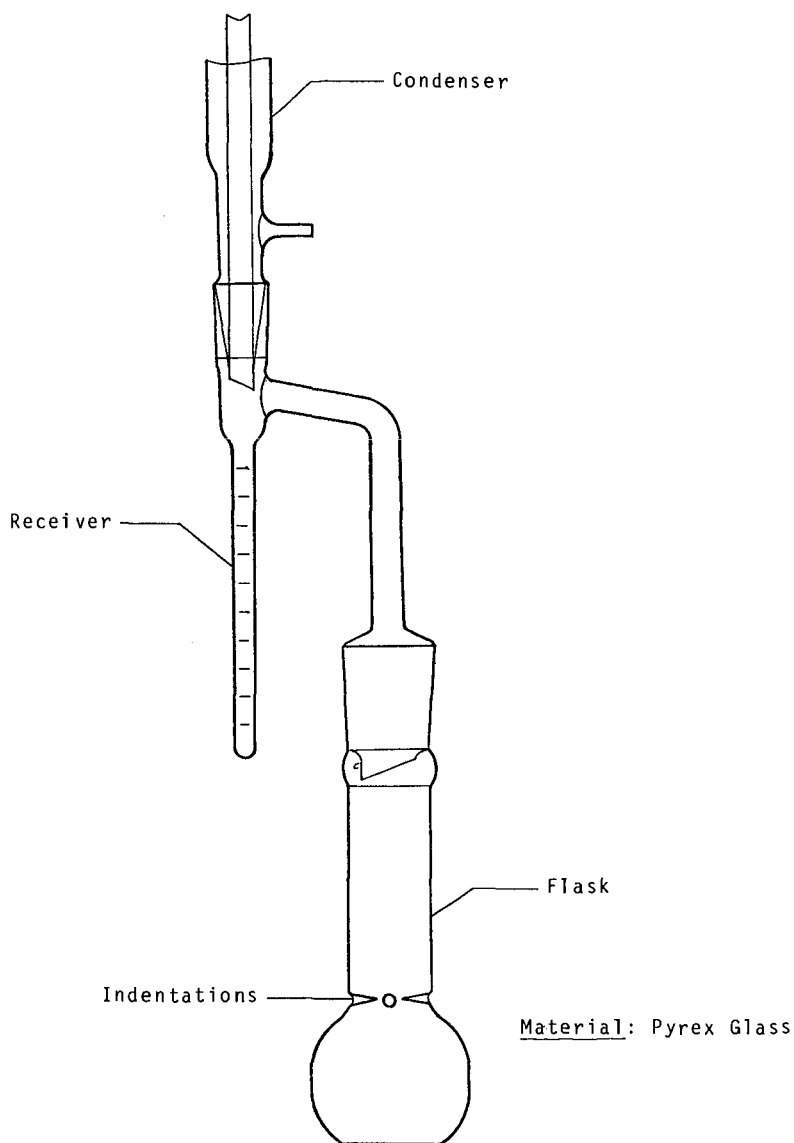


Figure 4. Dean & Stark Tube Assembly.

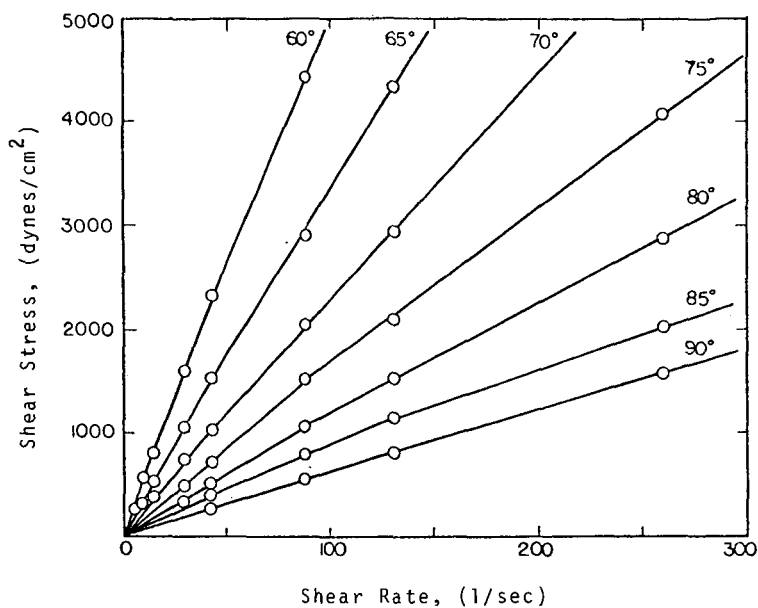


Figure 5. Flow Curves of Athabasca Bitumen.

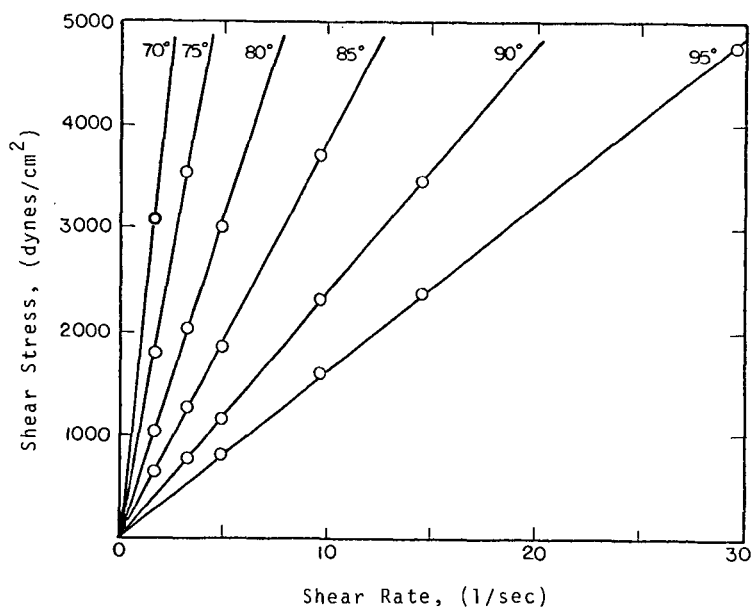


Figure 6. Flow Curves of Asphalt Ridge Bitumen.

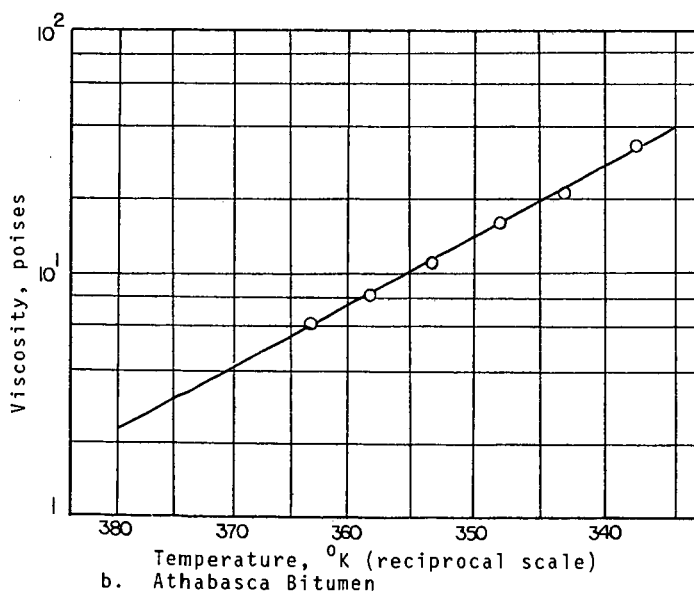
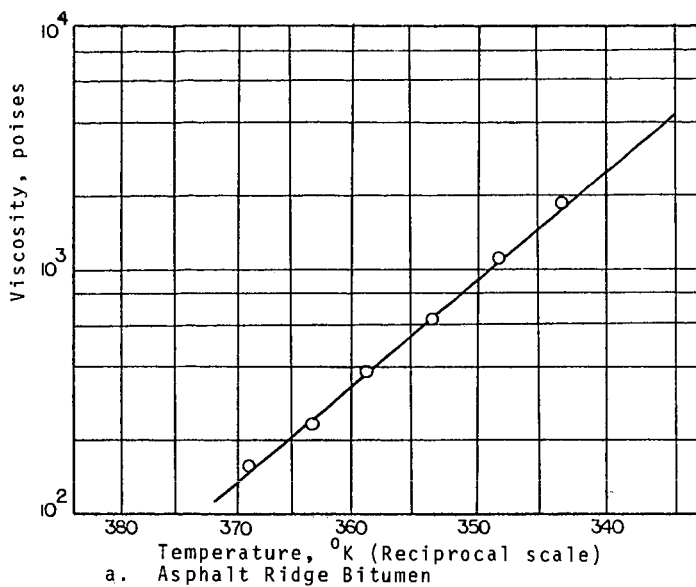


Figure 7. Effect of Temperature on the Viscosity of Asphalt Ridge and Athabasca Bitumens.

A PROPOSED DEVELOPMENT PLAN FOR A MODIFIED
HORIZONTAL IN SITU EXPERIMENT

R. L. Wise, H. G. Harris, and H. C. Carpenter

Laramie Energy Research Center
and The University of Wyoming
P. O. Box 3395 University Station
Laramie, Wyoming 82071

INTRODUCTION

The oil shales of Colorado, Utah, and Wyoming are a potentially important energy resource for the U.S., and a possible significant contributor to future national energy independence. Since approximately 80 percent of these shale deposits are on federal lands, the Government has a prime responsibility to ensure their efficient and environmentally sound utilization.

Primary efforts to develop oil shale to date have emphasized a combination of mining and surface retorting. An alternative approach, in situ (in place) retorting, has not been extensively investigated. If an economically viable in situ technology could be developed, however, it could increase the "recoverable reserves" of oil shale, reduce a shale oil industry's water requirements, and mitigate the environmental impacts normally associated with mining and aboveground processing.

An Accelerated National Oil Shale In Situ Research Program was accordingly formulated by a U.S. Government Interagency Oil Shale Panel (1) in March 1975.¹ A principal objective of the research and development program is to attempt to "advance the technology for in situ production of shale oil to the point of commercial feasibility by the early 1980's," with appropriate accompanying environmental safeguards. Both true in situ and modified in situ research projects to produce shale oil are included in the Accelerated Program.

ERDA assumed primary responsibility for implementing the research and development portion of the program, which closely relates oil shale leasing activities of the U.S. Department of the Interior with the activities of ERDA. The accelerated program development plan includes two main and coordinated phases. The first of these is the offering for sale of two tracts of Federal oil shale lands limited to development by in situ methods. The second phase is the research and development plan which is to be guided by the results (or lack of results) of the leasing phase.²

Lack of industrial interest in Wyoming oil shale, which is typical of lean, thin-seam oil shale deposits throughout Wyoming, Colorado, and Utah, as indicated by the absence of nominations, makes it imperative for the Government to assume a primary role in the long-range, high-risk research on the substantial thin-seam oil shale resource values. The present ERDA program on Wyoming oil shales consists of the research on true in situ processing now being conducted by the Laramie Energy Research Center.

¹ A joint announcement of the program was made by the Department of the Interior and ERDA at a Government/Industry Conference in Washington, D.C., March 19, 1975.

² Results from the Department of the Interior's call for nominations of in situ tracts in mid-1975 yielded six tracts nominated in Colorado and three tracts nominated in Utah. The nominations were made by six companies. No tracts were nominated in Wyoming. A tract selections committee selected one tract in Colorado and one tract in Utah. Two alternate tracts, both in Utah, were designated by the committee.

The proposed development plan is concerned with horizontal modified in situ research, as discussed in the Accelerated Program, and specifically with the technical, economical, and environmental feasibility of applying a combined horizontal mining and retorting technology to shale oil production from thin-seam oil shale deposits. The initial experiments are to be conducted in the 30- to 40-foot-thick shale strata of either the Laney or Tipton members of the Green River Formation on White Mountain, 5 miles northwest of Rock Springs, Wyoming.

The principal objectives of the proposed project are as follows:

1. Develop modified in situ recovery engineering expertise on lean, thin-seam oil shale deposits.
2. Determine optimum underground support design to minimize surface subsidence.
3. Develop mining and explosive blasting techniques to ensure desired void volume and to maximize resource utilization.
4. Design retort configurations to maximize resource recovery with minimum environmental impact.
5. Investigate heat effects during retorting, including temperature gradients of walls and surroundings.
6. Establish the effect of vertical versus horizontal sweep of the oxidizing or hot retorting gases.
7. Examine the effects of retorting variables (e.g. shale grade, porosity, gas composition) on shale oil yields and shale oil quality.
8. If possible, develop technology for sensible heat and additional hydrocarbon recovery from previously retorted shales.
9. Determine the economic feasibility of modified in situ horizontal retorting technology in thin-seam oil shale strata.

BACKGROUND

The Laramie Energy Research Center is a part of the nationwide facilities of the Energy Research and Development Administration. LERC was opened in July 1924, through a cooperative agreement with the Bureau of Mines and the University of Wyoming. Initial work was directed at developing petroleum resources in the Rocky Mountain region, and research was focused on improving methods of refining high-sulfur, asphalt-bearing crude oils of Wyoming.

A shift of emphasis at LERC to oil shale occurred as a result of the Synthetic Liquid Fuels Act enacted in 1944, and since that time an increasing fraction of the LERC research and development effort has been devoted to oil shale. Since the early 1960's, LERC oil shale work has been primarily concerned with in situ retorting techniques. LERC currently employs over 245 engineers, scientists, and supporting staff, and is responsible for directing several field programs.

Since the early 1960's, work on oil shale at the Laramie Energy Research Center has been concentrated on development of in situ retorting methods. The major effort directed at vertical retorting has been carried out in a 10-ton pilot-scale batch retort and a 150-ton semiworks batch retort. The overall objective of this experimental program has been to demonstrate the feasibility of forward combustion retorting of randomly sized, mine-run shale, i.e. the type of retorting that would most likely be employed in a vertical, in situ chimney retort.

In the Occidental modified in situ vertical process approximately 15 percent of the shale is mined away and blasting expands the remaining shale to create a chimney, called the retort. The expanded, or rubblized, shale is then ignited at the top and vertical retorting is employed for oil production. Air is carefully diluted with recycle gas to give the desired oxygen concentration. To date three chimnies (each with approximate dimensions of 30 feet x 30 feet x 70 feet) have been retorted; a substantially larger fourth chimney (120 feet x 120 feet x 270 feet) is currently being retorted.

Total investment by Occidental was expected to reach approximately \$38 MM by year end 1975.

While operating details of the Occidental process are proprietary, Occidental has acknowledged the importance of experience gained by LERC in guiding their development work. Initial experiments by Occidental were based primarily on results obtained in the 150-ton retort.

Occidental has reported (2) approximately 70 percent recovery of oil based on Fischer assay, while the net energy efficiency of this process varies from 55 to 80 percent for oil shale of from 10 to 40 gallons per ton assay. The ratio of energy output to energy input is from 10 to 24 for these shales. Occidental has stated that the energy efficiency could be increased by optimizing the process. For example, the energy required for gas compression was more than 50 percent of the total energy input and hence, should be carefully controlled for efficient operation.

In addition to these ongoing studies, numerous other laboratory and field tests have been proposed on variations of the modified in situ vertical retorting process. For example, Lawrence Livermore Laboratory has proposed a modified sublevel-caving mining method prior to in situ retorting, in which it is claimed would, if it were successful, allow \$6 to \$9 per barrel shale oil (3). Retort sizes of 100 x 100 x 300 feet and 250 x 250 x 1,000 feet have been proposed; smaller retorts of 50 x 50 x 120 feet have been termed "noncommercial retorts."

It should be noted that the proposed RISE program is conceptual only, and no such experiments have been conducted. In addition, the proposed development effort follows very closely the work currently underway by Occidental. Finally, this and other proposed techniques are applicable only to the very thick shale beds of Colorado; the thinner shale beds of Wyoming and Utah are not suitable for large-scale vertical retorting.

During World War II, underground pyrolysis of shale was attempted on a semiworks basis (4). Initial work was through private enterprise, but later efforts were supported by the German Navy. Under wartime pressure, premature operation on a larger scale was attempted. Horizontal chambers, 197 feet long, of rubblized shale produced by blasting were ignited at one end and gases exhausted at the other end. First, crosscuts 6.6 feet wide and 7.2 feet high were driven. The sides and roofs were drilled before rubblizing to a depth of 4.9 feet, and one pound of explosive per ton of shale was used. Since 30 to 35 percent of the shale was removed, voids were 30 to 35 percent. The deposits were about 28.2 feet thick, thus retorting the full bed thickness was not achieved due to the mining design. Progress of the combustion front along the top of the rubble was faster than through the bottom. This left unretorted shale at the bottom and resulted in excessive loss of oil by combustion, thus giving a yield of only 30 percent of Fischer assay. Presumably, gas recycle to reduce the oxygen content of the feed gas would have alleviated this, but was not tried. Modified in situ horizontal retorting was thus demonstrated to be feasible, but because of poor mining and retorting procedures resource recovery was poor.

Although not directly associated with modified in situ horizontal retorting, LERC has conducted for several years a field program directed toward development of true in situ horizontal retorting. Research on fracturing oil shale in place by non-nuclear means was initiated in the late 1960's. Three in situ recovery field experiments were designed and conducted by the Bureau of Mines following the fracturing studies. Each of these experiments was based on the concept of igniting the shale in an injection well and forcing hot gases and liquids horizontally through fractures to several recovery wells surrounding the injection well. The hot gases were produced by combustion with compressed air through the injection well.

PROPOSED OVERALL DEVELOPMENT PROGRAM

It is proposed that the overall development program for modified horizontal in situ retorting be divided into five consecutive phases extending over a total of 5 years.

Phase I. Preoperational Studies (approximately 12 months), including analyses of corehole and geologic data and selection of a field site; arrangements for access road rights-of-way; construction and maintenance of access roads; construction of on-site support facilities; arrangement for power, water, and other utilities; selection of subcontractors and consultants, and conduct environmental baseline studies.

Phase II. Preparation of Definitive Experimental Program (approximately 9 months), including development of final mining plan; selection of final retort configuration(s); overall design of experimental rubblizing and retorting program, and associated operation and measurement techniques; preparation of mathematical models of retorting methods; construction of special laboratory support facilities; selection of associated environmental studies.

Phase III. Initial Field Program (approximately 21 months), including development of horizontal mine and initial experimental retorts; conduct of first generation rubblizing and retorting experiments, using direct combustion and also hot gas injection; evaluation of data to identify critical parameters; performance of environmental research studies to quantify accompanying land, water, and air impacts; completion of associated laboratory analyses.

Phase IV. Expanded Field Program and Supporting Studies (approximately 18 months), including modification of initial retort designs; detailed evaluation of retorting parameters; determination of definitive heat and material balances and yields; characterization of product oils, gases, and spent shales; identification and measurement of air emissions, aqueous effluents, leachates, and solid wastes; assessment of environmental impacts on air, water, and land; design of suitable pollution control methods for future in situ field programs.

Phase V. Technical, Environmental, and Economic Evaluation of Commercial Operations (approximately 12 months), including establishment of design parameters for commercial-scale modified in situ retorting; assessment of technical feasibility of commercial-scale in situ plant; analysis of economics of full-scale in situ shale oil production; evaluation of environmental impacts of commercial-scale operations, and control methods required; recommendations regarding industrial in situ shale oil production from thin oil shale strata.

SITE LOCATION STUDIES

LERC has already conducted preliminary studies to identify potential field sites for the proposed research program. Three primary criteria were used to evaluate such sites. First, the shale deposit should be representative of the resource base which will be ultimately available for commercial development by a combined horizontal mining and retorting process. Based on this requirement, only shale deposits of 15 to 25 gpt average richness, with a thickness of approximately 50 feet were considered. Second, the shale deposit should outcrop in order to avoid expensive initial underground mining and site development. Third, location of the deposit should be accessible and in reasonable proximity to a population center, again to minimize field development costs and hardship to field workers.

It should be emphasized that these criteria were specifically employed in evaluation of potential sites for this program's initial field development work. However, results from the R & D program will be applicable to a wide range of thin-bed shales located over a wide geographical area. Other factors, of secondary importance, were

also considered and are discussed below. A number of possible sites were investigated in Colorado, Utah, and Wyoming. Based on the foregoing three criteria, however, the most favorable potential locations were determined to be in the White Mountain region of western Wyoming where two sites have been nominated.

White Mountain is an uplift in which weathering has exposed two members of the Green River oil shale Formation, viz, the Laney and the Tipton (in descending order). The geology and geochemistry of oil shale formation for this region have been described elsewhere (5). The crest of White Mountain runs in a northeasterly direction, and at its nearest point is within approximately 4 miles of Rock Springs, Wyoming. Both the Laney and the Tipton members outcrop in this region, and shales of suitable richness and thickness occur in these members. Thus, all primary criteria are met by this region. In addition, this region is only a few miles from LERC true in situ field test sites, and therefore offers a favorable strategic location for future project management.

In order to pinpoint specific sites suitable for the field studies, LERC initiated in 1974 a corehole program to accumulate data on both the Laney and Tipton members of the Green River oil shale Formation. Extensive corehole data has been obtained at two separate sites. To date six coreholes have been drilled and assayed at a total cost of approximately \$62,000, and further work is planned. Detailed information on the White Mountain corehole program is contained in LERC core analysis files (6). Location of the two sites is given in figure 1. Although both of the sites are considered suitable, site 1 in the Laney member is somewhat favored and has been used in preliminary planning and cost estimating. Final site selection will be based on preparation of the definitive experimental program.

In addition to the corehole program, environmental studies have been initiated in the White Mountain region and a report titled "An Environmental Reconnaissance Study for Sweetwater County In Situ Oil Shale Research" has been completed (7). The purpose of the report is to identify the regulatory requirements, agencies, and environmental components of concern in the research area. These data will be used in preparing the Environmental Assessment Report (EAR) for this project. To date approximately \$35,000 has been invested in the environmental studies. These preliminary studies represent a substantial effort in better defining the modified in situ horizontal retorting program.

MINING PROGRAM

Objectives

The mining related objectives of the program are as follows:

- (a) Develop blasting techniques to optimize oil yield by obtaining a uniform fragmentation and void distribution with the retort mass using conventional mine blasting agents and equipment.
- (b) Confirm theoretical design data relating to heat effects on mine pillars and openings.
- (c) Design retort configuration based on data from a and b.
- (d) Design general mine plan based on c, with adequate mine structural components to minimize environmental impact.

The first objective of determining the correct blast hole drilling and blasting procedures must be incorporated with retorting technology to complete the unit retort configuration.

In addition, the confirmation of the blasting method will define the void ratio which in turn determines the quantity of mined material to be handled and disposed of on surface.

Other mining costs such as tunnelling, raising, and blast hole drilling can be estimated with reasonable reliability.

The normal swell characteristic or increase in volume between a solid block and its blasted broken volume is 53 percent for most oil shale formations; this results in 35-percent voids. In order to reduce the void ratio below 35 percent, a finer granulometry of the rubble can be obtained by using more explosives, and varying the sequence of the detonation in order to vibrate or consolidate the broken mass to obtain the necessary volume and void ratio. The determination of the percentages of voids can only be ascertained by on-site testing due to the physical variations in all rock formations.

Occidental Oil Shale, Inc., operators of a large in situ demonstration project in Colorado have indicated that successful retorting has been accomplished using a 15-percent void volume while a 10-percent void volume resulted in poor oil recoveries. Therefore, the results of this research must determine the practical limits for the void volume.

Assuming ideal particle size and void distribution, the probably void volume would be 28 to 32 percent. This appears to be reflected by the German experience, as discussed in an earlier section, with regard to explosives consumption of 1 pound per ton of shale, which is double the quantity required for normal efficient blasting operations for room-and-pillar mining of shale. It is assumed the objective of the Germans was to obtain a large percentage of small-size fragments in the total granulometry.

Pilot Mining Plan

The pilot mining plan, as currently envisioned, will be to first drive a double tunnel access into an offset retort mining area. The entry adits or tunnels will be approximately 10 feet high x 12 feet wide and the retort area will be positioned as close as possible to the tunnel portal area, but beyond any effects of surface weathering and jointing. This is assumed to be approximately 400 feet from the portal. A retort access tunnel will then be driven a sufficient distance to initially permit laying out of several test areas. The location and direction of the mine workings will be oriented to work up the dip of the rock formation.

The portal bench will be leveled to provide space for a ventilating fan, administrative and change facilities, material storage and warehousing, and retort support facilities. The location will take into consideration potential flooding, waste rock disposal, accessibility, and the horizon to be mined. The bench size will be approximately 100 feet by 200 feet.

As the retort access drift is started from the adits at the floor level of the retort mine bed, a ramp access to the top level of the bed will be excavated and a top level retort access drift will be driven above the one on the main or floor level.

A width of 35 feet has been assumed as the thickness for the pillar walls. It is further assumed the mining horizon will be 40 feet thick and that the overburden will be approximately 800 feet. The 35-foot-wide pillars will have to be verified, particularly with regard to the effect of retorting temperature. The first experimental area will be set back 70 feet from the axis of the main access adits and 40 feet from the retort access drift.

The first retort stope area is suggested to be 40 feet x 40 feet and opened at the bottom level to begin testing drill hole and blasting methods. The minimum length of blast hole will be 20 feet, from which data can be derived in scaling up to longer and larger blasts. It will be necessary to excavate the rubble from this area to determine granulometry, and to assess the drill pattern efficiency. This

mined-out space can then be used for retorting experiments by recharging rubble to obtain results from a known or predetermined base.

The second retort will then be laid out to incorporate the experience of the first. Area will also be allowed to drive a second parallel retort access drift, if required, on both the main and top levels.

The development headings will be ventilated by exhausting through a vent pipe. The fans will be mounted in series as the distance from the portal increases. A raise to the surface will be bored for improved ventilation when the initial system reaches its limits of effectiveness.

The above-described pilot mining plan is presented schematically in figure 2.

Commercial Projection

A preliminary concept has been projected for a commercial, thin-seam, modified in situ oil shale project. Based on available information, it is believed that for a commercial project to be viable, surface retorts would have to be included to supplement in situ retorts. The surface retorts would process that shale which has to be mined to provide the void volume for in situ retorting.

A theoretical mining plan for a commercial in situ project has been developed and is shown schematically in figure 3. The horizontal retort having the dimensions of 40 feet high by 60 feet wide by 500 feet long would be prepared. In a single panel the first step would be to drive an entry 20 feet high by 40 feet wide by 500 feet long to provide a void volume of about 30 percent. A radial jumbo would be used to drill the blast holes. Blasting, or rubblizing, would be accomplished in 20-foot steps, while backing up through the entry. Before blasting each 20-foot section, a trench would be bored in the floor of the entry in which would be placed the combustion airline and a perforated oil drainline. The most economical, simplest system must be used for providing combustion air, oil draining, and flue gas removal.

The basis of the commercial projection is 50,000 bpd total oil production, using the following assumptions:

1. 50,000 tons/day of oil shale will be mined for creating the void volume; this material will be surface retorted.
2. 100,000 tons/day of oil shale will be rubblized for in situ retorting.
3. The shale seam will be 40 feet thick and will contain 20 gpt by Fischer assay.
4. The oil recovery for the surface retort will be 100 percent.
5. The oil recovery for the in situ retort will be 50 percent.
6. The combustion advance rate will be 1 ft/hr, which could be accomplished only by fine rubblizing.

For the commercial operation, 1-2/3 panels of the 40-foot by 60-foot by 500-foot panels would have to be mined and rubblized each day. To produce 25,000 bpd of in situ oil, 33 of the panels would simultaneously be in operation.

To give some concept of the aerial extent of the operation, the advance of the mining operation would be approximately 3 acres per day. The amount of surface area required for a 15-year operation would be around 20,000 acres or 30 square miles.

The purpose of pilot mining as described in the preceding subsection, would be to provide confirming data for the commercial operation.

RETORTING PROGRAM

Retorting Parameters

Modified horizontal retorting refers broadly to techniques for recovery of oil from shale by: (1) Horizontal mining to create the desired void fraction, (2) rubblization through explosive fracturing, and (3) retorting of the horizontal bed by injection of oxygen or hot sweep gases. The actual retorting process may be through horizontal sweep of the oxidizing or hot retorting gas, by vertical sweep of the gases via a gas distribution system, or by a combination of the two. A principal objective of the proposed program is to establish the efficiency of these possible retorting techniques.

It is generally accepted that there are five primary variables which control in situ retorting techniques: (1) Shale richness (gpt), (2) void volume associated with the shale rubble, (3) oxygen content of the retorting gas medium, (4) cross-sectional area of the retort, and (5) height or length of the retort. Secondary variables associated with each of these primary variables include product recovery (gas and oil), superficial gas velocity, swell factor, burn rate, retort life, retort production, and many more.

LERC has conducted tests using 10- and 150-ton aboveground retorts designed to simulate in situ retorting conditions since 1967. A great deal of the information from these retorts has been utilized by Garrett Research, Inc. (now Occidental Oil Shale Corp.) to develop their in situ process currently being tested near DeBeque, Colo. Since very little information is available concerning the Garrett process and its possible application to thin-bed shales, optimum values for the various retorting variables are not yet known. In order to provide this information, and specifically to develop in situ techniques to recovery oil from thin-seamed oil shale deposits, a series of tests have been designed to provide information concerning the retorting variables previously mentioned.

Based on results from the 10- and 150-ton aboveground retorts, oil recovery is a function of the superficial gas velocity and oxygen content of the retorting gas stream. Initial test conditions will be selected to coincide with ranges that have yielded the best results in the 150-ton retort. These conditions would have the following ranges.

<u>Retorting variable</u>	<u>Range</u>
void volume	15 - 40 pct
oxygen content	14 - 18 pct
air ratio	12,000 scf/ton
retorting rate	0.1-2.0 ft/hr
retorting area (width, length)	40 x 40 - 60 x 500 ft
retort height	25-40 ft

Methods of Heating

The major techniques for retorting the rubblized shale produced in the modified horizontal in situ program include (1) direct combustion of the carbonaceous residue on the spent shale, and (2) injection of hot gases (e.g., hot recycle gases) into the rubble bed. It is also possible to use hot fluids injection (e.g., superheated steam), but this is not initially contemplated for the White Mountain sites. Flexibility of experimental design will allow application of appropriate techniques at selected decision points.

Direct Combustion. This is the conventional method of in situ retorting, which is essentially an underground adaptation of surface gas combustion retorting. The bed of rubblized shale is ignited at the top with a mixture of air and gaseous fuel. As combustion proceeds, a downward-moving heat front retorts the shale beneath it. The shale oil vapors condense on the cold shale below. The resulting shale oil drains to the bottom and is pumped to the surface from collecting trenches

on the floor of the chimney. Approximately 45 percent of the retort gases produced are recycled to the rubble bed and burned for additional heat. The remaining gas is withdrawn. Net recovery of oil is expected to be approximately 50 percent of Fischer assay.

The major disadvantage of the process is the production of large quantities of low Btu gas (50 to 150 Btu/cu ft) at about 3 psig pressure. This gas cannot be vented directly to the atmosphere. In addition, if it is less than 100 Btu/cu ft heating value it will require either catalytic furnaces or supplemental fuel for disposal by burning. It might conceivably be used for power generation in specially designed turbines used on site, but this may not be economical.

Injection of Hot Gases. If hot gases are used for heating instead of in situ combustion with air, a retort offgas of 500 to 800 Btu/cu ft is obtained. One method of producing these hot gases is to heat recycle retort gases to around 1200° F in an external furnace, using approximately 5 percent of the recycle gas itself as a fuel in the furnace. The fuel gas portion of the recycle gas, of course, would require amine treatment for H₂S removal prior to use as external furnace fuel. Hydrogen sulfide removal would also be required for the 500 to 800 Btu/cu ft gas removed from the system for use in power generation, etc.

One alternative to the above method would be to utilize a heated gas other than retort recycle gases as a heating medium. Hot methane (hot natural gas) has been employed in the past for this purpose.

In order to recover the heat from the final bottom one-third of the rubble bed it has been suggested that, when exit gas temperatures from the bed reach approximately 200° F, the residual lower hot zone be advanced by recycling cooled product gases from an adjoining vertical retort.

Evaluation of Retorting Methods

General. The retorting methods selected from those described above will be evaluated on the basis of oil yield, oil quality, gas yield, gas quality, surface subsidence, thermal pollution, air pollution, subsurface pollution, and on-stream efficiency.

ENVIRONMENTAL RESEARCH PROGRAM

The environmental disturbances generated by the mining and in situ retorting covered in this proposal will be addressed by a concurrent research program designed to generate data on these concerns. The areas of research will involve impacts to land, water, and air resources. The overall environmental research program will be designed to accomplish the following: (1) To characterize the existing environment before research commences in the field, (2) to monitor, sample, and completely analyze the effluents from the various process steps, and (3) to continue residue studies and reconstitute the area after research work has progressed beyond the operational phase. A phasing diagram showing scheduling of necessary environmental work is shown in figure 4.

Close coordination of the research will be maintained with appropriate State of Wyoming departments and agencies. In addition, assistance of the University of Wyoming will be integrated into the program. Also, close on-site supervision of the environmental aspects of the experiment will be monitored by the office of the Environmental and Conservation coordinator of LERC for the Assistant Administrator of Fossil Energy.

Program Costs

A preliminary cost estimate for the total 5 year program was \$30,400,000. This includes \$1,700,000 total initial mining capital cost and \$2,900,000 processing and instrumentation capital cost.

The total project capital, operating, labor, and material costs for the 5-year program are as follows:

	Fiscal Year				
	1977	1978	1979	1980	1981
Capital	120	5,000	9,000	5,000	2,000
Subcontracts	210	1,890	2,760	1,500	720
Materials and Supplies	300	500	700	500	200
Total cost \$,000	630	7,390	12,460	7,000	2,920

Total, 5-year program \$30,400,000

CONCLUSIONS

1. Approximately one-third of known resources of oil shale occur in deposits that range from 15 to 25 gallons/ton in a seam thickness up to 50 feet at variable depths (100 to over 2,000 feet).
2. Much of the lean, thin-seam oil shale deposits occur on federal land, primarily in Utah and Wyoming, thus the U.S. Government has a very substantial investment in this area.
3. Economic recovery of this resource, using technology currently under development, is problematical. This fact was exemplified by industry when no bids were received on the Wyoming tracts.
4. Development of true in situ horizontal techniques to the point of commercialization requires a technological breakthrough. One promising alternative for development of thin-seam oil shale deposits is through modified horizontal retorting.
5. A modified horizontal experiment has been developed by the LERC engineering staff which includes two prospective sites with core analysis nearly complete, initial baseline environmental studies underway, a mining and retorting plan that indicate commercialization possibilities both from an economic and environmental standpoint, as well as an extensive environmental monitoring program.
6. LERC has a broad background and experience in collection of data and direction of field programs involving in situ oil shale development. This background should prove invaluable to ERDA in application to future in situ work.

REFERENCES

1. Accelerated Oil Shale In Situ Research--A National Program. Interagency Oil Shale Planning Panel, March 1975.
2. Cha, C. Y., and D. E. Garrett. Quart. Colo. School of Mines, v. 70, No. 3, 1975, pp. 31-39.
3. Lewis, A. E., and A. J. Rothman. Rubble In Situ Extraction (RISE): A Proposed Program for Recovery of Oil from Oil Shale. March 5, 1975.
4. Caldwell, J. M., and G. H. Smith. Wurttemberg Shale Fields. B.I.O.S. Trip No. 2409, October 1949.
5. Smith, J. W. Geochemistry of Oil-Shale Genesis, Green River Formation, Wyoming. Wyo. Geol. Assoc. Guidebook, 1967, pp. 185-190.

6. LERC Files. Available upon request to A. W. Decora, Laramie Energy Research Center, Laramie, Wyo.
7. Kerr, R. D., W. F. McTernan, et al. An Environmental Reconnaissance Study for Sweetwater County In Situ Oil Shale Research. Wyoming Water Resources Research Institute, June 19, 1975.

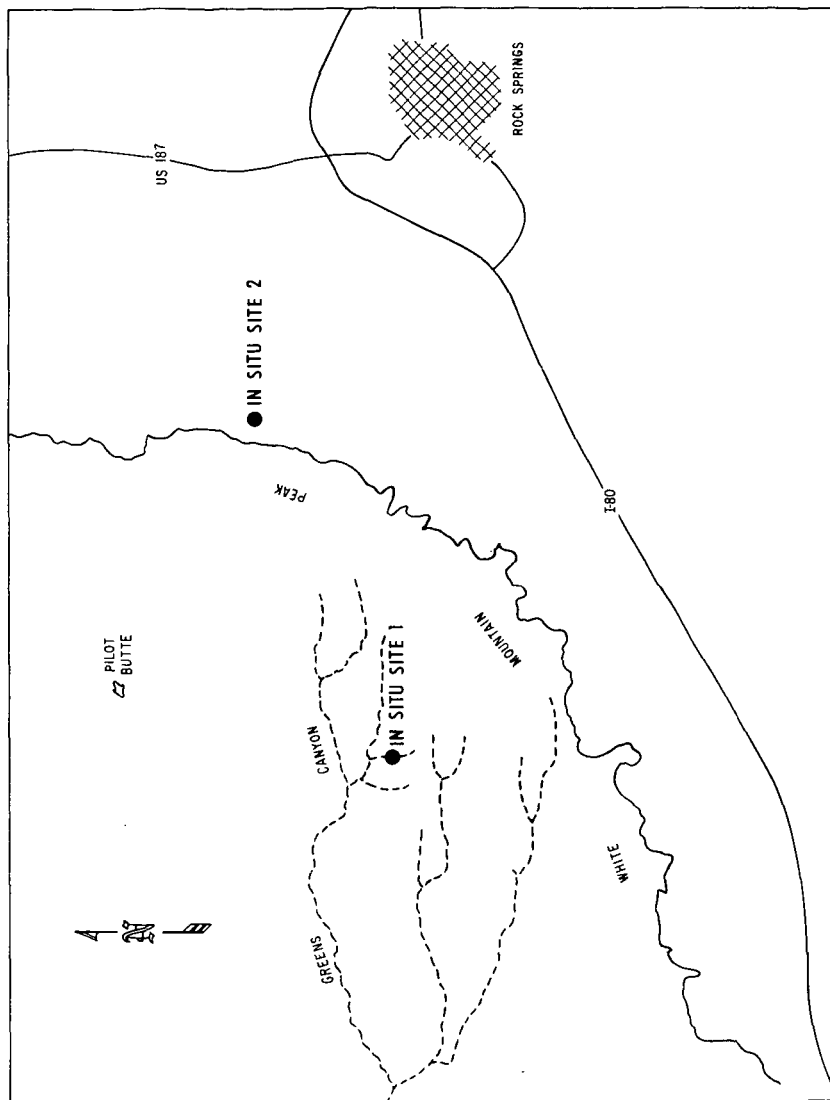


FIGURE 1. - AREA MAP FOR MODIFIED HORIZONTAL IN SITU EXPERIMENT

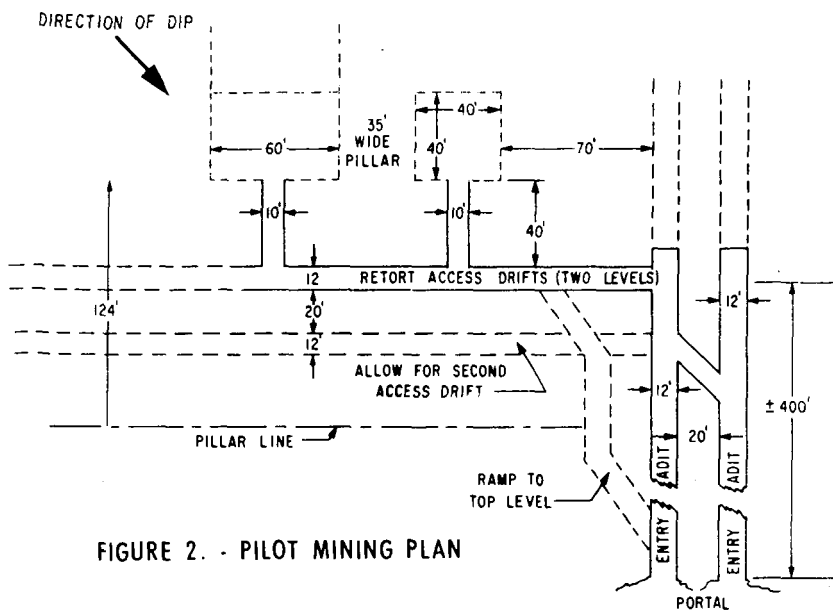


FIGURE 2. - PILOT MINING PLAN

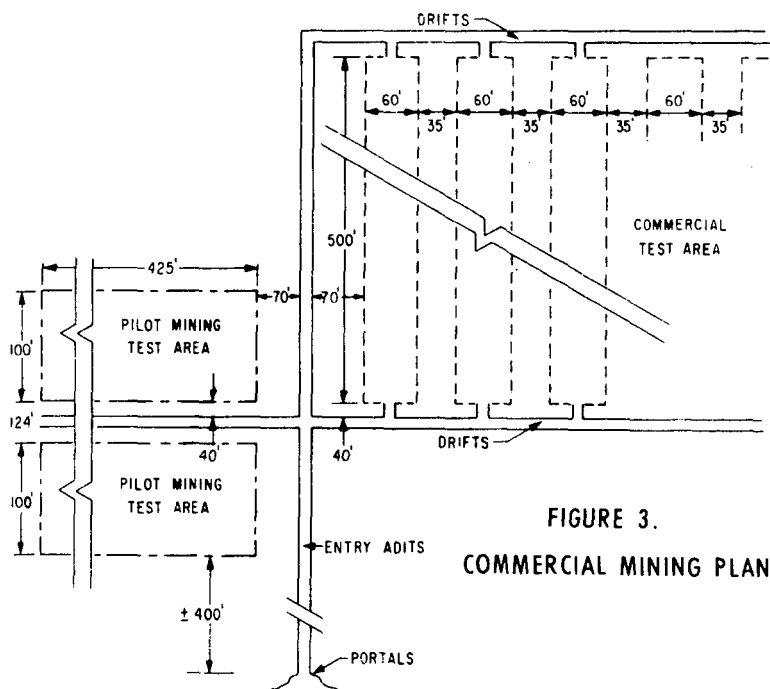


FIGURE 3.
COMMERCIAL MINING PLAN

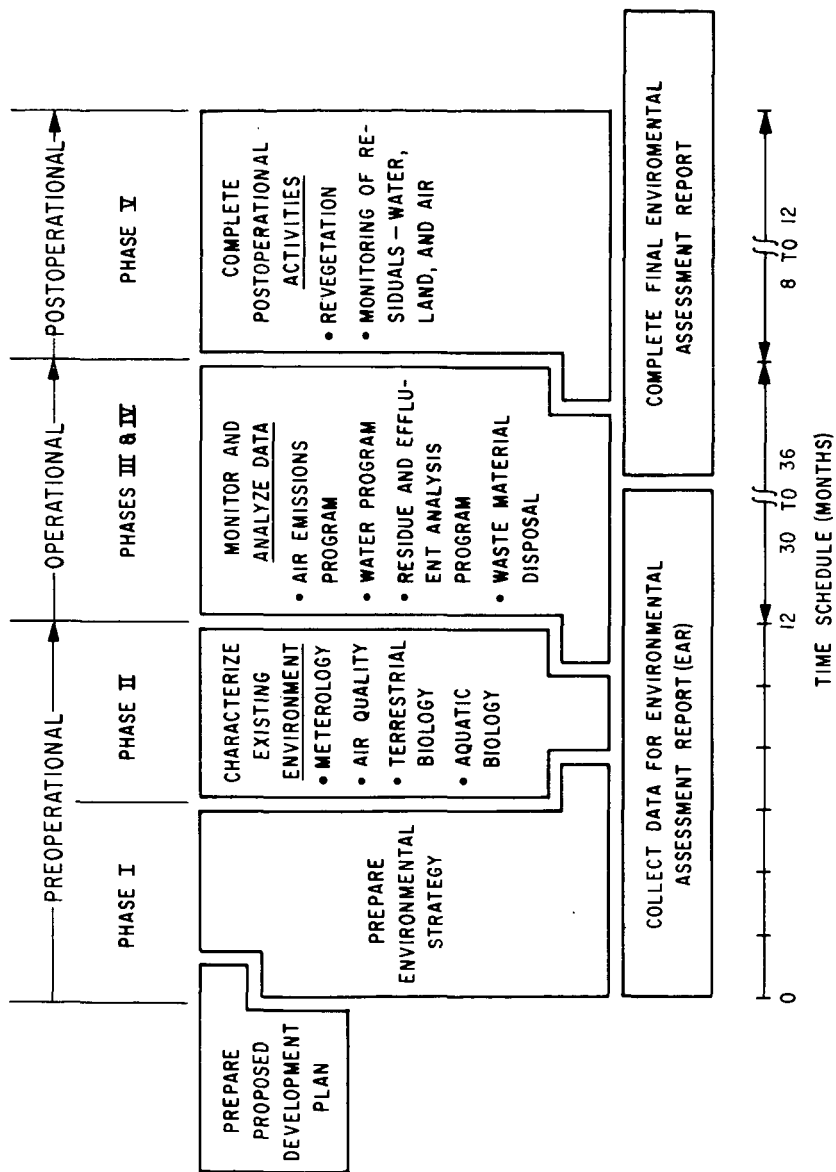


FIGURE 4. - PHASING DIAGRAM—ENVIRONMENTAL RESEARCH

OIL DEGRADATION DURING OIL SHALE RETORTING*

J. H. Raley and R. L. Braun

Lawrence Livermore Laboratory, University of California
Livermore, California 94550

INTRODUCTION

The Lawrence Livermore Laboratory is doing retorting research to support the development of modified in situ processes for production of oil from oil shale such as that described by Lewis and Rothman (1). Mathematical modeling studies (2,3) of in situ retorting indicate that the heat-up time for a shale particle can range from hours (combustion retorting) to months (hot gas retorting). A recent study at this Laboratory (4) reported the oil yields from powdered Colorado shale subjected to a wide variety of thermal histories. This study demonstrated that the oil yield from powdered shale is primarily determined by the amount of decomposition of the liberated oil. The present work supplies further data in support of this conclusion. Also, maximum rates for the thermal decomposition of shale oil are estimated and compared with pyrolysis rates for petroleum fractions.

EXPERIMENTAL

Detailed descriptions of the 92 ℓ /tonne (22 gal/ton) shale sample and of the retorting apparatus and method have been given previously (4). In the retorting procedure the temperature of the powdered ($<800 \mu\text{m}$; ca. 95 g) shale was raised at $12^\circ\text{C}/\text{min}$ (Fischer assay schedule) from ambient to the selected level and held constant for a period ranging from 2 to 800 hr (33 days). At the end of the isothermal period the temperature was increased, again at $12^\circ\text{C}/\text{min}$, to 500°C and finally held there for 40 min. The weight fraction of shale converted to oil (condensable at 0°C) by this procedure was compared with the assay value obtained by raising the temperature of an identical sample from ambient to 500°C without interruption, followed by the final 40 min period. This method, then, gives a direct measure of the effect on yield of the isothermal holding period. Isothermal temperatures covered the range from 150 to 450°C . In one set of experiments gas evolution from the retort at 65 to 100 kPa ($2/3$ to 1 atm) resulted only from that generated by the shale (autogenous atmosphere). In the other set, a flow of nitrogen at 1 atm was passed through the vessel during the entire experiment.

RESULTS

The effect on oil yield of isothermal holding periods of 8, 80, and 800 hr at 150 to 450°C is shown in Figure 1 for the autogenous atmosphere experiments. Yields relative to assay pass through minima of 81 to 92% at 350 to 400°C , depending on the length of the isothermal holding period. In Figure 2 the loss in oil yield is plotted against the amount of oil collected during the isothermal period, expressed as a fraction of the total oil collected over the entire experiment. The direct relationship shown between yield loss and oil produced during the isothermal holding period was observed for holding temperatures of 300 to 375°C . This relationship could not be followed to higher holding temperatures because of difficulty in distinguishing the oil produced isothermally from the large amount formed before the holding temperature was attained.

* This work was performed under the auspices of the U.S. Energy Research and Development Administration under contract No. W-7405-Eng-48.

Addition of nitrogen flow through the retort reduces or eliminates yield loss. Figure 3 illustrates this effect in terms of nitrogen space velocity or sweep rate, i.e., retort vapor volumes per min for the given holding temperatures and periods. The slopes of these curves over the 0 to 5 sweep rate range ($\Delta \text{yield}/\Delta \text{sweep rate}$) are also directly related to the quantities of oil produced during the isothermal periods in the non-sweep experiments (Figure 4).

Both observations support the conclusion that yield loss from powdered shale is due to degradation of oil after its release from the shale and while at high temperature in the retort. Interruption of a rapid rise in shale temperature by an isothermal period reduces the rate of oil and gas formation. Autogenous driving forces to remove oil from the retort — gas evolution and oil vaporization — are reduced correspondingly, residence times lengthened and oil degradation increased. Therefore, a direct relationship between yield loss and amount of oil formed during the isothermal period is the expected result. Similarly, the extent of reduction in yield loss by the sweep gas should be related directly to the quantity of extra-particle oil that otherwise would have a long residence time in the retort for degradation to proceed. As noted earlier (4), this degradation produces mainly a carbonaceous residue ("char") plus some gas.

OIL DEGRADATION RATE

The rates of oil degradation at 350 and 375°C can be estimated from the yields under autogenous atmosphere, the amounts of oil collected during the isothermal holding times, and the volatility of the oil produced from the assay heat-up schedule.

The rate of isothermal oil formation (R_1) is given by

$$R_1 = k_1 x_o e^{-k_1 t}, \quad 1)$$

where k_1 is the first order rate constant for oil formation and x_o is the mass of oil formed during the isothermal period, t_f . To calculate the rate of oil degradation (R_2), two regimes can be distinguished conceptually. In the first regime, R_1 is rapid and R_2 will be essentially constant, given by

$$R_2 = k_2 y_o, \quad 2)$$

where k_2 is the first order rate constant for oil degradation and y_o is the constant mass of oil in the retort. In the second regime, which begins when R_1 has decreased to the value of $k_2 y_o$, R_2 can be approximated by R_1 . That is,

$$R_2 = k_1 x_o e^{-k_1 t}. \quad 3)$$

Let t_e be the time at which $R_1 = k_2 y_o$. Then from Equation 3, t_e can be expressed as

$$t_e = \frac{1}{k_1} \ln \left(\frac{k_1 x_o}{k_2 y_o} \right). \quad 4)$$

The fraction of oil degraded during t_f is then given by

$$\alpha = \frac{1}{x_o} \int_0^{t_f} R_2 dt = \int_0^{t_e} \frac{k_2 y_o}{x_o} dt + \int_{t_e}^{t_f} k_1 e^{-k_1 t} dt. \quad 5)$$

This approximation neglects the small amount of oil in the retort which is degraded after oil formation becomes imperceptible. Integration of Equation 5 gives

$$\alpha = \frac{k_2 y_o t_e}{x_o} + e^{-k_1 t_e} - e^{-k_1 t_f} \quad (6)$$

With known values for α , k_1 , t_f , x_o , and y_o (derived in the Appendix), Equations 4 and 6 can be solved for t_e and k_2 by a series of approximations. The results are summarized in Table 1. It should be noted that estimation of y_o from simulated distillation analysis involves the assumption that oil exists in the retort only as vapor and spray, not as a discrete liquid phase. This assumption appears justified under conditions of rapid oil and gas generation, as is the case of a Fischer assay heating schedule (to 500°C in 1 hr). Under these conditions, yield from this apparatus that permits downflow escape of liquid oil is identical with that from a Fischer Assay apparatus, which allows only upflow escape (4). If a discrete liquid phase exists and flows from the retort more slowly than the spray, the estimated value of y_o is low and that of k_2 correspondingly high.

Table 1: Values for α , k_1 , t_f , t_e , x_o , y_o , and k_2

	350°C		375°C
α	0.180	0.190	0.162
$k_1 (10^{-5} s^{-1})$ (5)	0.72	0.76	4.0
$t_f (10^5 s)$	28.8	28.8	2.88
$t_e (10^5 s)$	4.35	4.03	0.818
$x_o (g)$	7.5936	8.0426	7.6580
$y_o (g)$	0.0560	0.0560	0.0532
$k_2 (10^{-5} s^{-1})$	4.3	5.1	22.0

Using the mean value of k_2 at 350°C, the rate constant can be expressed as:

$$k_2 = 1.00 \times 10^{13} e^{-49,400/RT} \quad (7)$$

As shown in Table 2, the values for k_2 at 350 and 375°C are substantially higher than the rate constants for pyrolysis of kerogen to oil and for thermal cracking of petroleum fractions. As noted above, the method used to estimate k_2 gives maximum values. On the other hand, the high olefin and heteroatom contents of shale oil (8) would be expected to impart thermal instability, especially with respect to condensation or polymerization processes. Such reactions of shale oil have been proposed previously (9) and have been observed in a closed vessel (10).

Table 2: Pyrolysis Rate Constants

	k_2 at 350°C (10^{-5} s^{-1})	k_2 at 375°C (10^{-5} s^{-1})	Activation energy (kcal/mole)
Shale Oil + Gas + Char	4.7	22.0	49.4
Kerogen + Oil (5) + Gas + Char	0.74	4.0	54.0
Asphalt (6)	1.6	7.6	49.7
California Petroleum (7)			
766 $\bar{M}^{a),b)}$	0.25	1.6	59.2
388 $\bar{M}^{a),c)}$	0.28	1.7	57.5

- a) \bar{M} represents the average molecular weight of the distilled fraction. The value of \bar{M} for assay shale oil in our experiments is about 330 (see Appendix).
- b) Conversion to lower boiling products only.
- c) Conversion to lower and higher boiling products.

CONCLUSIONS

Further evidence is supplied to show that the oil yield from retorting powdered Colorado oil shale is primarily determined by the extent of decomposition of the liberated oil. Yield losses occasioned by interrupting a rapid shale heating schedule with isothermal holding periods are directly related to the amounts of oil produced during the holding periods. These amounts are also related directly to the inert gas flow rates required to raise the yields to the assay value. The estimated maximum first order rate constant for thermal decomposition of the oil to char and gas is given by: $k_2 = 1.00 \times 10^{13} e^{-49,400/RT}$. Oil from Colorado shale apparently is more thermally unstable than virgin petroleum fractions. Additional experimental data are needed on the rate of shale oil thermal degradation.

ACKNOWLEDGMENTS

We are indebted to G. J. Koskinas, R. J. Opila, and N. D. Stout for supplying unpublished retorting data and to J. E. Clarkson for the simulated distillation results. We also thank Shell Development Company for permission to use unpublished data on pyrolysis of California petroleum fractions.

APPENDIX

Values of α , k_1 , t_f , x_o and y_o for Table 1

The values of α and t_f , the latter corresponding to 800 or 80 hr, were reported earlier (4).

With the assumption that all oil degradation occurs during the isothermal period, t_f , and since no oil was collected in the receiver after t_f ,

$$x_o = x_A - x_i$$

where x_A is the mass of oil obtained by assay and x_i is the mass of oil collected before t_f . Similarly,

$$x_f = x_t - x_i$$

where x_f is the mass of oil collected during t_f and x_t is the mass of oil collected during the entire experiment. The mass of oil degraded, x_d , then is:

$$x_d = x_o - x_f$$

and

$$\alpha = \frac{x_d}{x_o}$$

The experimental values of these quantities are (4,11) given in Table 3.

Table 3: Values of α and Oil Masses Collected

	350°C		375°C
Raw Shale Charge (g)	91.8983	96.7522	93.1773
Assay Oil (wt%)	8.407	8.407	8.407
x_A (g)	7.7259	8.1340	7.8334
x_i (g)	0.1323	0.0914	0.1754
x_o (g)	7.5936	8.0426	7.6580
x_t (g)	6.3561	6.6100	6.5942
x_f (g)	6.2238	6.5186	6.4188
α	0.180	0.190	0.162

As noted in the text, the mass of free oil in the retort, y_o , is assumed to consist only of vapor and spray. The fraction of oil vaporized can be estimated from the equilibrium flash vaporization (EFV) curve which, in turn, can be related to the molecular weight distribution. The EFV curve was constructed (12) from the gas chromatographic simulated distillation data (13) for oil produced under assay conditions (Figure 5). The molecular weight scale in Figure 5 is based on the relationship between molecular weight and boiling point of n-paraffins corrected

for the lower volatility of unsaturated components. The correction factor was taken from the ratio of the average molecular weight of the 388 M fraction of California petroleum to 421, the average molecular weight of the saturates contained therein (7).

The mass of free oil in the retort is

$$y_o = m_v + m_l,$$

where m_v is the mass of oil vapor in the retort and m_l is the mass of oil liquid as spray in the retort. The quantities m_v and m_l are calculated by the following relationships. First, the number of moles of oil vapor in the retort is

$$n_v = \frac{m_v}{M_v},$$

where M_v is the molecular weight taken from the EFV curve (Figure 5) at the appropriate temperature. Second, the number of moles of co-produced non-condensable gas in the retort is

$$n_g = \frac{0.22(m_v + m_l)}{21}.$$

This equation is based on the experimentally determined ratio of the mass production rate of non-condensable gas to that of oil, which is 0.22, and the gas molecular weight of 21 (11). Third, the total number of moles of oil vapor and non-condensable gas in the retort is calculated from the ideal gas law for the measured retort free volume of 35.1 cm³:

$$n_v + n_g = \frac{35.1}{(22400) \left(\frac{T}{273} \right)}.$$

Finally, the fraction of oil in the vapor state, taken from the EFV curve, is

$$f_v = \frac{m_v}{m_v + m_l}.$$

Combining the above equations yields the desired expression for the mass of free oil in the retort:

$$y_o = \frac{(n_v + n_g)}{\left(\frac{f_v}{M_v} + \frac{0.22}{21} \right)}.$$

Values of y_o calculated from these relationships are given in Table 1.

REFERENCES

1. Lewis, A. E. and Rothman, A. J., Rubble In Situ Extraction (RISE): A Proposed Program for Recovery of Oil from Oil Shale, Lawrence Livermore Laboratory, Rept. UCRL-51768 (1975).
2. Braun, R. L. and Rothman, A. J., "Research and Development on Rubble In-Situ Extraction of Oil Shale (RISE) at Lawrence Livermore Laboratory", Colorado School of Mines Quarterly, 70, 159 (1975).
3. Johnson, W. F., Walton, D. K., Keller, H. H., and Couch, E. J., "In-Situ Retorting of Oil Shale Rubble: A Model of Heat Transfer and Product Formation in Oil Shale Particles", Colorado School of Mines Quarterly, 70, 237 (1975).
4. Stout, N. D., Koskinas, G. J., Raley, J. H., Santor, S. D., Opila, R. J., and Rothman, A. J., "Pyrolysis of Oil Shale: The Effects of Thermal History on Oil Yield," Lawrence Livermore Laboratory, Rept. UCRL-77831 (1976); Colorado School of Mines Quarterly (in press).
5. Campbell, J. H., Koskinas, G. H., and Stout, N. D., "The Kinetics of the Decomposition of Colorado Oil Shale, Part I, Oil Generation", Lawrence Livermore Laboratory Rept., in preparation.
6. Nelson, W. L., Petroleum Refinery Engineering, (McGraw-Hill, New York, 1958), 4th ed., p. 651.
7. Data supplied by Shell Development Company from work of R. D. Mullineaux, J.H. Raley and D.H. Rowe.
8. Dinneen, G. U., Ball, J. S., and Thorne, H. M., "Composition of Crude Shale Oils", Ind. Eng. Chem., 44, 2632 (1952).
9. Schnackenberg, W. D.; and Prien, C. H., "Effect of Solvent Properties in Thermal Decomposition of Oil Shale Kerogen," Ind. Eng. Chem., 45, 313 (1953).
10. Hill, G. R., Johnson, D. J., Miller, L., and Dougan, J. L., "Direct Production of a Low Pour Point High Gravity Shale Oil", Ind. Eng. Chem. Product. Res. and Dev., 6, 52 (1967).
11. Data supplied by G. J. Koskinas, R. J. Opila, and N. D. Stout at this Laboratory.
12. Ref. 6, p. 113.
13. (a) ASTM D 2887-73, "Boiling Range Distribution of Petroleum Fractions by Gas Chromatography",
(b) ASTM D-2 Research Division 4, Study Group 2, "Proposed Method of Test for Boiling Range Distribution of Crude Petroleum by Gas Chromatography."

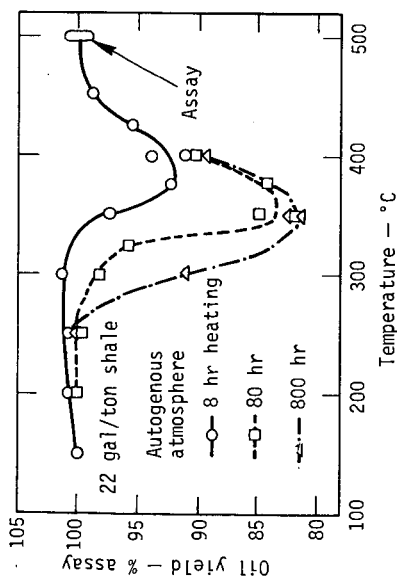


Figure 1. Effect of Isothermal Holding Periods on Oil Yields.

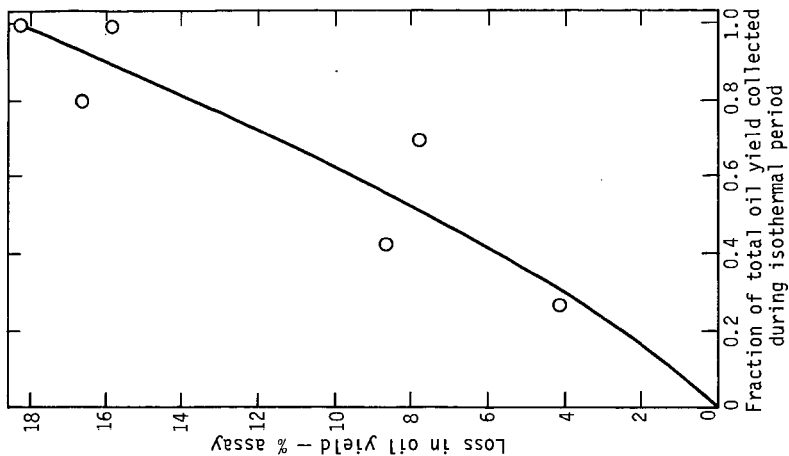


Figure 2. Correlation between Yield Loss and Oil Production During Isothermal Period.

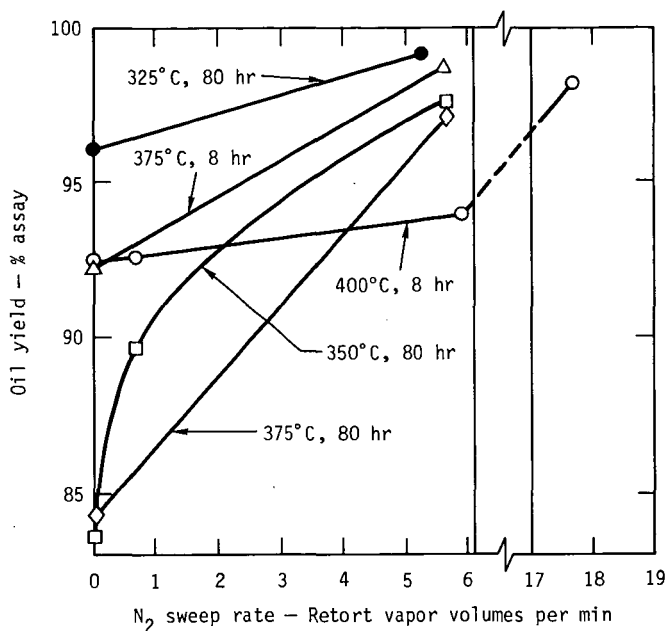


Figure 3. Effect of Nitrogen Sweep Rate on Oil Yield (Note abscissa scale change).

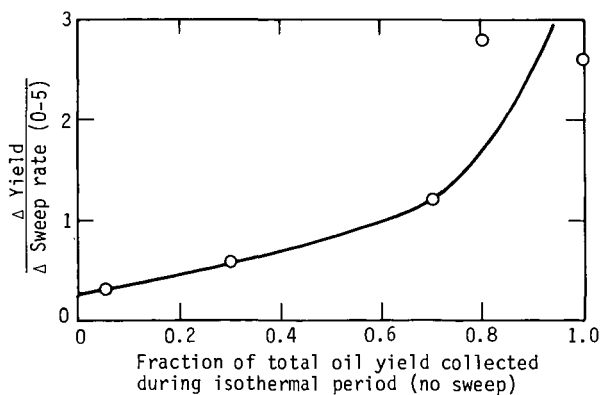


Figure 4. Correlation between Effect of Sweep Rate and Oil Production During Isothermal Period.

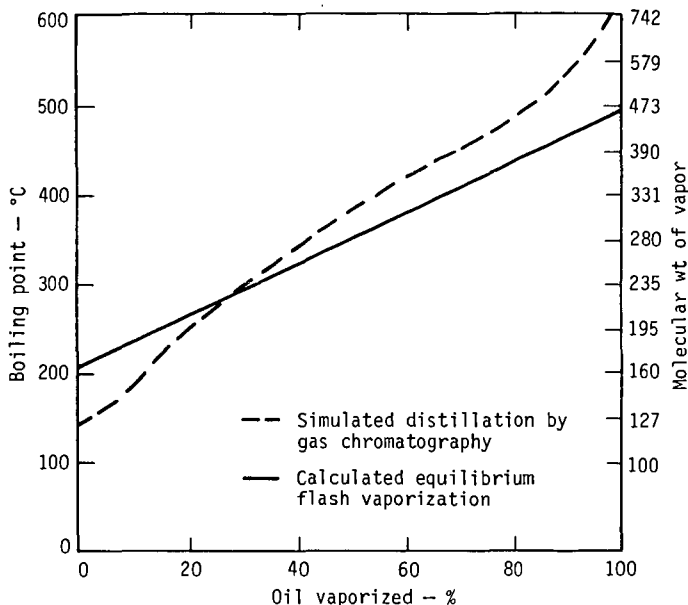


Figure 5. Oil Vaporization.

NOTICE

"This report was prepared as an account of work sponsored by the United States Government. Neither the United States nor the United States Energy Research & Development Administration, nor any of their employees, nor any of their contractors, subcontractors, or their employees, makes any warranty, express or implied, or assumes any legal liability or responsibility for the accuracy, completeness or usefulness of any information, apparatus, product or process disclosed, or represents that its use would not infringe privately-owned rights."

"Processing of Tar Sand Bitumens. Part I--
Thermal Cracking of Utah and Athabasca Tar
Sand Bitumens"

J. W. Bunger, S. Mori, and A. G. Oblad

Department of Mining, Metallurgy, and Fuels
Engineering
University of Utah, Salt Lake City, Utah 84112

Introduction

The tar sands deposits of Utah contain significant reserves of fossil energy. The bitumen, which is impregnated in sandstone, is a heavy, viscous, residue-like material and is not amenable to recovery by conventional primary or secondary techniques. Research and development efforts are currently being conducted in U.S. Government and in University laboratories to study the various recovery processes by hot water, fluid coking, and in situ combustion, etc. Additionally, efforts are being made to determine the optimum conditions for conversion of recovered bitumen to high quality products for use as fuel or the manufacture of chemicals.

The study of Utah tar sand bitumens has received relatively minor attention compared with Athabasca, Canada, bitumen. Virtually no literature exists regarding the processing of Utah bitumen whereas the Athabasca bitumen is being commercially processed. The thermal cracking of Asphalt Ridge and Sunnyside, Utah, bitumen was studied by Wenger, et al. (1) in the early 1950's. These studies were performed on bitumen which had been recovered via hot caustic water extraction followed by a solvent clarification step. This work provided valuable qualitative information about the yields and the nature of the products derived from Utah bitumens but results of these early studies are difficult to interpret in light of more recent information.

The thermal processing of Athabasca bitumen on the other hand, is well known and references to these studies are contained in an excellent overview by Camp. (2). The Great Canadian Oil Sands, Ltd., venture has selected delayed coking as the initial upgrading process and technology and processing conditions for the Athabasca bitumen are well established. However, Utah tar sands have been recently shown (3,4) to differ significantly from the Athabasca bitumen. This precludes the direct adaptation of existing technology and requires an additional research effort to identify the optimum processing conditions for this U.S. resource.

The work reported here represents our preliminary efforts to determine the processing characteristics and the value of the products derived from Utah tar sand bitumens. Thermal cracking was selected for our initial study because some variation of this general process will most likely be employed to upgrade bitumen to raw crude oil which can, in turn, be subjected to various hydrogenating/cracking sequences.

Our primary aim in this study was to provide a detailed comparison of the thermal cracking behavior of one bitumen to another and to compare tar sand bitumen generally with a petroleum residue. A direct comparison, under uniform, reproducible reaction conditions, provides a basis for determining the relative value of products derived as a function of the bitumen properties. In addition, the results of this study will provide a base from which to evaluate effects of varying the reaction conditions on yield and product properties.

In this study we subjected three Utah bitumens, one Athabasca bitumen and a Wilmington, Calif., petroleum residue to batch-type destructive distillation at atmospheric pressure and under an inert atmosphere. Properties and composition of the native bitumen are summarized and results of bench-scale thermal cracking are discussed in terms of the bitumen composition. Properties of the products from Utah bitumen are compared with that from Athabasca and the petroleum residue. General conclusions about the relative value of Utah bitumens as feeds for thermal cracking are made.

Experimental Procedure

Description of Samples - Four tar sand bitumens and one petroleum residue were thermally cracked in this work. Two tar sand bitumens, the Athabasca, Canada and P.R. Spring, Utah, were identical to the samples used in previous studies of one of the authors of the compound type analysis. (3,4) The Asphalt Ridge and Tar Sand Triangle, Utah, samples were similar to those two used in this previous work. Because property and elemental analysis data corresponded closely between the previous samples and present ones, we assumed bitumen composition to be respectively identical for purposes of interpreting the cracking yield data. The tar sand bitumens were extracted from the tar sand with benzene, filtered through 4.0 to 5.5 μ fitted glass filters, and flash distilled until final conditions of 75° to 80° C and 4 to 5 torr had been maintained for 1 hour.

The petroleum residue was a 485° C distillation residue from a Wilmington, Calif., crude oil. This sample was identical to that reported on earlier (3) and in conjunction with analysis resulting from American Petroleum Institute-U.S. Bureau of Mines Research Project 60. (5) This sample was determined to be the most similar to the P.R. Spring bitumen in terms of physical properties and composition and was included to establish a point of reference for our present work.

Description of apparatus- The Vycor thermal cracking reactor consisted of a common distillation flask design with the sidearm turned downward at the end. Heat was applied to the pot by use of a beaded heater and to the head and sidearm by use of heating tape. Temperature was monitored inside and outside of both the pot and head with thermocouples. The top of the reactor was closed off with a 19/38 joint which had been fitted with thermowells. Liquid products were collected in cold-finger type condensers using dry-ice/methanol for the final coldfinger coolant.

Description of procedure - Approximately a 10 g-sample of bitumen was pyrolyzed at a heating rate of about 5° C/min to an end point of 625° C. Reactor and condensers were preweighed and coke and liquid product yields were determined directly by weight. Gas volume rate production was determined by measuring the volume of water displaced

at atmospheric pressure and subsequently corrected to STP conditions. Weight of gas produced was estimated by difference and by analysis of gases produced.

Analysis of bitumen and products - Gas analysis was accomplished by GC using a 1/16-inch by 16-foot activated alumina column and by mass spectrometry. Elemental analysis and physical properties of the bitumen and products were determined by conventional means by U.S. Government and commercial laboratories. Heating value (H) was calculated from the formula (6)

$$H(\text{Kcal/K}_g) = 8,400(C) + 27,765(H) + 1,500(N) + 2,500(S) - 2,650(O).$$

Simulated distillation of bitumen and liquid products was accomplished by G.L.C. by procedures fully described elsewhere (7), using a 1/4-inch by 18-inch column packed with 5 percent UCW-98 on 60 to 80-mesh silanized chromosorb W. TGA and DTA were performed on a Mettler thermogravimetric analyzer. New infrared data reported here were gathered using a Beckman model 4860.

Results and Discussion

Bitumen, Composition and Properties

The extracted tar sand bitumens were characterized by methods adapted from those developed for the study of high boiling petroleum distillates and residues. Results of this study, which was conducted at the Laramie Energy Research Center (ERDA), will soon be published, (4) and are summarized here to provide an understanding of the nature of the bitumen. The elemental analysis and selected physical properties are given in table I. Comparison is made of the two sets of bitumens for which the sample used for cracking was similar to, but not identical to, that characterized. In the case of the Tar Sand Triangle sample, the two samples are nearly identical whereas some differences are noted for the Asphalt Ridge samples.

Results of our previous studies (4) have shown marked similarities between the two Uinta Basin samples (Asphalt Ridge and P. R. Spring) on the one hand and the Athabasca and Tar Sand Triangle on the other. These similarities extend beyond the elemental analysis and physical properties and include compound type analysis and boiling point distribution as well.

Comparison of the property and distillation data for the Uinta Basin samples with the high sulfur bitumens reveals a higher hydrogen and nitrogen content, lower sulfur, higher molecular weight and viscosity, and lower content of volatile material. These results are interpreted in conjunction with the compound type analysis to mean that Uinta Basin samples have a higher percentage of high boiling and residual saturated hydrocarbons with the aromatic portion reserved appreciably for the high boiling residue fraction. Conversely, the Tar Sand Triangle and Athabasca bitumens are comprised of generally lower molecular weight material with the aromatics and heteroatoms making up a comparatively large percentage of the volatile material.

There are a few notable compositional differences between the Wilmington residue and the tar sand bitumens which are likely to

Table I - Elemental analysis and physical properties
of bitumens*

Property	ATH ⁽⁴⁾	TST ₁ ⁽⁴⁾	TST ₂	AR ₁ ⁽⁴⁾	AR ₂	PRS ⁽⁴⁾	WIL ⁽⁷⁾
Carbon (wt-pct)	82.6	84.0	84.2	85.3	85.5	84.4	85.4
Hydrogen	10.3	10.1	10.2	11.7	11.3	11.0	10.6
Nitrogen	.47	.46	.52	1.02	1.03	1.0	1.08
Sulfur	4.86	4.38	4.48	.14	.42	.75	2.08
Oxygen	1.8	1.1	1.7	1.1	1.6	3.3	.8
C/H atomic ratio	.674	.695	.693	.611	.634	.641	.674
Average molecular wt. (VPO-benzene)	568	578	542	668	666	820	640
API gravity	11.6	11.1		14.4	12.0	10.3	8.6
Carbon residue (Ramsbottom), wt-pct	16.1	21.6	17.0	3.5	9.1	12.5	18.0
Asphaltene (pentane) wt-pct	16.4	26.0		3.4		16.0	12.8
Viscosity (poise) 77° F (cone-plate at 0.05 sec ⁻¹)	6,380	12,900	29,500			325,000	99,500
Pct volatile material (535° C)	60.4	54.5		50.3		49.9	(est)25

* ATH - Athabasca
TST - Tar Sand Triangle (previous study)
TST₁ - Tar Sand Triangle (this study)
TST₂ - Tar Sand Triangle (this study)
AR₁ - Asphalt Ridge (previous study)
AR₂ - Asphalt Ridge (this study)
PRS - P. R. Spring
WIL - Wilmington

influence the chemical behavior but are not apparent in the gross properties. Although the total heteroatom content of the Uinta Basin bitumen is similar to that of the Wilmington residue, there is a greater tendency (as a result of geochemical forces) to concentrate the heteroatoms in the high molecular weight compounds of the bitumens. Additionally, there is considerably more material associated with a given quantity of heteroatoms for comparable initial boiling point residues indicating that the average molecular weight for a 530° C residue of the Uinta Basin samples may be 1-1/2 to 2 times that of a 530° C Wilmington sample. The Athabasca and Tar Sand Triangle samples exhibit lesser tendencies to concentrate heteroatoms in the residue portion than the Wilmington residue. The comparative upper molecular weight of these samples is not known.

Quantitative Results of Pyrolysis

Product yields from the batch-type thermal cracking of the five bitumens are given in table II. Gas yields, which range from 4.8 to 7.5 percent, do not exhibit any obvious correlation with bitumen properties. The majority of the gas was produced above 500° C when condensate production was tapering off. The percent gas yield and the average molecular weight of the gas ran roughly parallel to each other.

Table II - Product yields

Product	ATH	TST	AR	PRS	WIL
Gases (C ₅ and lighter)	7.52	5.31	4.80	7.41	6.03
Liquid condensate (C ₆ -535° C)	76.52	72.82	82.85	76.05	77.04
Coke	15.96	21.87	12.35	16.54	16.93

Liquid condensate yields exhibit a good inverse correlation with carbon hydrogen atomic ratio. A secondary correlation appears to exist with molecular weight; for a given C/H ratio, the higher the molecular weight, the lower the yield. The Asphalt Ridge sample, which is a likely candidate for early commercial development, gave a high yield of almost 83 percent condensate.

Coke yield, which is directly related to carbon residue determination, also correlates well with the asphaltene content. Asphaltenes derived from tar sands are probably similar to petroleum asphaltenes in that they represent the high molecular weight, highly aromatic molecules present. These molecules contain significant quantities of heterocyclic structures with generally low alkyl and naphthenic carbon contents. These structural features explain their resistance to pyrolysis and their ability to form coke. Although the correlation between coke yield and asphaltene content is strong, a one-to-one precursor-product mechanism is not suggested. Many nonasphaltene aromatic molecules probably undergo polymerization and condensation as well, and asphaltenes can rupture to form lighter products. Comparison of the results of cracking a total bitumen with results from a deasphalted bitumen should prove interesting.

In order to provide assurances that yield and analytical results would be meaningful, it was imperative that high material and elemental

balance be achieved. This was one of the principal considerations in the experimental design. Table III shows the elemental balance for the Wilmington sample. Other bitumens showed similar results. The data illustrate that carbon and hydrogen recoveries were excellent, while nitrogen and sulfur were slightly low. Material balance was better than 99 percent in all cases.

Table III - Elemental balance (Wilmington residue)

	Wt-pct (O free basis)	
	Starting bitumen	Analysis of recovered products
Carbon	86.1	86.7
Hydrogen	10.7	10.8
Nitrogen	1.1	0.9
Sulfur	2.1	1.6

Characterization of Products

Gaseous products were analyzed by gas chromatography and mass spectrometry. All gaseous products showed the typical constitution of a pyrolysis gas. An example of mass spectral analysis for the products derived from the high sulfur Tar Sand Triangle bitumen is given in table IV. The oxygenated compounds are believed to be derived from bitumen oxygen compounds. Gases derived from the other bitumens were of a similar constitution with that from Asphalt Ridge having a relatively high concentration of olefins and that from the Wilmington having a relatively high concentration of methane.

Table IV - Composition of Tar Sand Triangle gases

Compound	Mole, pct (Helium-free basis)	Compound	Mole, pct (Helium-free basis)
Hydrogen	14.3	Cyclopentene	0.1
Methane	47.3	Pentenenes (noncyclic)	.7
Ethylene	1.6	Isopentane	.3
Ethane	10.9	n-pentane	1.3
Propylene	3.1	Ammonia	.7
Propane	5.5	Hydrogen sulfide	5.0
1,3-butadiene	0.1	Carbon monoxide	3.9
Butenes	2.6	Carbon dioxide	.4
Iso-butane	0.0		
n-butane	2.2	Total	100.0

Liquid products were characterized by elemental analysis, physical properties and application of the n-d-M method (9) for carbon type and ring structure, infrared spectroscopy, and simulated distillation. Elemental analysis and physical properties are given in table V. Generally, the bulk properties are remarkably similar for all samples. Carbon/hydrogen ratios exhibit moderate variation with values grossly following that in the original bitumen. The Tar Sand Triangle condensate exhibited a substantial increase in hydrogen content over the native bitumen while other samples exhibited less marked enrichment.

Table V - Liquid condensate properties

	ATH	Bitumen			
		TST	AR	PRS	WIL
Carbon (wt-pct)	84.7	85.2	87.1	86.5	86.5
Hydrogen	11.3	11.6	12.0	12.1	11.7
Nitrogen	.19	.16	.58	.57	.43
Sulfur	3.75	2.68	.32	.29	1.43
Oxygen	0 - trace	0 - trace	0 - trace	0 - trace	0 - trace
C/H atomic ratio	.631	.616	.615	.598	.618
Average molecular wt (VPO benzene)	279	280	282	280	313
Specific gravity (20/20)	.923	.910	.898	.895	.920
API gravity	21.9	24.0	25.8	26.5	22.3
Refractive index -n ²⁰	1.5191	1.5130	1.5106	1.5053	1.5174
Heating value (Btu/lb)	18,632	18,803	19,084	19,153	19,002

Sulfur and nitrogen contents reflect the relative concentrations of these elements present in the native bitumen. Oxygen has been completely removed, presumably as water and the oxides of carbon. Small amounts of water were produced at reaction temperatures of 350° to 400° C. Molecular weights are nearly identical for the tar sand bitumens while API gravity and refractive index show minor variations. The significance of the nearly constant physical properties can be seen in the results of the n-d-M analysis.

Application of the Van Ness and Van Weston (9) n-d-M method for estimating carbon structure was made with the recognition that these correlation charts were developed for virgin olefin-free petroleum samples. The presence of either cyclic or straight-chain olefins in a sample would probably add semiquantitatively to the aromatic carbon content largely at the expense of the naphthenic carbon. The percent of olefin carbon present in condensate products derived from the destructive distillation of Asphalt Ridge bitumen (1) and delayed coking of Athabasca bitumen (10) range from 10 to 12 percent. The n-d-M carbon type analysis was adjusted for the olefin content by subtracting the olefin carbon from the aromatic carbon and assuming that all olefins were present in a ring system. Typical ranges of carbon type and ring type are given in table VI. Inspection of the detailed data for products from each bitumen revealed minor differences, with the naphthenic carbon exhibiting the highest variability. These analyses further confirm the structural similarity of the pyrolysis condensates that were indicated by the similarities in the properties.

Table VI - Carbon and ring type analysis of condensates

Type	Atomic pct of carbon
Aromatic carbon	18-20
Naphthenic carbon (saturated)	9-16
Olefin carbon	10-12
Paraffinic carbon	55-60
Aromatic rings/molecule	0.7
Naphthenic-olefin rings/ molecule	0.8-1.2

Infrared spectra was employed to obtain additional qualitative information about the liquid condensate products. Virtually no adsorption exists in the free or bonded O-H or N-H region. The C-H region showed virtually no aromatic C-H and the intensity of the methyl C-H nearly equaled that of the methylene C-H. A broad, ill-defined adsorption peak centering about 1,705 cm^{-1} indicative of the presence of carbonyl compounds, is probably due to ketone artifacts generated upon exposure of the sample to air. A fairly sharp band centering about 1,640 cm^{-1} was attributed to unconjugated olefins. The existence of asymmetry on the high frequency side of the aromatic band (1,603 cm^{-1}) was attributed to the presence of conjugated olefins. Assignments were not made for several strong bonds present from 1,000-700 cm^{-1} .

The boiling point distribution was determined from simulated distillation by gas-liquid chromatography. Results are given in table VII. In this analysis significant differences are obvious. This is rather surprising in light of the similarities in the other properties

Apparently an "average structure" is defined by thermodynamic considerations but the actual distribution of molecular sizes relates back to some yet unknown structural feature of the feed bitumen. The Wilmington condensate is noticeably heavy which is consistent with its higher molecular weight and slightly higher degree of ring condensation.

Table VII - Simulated distillation yields, wt-pct

	ATH	TST	AR	PRS	WIL
Gasoline C ⁺ - 200° C	7.5	7.2	11.9	10.4	8.6
Kerosine 200-275° C	12.9	11.5	19.9	14.7	11.6
Gas oil 275-325° C	13.7	13.0	16.9	12.8	8.1
Heavy gas oil 325-450° C	48.0	51.4	34.0	46.6	38.5
Vacuum gas oil 450-535° C	17.9	16.9	17.3	15.6	28.2
Subtotal	100.0	100.0	100.0	100.0	95.0
Residue	0-4%	0-3%	0-5%	0-2%	5-10%

The coke was characterized by elemental analysis and heating value (table VIII). All of the cokes had a shiny appearance with infrequent pores. Coke from the Uinta Basin samples are extremely low in sulfur. Incomplete combustion in analysis is thought to cause low carbon values in some samples. Heating values were calculated from actual percentages because oxygen content is not known.

Table VIII - Coke analysis

	ATH	TST	AR	PRS	WIL
Carbon (wt-pct)	88.6	87.7	87.9	87.7	89.8
Hydrogen	2.5	2.8	3.0	2.6	2.9
Nitrogen	1.8	1.5	2.9	2.9	3.0
Sulfur	6.0	6.2	0.4	0.5	1.5
Heating value (Btu/lb)	14,960	14,950	14,860	14,720	15,165

Discussion of Results

The experimental design optimized sample definition. This procedure provides a base for comparison of results which can be derived from visbreaking, delayed coking, catalytic cracking and catalytic hydrogenation experiments. Although reaction conditions do not simulate commercial coking operations preliminary interpretation can be made of the thermal cracking characteristics of Utah tar sand bitumens. By relating results from Utah samples to those derived for Athabasca and a representative petroleum residue comparison is established with commercially processed samples. Results for the Athabasca sample compare favorably with literature results (2) with gas productions and compositions being similar to delayed coking operations while liquid yields are higher (77 vs 70) and coke yields are lower (16 vs 22) in the present study. These results are explained by the longer residence time under higher hydrocarbon partial pressures which enhances the condensation reactions.

Certain observations regarding the rate of light gas and liquid condensate production deserve attention. Plots of the rate of gas production as a function of temperature revealed a trimodal curve with the major rate of gas production occurring about 490° C with less prominent peaks occurring at 555° C and 610° C. These data suggest that several distinct molecular types may be present with discrete decomposition temperatures. Analysis of gases produced as a function of temperature revealed the expected increase in olefin to saturated hydrocarbon ratio but exhibited no clear enhancement of one component over another. At higher temperature the C_2-C_5/C_1 ratio was enhanced. Generally, more than half the gas production occurred after liquid condensate production had ceased (ca. 525° C). The peak gas production occurred some 40° C after peak condensate production. This suggests that precursors to light gases are largely short alkyl (or naphthene) groups attached to larger nonvolatile molecules. Cracking of medium volatility molecules or long chain alkyl substituents to light gases would give rise to simultaneous condensate production which is not observed.

Additional insight into the cracking behavior of these bitumens is obtained from thermal gravimetric analysis (TGA). Typically, the differential TGA curve (change in rate of weight loss vs temperature) exhibits a broad peak at 275° to 350° C followed by a well defined peak at 435° to 460° C. Comparison of TGA results with those of the simulated distillation, which determines volatility at short high-temperature residence times, reveal that initial thermal cracking may be taking place at temperatures as low as 150° C with appreciable cracking existing at 300° C. The susceptibility to thermal cracking was particularly apparent with the Wilmington sample where over 45 percent TGA weight loss had been experienced by 375° C when the nominal IBP was 485° C. Conversely, visual observation of the production of liquids from tar sand bitumens in the bench scale experiments showed substantially less liquid production at 375° C than was expected based on the simulated distillation data. The implication in these results is that even though thermal cracking apparently occurs at lower temperatures, mass transfer effects may be a limiting factor.

The thermal reactivity of tar sand bitumens is probably ultimately related to the overall severity of the geochemical maturation process. In this regard the Wilmington sample appeared noticeably more reactive than did the tar sand bitumens. This leads to the speculation that maturation conditions have been more severe for tar sands compared to the Wilmington crude oil. This factor will probably affect the optimum reaction conditions for upgrading bitumen to synthetic crude oil.

The work reported here is the result of a preliminary investigation at one set of reaction conditions. For this reason, further discussion of the mechanistic implications of our analytical work is reserved for future publications when the effects of varying the reaction conditions can also be discussed. Suffice it to say that knowledge of the total aromatic, naphthenic, paraffinic content and molecular weight data will not be adequate to explain the results. More subtle factors which may have significant effects on yield and yield structure include degree and type of alkyl substitution, the type of ring condensation and the presence of coke promoting heteroatoms such as pyridine type nitrogen. The model compound pyrolysis study of Madsen and Roberts (11) relates to the effects of these compositional features.

Conclusions

The raw liquid condensate from the low sulfur Uinta Basin samples show good potential for hydrotreating to produce a high quality synthetic crude oil amenable to conventional processing. Compared to the Athabasca bitumen sample, the Uinta Basin products are low in sulfur, high in hydrogen, are of comparable olefin content and are produced in higher yields. These comparative features will significantly enhance the value of this tar sand resource. Generally, the high sulfur bitumen from Utah, i.e., Tar Sand Triangle, will produce a similar product in thermal processing to the Athabasca bitumen.

Our preliminary evaluation of the thermal cracking of Utah and Athabasca tar sand bitumens showed that (1) conversion is primarily a function of hydrogen content, (2) bitumens show appreciable cracking at 300° C with maximum cracking at 450° C, (3) condensable product character, although considerably uniform from one bitumen feed to another, tends to correlate with bitumen character, (4) products derived from tar sand bitumens compare favorably with those derived from a representative petroleum residue, (5) coke generated from Uinta Basin, Utah, samples is extremely low in sulfur; (6) hydrogen demands in hydrotreating processes will probably be lower for Utah samples than for Athabasca samples.

Acknowledgements

The work reported here was supported by U.S. ERDA Contract E(29-2)-3659, NSF-Contract AER74-21867, and the State of Utah.

Acknowledgement is extended to S. M. Dorrence of the Laramie Energy Research Center (ERDA) for frequent technical discussions and for contributions to program coordination. We thank K. J. Voorhees of the Flammability Research Center of the University of Utah for helpful discussions on pyrolysis chemistry and for supplying TGA and DTA results.

The Tar Sand Triangle sample was supplied by Oil Development Co. of Utah, the P. R. Spring sample was supplied by Texaco and the Athabasca sample was supplied by Sun Oil. We are grateful for these contributions.

References

1. W. J. Wenger, R. L. Hubbard, M. L. Whisman, U.S. Department of Interior, Bureau of Mines, Report of Investigations 4871 (1952).
2. F. W. Camp, "The Tar Sands of Alberta, Canada," 2nd Ed., Cameron Engineers, Denver, Colo., 1974, 77pp (and references contained therein.)
3. J. W. Bunger "Characterization of a Utah Tar Sand Bitumen." Ch. 10, Advances in Chemistry Series--151 American Chemical Society, 1155 16th Street, N.W., Washington, D.C. (1976).
4. J. W. Bunger, K. P. Thomas, S. M. Dorrence, "Analysis of Compound Types and Properties of Utah and Athabasca Tar Sand Bitumens," Laramie Energy Research Center (ERDA). To be published.
5. D. M. Jewell, J. H. Weber, J. W. Bunger, Henry Plancher, and D. R. Latham. Anal. Chem., 44(8) 1391-1395 pp (1972)

6. Werner Boie, "Contributions to Pyrotechnic Computations," Wissenschaftliche Zeitschrift der Technischen Hochschule, Dresden, 2, PP. 687-718 (1952/53).
7. R. E. Poulson, H. B. Jensen, J. J. Duvall, F. L. Harris, and J. R. Morandi, Analysis Instrumentation (Instrument Society of America) 10, 193 (1972).
8. R. V. Helm and J. C. Petersen. Anal Chem 40, pp. 1100-1103 (1968).
9. K. Van Ness and H. A. Van Weston, Aspects of the Constitution of Mineral Oils, Elsevier Publishing Co., New York (1951).
10. W. A. Bachman and D. H. Stormant, Oil and Gas Journal, 65, pp. 1969-88 (1967).
11. John J. Madsen and Richard M. Roberts. Ind. Eng. Chem., 50 (2) 237-250 (1958).

COMPETING REACTIONS IN HYDROTREATING COKER DISTILLATES
FROM ATHABASCA BITUMEN ON UNPROMOTED AND PROMOTED CATALYSTS

R. Ranganathan, M. Ternan and B.I. Parsons

Energy Research Laboratories
Department of Energy, Mines & Resources
555 Booth Street
Ottawa, Ontario
K1A 0G1

INTRODUCTION

Hydrotreating crude distillates involves competing reactions such as desulphurization, denitrogenation and hydrogenation. Individual studies of these reactions have been described in the literature for several model compounds^{1, 2, 3}. In a few cases, the interaction of these competing reactions has been reported^{4, 5}. However, it is difficult to simulate all the properties of petroleum using model compounds. It was felt that a study with distillate fractions was required to determine the interaction of these competing reactions in the industrial hydrotreating process. The purpose of the present paper is to describe the interaction of the competing reactions for various catalysts and process conditions as they would be encountered in a refinery application. A coker kerosene distillate, derived from Athabasca bitumen⁶, was hydrotreated on unpromoted and promoted catalysts at various reaction temperatures.

EXPERIMENTAL

The catalysts used in this study were unpromoted MoO_3 /alumina containing 3, 6, 9 and 12 wt % of MoO_3 and promoted MoO_3 /alumina composed of 1.1 wt % CoO - 2.2 wt % MoO_3 /alumina, 1.1 wt % NiO - 2.2 wt % MoO_3 /alumina and 3 wt % CoO - 12 wt % MoO_3 /alumina. The catalysts were prepared by spraying aqueous solutions of metal salts on alumina powder (a mixture of 20 wt % Continental Oil Company "Catapal SB" and 80 wt % "Catapal N" alumina monohydrate) in a mix-muller⁷. The impregnated mixtures were dried in air at 110°C for 3 hours and then calcined at 500°C for 3 hours. The calcined powder was mixed with 2 wt % stearic acid and pressed into cylindrical pellets ($L = D = 3.2$ mm) in a continuous pelleting press. The pellets were recalcined at 500-550°C for 4 hours to remove the stearic acid. A commercial catalyst, 3 wt % CoO - 12 wt % MoO_3 /alumina (Harshaw CoMo 0603T, 3.2 mm pellets), was also used.

The feedstock used for the hydrotreating study was a coker kerosene distillate (193-279°C) supplied by Great Canadian Oil Sands Ltd. of Fort McMurray, Alberta. The properties of the feedstock are listed in Table 1.

The reaction measurements were carried out in a bench scale continuous flow system⁸ with the oil and hydrogen flowing up through a fixed bed of catalyst. The reactor was 0.025 m in internal diameter, 0.305 m long, and was made of 316 stainless steel. The reactor was filled sequentially from the bottom with 42 ml of berl saddles, 100 ml of catalyst pellets and 13 ml of berl saddles. The axial temperature profile was measured by a movable thermocouple in a thermocouple well located centrally in the reactor. The gas and liquid reaction products were separated in one of the two down-stream vessels. When steady-state conditions had prevailed for 1 hour, the product flow was routed to the second vessel where the liquid product was collected for subsequent analysis.

For all the experiments the reaction pressure, liquid space velocity and hydrogen flow rate were kept constant at $1.39 \times 10^7 \text{ N/m}^2$ (2000 psig), 2h^{-1} and $890.5 \text{ m}^3 \text{ H}_2/\text{m}^3$ oil (5000 scf H_2 /bbl oil) respectively. The reaction temperatures were varied in the following sequence: 400, 420, 360, 320 and 400°C . The second run at 400°C was undertaken to check the series and confirm the stability of the catalyst.

The product samples were analysed for sulphur, nitrogen, aromatics, olefins and saturates. The conversions of higher boiling fractions to lower boiling fractions were determined by atmospheric distillation and the sulphur concentration by X-ray fluorescence⁹. The sulphur apparatus was calibrated using a series of oil samples analysed by the bomb sulphur technique⁷. The nitrogen content was measured using a hydrogenation-microcoulometric apparatus developed and manufactured by the Dohrmann Division of Envirotech Corp., Mountain View, California¹⁰. The Dohrmann procedure was developed for oils containing 10-100 ppm and was calibrated using pyridine, carbazole and acetanilide. The samples having higher nitrogen were diluted to reduce the nitrogen concentration to the working range of the instrument. The aromatics, olefins and saturates were separated using the ASTM standard FIA method¹¹. The conversion of fractions boiling above 220°C to fractions boiling below 220°C was calculated using the distillation data in the following equation:

$$X_{\text{BP}} = \frac{(100-F) - (100-P)}{100 - F} \quad (1)$$

where $P = \text{wt \% of product boiling below } 220^\circ\text{C}$
 $F = \text{wt \% of feed boiling below } 220^\circ\text{C}$

RESULTS AND DISCUSSION

Catalyst Pretreatment:

Preliminary studies showed that the catalyst pretreatment conditions are important in obtaining stable activity¹². The oxides in the catalysts are slowly converted to sulphides by the hydrogen sulphide produced from the sulphur compounds in the feed. Large variations in catalyst activity have been related to differences in the extent of catalyst sulphiding. It was found that a pretreatment with the coker kerosene feedstock at reaction conditions of $1.39 \times 10^7 \text{ N/m}^2$ (2000 psig), 673°K , 2h^{-1} and $890.5 \text{ m}^3\text{H}_2/\text{m}^3$ oil (5000 cu ft/bbl) for 2 hours produced an adequate extent of catalyst stabilization.

Kinetics:

Mass transfer effects in catalysts are known to be important, particularly when hydrotreating high boiling petroleum fractions¹³. However, for the system used in this work there were strong indications that mass transfer was not controlling. The fact that the different catalysts had markedly different activities suggests that the effect of external mass transfer was negligible. Other experiments undertaken in this laboratory with a higher boiling gas-oil over extruded catalysts, having different dimensions (0.317 mm and 0.159 mm) but the same chemical composition, also produced the same activity¹⁴. This indicated that pore diffusional resistance was not controlling. Additional evidence for minimal diffusional effects is obtained when one compares the desulphurization and denitrogenation reaction data of two catalysts having the same metals content (Table 2). For 1.1 wt % NiO - 2.2 wt % MoO_3 /alumina, the denitrogenation conversion improved relative to desulphurization conversion with increasing temperature. For 3 wt % MoO_3 /alumina, the desulphurization improved relative to denitrogenation conversion with increasing temperature. Such changes indicate that the differences in desulphurization and denitrogenation are not due to pore diffusion effects and can be attributed to kinetics.

The kinetics of denitrogenation, desulphurization and hydrogenation were studied on 3 wt % CoO - 12 wt % MoO_3 /alumina catalyst. Denitrogenation followed first order kinetics (Figure 1 A) as reported by others¹⁵. The desulphurization followed second order kinetics (Figure 1 B).

Similar desulphurization kinetics have been observed by others for high sulphur crudes¹⁶. However, for low sulphur crudes, first order kinetics have also been reported¹³. Beuther et al¹⁶ and Schuit et al¹⁷ suggest that desulphurization is first order for individual sulphur compounds and appears to be second order in a feedstock containing different types of sulphur compounds.

In the literature, the hydrogenation of aromatics is reported to follow reversible first order kinetics¹⁸. However, in the work discussed here the data did not fit zero order, first order irreversible, first order reversible or second order irreversible kinetics. This is probably due to the inhibition of the hydrogenation process by sulphur compounds. Voorhoeve and Stuiver¹⁹ reported that the hydrogenation of cyclohexane deviated from first order kinetics when carbon disulphide was present. They suggest that the hydrogenation sites are blocked by the preferential adsorption of CS_2 . In the present case it is entirely possible that the sulphur compounds in the feedstock complicated the hydrogenation kinetics in this way.

Effects of Metal Oxide Concentration:

Several catalysts of varying MoO_3 concentration were evaluated. Figure 2 A shows that the % conversion of sulphur increases with MoO_3 concentration and reaches a plateau after 9 wt % MoO_3 . The denitrogenation results (Figure 2 B) show similar trends. However, at 320°C the rate of increase of conversion with metal oxide concentration was considerably greater for denitrogenation. At all temperatures studied the denitrogenation conversion is higher than desulphurization for the whole series of unpromoted MoO_3 /alumina catalysts. Qader et al²⁰ also reported that the denitrogenation conversion was higher than desulphurization conversion for low temperature distillate from coal tar (200 - 325°C, 0.83 wt % S and 0.40 wt % N) on a WS_2 catalyst at pressures above 1000 psig. However, Williams et al²¹ found that desulphurization conversions were greater than denitrogenation conversions for a heavy gas-oil (345 - 525°C, 3.59 wt % S and 0.38 wt % N) on unpromoted MoO_3 /alumina catalysts at 2000 psig. The combined results indicate that the nitrogen in the heavier fractions is much more difficult to remove.

Hydrogenation of aromatics in coker kerosene distillate showed a trend different from denitrogenation and desulphurization (Figure 2 C). A 3 wt % MoO_3 /alumina catalyst showed significantly higher hydrogenation conversion than the pure alumina support. However, further increases in MoO_3

concentration only slightly improved the hydrogenation of aromatics.

The conversion of fractions boiling above 220°C to fractions boiling below 220°C (equation 1) was measured for all catalysts studied. At 400°C, the per cent conversion increased with increasing metal oxide concentration up to 9 wt % MoO₃ and decreased above 9 wt % (Figure 2 D). At 320°C, the maximum was at 6 wt % MoO₃. The findings of Seshadri et al²² may provide a partial explanation for the maximum in conversion. They found that, for MoO₃/alumina catalysts, the catalytic activity in vapour-phase aldol condensation of n-butyraldehyde and the esr signals (indicating Mo⁵⁺ concn.) showed maxima at 9 wt % in MoO₃, suggesting that Mo⁵⁺ centers may be responsible for molecular weight reduction. Desulphurization, denitrogenation and hydrogenation conversions did not show these maxima. It would appear that quite different sites are involved for molecular weight reduction than for the refining reactions.

Effects of Promoters:

At low reaction temperatures the addition of promoters to MoO₃/alumina catalysts affected the desulphurization, denitrogenation and hydrogenation processes differently. Comparing catalysts containing 2.2 wt % MoO₃/alumina and 1.1 wt % CoO - 2.2 wt % MoO₃/alumina, the conversions at 320°C for desulphurization, denitrogenation and aromatic hydrogenation increased from 20 to 76.7%, 30 to 48% and 31 to 43% respectively (Figures 1 A, 1 B and 1 C and Table 2). A laboratory catalyst containing 12 wt % MoO₃/alumina was compared with a commercial catalyst having 3 wt % CoO - 12 wt % MoO₃/alumina. In this case the conversions improved from 38.8 to 93.5%, 57.2 to 79.3% and 40.5 to 49.2% respectively. The promotion of MoO₃/alumina with nickel showed similar increases in desulphurization, denitrogenation and hydrogenation (Table 2). At 320°C the increase in conversions due to promoter addition varied in the following order:

desulphurization > denitrogenation > aromatic hydrogenation

The results show that the addition of cobalt or nickel to molybdenum/alumina significantly increases the selectivity for the desulphurization reaction in particular. The promoter would appear to change the chemisorption characteristics of sulphur compounds in such a way as to selectively improve desulphurization.

Similar results were obtained by Williams et al²¹ showing that the addition of a promoter selectively increased the desulphurization conversion. They found that, at 380°C for 3 wt % CoO - 12 wt % MoO₃ catalysts, the desulphurization and denitrogenation conversions were 78% and 24% respectively compared to 35% and 16% for 12 wt % MoO₃ catalysts. The important point to note is that the different types of compounds present in the low boiling coker kerosene and the heavy gas-oil feedstocks did not affect the promotion of desulphurization by cobalt or nickel.

Comparison of Denitrogenation and Desulphurization at Different Temperatures:

The rate constants calculated using the first order equations for denitrogenation and the second order equations for desulphurization are shown in Arrhenius plots (Figures 3 & 4). The results obtained for both promoted and unpromoted catalysts are given. It is seen from Figure 3 that the activation energies (proportional to the slopes of the lines) for denitrogenation decrease with increasing concentrations of unpromoted MoO₃ on alumina. On the other hand, for desulphurization (Figure 4) the activation energies increase with increasing MoO₃ concentration. Cremer²³ suggests that one of the reasons for variations in activation energies and frequency factors is the difference in the strength of adsorption. In the present work, the variations in activation energies also suggest that the differences in denitrogenation and desulphurization conversions on MoO₃/alumina are caused by differences in strengths of chemisorption of sulphur and nitrogen compounds on the catalyst. When Ni or Co promoter was added the activation energies for both denitrogenation and desulphurization decreased, but there was a large increase in the frequency factor for the desulphurization reaction compared to the denitrogenation reaction.

Satterfield et al⁴ suggest that the interaction between desulphurization and denitrogenation is temperature-dependent. They studied the desulphurization of model compounds such as thiophene and the denitrogenation of pyridine on commercial CoMo, NiMo and NiW sulphided catalysts at temperatures up to 425°C and pressures up to 1.1×10^3 kN/m² (11 atm). At low temperatures, thiophene inhibited denitrogenation and at high temperatures the sulphur compounds enhanced the denitrogenation. The results obtained with distillate fractions and the promoted catalysts both in the present work and by Williams et al²¹ support the observations of Satterfield et al⁴. With the coker distillate over Co and Ni promoted catalysts, the desulphurization was much

higher than denitrogenation at 320°C, but the denitrogenation conversion improved relative to desulphurization with increasing temperature (Table 2). Also, Williams et al found that for similar promoted MoO₃/alumina catalysts (Table 3), the differences between the conversions for denitrogenation and desulphurization decreased at higher reaction temperatures.

With the unpromoted catalysts, on the other hand, the hydrotreating data shows a reverse trend. The results for the unpromoted catalysts (Figures 1 A, 1 B and Table 2) with the coker distillate and of Williams et al on gas-oil (Table 3) show that with increasing reaction temperature, the desulphurization reaction conversion improves relative to denitrogenation conversion. A comparison of relative conversions for desulphurization and denitrogenation at different temperatures definitely indicates that the interaction of these reactions depends on whether the catalyst is promoted or not.

CONCLUSIONS

Comparison of molecular weight reduction and the refining reactions on unpromoted MoO₃ catalysts indicates that quite different active sites are involved for molecular weight reduction than for the refining reactions. Variations in trends for apparent activation energies of desulphurization and denitrogenation on unpromoted catalysts indicate differences in chemisorption characteristics of nitrogen and sulphur compounds.

With the promoted catalysts, the kinetics observed with the distillate fractions generally agrees with the results of the pure compound studies. The trend of the data was the same regardless of the boiling range of the distillate. However, in the case of unpromoted catalysts, the boiling range of the feed-stock has a considerable influence on the reaction rates. Comparison of the high pressure data for coker kerosene reported here, the high pressure data of Williams et al²¹ and the low pressure data reported by Satterfield et al⁴ indicates that with increasing reaction temperature, the presence of sulphur compounds enhances denitrogenation relative to desulphurization on promoted catalysts but not on unpromoted catalysts.

ACKNOWLEDGEMENTS

The authors wish to thank R.G. Draper, E. Kowalchuk, G.R. Lett, S. Soutar, E. McColgan, R.J. Williams and R.W. Taylor for their technical assistance.

REFERENCES

1. Amberg, C.H. and Owens, P.J., *Advances in Chemistry Series* 33, 182 (1961)
2. Doleman, J. and Vlugter, J.C., *Proceedings of Sixth World Petroleum Congress, Frankfurt, West Germany, Section 111*, 247 (1964)
3. Voorhoeve, R.J.H., *J. Catalysis* 23, 236 (1971)
4. Satterfield, C.N., Modell, M. and Mayer, J.F., *A.I.Ch.E. Journal*, 21 (6), 1100 (1975)
5. Rosenheimer, M.O. and Kiovsky, J.R., *ACS Preprints (Petroleum) Chicago Meeting, Sept. 11, 1967*, p B-147
6. Bachman, W.A. and Stormont, D.H., *Oil and Gas J.*, 65 (43), 69 (1967)
7. Williams, R.J., Draper, R.G. and Parsons, B.I., *Technical Bulletin TB 187, Department of Energy, Mines & Resources, Ottawa, Canada* (1973)
8. Takematsu, T., and Parsons, B.I., *Technical Bulletin TB-161, Dept. of Energy, Mines & Resources, Ottawa, Canada* (1972)
9. Frechette, G., Herbert, J.C., Thinh, T.P. and Miron, T.A., *Hydrocarbon Processing*, 54 (2), 109 (1975)
10. Fabbro, L.A., Filachek, L.A., Iannacone, R.L., Moore, R.T., Joyce, R.J., Takahashi, Y. and Riddle, M.E., *Anal. Chem.* 43, 1671 (1971)
11. ASTM Method D-1319
12. Ranganathan, R., Ternan, M., and Parsons, B.I. - publication in "Fuel" (in preparation)
13. Schuman, S.C. and Shalit, S.C., *Catalysis Reviews* 4 (2), 245 (1970)
14. Whalley, M. and Ternan, M. - unpublished results
15. Flinn, R.A., Larson, O.A. and Beuther, H., *Hydrocarbon Processing* 42 (9), 129 (1963)
16. Beuther, H. and Schmid, B.K., *Proc. 6th World Petroleum Cong., Frankfurt*, 3, 297 (1963)

17. Schuit, G.C.A. and Gates, B.C., A.I.Ch.E. Journal 19 (3), 417 (1973)
18. Gully, A.J. and Ballard, W.D., Adv. in Pet. Chem. and Ref. 7, 240 (1963)
19. Voorhoeve, R.J.H. and Stuijver, J.C.M., J. Catalysis 23, 228 (1971)
20. Qader, S.A., Wiser, W.H. and Hill, G.R., Ind. and Eng. Chem. Proc. Des & Dev. 7 (3), 390 (1968)
21. Williams, R.J., Ternan, M. and Parsons, B.I., Report ERP/ERL 75-85 (R), Energy Research Laboratories, Dept. of Energy, Mines and Resources, Ottawa, Canada (1975)
22. Seshadri, K.S. and Petrakis, L., J. Phys. Chem. 74, 4102 (1970)
23. Cremer, E., Advances in Catalysis 7, 83 (1955)

TABLE 1

PROPERTIES OF THE FEEDSTOCK

Properties		Coker Kerosene Distillate
Boiling range,	°C	193 - 279
Specific Gravity 60/60	°F	0.871
Sulphur,	wt %	2.32
Nitrogen,	ppm	430
Pour Point,	°F	Below -60
Cloud Point,	°F	Below -60
Flash Point,	°F	116
Vanadium,	ppm	0.40
Nickel,	ppm	0.36
Iron,	ppm	0.50
Ramsbottom Carbon		
Residue (10% bottoms),	wt %	0.29
Aromatics + olefins,	vol %	58
Saturates,	vol %	42

TABLE 2

DESULPHURIZATION, DENITROGENATION AND HYDROGENATION
OF COKER KEROSENE ON PROMOTED AND UNPROMOTED CATALYSTS

Catalysts	Promoted								Unpromoted			
	1.1 wt % CoO-2.2 wt % MoO ₃ /alumina				1.1 wt % NiO-2.2 wt % MoO ₃ /alumina				3 wt % MoO ₃ /alumina			
Concn metal oxides												
Reaction temperature, °C	320	360	400	420	320	360	400	420	320	360	400	420
% desulphurization	76.7	92.7	96.6	96.6	71.1	94.0	96.1	96.1	26.7	56.5	87.1	92.2
% denitrogenation	48.1	82.3	95.3	97.7	50.9	86.1	96.3	98.6	34.4	68.6	91.2	94.0
% hydrogenation	43.2	54.1	56.6	56.8	42.9	52.2	55.8	57.5	34.9	43.4	55.3	56.3

TABLE 3

GAS OIL HYDROTREATING ON
PROMOTED AND UNPROMOTED CATALYSTS
Williams et al (21)

Catalyst	Promoted	Unpromoted					
		3 wt % CoO - 12 wt % MoO ₃	3 wt % MoO ₃	6 wt % MoO ₃	9 wt % MoO ₃	12 wt % MoO ₃	
Concn metal oxides							
Reaction temperature, °C	380	450	380	450	380	450	450
% desulphurization	78	93	26	74	29	81	35
% denitrogenation	24	73	0	24	0	45	16
							63

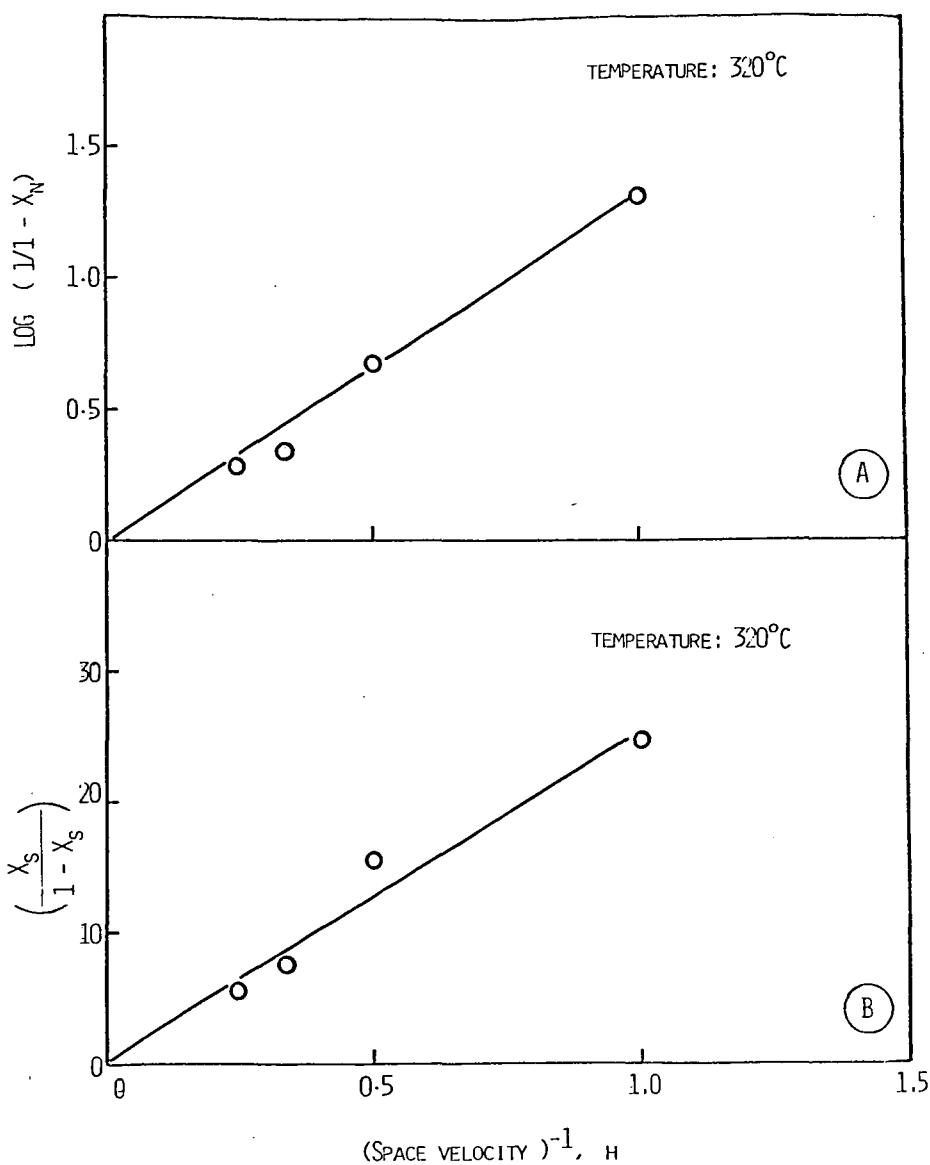


FIGURE 1 A FIRST ORDER PLOT FOR DENITROGENATION
(X_N - FRACTIONAL NITROGEN CONVERSION)

FIGURE 1 B SECOND ORDER PLOT FOR DESULPHURIZATION
(X_S - FRACTIONAL SULPHUR CONVERSION)

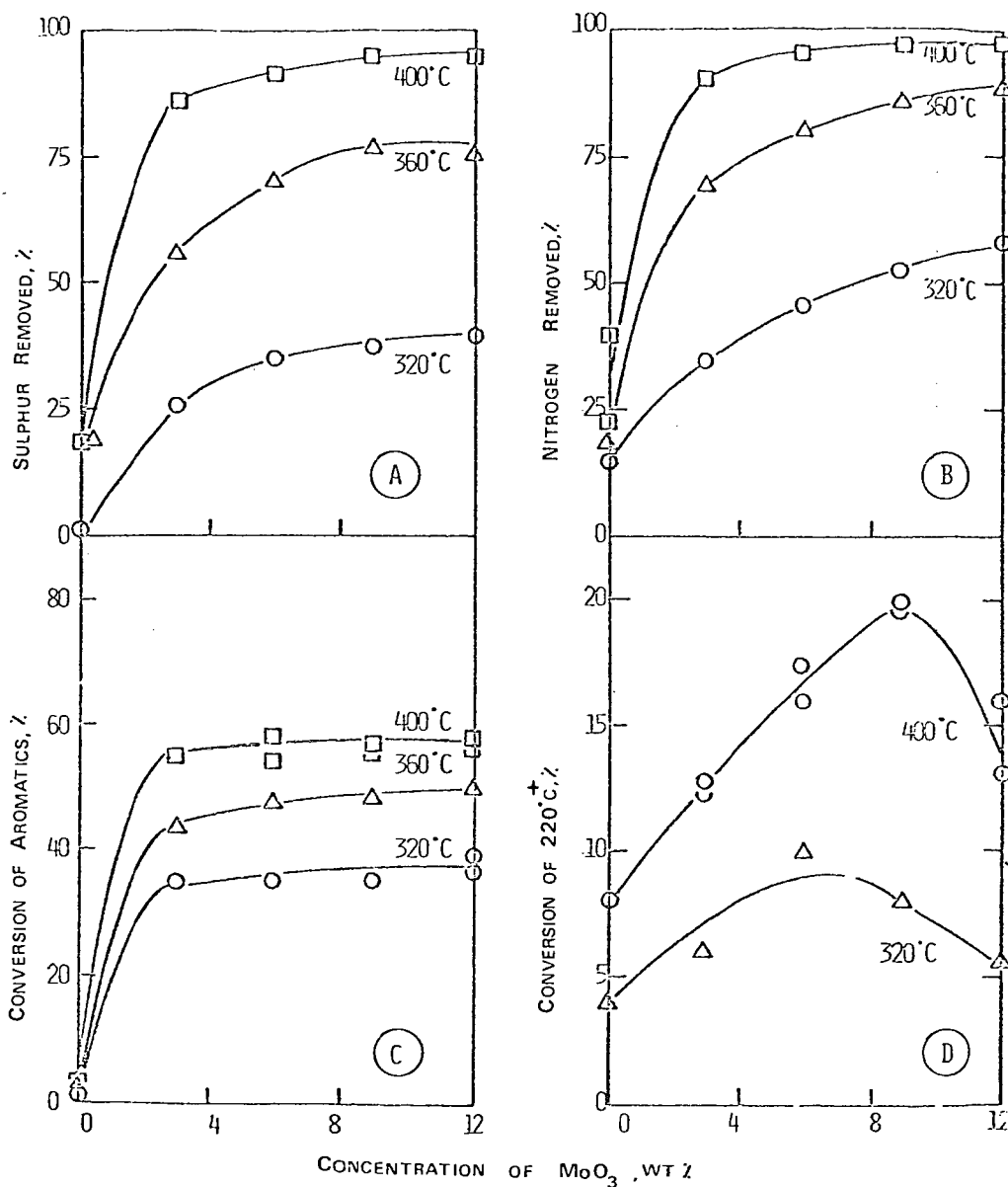


FIGURE 2 - EFFECT OF METAL OXIDE CONCENTRATION ON: A-DESULPHURIZATION CONVERSION
 B-DENITROGENATION CONVERSION
 C-HYDROGENATION OF AROMATICS
 D-CONVERSION OF FRACTIONS BOILING ABOVE 220°C

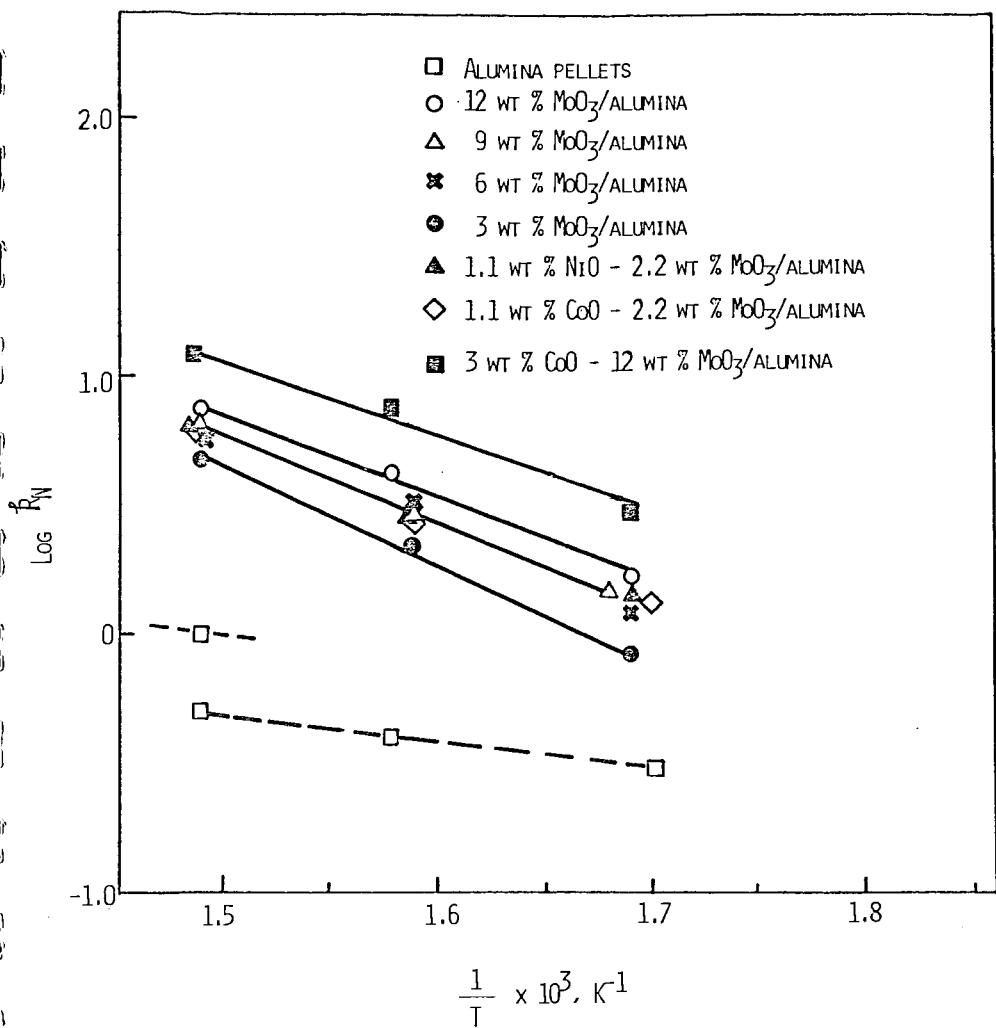


FIGURE 3 - ARRHENIUS PLOT FOR DENITROGENATION
(k_N - FIRST ORDER RATE CONSTANT)

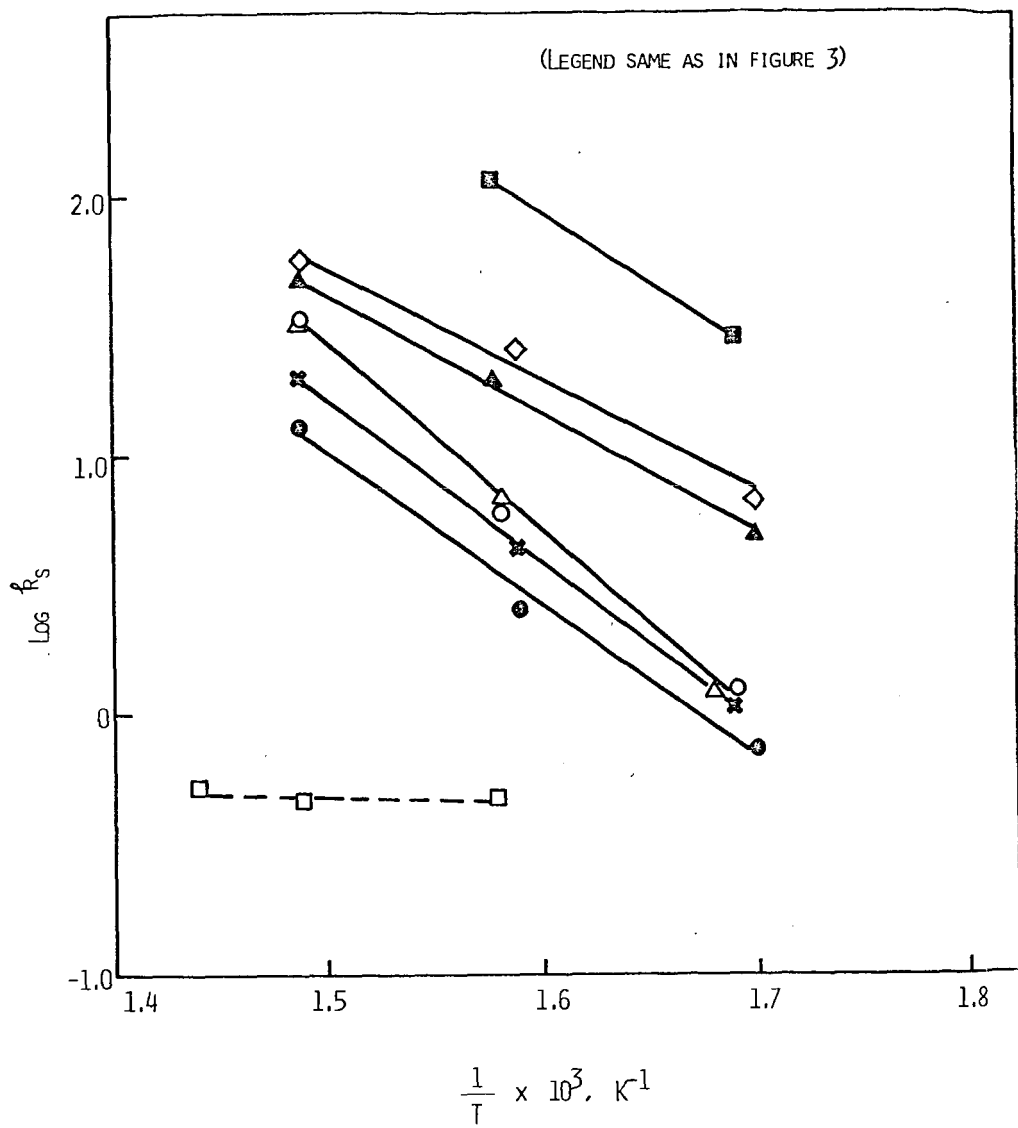


FIGURE 4 - ARRHENIUS PLOT OF DESULPHURIZATION
(k_s - SECOND ORDER RATE CONSTANT)

HYDROCRACKING OF IN SITU SHALE OIL

P. L. Cottingham and L. G. Nickerson

Energy Research and Development Administration
Laramie Energy Research Center, Laramie, Wyoming 82071

ABSTRACT

A group of once-through laboratory hydrocracking experiments was made with crude in situ shale oil from underground combustion retorting of Green River oil shale. Nickel oxide-molybdenum oxide catalyst on a silica-stabilized alumina support was used at 1500 psig pressure, 700°, 750°, and 800° F, and space velocities of 0.6, 1.0, and 2.0 volumes of oil per volume of catalyst per hour. Yields and properties of gasoline-boiling-range naphthas and broad-cut diesel fuels are given.

EFFECTS OF THERMAL HYDROCRACKING ON THE
COMPOUND-TYPE DISTRIBUTION IN ATHABASCA BITUMEN

A.E. George, R.C. Banerjee, G.T. Smiley and H. Sawatzky

INTRODUCTION

Upgrading Athabasca bitumen requires the use of pyrolytic processes. The currently-used coking processes are wasteful, and alternatives such as the thermal hydrocracking process are sought (1). This report deals with the hydrocarbon-type conversions involved in hydrocracking this asphaltic sulphurous bitumen.

Five samples of hydrocracked bitumen, selected to represent increasing severities of treatment as expressed in pitch conversion to distillable fractions, were subjected to analysis by liquid-solid chromatography.

EXPERIMENTAL

A schematic diagram of the procedure and the breakdown to compound types is shown in Figure 1.

Thermal Hydrocracking

The hydrocracking pilot plant and its operation have been described in a previous report (1). The reactor is a vertical vessel to which the total Athabasca bitumen and hydrogen are fed at the bottom. Any gases formed can escape upwards immediately and are removed in a scrubber before the hydrogen is recycled with the fresh make-up hydrogen to the reaction vessel. Five samples representing increasing degrees of hydrocracking were selected for investigation. Three of these samples are representative of steady state conditions of a liquid hourly space velocity of 2, a feed rate of 8000 grams per hour and temperatures of 435, 445 and 455°C respectively. Similarly, the other two samples were obtained at a liquid hourly space velocity of 1, a feed rate of 4000 grams per hour and temperatures of 445 and 460°C respectively. All the samples resulted from processing at 2000 psi operating pressure and a hydrogen recycle rate of 1.5 cu ft/hr at operating pressure and 25°C. The hydrogen purity was 85%. The product was separated into a light and a heavy oil in a hot receiver vessel.

Distillation

The light oil was separated by distillation (ASTM D216-54) to light ends boiling below 200°C and the fraction boiling above 200°C. The heavy oil

did not contain any light ends boiling below 200°C. The distillation residue above 524°C is defined as pitch.

Deasphalting

The asphaltene portion of the heavy oil was precipitated through the addition of twenty volumes of pentane to one volume of oil. The asphaltenes were separated by filtration, extracted with pentane in a soxhlet extractor and dried first on a water bath, then under reduced pressure at 50°C. The main pentane solubles and washings were combined and n-pentane was completely evaporated from these maltenes.

Compound-Type Separation

The light ends distilling below 200°C were analyzed for saturate, aromatic and olefinic contents on silica gel using the fluorescent indicator adsorption method (ASTM D1319-70).

The light oil fraction boiling above 200°C and the deasphalted heavy oil (maltenes) were separated into compound-type concentrates of saturates, monoaromatics, diaromatics, polyaromatics, polar material and basic compounds in a dual-packed (silica gel and alumina gel) liquid-solid chromatographic column developed by the API project 60 (2), and modified in our laboratory (3). The modification consisted of scaling down the original procedure by a factor of 10 and applying pressure to increase the speed of separation. The polyaromatics were eluted by benzene; the polar material was eluted by a mixture of polar solvents (methyl alcohol, ethyl ether and benzene) and the basic compounds were eluted by pyridine at 100°C (Figure 1).

The number of moles of the various types of structures were determined using average molecular weights that were obtained by vapour pressure osmometry for the light oil and heavy oil. The average molecular weights of the light oil fraction below 200°C were determined from gas chromatographic simulated distillation data, assuming that the material distilling when half of the sample had distilled represented the average molecular weight. The aromatics in the light ends distilling below 200°C were assumed to be mononuclear aromatics.

The number of sulphur-bearing structures in each fraction was determined assuming that there was one sulphur atom per molecule. The number of sulphur-free structures was then obtained by difference.

Mass Spectrometric Analyses

Analyses of the approximate compositions of the cyclic saturates were performed on a C.E.C. 21-104 mass spectrometer, operated at an ionization potential of 70eV and using electric scan.

RESULTS

The Athabasca bitumen is a heavy, sulphurous oil with high asphaltene and metal contents. The chemical nature of its hydrocarbons is mostly aromatic, 75% by wt, with a prevalent polyaromatic-polar composition of 70% of the aromatics. The properties of the bitumen are given in Table 1.

Effect of Thermal Hydrocracking on the Gross Composition

Increasing hydrocracking severity causes a steady increase in the amounts of light oil (Table 2) at the expense of the heavy oil and asphaltene contents. The asphaltene content diminishes from 15.3% in the feedstock and 13.4% at 435°C (LHSV-2) to 2.7% at 460°C (LHSV-1). This is an appreciable decrease, considering that the molecular weights of the treated asphaltenes also decline. In these cracking reactions, asphaltenes could be formed as well as destroyed. The presence of hydrogen pressure would suppress asphaltene formation. The percentage of heavy oil in the product decreases steadily to 54% of its content when the severity of the operating temperature was increased from 435°C (LHSV-2) to 460°C (LHSV-1). This effect is even more pronounced considering the lower molecular weight of the products.

The severity of hydrocracking is more pronounced at the lower liquid hourly space velocity due to the increased residence time of the liquids in the reactor. A comparison of the pitch conversions of the two experiments at 445°C and space velocities of 1 and 2 is given in Table 2.

Effect of Thermal Hydrocracking on the Compound-Type Distribution

The compound-type distribution on a weight basis is shown in Table 3. The sulphur is included with the aromatic and polar types. Tables 4 and 5 show the number of moles per 100g of bitumen for the hydrocarbons and for the sulphur compounds respectively.

Saturated Hydrocarbons:

The total percentage of saturates in the liquid products of the bitumen increases markedly with increasing severity of hydrocracking, particularly in the light ends. Although the saturate content remains almost constant in the light oil fraction above 200°C, the increasing percentage of this fraction in the total product increases the total saturate content.

An approximate mass spectrometric ring analysis of the saturates of the Athabasca bitumen shows that they are mainly cyclic with little or no alicyclics. About 90% of the cyclic material is dicyclic, tricyclic and tetracyclic in equal proportions. Monocyclics are absent, and pentacyclics or higher ring systems are present in only small amounts. The alicyclic hydrocarbons developed because of hydrocracking. The dicyclic and tricyclic systems prevailed, followed by the monocyclics, then the tetracyclics, or the reverse, depending on the investigated boiling range. Pentacyclic molecules decreased to trace amounts, while 6- and higher- ring structures disappeared.

The saturate content includes olefinic hydrocarbons ranging in the light oil below 200°C from 8.0% to 5.2% in the least and most severely hydrocracked products respectively. It ranges from 14.6% to 3.0% in the light oil products above 200°C.

Mononuclear Aromatics:

The monoaromatic content of the bitumen increases drastically (175%) at the highest pitch conversion rate and about half of this increase takes place at the mildest treatment (Table 3). The number of aromatic rings, however, increases 3.7 times (Table 4), mostly in the form of benzene structures in the light oil. Benzene compounds are valuable as chemical feedstocks and because of their combustion characteristics.

The numbers of sulphur structures in the monoaromatic concentrate, mostly thiophenes, double on the mildest treatment and then remain almost constant (Table 5).

Dinuclear Aromatics:

This fraction's weight per cent decreases slightly on hydrocracking (Table 3) but the number of its diaromatic rings doubles (Table 4). The thermal stability of the associated sulphur structures are indicated by their slight decrease (Table 5) with no evidence of formation from the destruction

of higher molecular weight components. We have evidence (6) that most of these sulphur compounds are alkyl benzothiophenes.

Polynuclear Aromatics:

The weight per cent of this fraction decreases by more than 50% on hydrocracking, and 54% of this decrease occurs at the least severe treatment (Table 3). However, the number of the polyaromatic structures increases 2.75 times in the mildest treatment, then gradually to 5 times at 460°C (Table 4). The associated sulphur components are unstable relative to the diaromatic sulphur structures (Table 5) and they decrease by 30% with the mildest treatment. This percentage increases gradually to 65% at 460°C.

Polar Components:

Although this fraction diminishes in weight with hydrocracking similar to the polynuclear aromatics (Table 3), the number of these polar structures increase (Table 4). The joining sulphur structures are thermally unstable and decrease to 40% at 460°C (Table 5).

Basic Compounds:

More than half of these compounds are destroyed at the mildest temperature, and only 15% remain at 460°C.

DISCUSSION

The increase of the saturated hydrocarbons content is caused by the cleavage of aliphatic components from the aromatic, polar and asphaltenic structures. At the mildest treatment this fraction appears to increase mostly at the expense of the polynuclear aromatics and the polar materials. The other types would also lose paraffinic and cyclic portions to the saturate fraction and in the meantime receive the same from the higher molecular weight complex fractions. The saturated hydrocarbons could, to a large extent, represent cleavage products from the asphaltenes, especially in the last two treatments. There is a strong relationship between the rate of asphaltene destruction and the increase in saturates content (Tables 1, 2 and Figure 2).

There is also a relationship between the mole increase of the sulphur-free monoaromatic structures (benzenes) and the degree of asphaltenes

conversion (Figure 2) which suggests that these benzenes are cleaved from the complex asphaltenic structures. However, they could be generated by the aromatization of cycloalkanes.

Asphaltenes are considered to consist mainly of large substituted polynuclear aromatic structures (4) and to contain more heteroatoms than the other bitumen fractions. Therefore, it would be expected that their cleavage during cracking should increase the polynuclear aromatic structures as well as the polar compounds. While there is a steady increase in these fractions (Table 4), there is no direct relationship between this increase and the rate of asphaltene destruction.

The only compound types that increase in sufficient quantity to explain the diminishing asphaltene content in the two most severe treatments are the saturates and the mononuclear aromatics. Since it is not plausible to assume that the asphaltenes consist largely of benzene structures, a hydrogenation step of the asphaltene clusters before undergoing cracking must be considered to explain the increase in monoaromatics.

It is unlikely that hydrogenation consumes appreciable molecular hydrogen and the major consumption is probably due to reaction with free radicals formed on cracking, unless some inorganic components in the bitumen catalyze hydrogenation. Probably the hydrogenation of most of the polynuclear aromatic clusters in the asphaltenes and some of the polynuclear aromatic fractions occur by hydrogen transfer reactions. Tetralins are good hydrogen donors in these reactions but, if this is the case, then there would be an appreciable increase in the dinuclear aromatic structures of the products where asphaltenes decrease sharply. This was not observed.

It is known that cyclohexanes are not good hydrogen donors but decalins are (5). If the addition of one aliphatic ring to cyclohexane would increase its hydrogen-donating capability greatly, then it can be inferred that the addition of more saturated rings would result in even better donors. The saturated hydrocarbons are highly cyclized and thus should be effective hydrogen donors. For these reasons, it can be argued that the large complex aromatic clusters become hydrogenated during the hydrocracking reactions by hydrogen resulting from aromatization of saturated structures and that the hydrogenated structures undergo more extensive cracking. This explains the large increase in both the benzene structures and saturated hydrocarbons.

ACKNOWLEDGEMENT

The authors are grateful to the Process Engineering Section for the provision of samples and the processing data.

LITERATURE

- (1) Merrill, W.H., Logie, R.B. and Denis, J.M., Mines Branch Report R-281 (1973)
- (2) Hirsch, D.E., Hopkins, R.L., Coleman, H.J., Cotton, F.O. and Thompson, C.J., ACS Preprints, Div. of Petrol. Chem., p. A65 (1972)
- (3) Sawatzky, H., George, A.E., Smiley, G.T. and Montgomery, D.S., Fuel, 55, 16 (1976)
- (4) Yen, T.F., Energy Sources, 1, 447 (1974)
- (5) Carlson, C.S., Langer, A.W., Stewart, J. and Hill, R.M., Industrial and Engineering Chemistry, 50, No. 7, 1067 (1958)
- (6) Clugston, D.M., George, A.E., Montgomery, D.S., Smiley, G.T. and Sawatzky, H., ACS Fuel Division preprints, 19, No. 2, 202 (1974)

TABLE 1

PROPERTIES OF ATHABASCA BITUMEN

Specific Gravity, 60/60°F	1.009
Sulphur, wt%	4.63
Ash, wt%	0.68
Viscosity, cSt at 210°F	152.2
Conradson Carbon Residue, wt%	12.8
Asphaltene (pentane insolubles), wt%	15.3
Benzene Insolubles, wt%	0.9
Nickel, ppm	70.
Vanadium, ppm	190.

TABLE 2

GROSS COMPOSITION OF ATHABASCA BITUMEN AND

HYDROCRACKING PRODUCTS

(wt % of total bitumen)

SAMPLE	PITCH CONVERSION* wt %	GAS*	LIGHT OIL		HEAVY OIL	
			Below 200°C	Above 200°C	MALTENES	ASPHALTENES
FEED			1.4	(83.3% maltenes above 200°C)	15.3	
LHSV-2, 435°C	59.1	3.9	7.0	10.2	65.5	13.4
LHSV-2, 445°C	68.9	4.0	11.5	10.2	62.0	12.3
LHSV-2, 455°C	77.4	5.9	13.1	10.8	59.7	10.5
LHSV-1, 445°C	80.0	6.8	13.5	25.7	47.0	7.0
LHSV-1, 460°C	91.4	9.2	18.5	34.0	35.6	2.7

(*) Reference 1

TABLE 3

DISTRIBUTION OF THE TOTAL COMPOUND-TYPES
IN THE FEED AND HYDROCRACKED
PRODUCTS OF ATHABASCA BITUMEN
 (Wt % of total bitumen)

<u>SAMPLE</u>	<u>SATURATES</u>	<u>MONOAROMATICS</u>	<u>DIAROMATICS</u>	<u>PNA*</u>	<u>PM*</u>	<u>BC*</u>
Feed	21.0	9.6	9.3	20.1	19.0	5.7
LHSV-2, 435°C	31.3	13.1	8.2	14.2	12.8	2.3
LHSV-2, 445°C	32.8	15.0	8.4	12.9	11.6	2.1
LHSV-2, 455°C	36.0	14.7	8.7	11.7	9.8	1.6
LHSV-1, 445°C	39.0	15.0	7.7	11.1	10.5	1.2
LHSV-1, 460°C	44.1	16.8	7.2	9.1	8.8	0.9

* PNA = Polynuclear aromatics
 PM = Polar material
 BC = Basic compounds

TABLE 4

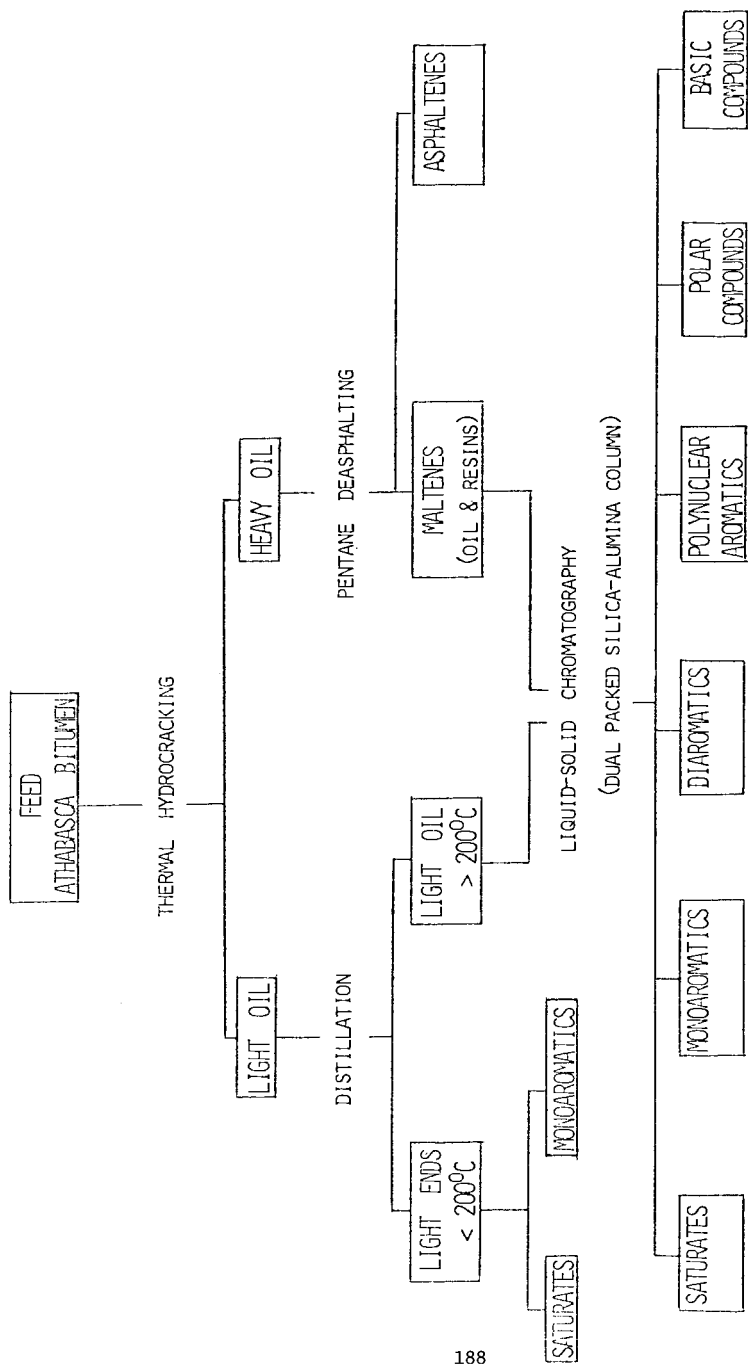
MOLES OF STRUCTURE TYPES
PER 100 GRAMS BITUMEN (SULPHUR COMPOUNDS NOT INCLUDED)

<u>SAMPLE</u>	<u>MONOAROMATICS</u>	<u>DIAROMATICS</u>	<u>POLYAROMATICS</u>	<u>POLAR MATERIAL</u>
FEED	0.021	0.010	0.004	-
LHSV-2, 435°C	0.043	0.015	0.011	0.005
LHSV-2, 445°C	0.058	0.015	0.014	0.008
LHSV-2, 455°C	0.059	0.019	0.015	0.010
LHSV-1, 445°C	0.065	0.020	0.021	0.010
LHSV-1, 460°C	0.078	0.021	0.020	0.013

TABLE 5

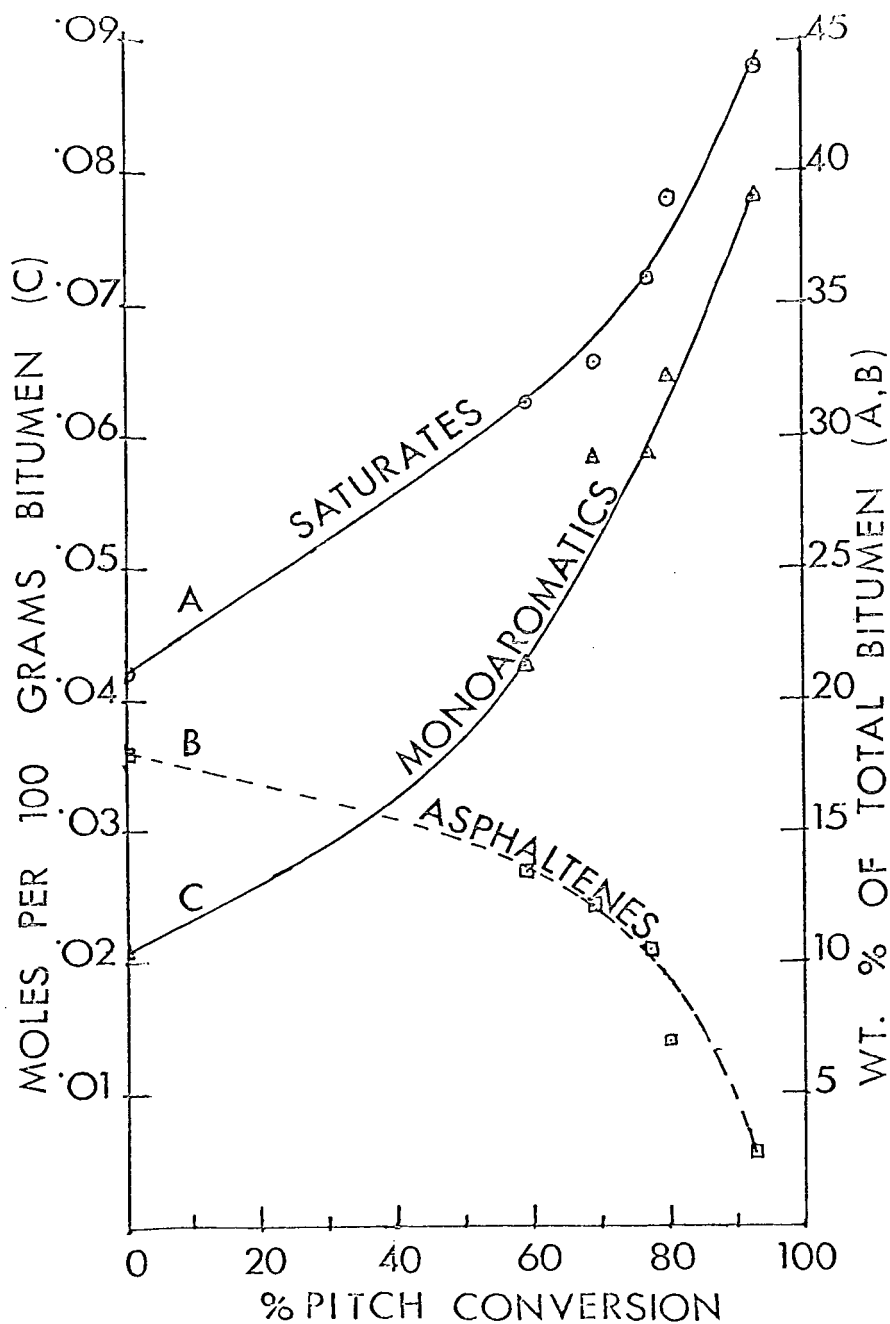
MOLES OF SULPHUR STRUCTURE TYPES
PER 100 GRAMS BITUMEN

<u>SAMPLE</u>	<u>MONOAROMATICS</u>	<u>DIAROMATICS</u>	<u>POLYAROMATICS</u>	<u>POLAR MATERIAL</u>
FEED	0.006	0.014	0.043	0.040
LHSV-2, 435°C	0.012	0.013	0.030	0.025
LHSV-2, 445°C	0.013	0.013	0.026	0.022
LHSV-2, 455°C	0.012	0.013	0.024	0.018
LHSV-1, 445°C	0.011	0.010	0.019	0.018
LHSV-1, 460°C	0.011	0.010	0.015	0.016



HYDROCRACKING AND SEPARATION SCHEMATIC

FIGURE 1



THE EFFECT OF HYDROCRACKING ON SATURATE, MONOAROMATIC AND ASPHALTENE CONTENTS IN ATHABASCA BITUMEN

FIGURE 2

PYROLYSIS OF A HYDROGENATED COAL LIQUID

A. Korosi, H.N. Woebecke, and P.S. Virk

Stone & Webster Engineering Corporation, Box 2325, Boston, Ma 02107

Introduction.

The present work forms part of an effort at Stone & Webster to assess how the production of olefins might be affected by changes in feedstock origin from petroleum to coal. In what follows, we focus on experimental results concerning the characterization, hydrogenation, and pyrolysis of a coal-derived liquid; for comparison, data are also presented for the pyrolysis of a petroleum distillate, having a boiling range and hydrogen content similar to those of the coal liquid, as well as for pyrolysis of decahydronaphthalene, a model alicyclic substrate. Some economic implications of these results will be reported separately; related work in progress includes theoretical and experimental study of alicyclic pyrolysis pathways.

Sample Preparation and Characterization.

Our investigation commenced with a sample of 'Synthoil' coal liquid, produced from a Kentucky hvAb coal by a USBM process recently described by Akhtar et. al. (1). The Synthoil coal liquid was separated into seven fractions by refluxed batch distillation at subatmospheric pressures, of order 10 mm Hg. The second fraction (abbr. CLF), with atmospheric boiling range from 250 C to 380 C, comprised 36 weight percent of the original sample and this fraction was catalytically hydrogenated to yield the hydrogenated coal liquid sample (abbr. HCL) finally pyrolysed.

The coal liquids were characterized by standard analytical procedures, with application of the SARA separation technique (2) to enhance mass-spectrometric analyses. The principal SARA classification categories are Saturated hydrocarbons, Aromatic hydrocarbons, Resins, and Asphaltenes, with some further subdivisions, e.g., mono-, di-, tri-nuclear aromatic hydrocarbons. Pertinent results are presented in Table 1, (a) elemental analyses, and (b) SARA separation data. Individual compounds detected in the hydrocarbon fractions of the Synthoil coal liquid sample appeared to possess predominantly the pyrene and phenanthrene types of skeleta; the number of aromatic rings per molecule averaged two, i.e. the naphthalene type of pi-electron system, with a range from zero (alicyclic) to five (benzopyrene). It is noteworthy that coal liquids derived from other catalytic coal conversion processes (3) also show a preponderance of compounds with pyrene and phenanthrene structures.

Catalytic Hydrogenation.

The coal liquid fraction, sample CLF, was catalytically hydrogenated in two stages, with operation temperature, hydrogen partial pressure, LHSV, respectively (350 C, 125 bar, 0.25 inv. hr) and (300 C, 125 bar, 0.50 inv. hr). The first stage employed a presulfided nickel-tungsten catalyst on alumina, a formulation of

the type commonly used in hydrogenation of aromatic feedstocks. Although detailed intermediate analyses were not obtained, it is estimated that the first stage reduced the aromatics content of the coal liquid from about 75 wt % to about 25 wt %. The second stage employed a proprietary catalyst formulation which included a Pt group metal carried on alumina; this further reduced the aromatics content to about 12 wt %, its final value.

Approximate analyses of the coal liquids before and after hydrogenation are indicated by Table 2, in terms of a matrix of the major compound types detected. Each row in Table 2 represents a particular structural skeleton, while each column represents a particular aromatic nucleus; carbon numbers increase from the bottom upwards and the extent of hydrogenation increases from left to right. Each element of the matrix is labelled by the structure of the compound, and by two numbers representing the respective weight percentages of that compound in the coal liquid samples before (CLF) and after (HCL) hydrogenation. Table 2 shows clearly the predominance of pyrene and phenanthrene structures in both the CLF and HCL samples. The total amount of 3-ring compounds was approximately the same, ≈ 40 wt %, before and after hydrogenation but compounds with ≥ 4 rings seemed to decrease while those with ≤ 2 rings increased following hydrogenation, suggestive of some associated hydrogenolysis. It should also be noted that the aromatic compounds remaining in the hydrogenated coal liquid were mainly benzenes substituted with alicyclic structures.

Pyrolysis Experiments.

The pyrolysis experiments were conducted in an electrically-heated once-through tubular flow reactor, designed to simulate the time-temperature history experienced in commercial steam-cracking operations. Reactor effluent compositions were ascertained by gas-chromatograph and mass-spectrometer analyses. Three feedstocks were pyrolysed: the hydrogenated coal liquid sample (HCL) described earlier, a petroleum distillate (LGO), of Kuwaiti origin, and decahydronaphthalene (DHN) of 99.99 wt % purity with cis-trans isomer percentages 47-53.

Pyrolysis results are summarized in Table 3, parts (a), (b), and (c) of which respectively concern feedstock characterization, pyrolysis conditions, and product yields.

Comparison of HCL and LGO feedstocks in Table 3(a) reveals substantial similarities in their physical properties, i.e. specific gravity and distillation data, but striking contrasts in chemical constitution, the respective paraffin, alicyclic, aromatic contents being HCL(1.0, 83.1, 12.8) and LGO(56.9, 23.0, 20.1). Pronounced differences also exist within each of the respective alicyclic and aromatic groups. Thus the HCL contains mainly 3-ring alicyclics lacking side chains, while the LGO has mainly single ring alicyclic compounds with substantial aliphatic side chains. Single aromatic ring compounds dominate the aromatic fractions in both the HCL and LGO but the benzene ring substitutions differ, the HCL containing cata-condensed alicyclic substituents, e.g. octahydrophenanthrene, whereas the LGO contains open chain alkyl substituents, e.g. n-octyl benzene. The HCL characterization suggests that it should be well modelled by an alicyclic compound of 2 to 3 rings, i.e., decahydronaphthalene or perhydrophenanthrene. Table 3(a), column 3 shows that the DHN specific gravity and hydrogen content are indeed very

close to those of the HCL.

All three feedstocks were pyrolysed under substantially similar conditions, given in Table 3(b), with steam to hydrocarbon weight ratios 0.75 ± 0.25 , reactor residence times 0.35 ± 0.05 sec, exit pressures 1.80 ± 0.05 bar, and exit temperatures 862 ± 12 C.

Pyrolysis product spectra, shown in Table 3(c), merit comparisons between the HCL and LGO, and also between the HCL and DHN feedstocks.

Relative to the LGO, the HCL yielded somewhat less ethylene, and about half the propylene. Yields of 1,3 butadiene were about equal in both cases, but the HCL yielded only half the butenes, making for a greater proportion of the butadiene in the C4 fraction. In the aromatic 'BTX' fraction, the HCL produced roughly twice as much of each component, the ratio of C6:C7:C8 aromatic compounds being approximately the same 1.0:0.5:0.25 for each feedstock. The pyrolysis fuel oil fraction, with atmospheric boiling point ≥ 205 C, was approximately equal in each case. The respective fuel oil samples were both aromatic, had similar hydrogen contents of 6.85 ± 0.15 wt %, and analogous Rayleigh distillation curves, but differed in chemical constitution, the fuel oil from HCL containing major amounts of pyrenes and phenanthrenes whereas naphthalenes were the predominant constituents, ≈ 47 wt %, of the fuel oil from LGO.

Product yields from the HCL and DHN feedstocks showed striking similarities, the yields of compounds from hydrogen through to the C5 fraction being virtually identical. Total BTX yields from HCL and from DHN were roughly in the ratio 2:3, with proportions of the C6-C8 aromatic compounds the same in each case. The HCL yielded twice as much pyrolysis fuel oil as DHN. The respective fuel oil samples were both aromatic, and had similar hydrogen contents and distillation curves, but their chemical compositions differed, the sample from DHN containing a broad distribution of aromatic compound types with naphthalenes, ≈ 15 wt %, somewhat more abundant than any other group.

Discussion.

Hydrocarbon pyrolysis involves mainly free radical and pericyclic types of reactions, the principles of which are known well enough (4,5) to permit inference of likely pyrolysis pathways for any given molecule. Two simplified examples, pertinent to the present experiments, are illustrated in Figure 1, which shows a plausible pathway for each of (a) perhydrophenanthrene and (b) octahydrophenanthrene, these compounds being respectively representative of the alicyclic and aromatic constituents of the HCL sample. The pathway in Figure 1(a) commences in classical Rice-Herzfeld fashion, with hydrogen abstraction from the 10 position; the resulting radical undergoes three successive beta C-C bond scissions and a final hydrogen atom elimination, leading to the 'primary' unsaturated products of ethylene, 1,3 butadiene and 1,3,5 hexatriene. The hexatriene is unstable relative to its 1,3 cyclohexadiene isomer, the pericyclic pathway shown proceeding through electrocyclic ring closure of a butadiene moiety to cyclobutene, followed by a 1,3 sigmatropic alkyl migration (alternately, the hexatriene could isomerize to the all-cis form which undergoes

electrocyclic ring closure). Finally, 1,3 hexadiene pyrolysis leads to benzene in high yields (6), by a radical mechanism. The pathway in Figure 1(b), with an aromatic substrate, starts with hydrogen abstraction from the 2 position; this leads to a radical in which beta scission either requires rupture of the strong 1-11 bond or forms a non-propagating benzylic radical at the 4 position, making hydrogen atom elimination a likely alternative. The molecule produced now contains a 1,4 dihydronaphthalene moiety, which is prone to pericyclic group transfer (1,4 elimination) with formation of the corresponding naphthalene moiety. This type of pathway will evidently cause any originally hydro-aromatic substrate to revert to its fully aromatic analog.

Application of the foregoing provides some insight into the product yield spectra resulting from the HCL, LGO, and DHN feedstocks. In regard to the appreciably lower propylene yields obtained from HCL (also DHN) relative to LGO, we note that propylene is primarily produced by beta scission from 4-carbon moieties of the n- and iso-butyl type, following H abstraction from the 2 and 1 (or 1') positions respectively. Such moieties are abundant in normal- and iso-paraffin compounds, which comprise a major portion of the LGO feedstock, but are absent in alicyclic structures, which predominate in the HCL. Incidentally, the propylene yield from the HCL is far from negligible because pyrolysis of the primary substrate molecules produces others which contain the requisite moieties; e.g. in Figure 1(a), the primary radicals formed after steps 3 and 6 could each abstract hydrogen from the substrate, with the resulting molecules both containing n-butyl moieties. There are two possible reasons why the ethylene yield from HCL was lower than that from LGO. First, at the present experimental conditions, appreciable amounts of ethylene arise from propylene decomposition, with reduced yields of such 'secondary' ethylene a consequence of the observed lower propylene yields. Second, the aromatic molecules in the LGO probably contribute more ethylene than those in the HCL. Ethylene production from substituted aromatic molecules requires alkyl carbon atoms more than two sigma bonds distant from the aromatic ring periphery, e.g., n-octyl benzene contains six such C atoms whereas 1,2,3,4,5,6,7,8 octahydrophenanthrene contains none. It had earlier been pointed out that the aromatics in LGO included alkyl benzenes, whereas those in the HCL were akin to octahydrophenanthrene. The BTX fraction is another major product of both HCL and LGO pyrolyses. The relatively greater amount of benzene, and associated C7 and C8 benzenes, obtained from the HCL seems related to the tendency of polynuclear alicyclic compounds to yield vinyl butadienes as primary pyrolysis products which can then follow facile pathways via hexadiene to benzene, possibly along lines indicated in Figure 1(a). The HCL and LGO produced roughly equal amounts of pyrolysis fuel oil, the differing chemical constitutions of which mainly reflect differences in the aromatic portions of the respective feedstocks.

The congruence between HCL and DHN product yield spectra for compounds containing less than eight carbon atoms implies a close similarity of pyrolysis pathways. Essentially the only difference arises in the pyrolysis fuel oil yields, in which regard the yield from DHN might reasonably be considered characteristic of polynuclear alicyclic pyrolysis under the present conditions. The alicyclic portion of the HCL would therefore be expected to yield about

0.85x11.6 \pm 10 wt % out of the observed 22.5 wt % fuel oil, the remainder, 12.5 wt %, corresponding closely with the amount of aromatic compounds, 12.8 wt %, in the HCL feedstock. This suggests that the hydro-aromatic compounds present in the HCL were mainly pyrolysed to polynuclear aromatic compounds eventually contained in the fuel oil fraction; it is likely that pathways of the type shown in Figure 1(b) contribute to this conversion.

Finally, the foregoing has two interesting implications concerning catalytic hydrogenation of coal-derived liquids to provide pyrolysis feedstocks. First, the polynuclear aromatic molecules contained in coal liquids must be hydrogenated to their fully alicyclic analogs in order to provide desirable pyrolysis products; partial hydrogenation leads to hydro-aromatic molecules which tend to revert to their fully aromatic form upon pyrolysis, contributing mainly to the relatively undesirable fuel oil fraction. Put another way, the incremental yield of desirable olefinic products increases most strongly as the feedstock aromatics content approaches zero. Second, since the final stages of hydrogenation are of decisive importance, the most appropriate catalysts should be those capable of converting multiply substituted benzenes, i.e., catalysts which are relatively insensitive to the steric effects resulting from substitution around the aromatic ring periphery.

Acknowledgements. Dr. Sayeed Akhtar, of the the Bureau of Mines, Pittsburgh, kindly provided the 'Synthoil' coal liquid sample. Pyrolysis experiments were conducted in the Stone & Webster pilot plant facilities at the Institute of Gas Technology, Chicago, with the assistance of Mr. R. Miller.

References.

1. S. Akhtar, N.J. Mazzocco, M. Weintraub, and P.M. Yavorsky, "Synthoil Process for Converting Coal to Non-polluting Fuel Oil." Paper to the Fourth Synthetic Fuels from Coal Conference, Stillwater, Oklahoma (1974).
2. D.M. Jewell, J.H. Weber, J.W. Bunger, H. Clancher, and D.R. Latham, Anal. Chem. 44, 1391 (1972).
3. J.T. Swansiger, F.E. Dickson, and H.T. Best, Anal. Chem. 46, 730 (1974).
4. J.K. Kochi, "Free Radicals," John Wiley & Sons (1973).
5. R.B. Woodward and R. Hoffman, "The Conservation of Orbital Symmetry," Verlag Chemie/Academic Press (1970).
6. S.W. Benson and R. Shaw, J. Amer. Chem. Soc. 89, 5351 (1967).

Table 1. Analyses of Coal Liquid Samples.

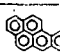
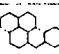
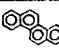
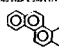
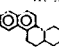
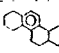
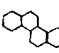
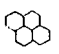

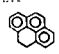
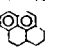
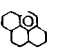
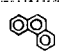
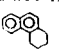
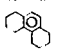
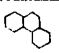
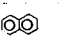
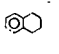
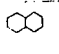
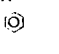
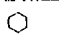
(a) Elemental Analyses.

Sample	H	C	N	O	S	C/H atomic
	percent by weight					
Coal Source (hvAb, MAF)	5.7	72.7	1.4	13.6	6.6	0.94
Synthoil Coal Liquid	9.07	87.14	0.83	2.06	0.90	1.25
Coal Liquid Fraction 2	10.47	87.50	0.38	1.52	0.13	1.44
Hydrogenated Coal Liquid	12.76	87.14	0.03	0.07	0.001	1.76

(b) SARA Separation Data

Sample	Satur HC	Arom HC	Resins	Asphaltenes
	percent by weight			
Synthoil Coal Liquid	13.6	37.4	17.7	31.3
Coal Liquid Fraction 2	25.7	62.6	11.7	0.0
Hydrogenated Coal Liquid	84.1	12.8	3.1	0.0

Table 2. Approximate Compositions of Coal Liquid Samples Before and After Hydrogenation.

 1.0 0.3						 0.9 0.0
 2.5 0.8		 0.6 0.0	 1.5 0.2	 4.0 1.6	 +	 5.3 14.7
	 3.1 0.4	 2.8 0.2	 7.7 0.2	 5.0 1.9		
		 0.4 0.0	 13.6 0.6	 16.7 4.5	 9.6 35.0	
			 1.2 0.0	 9.5 2.5	 6.4 22.0	
				 1.1 0.0	 4.4 13.8	

Note: Figures in table are percentages by weight of the compound. In each row, upper figures refer to Coal Liquid Fraction 2 before hydrogenation (sample CLF), while lower figures refer to Hydrogenated Coal Liquid (sample HCL).

Table 3. Summary of Pyrolysis Experiments.

(a) Feedstock Characterization.

Feedstock Sample*	HCL	LGO	DHN
Specific Gravity, 15/15 C	0.895	0.828	0.883
Elemental Analysis: H wt %	12.76	13.70	13.12
C wt %	87.14	86.16	86.88
Distillation, ASTM D86, vol % vs. deg C			
0 (IBP)	184	193	187
10	245	238	
30	268	271	
50	285	293	191
70	304	318	
90	333	351	
100 (EP)	348	389	196
Hydrocarbon Group Types, wt %:			
n-paraffins	0.0	23.50	0.0
i-paraffins	1.0	33.40	0.0
alicyclics	83.1	23.00	100.0
aromatics	12.8	20.10	0.0

(b) Pyrolysis Conditions.

Steam/Hydrocarbon weight ratio	1.0	0.5	0.5
Residence time, sec	0.3	0.4	0.35
Reactor exit pressure, bar abs	1.85	1.80	1.75
Reactor exit temperature, deg C	875	854	854

(c) Product Yields, in weight percent.

Hydrogen	1.03	0.60	1.05
Methane	11.66	12.00	10.35
Acetylene	0.49	0.39	0.54
Ethylene	18.83	22.66	19.36
Ethane	2.40	3.96	2.86
Propadiene, Propyne	0.58	0.41	0.29
Propylene	7.83	13.02	6.57
Propane	0.21	0.34	0.20
1,3 Butadiene	4.68	4.82	4.65
Butenes	1.63	3.12	1.41
C5 olefins, diolefins	2.56	2.72	2.24
Benzene	12.15	6.71	17.97
Toluene	6.76	3.51	10.34
C8 Aromatics	3.43	2.11	4.88
Other C6, C7, C8	0.48	0.50	0.42
C9+ to 205 C	2.82	2.61	5.21
Pyrolysis Fuel Oil (\geq 205 C)	22.46	20.51	11.66
Total	100.00	100.00	100.00

* Feedstock abbreviations as follows:

HCL Hydrogenated Coal Liquid sample.

LGO Light Gas Oil petroleum distillate (Kuwait, desulfurized).

DHN Decahydronaphthalene.

AN INVESTIGATION OF OXYGEN FUNCTIONS IN BITUMEN FRACTIONS

By

Speros E. Moschopedis and James G. Speight
Fuel Sciences Division,
Alberta Research Council,
11315-87 Avenue,
Edmonton, Alberta,
Canada, T6G 2C2.

INTRODUCTION

The function of hetero-atoms (i.e. nitrogen, oxygen and sulphur) within a bitumen or petroleum has not yet been evaluated but on the basis of work carried out with a variety of petroleum asphaltenes and resins (1), it appears that they play an important part in the intermolecular forces which are necessary for the colloidal stability of petroleum, bitumens and asphalts. For example, the asphaltenes themselves are insoluble in the oils but are able to exist in bitumens (or petroleum) as micellular dispersions due to the peptising effect of the resins. Thus, the stability of the system primarily depends upon the relation of asphaltenes and resins and finally upon the relationship between the micelles and the oily medium. Whilst very little is known about the locale of the hetero-atoms in bitumens and asphalts, preliminary attempts have been made to place the hetero-atoms in aromatic or non-aromatic locations, within the Athabasca bitumen, by virtue of their retention in the cokes formed during pyrolysis (2-4). It therefore seemed worthwhile to examine the bitumen chemically and spectroscopically in order to gain some knowledge of the hetero-atom types in this material. Thus, the results of investigations pertaining to the nature of the oxygen atoms within the asphaltene and resin fractions of the bitumen are now reported.

EXPERIMENTAL

Deasphalted (pentane) Athabasca bitumen was mixed with twenty (20) parts by weight of Fuller's earth whereby extraction with pentane yielded the oil fraction. Subsequent extraction with pyridine yielded the resin fraction. Further separation of the oil fraction by a standard chromatographic technique using a silica gel-alumina column with pentane and benzene yielded the saturates and aromatics, respectively. Infrared spectra were recorded as films on sodium chloride plates using a Perkin Elmer 221 Double Beam Infrared Spectrophotometer; the films were deposited from methylene chloride solution by evaporation of the solvent.

Resin Interactions

Sodium salt of resins: The resins were dissolved in dioxane and the solution heated under reflux with normal aqueous sodium hydroxide solution for 4 hr. The sodium salt of the resins was isolated by evaporation of the aqueous dioxane under reduced pressure.

Resin acids The sodium salt was dissolved in ether and treated several times in an extraction funnel with normal hydrochloric acid solution. The ethereal solution was washed with distilled water until acid free (Congo paper), dried (anhy. sodium sulphate) and the products isolated by evaporation of the ether under reduced pressure.

Acetylated resins: Resins and acetic anhydride were heated under reflux for 24 hr. The acetic anhydride was removed by distillation under reduced pressure at 65°C. The residue was repeatedly dissolved in dry toluene and dried as before to ensure complete removal of the acetic anhydride.

Methylated resins: Resins were methylated with diazomethane in ethereal solution.

Asphaltene Interactions

Acetylated asphaltenes: Method A Asphaltenes (5 g.), acetic anhydride (50 ml.) and pyridine (2 ml.) were heated under reflux for 24 hr. The product was isolated by removal of the liquids under reduced pressure at 65°C. The residue was repeatedly dissolved in toluene and the solvent removed as before to ensure complete removal of the acetic anhydride, extracted with ether (Soxhlet) and dried (70°C/20 mm Hg); the ether extract amounted to 4% w/w of the material. The ether-insoluble material was finally purified by washing a toluene solution with water and, after drying over anhydrous sodium sulphate, the solvent was removed in the usual manner.

Method B The asphaltenes were extracted with ether (Soxhlet) prior to treatment of each fraction with acetic anhydride. As above, the ether soluble fraction amounted to 4% w/w of the asphaltenes. Thus, the asphaltene fraction (5 g.) was acetylated as described in Method A using toluene (50 ml.) as a solvent and the product was purified in a similar manner but the ether extraction step was omitted.

Acetyl group determinations were carried out by the Alfred Bernhardt Microanalytical Laboratory, Elbach über Engelskirchen, West Germany.

Hydrolysis of phthalic and n-butyric anhydrides: The anhydride (1 g.) and aqueous potassium bicarbonate (10% w/w, 50 ml.) were stirred at room temperature for 30 min. After acidification with normal hydrochloric acid solution, the organic product was extracted with ether and the ethereal solution was washed (water) and dried (anhy. sodium sulphate). If a precipitate formed as a result of acidification, the material was isolated by filtration, washed (water) and dried (70°C/20 mm Hg). Refluxing the reactants for 15 min. gave essentially the same results.

Acetylated asphaltenes - aqueous potassium bicarbonate: Acetylated asphaltenes (1 g.) and aqueous potassium bicarbonate (10% w/w, 75 ml.) were stirred vigorously for 30 min. at room temperature. The asphaltenes were separated by filtration, washed with normal hydrochloric acid solution, water and dried (70°C/20 mm Hg). Alternatively, a solution of acetylated asphaltenes (1 g.) in chloroform (20 ml.) was stirred vigorously with aqueous potassium bicarbonate (10% w/w, 75 ml.) for 30 min. at room temperature. The organic layer was washed with normal hydrochloric acid, water and dried (anhy. sodium sulphate). The solvent was removed under reduced pressure.

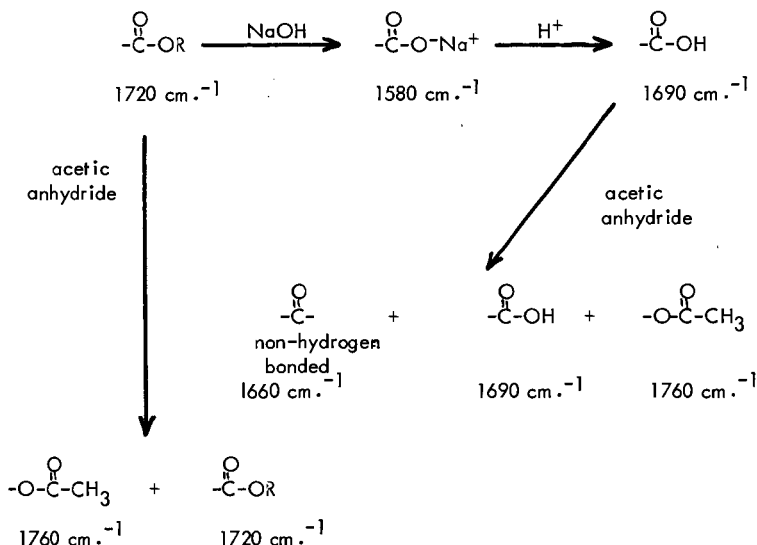
- aqueous sodium hydroxide: A solution of acetylated asphaltenes (1 g.) in benzene (50 ml.) and normal aqueous sodium hydroxide (25 ml.) was heated under reflux for 30 min. The sodium salt of the reaction product was isolated by evaporation of the liquids on a steam bath and was finally dried under reduced pressure (70°C/20 mm Hg).

RESULTS AND DISCUSSION

The use of infrared spectroscopy to identify oxygen functions, especially those responsible for carbonyl absorptions, produced during the oxidation of asphalts has received considerable attention (5). However, the recognition of organically-bound oxygen in unoxidised asphalts and bitumens has mainly been restricted to analytical data (6) and, with few exceptions (7), there has been little, or no, attempt to identify the oxygen types in natural asphalts or bitumens.

Preliminary infrared spectroscopic examination of the bitumen itself and the fractions derived therefrom (Figure 1) shows that the resin fraction exhibits the strongest absorption in the carbonyl region of the infrared (1720 cm^{-1}) and therefore was chosen as the starting material for these investigations. The infrared spectrum of the resins (Figure 2a) is characterised by two absorption bands in the $1500 - 1800\text{ cm}^{-1}$ region which are centred at 1600 cm^{-1} and 1720 cm^{-1} . The former is attributed to double bonds between carbon atoms whilst the latter is assigned to carbonyl oxygen (8). After hydrolysis, the sodium salt of the reaction product exhibits a strong absorption at 1580 cm^{-1} (Figure 2b); the original carbonyl band at 1720 cm^{-1} has completely disappeared whilst the 1600 cm^{-1} band is presumably masked by the strong and broad absorption band centred at 1580 cm^{-1} . These changes in the infrared spectra of the resins suggest formation of carboxylate anions which are derived from the hydrolysed carboxylic acid esters originally present in the resin entities. Furthermore, treatment of the resin sodium salt with hydrochloric acid results in displacement of the sodium ion and formation of the free acid. The infrared spectrum of the resin acids (Figure 2c) shows two bands centred at 1600 cm^{-1} and 1690 cm^{-1} . The latter band is assigned to the carbonyl absorption of hydrogen-bonded carboxylic acid groups. These derivatives also exhibit broad absorption in the $3200 - 3500\text{ cm}^{-1}$ region of the infrared due to the stretching vibrations of hydrogen-bonded hydroxyl groups. When the hydrolysed resins are refluxed with acetic anhydride, the result is a product with a more complex infrared spectrum. As illustrated (Figure 2d), two new bands - centred at 1660 cm^{-1} and 1760 cm^{-1} - appear. The absorption at 1600 cm^{-1} is greatly reduced when compared with the 1690 cm^{-1} band of the resin acids (Figure 2c) and the broad absorption in the $3200 - 3500\text{ cm}^{-1}$ region is also greatly reduced. It appears that reaction with acetic anhydride has caused acetylation of the free and hydrogen-bonded phenolic hydroxyl groups present in the hydrolysed resins giving rise to the absorption bands at 1660 cm^{-1} and 1760 cm^{-1} which have previously been attributed to non-hydrogen-bonded carbonyl of a ketone and/or quinone and phenyl acetates, respectively (9).

In order to obtain stronger evidence and to substantiate further the weak absorption band at 1660 cm^{-1} , methylated resins were treated with refluxing acetic anhydride in the absence of a catalyst. This method has been found effective by Moschopedis (9) on coal humic acids and was later employed by Mathur (10) during studies of soil humic acids. Thus, examination of the infrared spectrum of the product (Figure 2f) again showed prominent absorptions at 1660 cm^{-1} and 1760 cm^{-1} . It was also noted that the 1660 cm^{-1} carbonyl band was much more intense when the resins were methylated prior to treatment with acetic anhydride in agreement with previous work (9-12) that acetylation takes place much more readily after the material has been methylated. In an attempt to ascertain the proximity of the various oxygen functions in the natural resins with respect to each other, the resins and the hydrolysed resins were heated in sulpholane under reduced pressure in the manner outlined elsewhere (11). In both cases, anhydride formation failed to occur thus indicating that any carboxylic acid functions in the original resins and, for that matter, similar functions in the hydrolysed material are not located in such close proximity which would be conducive to anhydride formation (11). It is also noteworthy here that whilst such carbonyl oxygen functions exist in isolated locations, the results of preliminary studies into the quantitative analysis of oxygen functions in the resins indicate that esters are the predominant locale for oxygen in the resin fraction. These latter observations notwithstanding, the results described above lead to the conclusion that the 1720 cm^{-1} infrared absorption band of the natural resins is mainly due to the presence of esters in this material and, thus, the following transformations are proposed:



At this stage, attention was turned to the asphaltene fraction of the bitumen. An examination of the infrared spectrum of the asphaltene (Figure 1) shows that characteristic absorptions due to oxygen-containing functional groups are largely restricted to the 3200-3500 cm.^{-1} region; this broad absorption has previously been assigned to hydrogen-bonded hydroxyl groups (13, 14). Lack of any absorption in the 1670 - 1800 cm.^{-1} region of the spectrum indicates that carboxylic acid carbonyl groups are absent from the asphaltene molecule (14). Nevertheless, it is known that hydrogen-bonded carbonyl groups of ketones and/or quinones appear in the 1600 cm.^{-1} region (14) and, consequently, will be masked by the 1590 cm.^{-1} band present in the asphaltene spectrum; the 1590 cm.^{-1} band in the infrared spectrum of asphaltene has been mainly assigned to carbon-carbon double bonds (8).

When asphaltene is heated with acetic anhydride in the presence of pyridine, the infrared spectrum of the product (Figure 3a) exhibits prominent absorptions in the 1680 - 1800 cm.^{-1} region. Examination of the expanded infrared spectrum shows that the infrared bands of the acetylated material are centered at 1680 cm.^{-1} , 1730 cm.^{-1} and 1760 cm.^{-1} . The relative intensities of the 1730 cm.^{-1} and 1760 cm.^{-1} bands appears to depend upon the method by which the asphaltene was treated with acetic anhydride. For example, when the asphaltene was acetylated in suspension (Method A) the 1760 cm.^{-1} absorption was more intense than the 1730 cm.^{-1} band. The converse is true when the asphaltene was acetylated in solution (Method B); in this case the 1730 cm.^{-1} band was more pronounced. Therefore, it is apparent that when asphaltene was treated in toluene solution acetylation is much more extensive and presumably includes acetylation of hydroxyl groups which may otherwise be

sterically hindered when the material is in suspension and which are relatively difficult to acetylate in this state.

The observed changes in the infrared spectrum of the asphaltenes as a result of treatment with refluxing acetic anhydride suggest acetylation of free and hydrogen-bonded phenolic hydroxyl groups which are present in the asphaltenes (13). The absorption bands at 1680 cm^{-1} and 1760 cm^{-1} have previously been attributed to non-hydrogen bonded carbonyl of a ketone and/or quinone and to phenolic acetates, respectively (9). If the 1680 cm^{-1} band is, in fact, due to the presence of non-hydrogen bonded ketones or quinones, the appearance of this band in the infrared spectra of the products could conceivably arise by acetylation of a nearby hydroxyl function which had served as a hydrogen-bonding partner to the ketone (or quinone) thereby releasing this function and causing the shift from ca. 1600 cm^{-1} to higher frequencies.

The 1730 cm^{-1} band, the third prominent feature in the spectrum of the acetylated products is also ascribed to phenolic acetates and, like the 1760 cm^{-1} band, falls within the range $1725 - 1760\text{ cm}^{-1}$ assigned to esters of polyfunctional phenols suggesting that a considerable portion of the hydroxyl groups present in the asphaltenes may occur as collections of two, or more, hydroxyl functions on the same aromatic ring or on adjacent peripheral sites or on sites adjacent to a carbonyl function in a condensed aromatic system (11).

To check the possibility of anhydride formation which could also account for the 1730 cm^{-1} and 1760 cm^{-1} absorption bands in the products, the acetylated asphaltenes were treated at room temperature with aqueous potassium bicarbonate. The failure of this procedure to cause any changes in the spectra of the acetylated asphaltenes, when model anhydrides were hydrolysed by this reagent, is strong evidence for the exclusion of anhydrides from the products of the acetylation process.

The infrared spectrum of the ether-soluble asphaltene fraction (Figure 1d) is characterised by a broad absorption band at $3200-3500\text{ cm}^{-1}$ and a moderately strong band centred at 1690 cm^{-1} . The former band is assigned to hydrogen-bonded hydroxyl groups of phenols and/or carboxylic acids whilst the latter band is assigned to the carbonyl group of carboxylic acids (14). After refluxing in an acetic anhydride-pyridine mixture, the product also had a band at 1690 cm^{-1} but with shoulders on the high frequency side which consisted of absorptions at 1730 cm^{-1} and 1760 cm^{-1} . These two bands are again assigned to the presence of polyfunctional phenol acetates since, after treatment with aqueous potassium bicarbonate, no changes were observed in the position of these two bands in the infrared. Additional evidence for the assignment of the 1730 cm^{-1} and 1760 cm^{-1} absorptions to phenol acetates was obtained by hydrolysis of the acetylated products, in particular hydrolysis of the acetylated ether-soluble asphaltene as the original material contains carboxyl functions (Figure 3d) which could conceivably lead to anhydride formation. Thus, treatment of the acetylated product with normal aqueous sodium hydroxide yielded a product with a strong absorption centred at 1580 cm^{-1} (Figure 4), assigned to the presence of the carboxylate ion (14), with no absorptions in the $1700-1800\text{ cm}^{-1}$ region. Since treatment with aqueous potassium bicarbonate did not cause any changes in the infrared but hydrolysis with aqueous sodium hydroxide caused marked changes in the infrared spectrum, it is evident that the 1730 cm^{-1} and the 1760 cm^{-1} absorption bands are due to phenolic acetates and not to carbonyl functions of anhydrides.

Finally, acetyl group determination in the products produced some interesting information (Table). The results showed that 40 - 60% of the oxygen present in the unreacted asphaltenes is accessible to acetylation and, in accordance with the absorption band at 1200 cm^{-1} in the infrared spectra of the acetylated materials, is presumed to be in the form of phenolic hydroxyl groups (14). However, it seems that some of these particular groups may

be inaccessible to acetylation because of steric factors since infrared spectroscopic examination of the acetylation products in dilute solution (13) showed the presence of absorption bands due to non-hydrogen bonded hydroxyl groups. It is conceivable that groups of this type may be sterically hindered by virtue of their location in "hole" structures - if such structures do in fact exist within the asphaltene molecule (15). Nevertheless, it is apparent that the majority of the oxygen in the asphaltenes is in the form of hydroxyl groups. The remainder of the oxygen, apart from that in sterically-hindered hydroxyl groups, could well exist as carbonyl functions (such as ketones and quinones), ethers, sulphur-oxygen functions as well as carboxyl functions in the ether-soluble fraction.

Acknowledgements

We thank Syncrude Canada Ltd. for gifts of dry bitumen.

REFERENCES

1. Koots J.A. and Speight J.G., *Fuel*, **54**, 179 (1975).
2. Bowman C.W., *Proc. 7th World Petrol. Cong.*, **3**, 583 (1967).
3. Speight J.G., *Preprints, Am. Chem. Soc., Div. Petrol. Chem.*, **15** No. 1, 57 (1971).
4. Speight J.G., *Alberta Sulphur Recovery Research Workshop, Red Deer, Alberta*, June 3 & 4, 1975.
5. Petersen J.C., Barbour F.A., and Dorrence S.M., *Anal. Chem.*, **47**, 107 (1975).
6. Barth E.J., "Asphalt Science and Technology," Gordon and Breach, New York (1968), p. 10 et seq.
7. Petersen J.C., Barbour R.V., Dorrence S.M., Barbour F.A., and Helm R.V., *Anal. Chem.*, **43**, 1491 (1973).
8. Speight J.G., *Appl. Spectroscopy Revs.*, **5**, 211 (1972).
9. Moschopedis S.E., *Fuel*, **41**, 425 (1962).
10. Mathur S.P., *Soil Sci.*, **113**, 136 (1972).
11. Wood J.C., Moschopedis S.E., and den Hertog W., *Fuel*, **40**, 491 (1961).
12. Greenhow E.J., and Sugowdz G., *Austral. J. Appl. Sci.*, **12**, 246 (1961).
13. Moschopedis S.E., and Speight J.G., *Fuel*, **55**, in press (1976).
14. Bellamy L.J., "The Infrared Spectra of Complex Organic Molecules", John Wiley and Sons Inc., New York, (1966).
15. Speight J.G., *Proc. Nat. Sci. Found. Workshop on the Fundamental Structure of Coal*, Knoxville Tenn., July 17-19 (1975).

TABLE

Sample	Unreacted material		Product	
	%O	m.eq./g.	% acetyl	m.eq./g.
Asphaltene product (Method A)	---not determined---		2.73	0.63
Asphaltene (ether- insoluble) product (Method B)	2.49	1.56	3.08	0.72
Asphaltene (ether- soluble) product (Method B)	1.82	1.14	2.74	0.64

FIGURE 1 Infrared spectra of Zirconium-Ethylene on acrylonitrile fractions

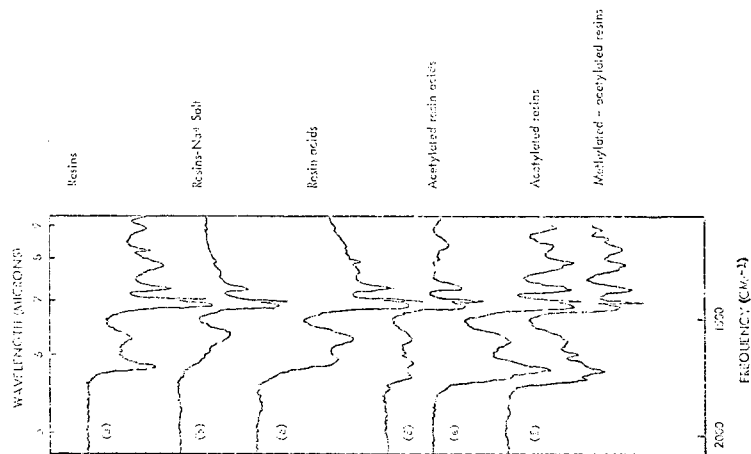
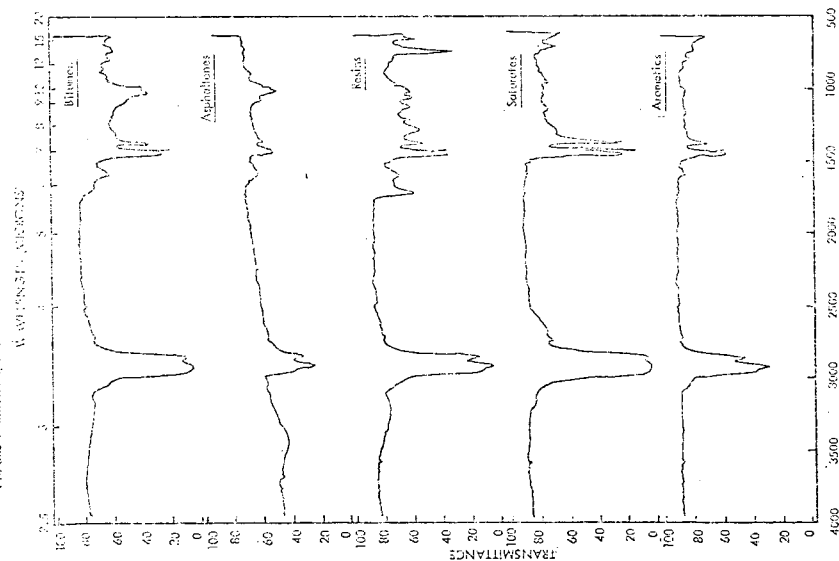


FIGURE 2 Infrared spectra of the resin fraction and derived products

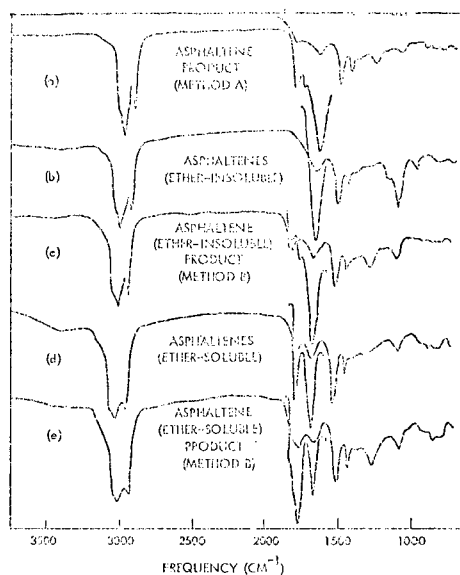


FIGURE 5: Infrared spectra of acetylated products

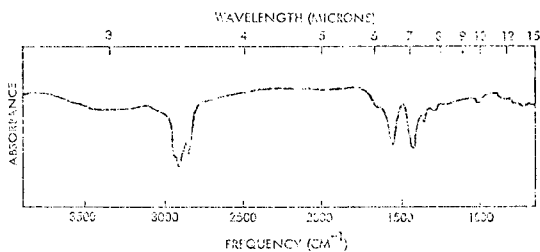


FIGURE 6: Infrared spectrum of acetylated (Method A) ether-insoluble asphaltene after hydrolysis (aq. NaOH)

STEAM PYROLYSIS OF TOSCO SHALE OIL FOR PRODUCTION OF CHEMICAL INTERMEDIATES

C.F. Griswold, V.F. Yesavage, and P.F. Dickson
Colorado School of Mines, Golden, Colorado

INTRODUCTION

The recent national concern for developing new sources of energy has increased interest in creating ways to utilize the vast reserves of oil shale in the U.S. This attention is evidenced in the numerous commercial projects being undertaken for the production of synthetic fuels from oil shale (1). Research and development of synthetic fuels from oil shale has been directed toward processing schemes involving retorting followed by a combination of coking, hydrostabilization, hydrodenitrogenation, reforming, and cracking (2).

Typically, crude shale oil has a high content of organic nitrogen (2% by weight) as reported by Sladek (3) and Atwood (4) and comprehensively characterized by Poulson, et al. (5) and Cook (6). Since nitrogen is a poison for current refinery catalysts, existing refineries would not be able to cope with the high nitrogen content of raw shale oil if it were a substantial part of the refinery feed (2,7). Frost, et al. (7) reports that the National Petroleum Council has suggested that crude shale oil be upgraded at the retorting site. The Energy Research and Development Administration in Laramie has developed a method for refining shale oil that involves the upgrading proposed by the National Petroleum Council (8). The upgrading would require severe prerefining steps. Thus, any alternative use of shale oil that does not require prerefining may be both practical and economical.

An alternative use of shale oil is as a feedstock for production of chemical intermediates such as ethylene, propylene, benzene, toluene, and xylene. Steam pyrolysis of hydrocarbon feedstocks is the most extensively used method for production of petrochemical intermediates (9). Since steam pyrolysis is not a catalytic process, it may not require severe prerefining of the feedstock. It therefore becomes an attractive alternative.

Previous studies of the utilization of shale oil as a steam pyrolysis feedstock have been undertaken by the U.S. Bureau of Mines (10) and the Institute of Gas Technology (11) with significant results. Chambers and Potter (12) report maximization of ethylene should be the objective of steam pyrolysis.

The role of ethylene as a chemical building block in the petrochemical industry is great and will not be further discussed here. Traditionally, most ethylene has been produced by cracking ethane and propane due to the high product yields possible. However, recently the availability of ethane and propane for feedstocks has not kept up with the demand. The continuity of feedstock supply is almost more important than feedstock price (13). Recently naphtha and heavier feedstocks have been used as alternative feedstocks for ethylene production.

"Developmental studies of crude oil pyrolysis indicate that ethylene and other olefins can be produced at lower cost and higher return on investment than by conventional naphtha pyrolysis." (14)

Thus, crude shale oil may be utilized as an economical, readily available feedstock for ethylene production.

An overall research program has been developed to study the utilization of shale oil produced from several retorting processes as a feedstock for steam pyrolysis. The effects of feed composition, operating variables, and nitrogen

level on product distribution will be studied. The objective of this first stage of the overall research program is to develop a steam pyrolysis unit to study the utilization of shale oil produced from the TOSCO II retorting process as a feedstock for steam pyrolysis with a major goal of obtaining maximum ethylene production.

EXPERIMENTAL BASES

Previous Work

Pyrolysis has been established as an effective process for producing chemical intermediates. Processes have been proposed and/or developed for cracking crude (13,14,15,16,17), vacuum gas oil (18), and vacuum residuum (19). The previous significant experimental work with shale oil has been done by the Laramie Energy Research Center of the Energy Research and Development Administration (10,20) and the Institute of Gas Technology (11).

One series of tests by the Laramie Center involved the retorting of pulverized oil shale, entrained in steam or other gaseous media, in a vertical tube high temperature retort. In another series, shale oil from a conventional retort was pyrolyzed for comparison purposes. The latter series is the one relevant to this study. The results show a significant conversion to the chemical intermediates of interest; however, all runs were made below 1200°F, which is below the temperature interval of interest in this study.

The studies made by the Institute of Gas Technology involved the steam pyrolysis of a crude shale oil in a continuous flow vertical tube reactor. The experimental runs were made at higher temperature than the Laramie tests. The shale oil studied was produced from Green River formation shale by the Bureau of Mines gas combustion and the Union Oil Co. processes. The experiments were run for reaction times over the 1- to 4.5-second range at 1400, 1470, and 1550°F for gasification at atmospheric pressure, at partial pressures of the product gas from 0.64 to 0.76 atm. Thus, while the temperature range is sufficiently high, the reaction times are relatively high. The results obtained by IGT will provide a basis for comparison.

Reaction Variables

Feed composition: The ultimate yields of chemical intermediate products is greatly dependent on the composition of the feedstock. Numerous studies have been conducted to determine the yields from both pure compounds and commercial feedstocks. The ease of conversion of various feedstocks to ethylene has been summarized by Zdonik, et al. (18) and Vanderkooi (21). The feedstocks in order of decreasing convertability are:

1. normal-Paraffins
2. iso-Paraffins
3. naphthenes
4. olefins
5. aromatics

Feeds and corresponding products of interest are summarized below:

<u>Feed</u>	<u>Product</u>	<u>Reference</u>
Paraffin	Light olefins	18,21
Light Olefins	Benzene + Toluene other light olefins	22,23
Naphthenes	Light olefins aromatics	18
Aromatics	Unconverted	18,21

Generally, yields of olefinic and aromatic products decrease as the weight of the feedstock increases. Additionally, the lighter olefins may undergo secondary reactions with each other to condense into monoaromatics (22,23). Thus, feedstocks having different paraffin-olefin-naphthene-aromatic (PONA) compositions and different weights will produce different product compositions.

The shale oil to be pyrolyzed in this study is from a TOSCO II process retort with properties (24):

Gravity	21 API
Sulfur	0.7 wt %
Nitrogen	1.9 wt %
Molecular Weight	300

Distillation curves for the TOSCO oil and crude shale oils from the gas combustion retorting process and the Union Oil retorting process (the oils used by the Institute of Gas Technology) are readily available (25).

Temperature: Chambers and Potter (12) report that cracking reactions at highest temperature gave maximum ethylene yields. As temperature is increased, hydrogen, methane, and ethylene yields go up, propanes, butanes, and pentanes go up then down, and hexanes and non-aromatics go down (21). The Institute of Gas Technology (11) conducted their pyrolysis tests between 1400 and 1550°F. Dow Chemical (21) operates between 1382 and 1562°F.

Time: For maximum yields of light olefins, low hydrocarbon residence time is essential (26). The previous studies have been made with residence time ranges of 0.5-1.5 seconds (21) and 1.0-4.5 seconds (11). The importance of low residence times is explained by Kamptner (17):

"The chronological course of the reaction influences the occurrence of disturbing secondary reactions which are generally noticeable in a reduction in the yield of valuable primary cracked products."

The residence time is based on the reactor void volume, the volume of steam flow at atmospheric pressure and reaction temperature, and the ideal-gas volume of 300-molecular-weight oil at atmospheric pressure and reaction temperature.

Steam-oil ratio: In steam pyrolysis, the steam acts as a diluent to prevent excessive coke formation, as an oil preheat heat source, and as a carrier medium. In the temperature range of interest the steam does not participate in the reactions. Studies have been made with steam-hydrocarbon mass ratios of 0.2-0.8 (21) and 0.5-1.0 (26) for feedstocks in the range light naphtha to heavy gas oil.

Pyrolysis severity factor: Numerous severity factors have been developed and/or utilized for correlating pyrolysis results (11,12,21,26,27,28). The most common severity factor is that used by the Institute of Gas Technology which takes the form:

$$S = T\theta^{0.06} \quad 1)$$

where S is pyrolysis severity factor

T is reaction temperature, F

θ is residence time, sec.

The results of this study are correlated with the IGT severity factor with an additional factor to account for the effect of steam-hydrocarbon ratio.

APPARATUS AND PROCEDURE

The continuous flow reactor used in this study (Figure 1) consisted of a 12-inch externally heated section of 1-inch schedule-40 stainless steel pipe. The

reactor was packed with 1/2-inch porcelain balls. Chromel-alumel thermocouples connected to a temperature recorder monitored the temperature within the reaction zone. The heat was supplied by a Linberg single-zone tube furnace. The current to the heated zone was controlled with a Lindberg single-zone control unit that responded to a Platinel II thermocouple in the middle of the heated zone.

Below the reactor was a heavy oil separator in which the steam and heavy oil was condensed and collected. The remaining vapor then passed through a series of water and ice-water condensers and a filter to remove any remaining condensables.

The oil was fed to the reactor with an adjustable-stroke positive-displacement pump. Distilled water was fed through a boiler and superheater and mixed with the oil at the entrance of the reactor. Liquid feed rates were determined by direct measurement of volume flowed during the reaction period.

Gaseous products flow rates were measured with a wet-test meter. Gaseous product compositions were determined by conventional gas chromatography. Solid carbon deposition in the reactor was determined by measuring the weight gain of the reactor packing.

RESULTS

A series of experimental runs were made to determine the relationship between the reaction variables and product yields. A detailed compilation of the reaction conditions and corresponding product analyses is available elsewhere (29). The effects of the reaction variables are discussed in the following sections.

Temperature

Tests for temperature effects were made at temperatures of 1300, 1450, and 1600°F for 0.8 sec residence time and 0.8 steam-hydrocarbon ratio. In Figure 2 the volumetric gaseous product yields are plotted as a function of reaction temperature.

Increasing temperature rapidly increases both the weight percent of the feed converted to gaseous products and the total volume of gaseous products. Gaseous product yields ranged from 3.96 standard cubic feet per pound and 31.46 weight percent converted at 1300°F to 9.23 standard cubic feet per pound and 56.68 weight percent converted at 1600°F.

As can be seen in Figure 2, increasing temperature significantly increases the yields of hydrogen, methane, and ethylene. Higher temperatures promote extensive additional cracking of the vaporized oil and thus the increased production of the lighter gaseous products. Ethylene production increased from 1.17 standard cubic feet per pound at 1300°F to 3.27 standard cubic feet per pound at 1600°F. Corresponding increases of methane from 0.86 to 3.93 and hydrogen from 0.18 to 0.49 were obtained. Propylene production increased from 0.71 standard cubic feet per pound at 1300°F to 0.97 at 1450°F and then decreased to 0.52 at 1600°F due to further cracking to lighter products.

Residence Time

The effect of residence time within the reactor was investigated at times of 0.4, 0.8, and 1.2 sec for 1450°F temperature and 0.8 steam-hydrocarbon ratio. The volumetric gaseous product yields are plotted as a function of residence time in Figure 2.

For the low residence times investigated a great variation in product yields and compositions was not expected as shown in Figure 2. As residence time is increased from 0.4 to 1.2 sec the weight percent converted to gaseous product

increases from 50.06 to 54.44, and the volumetric gaseous product yields increase from 6.78 to 7.84 standard cubic feet per pound. As residence time was increased from 0.4 to 1.2 sec, hydrogen yields increased from 0.31 to 0.45 standard cubic feet per pound, methane yields increased from 1.92 to 2.46, and ethylene yields increased from 2.44 to 2.78. Propylene yields remained essentially constant at 1.0 standard cubic feet per pound.

Steam-hydrocarbon Ratio

Experimental runs were made to investigate the effect of steam-hydrocarbon ratio on product yields and compositions at ratios of 0.4, 0.8, and 1.2 for 1450°F temperature. The volumetric gaseous product yields are plotted as a function of steam-hydrocarbon ratio in Figure 2.

As shown in Figure 2 the effect of increasing the steam-hydrocarbon ratio is similar to increasing the residence time. As the ratio is increased from 0.4 to 1.2, the weight percent conversion to gaseous products increases from 49.31 to 55.63, and the volumetric gaseous product yields increase from 7.02 to 7.88 standard cubic feet per pound.

Although increasing the ratio increases cracking, the cracking tends more toward production of ethylene rather than methane. As the ratio was increased from 0.4 to 1.2, hydrogen yields increased from 0.34 to 0.48 standard cubic feet per pound and ethylene increased from 2.41 to 2.87. Methane production remained nearly constant between 2.2 and 2.3 standard cubic feet per pound. Propylene yields remained essentially constant at 1.0 standard cubic feet per pound.

Pyrolysis Severity Factor

The pyrolysis severity factor combines the effects of all the reaction variables on product compositions and yields into one variable. The IGT severity factor (11) will be used with an additional factor to account for the effect of steam-hydrocarbon ratio. The relation that will be used for correlation is:

$$S = T^{0.06} \text{ ratio}^{0.05} \quad 2)$$

where ratio is the steam-hydrocarbon mass ratio.

Figure 3 shows the effect of pyrolysis severity factor on volumetric gaseous product yields. Greater severity of operation yields greater volumes of paraffins (mainly methane) and light olefins.

Figure 4 shows the gas composition in mole percent as a function of the pyrolysis severity factor. Greater operation severity results in increased hydrogen and methane contents and decreased contents of higher paraffins and olefins. Except for the low temperature run, the ethylene content was nearly constant in the range 34.37-36.39 mole percent.

The effect of severity on light olefin production is shown in Figure 5. Greater severity of operation results in the following trends: ethylene production first increases rapidly and then tapers off to a steady rise. If severity were increased beyond the range of this study then an eventual decrease in ethylene production can be expected via secondary reactions as predicted by Kampthner (17) and obtained by IGT (11). The maximum yield of ethylene obtained was 3.3 standard cubic feet per pound which corresponds to 24.2 weight percent of the feed. Propylene production gradually increases, then gradually decreases due to further cracking via secondary reactions. Propylene yield peaked at 1.0 standard cubic feet per pound or 10.8 weight percent of the feed. Combining both ethylene and propylene yields into a total light olefin yield results in a rapid initial increase which levels off to a constant production rate and then begins to decrease

at high severity. The maximum total light olefin yield was 3.8 standard cubic feet per pound and 31.8 weight percent of feed.

Figure 6 shows the effect of severity on solid products. Carbon deposits increase approximately linearly with pyrolysis severity.

Comparison with IGT

Figure 7 compares the results of a study of crude shale oil pyrolysis by the Institute of Gas Technology with the experimental results of this study. Total gaseous product volumetric yields and ethylene yields are compared. The IGT tests were made on crude shale oil from the gas combustion retorting process and the Union Oil retorting process, while crude shale oil from a TOSCO II process retort was used in this study. The TOSCO oil has a much greater quantity of light ends than the other two oils. Thus a higher total gas and ethylene production would be expected. Figure 7 shows the expected higher production. The total volume of gaseous products from the TOSCO oil is consistently higher than the total volume from the IGT tests for constant reaction severity. Significantly greater yields of ethylene were also obtained at constant reaction severity.

The comparison of the two studies is limited to a qualitative comparison only. The uncertainty is caused by different procedures for calculating residence time. Reaction times for IGT's tests were calculated on the basis of the final product rate, the "average indicated" reaction temperature, reactor pressure, and the reactor volume. However, the method of determining the "average indicated" reaction temperature was not reported. The residence times for this study were calculated on the basis of the reactor void volume, the volume of steam flowed at atmospheric pressure and reaction temperature, and the ideal gas volume of 300-molecular-weight oil at atmospheric pressure and reaction temperature. Additionally, temperature profiles were measured along the length of the reactor. The measurements showed that the temperatures at the exit and entrance of the reactor were considerably lower than the reaction temperature.

CONCLUSIONS

The results of the study of steam pyrolysis characteristics of a TOSCO II shale oil were reasonably successful. Up to 24 weight percent of the feed was converted to ethylene, and up to 6 weight percent was converted to propylene. The results are comparable with reported results and predictions for crude oil, gas oil, and shale oil. For example, Sherwin and Fuchs (30) have predicted yields of 23 weight percent ethylene and 5 weight percent propylene for cracking unrefined shale oil. Additionally, Stork, et al. (13) report expected ethylene yields greater than 20 weight percent for several proposed petrochemical refinery schemes.

Within the ranges studied, an increase in any one of the reaction variables resulted in an increase of severity of operation. The effect of increasing the temperature was extreme, while increasing the residence time or steam-oil ratio had a much smaller effect. A modified form of a commonly used pyrolysis severity factor satisfactorily correlated the experimental results. Increasing the severity of operation resulted in increases in weight percent of feed converted to gaseous and solid products, in total volume of gaseous products, and in volumetric yields of methane and ethylene. The total light olefin yields increased sharply, then leveled off and began to decrease with increasing severity.

The yields obtained from the TOSCO oil were greater in total gas and ethylene than crude shale oil from the gas combustion retort.

LITERATURE CITED

1. Cameron Engineers, 1975, Status of synfuels projects: Synthetic Fuels, v. 12, n. 3, p. 1-3.
2. Montgomery, D. P., 1968, Refining of pyrolytic shale oil: I&EC Product Research and Development, v. 7, no. 4, p. 274-282.
3. Sladek, T. A., 1975, Recent trends in oil shale: Mineral Industries Bull., v. 18, n. 2, p. 6.
4. Atwood, M. T., 1975, Raw shale oils inspections: Golden, Colo., The Oil Shale Corp., 19 p.
5. Poulson, R. E., C. M. Frost, and H. B. Jensen, 1972, Characteristics of synthetic crude from crude oil produced by in-situ combustion retorting: ACS Div. of Petroleum Chemistry Preprints, v. 17, n. 2, p. 175-182.
6. Cook, G. E., 1965, Nitrogen compounds in Colorado shale oils: ACS Div. of Petroleum Chemistry Preprints, v. 10, n. 2, p. C35-C38.
7. Frost, C. M., R. E. Poulson, and H. B. Jensen, 1972, Production of synthetic crude shale oil produced by in-situ combustion retorting: ACS Div. of Petroleum Chemistry Preprints, v. 17, n. 2, p. 156-168.
8. Carpenter, H. C., C. B. Hopkins, R. E. Kelley, and W. I. R. Murphy, 1956, Method for refining shale oil: Ind. Eng. Chem., v. 48, n. 7, p. 1139-1145.
9. Goldstein, R. F. and A. L. Waddams, 1967, The petroleum chemicals industry: London, E.&F.N. Spon Ltd., p. 97.
10. Sohns, H. W., E. E. Jukkola, and W. I. R. Murphy, 1959, Development and operation of an experimental entrained-solids, oil-shale retort: U.S. Bureau of Mines, RI 5522, 45 p.
11. Shultz, E. B., J. J. Guyer, and H. R. Linden, 1955, Pyrolysis of crude shale oil: Ind. Eng. Chem., v. 47, n. 12, p. 2479-2482.
12. Chambers, L. E. and W. S. Potter, 1974, Design of ethylene furnaces: part 1, maximum ethylene: Hydrocarbon Processing, v. 53, n. 1, p. 121-126.
13. Stork, Karl, M. A. Abrahams, and A. Rhoe, 1974, More petrochemicals from crude: Hydrocarbon Processing, v. 53, n. 11, p. 157-166.
14. Wilkinson, L.A. and S. Gomi, 1974, Crack crude for olefins: Hydrocarbon Processing, v. 53, n. 5, p. 109-111.
15. McKinley, D. L., P. E. Boliek, and W. H. Hoffmann, 1967, The Wulff process for feed and product flexibility in the production of olefins: ACS Div. of Petroleum Chemistry Preprints, v. 12, n. 2, p. D138-D143.
16. Jensen, J. T. and M. F. Stewart, 1969, The chemical refinery in perspective: ACS Div. of Petroleum Chemistry Preprints, v. 14, n. 4, p. D77-D84.
17. Kamptner, H. K., 1968, Theory and technique of the high-temperature pyrolysis of petroleum hydrocarbons and their influence on some manufacturing processes: ACS Div. of Petroleum Chemistry Preprints, v. 13, n. 4, p. A23-A35.
18. Zdonik, S. B., E. J. Bassler, and L. P. Hallee, 1974, How feedstocks affect ethylene: Hydrocarbon Processing, v. 53, n. 2, p. 73-81.
19. Cusack, J. and R. H. Mashford, 1974, Paccal makes ethylene from resid: Hydrocarbon Processing, v. 53, n. 1, p. 127-129.
20. Brantley, F. E., R. J. Cox, H. W. Sohns, W. I. Barnet, and W. I. R. Murphy, 1952, High temperature shale oil: Ind. Eng. Chem., v. 44, n. 11, p. 2641-2650.
21. Vanderkooi, W. N., 1974, Pyrolysis experimentation and computations: ACS Div. of Petroleum Chemistry Preprints, v. 19, n. 1, p. 124-139.
22. McConaghy, J. S. and R.N. Moore, 1971, The mechanism of aromatic formation in hydrocarbon pyrolysis: ACS Div. of Petroleum Chemistry Preprints, v. 16, n. 1, p. B88-B95.
23. Sakai, T., K. Soma, Y. Sasaki, H. Tominaga, and T. Kunugi, 1969, Secondary reactions of olefins in pyrolysis of petroleum hydrocarbons: ACS Div. of Petroleum Chemistry Preprints, v. 14, n. 4, p. D40-D53.
24. Atwood, M. T., Sept. 3, 1975, personal communication.
25. Hendrickson, T.A., 1975, Synthetic fuel data handbook: Denver, Cameron Engineers Inc., 112 p.

26. Chambers, L. E. and W. S. Potter, 1974, Design ethylene furnaces: part 2, maximum olefins: Hydrocarbon Processing, v. 53, n. 3, p. 95-100.
27. Davis, H. G. and T. J. Farrell, 1972, Relative rates of decomposition of light paraffins under practical operating conditions: ACS Div. of Petroleum Chemistry Preprints, v. 17, n. 2, p. B60-B68.
28. Farrell, T. J. and H. G. Davis, 1972, An approach to obtaining first order rate constants for the pyrolysis of pure components in mixed liquid feedstocks: ACS Div. of Petroleum Chemistry Preprints, v. 17, n. 2, p. B72-B78.
29. Griswold, C. F., 1976, Master's Thesis, Colorado School of Mines, Golden, Colo.
30. Sherwin, M. B. and W. Fuchs, 1975, Petrochemicals from coal and shale--an overview: Presented at the 79th National AIChE meeting, March 16-20, 1975, Houston, Texas.

ACKNOWLEDGMENTS

The financial support from the National Science Foundation and the Gulf Oil Foundation is acknowledged. Appreciation is also extended to The Oil Shale Corporation for providing the shale oil used in this study.

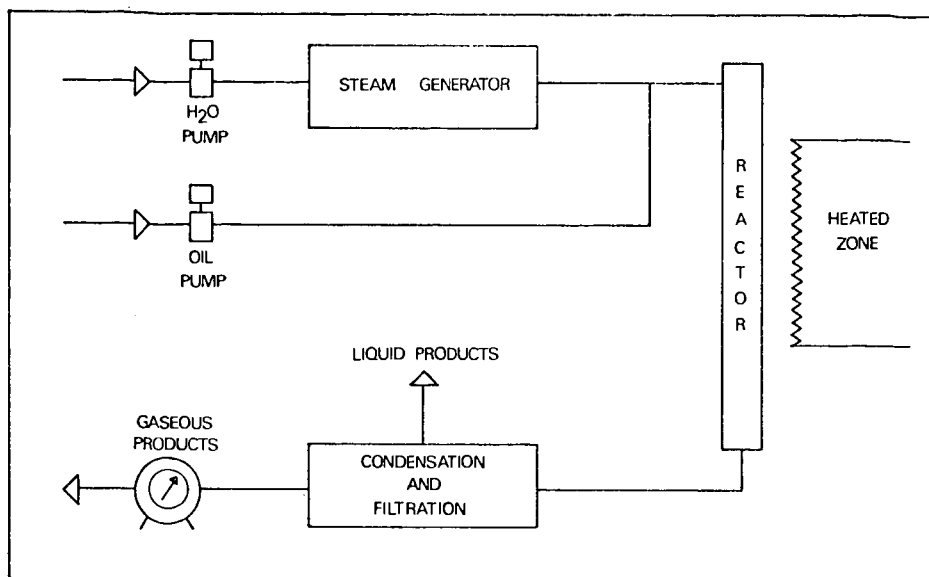


Figure 1. Reactor system

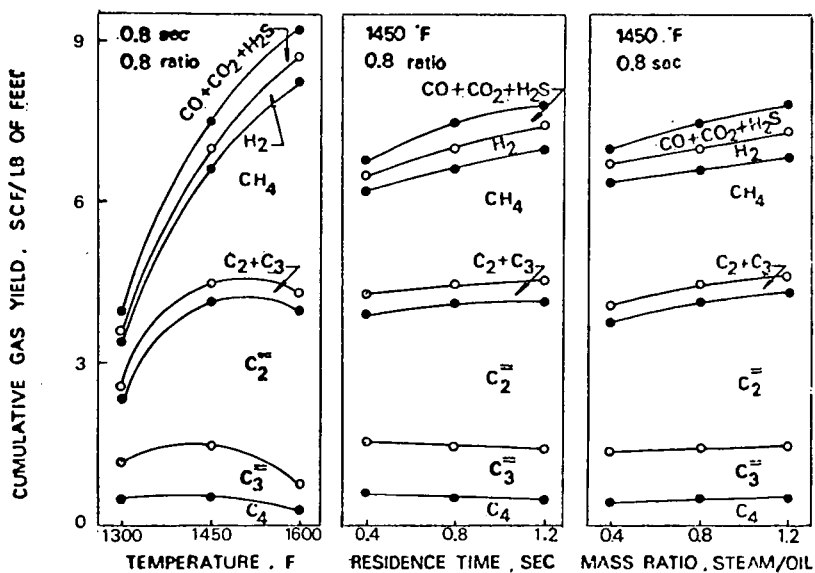


Figure 2. Effect of reaction variables on cumulative gas yields

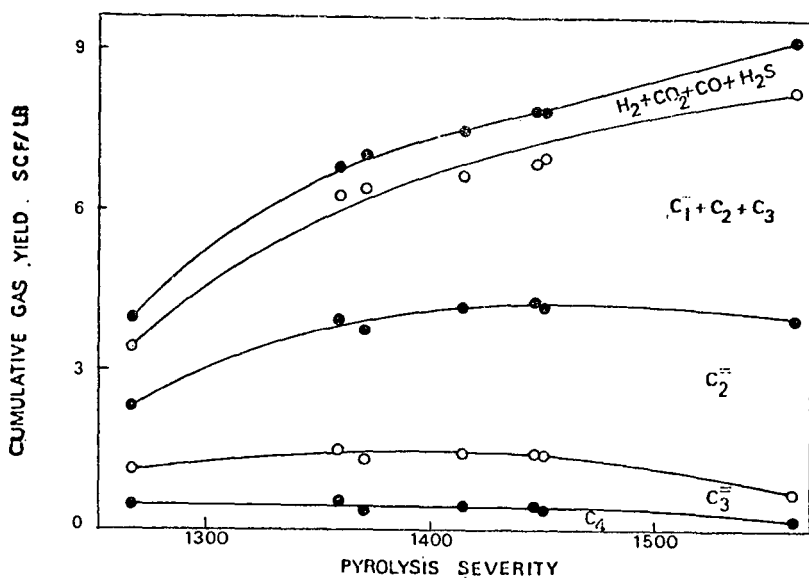


Figure 3. Effect of pyrolysis severity on volumetric gas yields

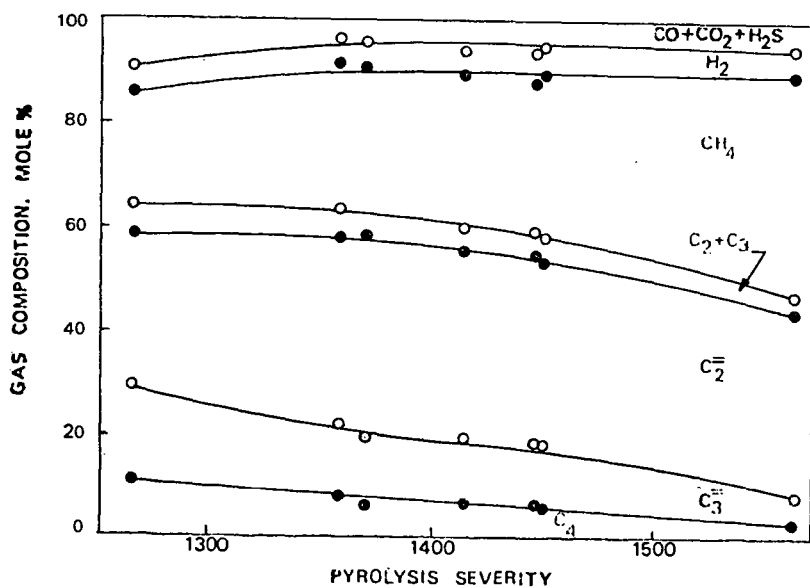


Figure 4. Effect of pyrolysis severity on product gas composition

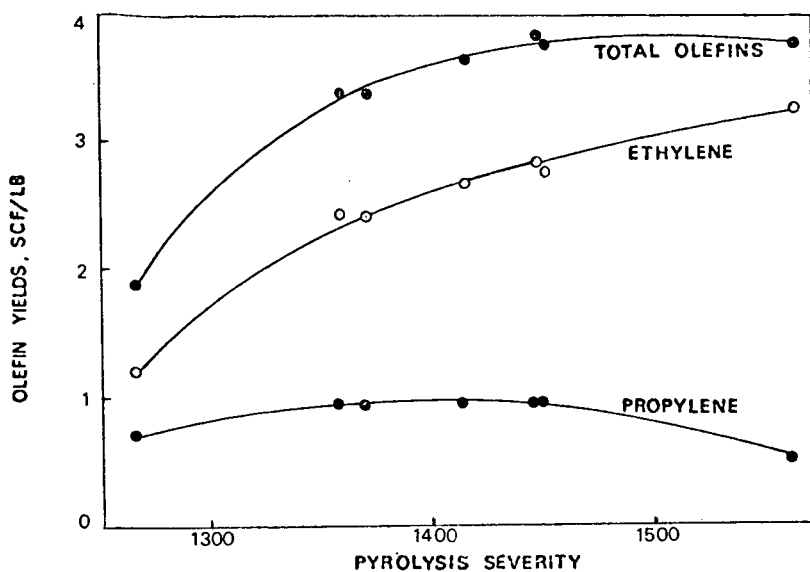


Figure 5. Effect of pyrolysis severity on olefin yields

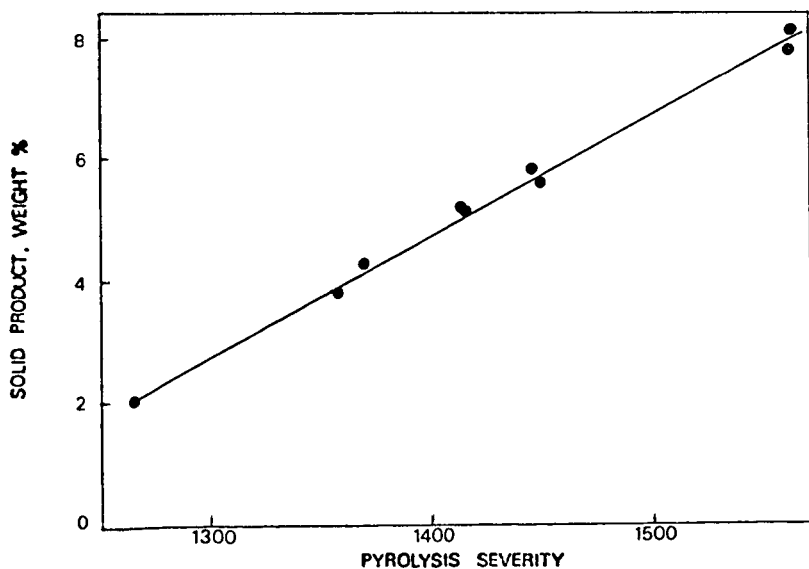


Figure 6. Effect of pyrolysis severity on solid product yields

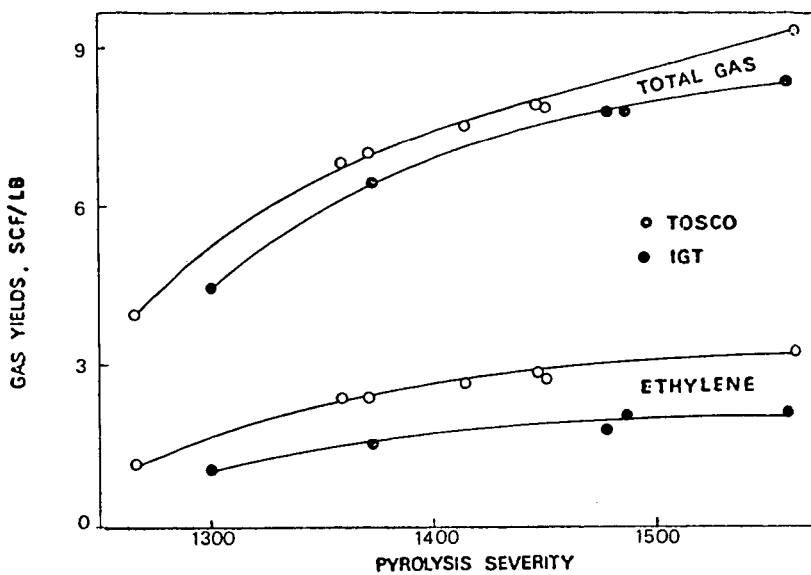


Figure 7. Yield comparisons between TOSCO and IGT oils

PROPERTIES AND COMPOSITION OF JET FUELS
DERIVED FROM ALTERNATE ENERGY SOURCES
PART I. BACKGROUND AND N-ALKANE CONTENT

ROBERT N. HAZLETT AND JAMES M. HALL

Naval Research Laboratory
Washington, D. C. 20375

JEFFREY SOLASH

Naval Air Propulsion Test Center
Trenton, New Jersey 08628

INTRODUCTION

In the current climate of dwindling domestic production of petroleum, increased importing of petroleum, potential oil embargoes, and escalating prices, the Department of Defense has begun significant new fuels programs. These programs are evaluating the military potential of liquid transportation fluids derived from alternate fossil fuels - shale oil, tar sands and coal. Of major import to the U.S. Navy are fuels used primarily for aircraft propulsion, JP-5, and ship propulsion, Diesel Fuel Marine. The discussion in this paper will be limited to the former, jet fuel for naval aircraft. It should be noted however, that JP-5 is sometimes used as a substitute ship propulsion fuel.

CRITICAL PROPERTIES OF JET FUEL .

JP-5 must meet many stringent requirements if satisfactory performance in aircraft and fuel handling and storage systems is to be attained (1). In considering JP-5 derived from alternate fossil fuels, several critical properties stand out. With one or two exceptions, these key properties are affected more by the chemical characteristics of the fuel than by the physical properties. The important specification requirements may be primarily controlled by elemental composition, the amounts of each of the hydrocarbon classes - paraffin, naphthene, aromatic, olefin - or by specific chemical compounds. The critical properties are discussed briefly below.

A. Heat of Combustion - This property directly controls the range of a jet aircraft and it is desirable to maximize the value. Hydrocarbon fuels which are liquid at ambient temperatures have net heating values between 16,000 and 20,000 BTU/lb and the minimum specification limit for JP-5 is 18,300 BTU/lb (1). Martell and Angello have shown that the heat of combustion for jet fuels increases linearly with hydrogen content (2). The amounts of nitrogen and oxygen in jet fuel are negligible with respect to heat of combustion and the variation of sulfur in the allowable range of 0.0 to 0.4% would exert a maximum effect of 40 BTU/lb.

B. Freezing Point - Jet aircraft are exposed to low temperatures and the fuels must not interfere with flying operations by freezing and plugging filters. Commercial jet fuel (Jet A) has a specification requirement of -40°F maximum but that for military fuels is lower. JP-5 must freeze below -51°F because the Navy jets operate world wide as well as at higher altitudes than commercial jets. U.S. Air Force bombers require an even lower freezing point, -72°F maximum, since long flights at high altitudes permit the fuel to reach lower temperatures. It has not been practical to make JP-5 from some petroleum crudes because the freezing point cannot be met along with the required flash point. Dimitroff et al (3) examined the influence of composition on freezing point of several types of fuels. They found the saturate fraction of a fuel usually exerted the greatest effect on freezing point but the aromatic fraction seemed to be important in some cases.

C. Flash Point - The Navy requires a high flash point for all fuels carried onboard ships except for a small amount of aviation gasoline which is carried on some aircraft carriers. The Avgas is stored in an armored box in the center of the carrier and air/fuel vapors are minimized in the storage tanks by using a water displacement system. JP-5, which is stored in the wing tanks (flush with the hull), has a minimum flash point of 140°F in order to reduce the hazard from this and other exposure situations. The flash point of a mixture such as a fuel is controlled by the quantity and volatility of the front ends (4). The flash point and other flammability properties of some alternate jet fuels is considered in another paper at this Symposium (5).

D. Combustion Properties - Jet engines give high combustion efficiencies (98-100%) for conversion of fuel to CO₂ and H₂O. Other combustion characteristics can be deficient under such conditions, however. Flame radiation to the combustor walls can raise the temperature of the walls above desired levels (6,7). Soot deposition can also affect combustor wall temperatures. Smoke in the exhaust must be controlled both for military and environmental reasons.

The flame radiation, soot deposition, and smoke production may be closely related chemically. These three properties of a jet fuel are controlled by passing a simple wick burning test, the smoke point, or a slightly more complicated burner test, the luminometer number. The minimum smoke point for JP-5 is 19 mm and the minimum luminometer number is 50.

A secondary control on combustion properties is obtained by limiting the aromatic content to 25% (1). Condensed polynuclear aromatics are significantly more detrimental to smoke point than monocyclics (8).

E. Thermal Oxidation Stability - Jet fuel cools several systems in a jet aircraft. In a subsonic plane, the major heat load comes from the engine lubricant but for aircraft flying faster than Mach 2.2, the structure must also be cooled. The ability of a fuel to withstand this thermal stress is the most critical fuel property for high speed aircraft (9).

Degradation of the fuel is stimulated by the dissolved oxygen present in equilibrium with air (50-70 mg/l). Poor fuels form solids which coat heat exchanger surfaces and/or plug combustor nozzles. The Jet Fuel Thermal Oxidation Tester estimates these two properties by examining varnish formation on a heated metal tube and measuring the pressure drop through a filter. A satisfactory fuel passes a 2 1/2 hr test at 500°F.

Little research has been reported on the effect of chemical structure on thermal oxidation stability at 500°F but Taylor has reported on tests in the 200-400°F temperature range. He found that olefins, particularly multifunctional ones, increased deposit formation (10). At 275°F, 10 wt % indene in decane increased deposit formation 39-fold but some other aromatics decreased the deposit rate. Some sulfides and disulfides enhance deposit formation at concentrations as low as 1000 ppm sulfur (11) and nitrogen compounds also participate in deposit formation (12).

F. Gum Formation - The low temperature stability of JP-5 is estimated by the Existent Gum Test. A maximum of 7.0 mg/100 ml gum is allowed in this test. Schwartz et al. have found for gasoline that sulfur compounds are the most significant participants in gum formation but that nitrogen compounds, indanes, tetralins and olefins are also involved (13).

PROPERTIES OF ALTERNATE JET FUELS

Jet fuels made from oil shale, tar sands and coal were examined in this study. A brief outline of the processes involved in production of the fuels are listed in

Table I. Further information on processing and fuel properties can be found in another paper in this symposium (14) and in the references cited in Table I.

Table II lists the properties of the fuels pertinent to this paper. The Laramie Energy Research Center in-situ shale fuels were not produced to meet the JP-5 specs but had a boiling range (350-550°F) similar to JP-5. Since only limited amounts of the LERC samples were available, complete specification tests were not run. The discussion which follows compares, where possible, the alternate fuel properties with petroleum jet fuel properties taken from the literature. The effect of composition on properties is also described.

A. Heat of Combustion - The heat of combustion of alternate fuels is plotted in Figure 1 versus percent hydrogen. The graph shows data for the five COED, the tar sand, and the Paraho shale oil fuels. The line on this graph is curve D in Figure 3 of reference (2) and is based on 41 jet fuels derived from petroleum. The alternate fuel data fit the curve very well. The three COED fuels with high aromatic contents fall to the left. COED-1 and COED-5 fall slightly below the JP-5 requirement of 18,300 BTU/lb. Decreasing the aromatic content from about 25% to 5% (COED-1 to COED-3 or COED-2 to COED-4) increases the heat of combustion about 90 BTU/lb. The tar sands and Paraho shale fuels have higher heating values than the COED samples with similar aromatic contents. We feel this is due to a high naphthene content in the coal fuels, an expected consequence of hydrogenation of the highly aromatic syncrude obtained by coal pyrolysis (21).

B. Freezing Point/Flash Point - Most of the alternate fuel samples met the flash point requirement for JP-5. The flash point can be changed usually by the adjustment of the initial boiling point. The freezing point of several of the alternate jet fuels was too high, however. The freezing point/flash point relationships for the five COED (C-1 to C-5), tar sands (TS), and Paraho shale oil (OS) are depicted in Figure 2. No consistent pattern is evident for these fuels.

For comparison, the properties of 29 petroleum derived jet fuels are also shown on the graph. These latter fuels, which were part of the Coordinating Research Council (CRC)-Air Force (AF) fuel bank (22), did not meet all specifications in some cases. Examination of the CRC fuels is useful, however, to see the wide range in freezing points encountered for fuels with similar flash points. In Figure 2, the display is simplified by grouping the fuels by 10°F intervals for flash point. As an example, four petroleum derived fuels had flash points between 161 and 170°F. The freezing points for these same fuels were -26, -32, -62 and <-76°F. One alternate fuel sample, COED-3 had a flash point in this range and it had a freezing point of -58°F.

It is noteworthy that COED-2 and COED-4, both produced from Utah coal, had higher freezing points than the COED fuels made from Western Kentucky coal. This was the case even though COED's 1 through 4 had similar distillation ranges. The Paraho shale oil sample was far above the JP-5 fuel freezing point spec of -51°F. The LERC in-situ shale samples also had very high freezing points, -16°F for the multistep product and -15°F for the single step material. Flash points were not available for these two shale fuels.

C. Combustion Properties - The smoke points of several alternate jet fuels are displayed in Figure 3 as a function of aromatics content. In addition, this graph presents the smoke point vs. % aromatic relationship for 29 CRC-AF petroleum-derived fuels (22). The general control of smoke point by aromatic content is apparent both for the petroleum-derived and the alternate fuels. Some fuels with low aromatic contents exhibit low smoke points, however, and do not fit the primary relationship. The four petroleum fuels which show this behavior possess high naphthene content, 80% or higher. COED-3 and COED-4, which have been derived by severe hydrogenation (3000 psig to afford a low aromatic content) of a highly aromatic syncrude (21),

should also contain high concentrations of naphthenes. Hence, the anomalous smoke point behavior shown, both by alternate and petroleum-derived jet fuels, can be explained on the basis that naphthenes influence this property if the aromatic content is low.

Smith (23) has suggested a formula for calculating the smoke point of kerosenes based on paraffin, naphthene and aromatic content but it is not useful for the fuels discussed in this paper. The broad definition of aromatic and naphthene is not adequate for combustion considerations. For instance, one mole/l of either butyl benzene or naphthalene would give about the same aromatic concentration by the specification test but the latter compound would have a much greater effect on the smoke point.

D. Stability - The thermal oxidation stability and gum forming tendencies of the alternate fuels are listed in Table II. COED-1 and COED-5 fail the 500°F thermal stability test by slight amounts but the Paraho shale oil material fails by 50°F. Further, this shale oil is the only fuel to fail the existent gum requirement of 7 mg/100 ml. The sulfur content of all of the alternate fuels is about the same and well below the 0.4% specification limit. Although jet fuel has no limit on nitrogen, the shale fuel is much higher in nitrogen than the other alternate and petroleum jet fuels.

Clay filtration of the shale jet fuel raised the breakpoint for thermal oxidation stability to 475°F but the existent gum remained high, 64 mg/100 ml, as did the nitrogen. Acid treatment (≈ 2 lb 98% H_2SO_4 /bbl) reduced the basic nitrogen to zero, enabled the thermal stability requirement to be met but did not greatly improve the gum formation. Distillation to a 90% recovery gave a product which passed both thermal stability and gum (1.2 mg/100 ml) tests. Basic nitrogen remained high, however. These results do not delineate the role of nitrogen in fuel stability and additional work will be needed to clarify the stability behavior of shale fuels.

It is noteworthy that severe hydrogenation to reduce the aromatic content of coal liquids (COED-1 to 3 and COED-2 to 4) significantly improved the thermal oxidation stability (to $>700^\circ F$).

E. n-Alkane Content - Since n-alkanes are likely to be related to the high freezing points of some of the alternate fuels, the concentration of these compounds was determined.

The saturate fractions were separated from the aromatics by pentane elation from activated silica gel (Davison Grade 923). Each saturate fraction was then analyzed by gas chromatography (GC) on a 300 ft. Apiezon L capillary column at 140°C. A sample of 0.1 microliter was split 100:1 ahead of the column and the helium flowrate through the column was 1.0 cc/min. This column, when operated under the described conditions, had an efficiency of 184,000 theoretical plates for n-tetradecane. A known amount (5.0 wt %) of n-octane was added as an internal standard and the weight % of each n-alkane was calculated by comparing electronic integrator counts to the octane count. Identification of the n-alkane peaks was made on a Hewlett-Packard 5982 GC-MS system using a 100 ft. OV-101 support coated open tubular column - temperature programmed from 100 to 160°C and with a helium flowrate of 3 cc/min. Corroborating identification came from matching GC retention times for fuel components on the Apiezon L column with standards on the same column.

The n-alkanes were the major peaks in most of the saturate fractions. The n-alkanes from nonane to hexadecane were found in most of the alternate fuels. In addition, small amounts of n-heptadecane were found in the shale fuels. The n-alkane concentrations are listed in Table III. The sum of the n-alkanes in the fuels decreases in the order: Paraho shale, LERC shales, petroleum, tar sands, Utah COED's, W. Ky. COED's. This order holds for individual n-alkanes in the middle

of the distillation range - C_{12} , C_{13} and C_{14} - but varies for smaller or larger compounds because of differences in initial boiling point or end point.

The total n -alkane concentration does not afford a significant relationship with freezing point. However, the freezing point does show some dependence on the amount of the larger hydrocarbons present in fuel samples. This is illustrated for n -hexadecane in Figure 4. The $\log (\% C_{16})$ vs. the reciprocal freeze point of the 11 fuels listed in Table II indicates a reasonable adherence to a solubility plot. This is remarkable in view of the different distillation ranges, the variation in aromatic/naphthene contents, and the neglect of other n -alkanes in this consideration.

The Paraho jet fuel was treated with urea to remove n -alkanes (24). The percent of the n -alkanes removed by this process and the amount remaining in the fuel are shown in Table IV. Overall, 47% of the n -alkanes (17% of the total fuel) were removed. The percent removed increased with molecular weight. The removed material was 98% n -alkanes with the remainder being identified by GC-MS as mostly 2-methyl alkanes and 1-alkenes. The stripped sample with an n - C_{16} content of 0.17%, had a freezing point of -54°F which places it close to the curve in Figure 4.

DISCUSSION

Suitable jet fuels can be made from any of the alternate energy sources - oil shale, tar sands or coal. However, refining processes may have to be modified from those used with petroleum crude and processing conditions may have to be more severe, particularly for oil shale and coal liquids. Since crudes from oil shale, tar sands and coal are closer in properties to the lower API gravity petroleum crudes, hydrocracking and delayed coking will be used extensively in producing military fuels from these alternate sources.

The jet fuel properties which are of greatest concern with the new fuels are the freezing point, combustion properties, and stability, both thermal oxidative and storage. Additional understanding is required on the effect of composition on these properties. Development of such information will aid in selecting or modifying refining processes to produce suitable fuels at reasonable costs. Techniques to remove nitrogen from shale oil and to convert n -alkanes to lower freezing compounds are needed. Cheaper hydrogenation processes must be developed for economical conversion of coal liquids to jet fuels with satisfactory heats of combustion.

The high concentrations of n -alkanes found in the shale oil samples affords clues on the nature of the organic material in shale. This information indicates that oil shale contains many long, straight chain components. When thermally stressed, as in retorting or coking, such constituents would yield smaller fragments which would also have straight chains (25). The major products would be n -alkanes and 1-alkenes. Since the latter hydrogenate to the former, n -alkane concentration could be considerable. It is interesting that the three shale jet fuels studied in this work were high in n -alkanes. This is in spite of differences in production, refining and hydrogenation processes.

Work will continue in relating composition to properties of the alternate jet fuels. This will include attention to non-specification properties and those properties which may be inherently different due to the origin of the base stock.

ACKNOWLEDGEMENT

The authors thank the Naval Air Systems Command for support to accomplish this research. The opinions expressed are the author's and do not necessarily reflect those of the U.S. Navy.

LITERATURE CITED

1. MIL-T-5624J, Turbine Fuel, Aviation, Grades JP-4 and JP-5, 30 Oct., 1973
2. C. R. Martell and L. C. Angello, "Hydrogen Content As a Measure of the Combustion Performance of Hydrocarbon Fuels", AFAPL-TR-72-103, Wright-Patterson Air Force Base, Ohio, May 1973.
3. E. Dimitroff, J. T. Gray, Jr., N. T. Meckel and R. D. Quillian, Jr., Seventh World Petroleum Congress, Individual Paper No. 47, Mexico City, Mexico, Apr. 2-9, 1967.
4. W. A. Affens and G. W. McLaren, J. Chem. & Eng. Data, 17, 482 (1972).
5. W. A. Affens, J. T. Leonard, G. W. McLaren and R. N. Hazlett, 172nd ACS Meeting, Division of Fuel Chemistry, this symposium.
6. Coordinating Research Council, "Evaluation of CRC Luminometer", New York, N.Y., June 1959.
7. R. M. Schirmer and E. W. Aldrich, "Microburner Studies of Flame Radiation as Related to Hydrocarbon Structure", Phillips Petroleum Company, Prog. Rpt. No. 4 on Navy BUWEPS Contract NOW63-0406-d, May 1964.
8. M. Smith, Aviation Fuels, Ch. 49, G. T. Foulis and Co., Ltd., Henley-on-Thames, England, 1970.
9. H. Ravner, C. Singleterry and R. N. Hazlett, "Aircraft Propulsion; Advanced Fuels and Lubricants R&D Goals - - 1970 to 1980," Naval Air Systems Command Committee Report, June 1971.
10. W. F. Taylor, I&EC Prod. R&D, 8, 375 (1969).
11. W. F. Taylor and T. J. Wallace, I&EC Prod. R&D, 7, 198 (1968).
12. W. F. Taylor, Paper 680733, SAE Aeronautic and Space Eng. Mtg., Los Angeles, CA. Oct. 1968.
13. F. G. Schwartz, M. L. Whisman, C. S. Albright and C. C. Ward, "Storage Stability of Gasoline," Bureau of Mines Bulletin 626, 1964.
14. J. Solash and R. F. Taylor, 172nd ACS Meeting, Division of Fuel Chemistry, this symposium.
15. H. Bortick, K. Kunchal, D. Switzer, R. Bowen and R. Edwards, "The Production and Refining of Crude Shale Oil into Military Fuels," Applied Systems Corp., Vienna, Va., Navy Contract N00014-75-C-0055, Aug. 1975.
16. C. M. Frost, R. E. Poulson and H. B. Jensen, 167th ACS Meeting, Division of Fuel Chemistry, 19, No. 2, 1974, p. 156.
17. R. E. Poulson, C. M. Frost and H. B. Jensen, 167th ACS Meeting, Division of Fuel Chemistry, 19, No. 2, 1974, p. 175.
18. C. M. Frost and R. E. Poulson, 169th ACS Meeting, Division of Fuel Chemistry, 20, No. 2, 1975, p. 176.
19. C. J. Nowack, "Endurance and Emission Tests of a T63-A-5A Engine Using a Tar Sands Derived JP-5," Naval Air Propulsion Test Center, Rpt. NAPTC-L-75-29, 23 June 1975.
20. R. D. Humphreys, Chem. Eng. Prog., 70(9), 66 (1974).
21. F. S. Eisen, "Preparation of Gas Turbine Engine Fuel From Synthetic Crude Oil Derived From Coal," Sun Oil Co. Final Rpt. on Navy Contract N00140-74-C-0568. Feb. 6, 1975.
22. Coordinating Research Council, Inc. Rpt. No. LD-148, "Fuel Inspection and Thermal Stability Data," 1 July 1965, New York.
23. M. Smith, Op. Cit., p. 85.
24. A. Hoppe, "Dewaxing with Urea," in Advances in Petroleum Chemistry and Refining, Vol. VIII, ed., John J. McKetta, John Wiley & Sons, New York, 1964.
25. B. M. Fabuss, J. O. Smith, and C. N. Satterfield, Advances in Petroleum Chemistry and Refining, Vol. IX, 157 (1964).

TABLE I

ALTERNATE FUEL SOURCES AND PROCESSES

<u>Fuel Source*</u>	<u>Method of Production</u>	<u>Method of Refining</u>	<u>Hydrotreat</u>	<u>Reference</u>
Shale-Paraho	Retort	Delayed Coking and Fractionation	Standard Pressure (Co-Mo)	15
Shale-LERC Multistep	In-Situ	Delayed Coking and Fractionation	1500 psig (Ni-Mo)	16,17
Shale-LERC Single Step	In-Situ	Fractionation after Hydrotreat	Total Oil 1500 psig (Ni-Mo)	18
Tar Sands-GCOS	Hot Water	Delayed Coking and Fractionation	Not Available	19,20
COED-1 FMC W.Ky. Coal	Pyrolysis	Fractionation	1500 psig (Ni-Mo)	21
COED-2 Utah Coal	Pyrolysis	Fractionation	1500 psig (Ni-Mo)	21
COED-3 W.Ky. Coal	Pyrolysis	Fractionation	1st stage 1500 psig (Ni-Mo) 2nd stage 3000 psig (Pt)	21
COED-4 Utah Coal				
COED-5 W.Ky. Coal	Pyrolysis	Fractionation	3000 psig (Ni-Mo)	21
Petroleum-A	Drilling	Not Available	Not Available	--
Petroleum-B	Drilling	Not Available	Not Available	--

* Paraho-Paraho Development Corp.; LERC-Laramie Energy Research Center; GCOS-Great Canadian Oil Sands, Ltd., FMC-Food Machinery and Chemical Co.

TABLE II

ALTERNATE FUEL PROPERTIES

Fuel	Thermal* Stability (°F)	Gum Existent (mg/100 ml)	Nitrogen (ppm)	Sulfur (wt. %)	Aromatics (percent)	Smoke Point (mm)	Viscosity at -30°F (cgs.)	Freezing Point (°F)	Heat of Combustion (BTU/lb)	Hydrogen (percent)
Shale-Paraho	450	81.7	680	0.05	26.0	22.0	frozen	-28	18,532	13.74
Shale-LERC Multistep	--	--	79	0.0001	23.7	--	--	-16	--	--
Shale-LERC Single Step	--	--	5	0.0005	21.3	--	--	-15	--	--
Tar Sands	Pass	1.2	--	0.01	19.3	20.0	12.85	-64	18,436	13.50
COED-1	495	0.0	40	0.05	24.8	17.0	23.69	-54	18,294	12.80
COED-2	510	0.1	42	0.04	24.1	17.0	22.94	-40	18,372	12.98
COED-3	>700	0.0	40	0.05	4.7	22.0	25.95	-58	18,383	13.34
COED-4	>700	0.1	43	0.03	6.1	22.0	23.03	-40	18,465	13.62
COED-5	485	0.1	37	0.03	24.1	18.0	9.04	<-70	18,282	12.81
Petroleum-A	Pass	<7	--	0.11	18.2	23.0	<16.5	-56	18,518	--
Petroleum-B	Pass	<7	--	<0.40	16.2	>19.0	<16.5	-59	--	--

*JFTOT Test, ASTM D3241, Pass indicates 500°F or higher

TABLE III

N-ALKANE CONTENT OF JET FUELS
FROM ALTERNATE SOURCESWEIGHT PERCENT

	C ₉	C ₁₀	C ₁₁	C ₁₂	C ₁₃	C ₁₄	C ₁₅	C ₁₆	C ₁₇	Σ
Shale Paraho	0.90	3.28	7.46	7.12	6.66	5.14	3.32	2.45	0.3*	36.33
Shale-LERC Multistep	0.002	0.11	3.11	6.08	5.81	4.26	3.48	2.46	0.6*	25.31
Shale-LERC Single Step		0.05	3.00	5.66	5.36	3.91	3.17	2.58	0.8*	23.73
Tar Sands-2	0.26	0.54	1.48	2.59	2.43	1.32	0.73	0.15	--	9.50
Coed-1		0.08	1.18	0.73	0.66	0.56	0.46	0.2	--	3.90
Coed-2		0.04	1.08	1.50	1.51	1.27	1.08	0.66	--	7.14
Coed-3	0.01	0.11	0.99	0.68	0.70	0.55	0.42	0.27	--	3.73
Coed-4		0.06	1.42	1.49	1.53	1.28	1.01	0.66	--	7.45
Coed-5	0.02	0.63	2.33	1.23	0.76	0.38	0.11	(0.02)	--	5.48
Petroleum-A	0.20	1.72	3.63	3.88	3.49	2.13	0.81	0.14	--	16.00
Petroleum-B	0.29	1.97	3.85	3.38	3.13	1.82	0.72	0.05	--	15.71

*C₁₇ peak broad, integration not accurate, not included in total

TABLE IV

RESULTS OF UREA STRIPPING OF PARAHIO
SHALE JET FUEL

<u>N-Alkane</u>	<u>Starting Material</u>	<u>Concentration (Percent) Product</u>	<u>N-Alkane Concentrate</u>	<u>Percent ** Removed</u>
Nonane	0.90	0.73	0.96	19
Decane	3.28	2.65	3.86	19
Undecane	7.46	5.43	11.54	27
Dodecane	7.12	4.66	16.50	35
Tridecane	6.66	3.33	19.13	50
Tetradecane	5.14	1.73	18.71	66
Pentadecane	3.32	0.67	15.16	80
Hexadecane	2.45	0.17	9.47	93
Heptadecane	0.3*	0.00	1.38	--
Total	36.33	19.37	98.0	

* Broad peak, integration not accurate, not included in total

** Based on comparison between product and starting material

NET HEAT OF COMBUSTION VS. PERCENT HYDROGEN

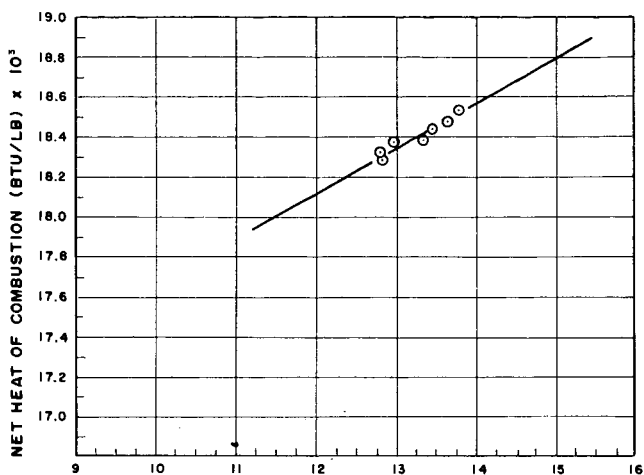


Figure 1 PERCENT HYDROGEN BY WEIGHT
 ○ JET FUELS FROM ALTERNATE ENERGY SOURCES

FREEZING POINT vs FLASH POINT

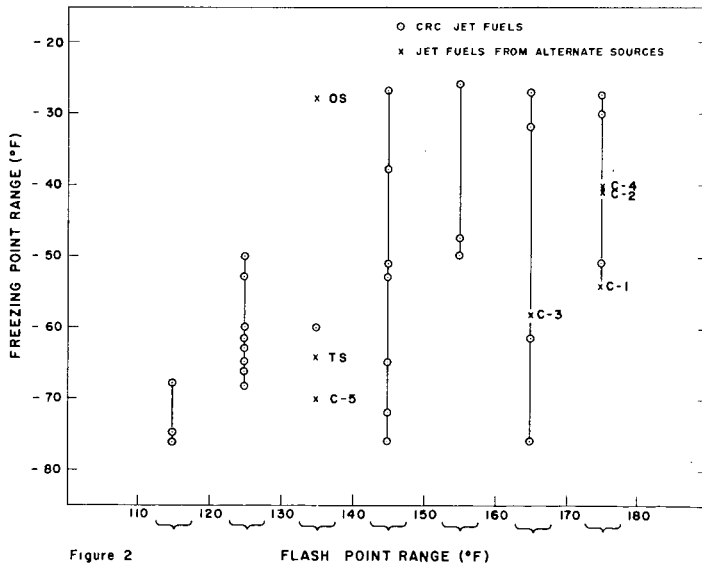
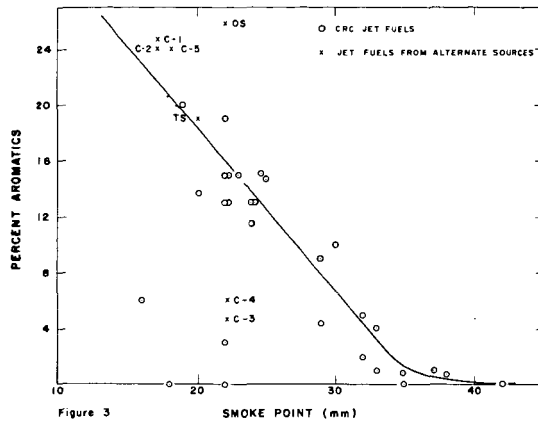
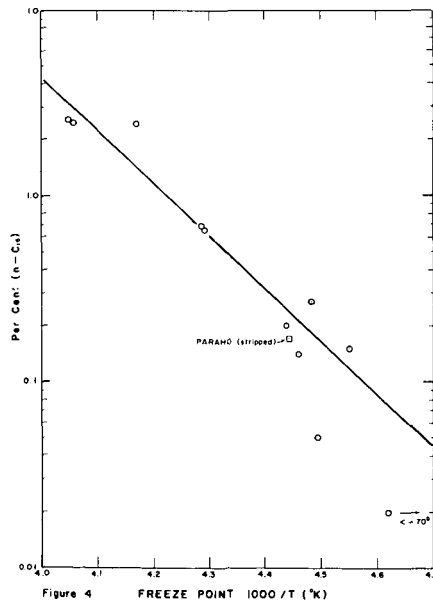


Figure 2 FLASH POINT RANGE (°F)

SMOKE POINT vs AROMATIC CONTENT



EFFECT OF N-HEXADECANE ON FREEZING POINT



CHARACTERIZATION OF AROMATIC FRACTIONS FROM
NON-PETROLEUM DERIVED JP-5 TYPE FUELS

Jeffrey Solash and Renee F. Taylor

Naval Air Propulsion Test Center, Trenton, NJ 08628

Introduction

The Department of Defense has initiated programs aimed at evaluating liquid hydrocarbon fuels which are derived from alternate (fossil) sources: coal, oil shale and tar sands. Of major importance to the Navy are aircraft fuels (JP-5) and ship diesel fuels (DFM). The properties of these kerosene fuels are controlled by means of stringent specifications tests. However, complete knowledge of fuel chemical composition defines the properties of the fuel. Certain properties which are of critical importance to the Navy can be altered by simple physical methods (i.e., flash point (1)). However, other fuel properties depend strongly on fuel composition and therefore, are not subject to facile alteration.

In order to gain a clearer understanding of the effects of chemical composition on fuel properties, a detailed analysis was undertaken. The discussion in this paper will be limited to jet fuels used in Naval aircraft (JP-5). Jet fuels derived from coal, oil shale and tar sands were analyzed. The normal alkane analysis has been reported elsewhere (1). Reported below are the results of analysis of the aromatic components of these fuels.

Production of Fuels

Coal Derived Fuels

The coal derived fuels used in this work were obtained by liquefaction of a Western Kentucky and a Utah coal via the COED process (2). In this process, coal is pyrolyzed in an ebullated bed retort at temperatures ranging from 600 to 1600°F. The condensed oil is hydrotreated over Ni-Mo catalyst (~2500 psig H₂, 7-800°F) to produce a low sulfur crude oil. The crude oil was then refined by hydrotreatment (3) and distilled to give the JP-5 grade fuels, Sun 1 (Western Kentucky coal), Sun 2 (Utah coal) and Sun 5 (Western Kentucky coal). A schematic of the major process steps used in the production of these fuels is shown in Figure 1.

Alternative methods of refining coal derived crude oils were examined. One such method involved selective removal of heavy aromatics and polar organics (containing N, S, O) by solvent extraction. In a method developed by the Navy (4), a straight run middle distillate from Utah coal derived crude oil (bp 350-550°F) was consecutively treated with sulfuric acid and furfural. The resultant fuel (designated "Sol. Extr.") was used directly without further processing.

Oil Shale Derived Fuel

Green River oil shale was mined and surface retorted by the Paraho Development Corporation. A sample of JP-5 grade kerosene derived from this oil shale was supplied to the Navy by Applied Systems Corporation, under a contract let by the Office of Naval Research. In the Paraho process, crushed and sized oil shale is fed by gravity into a vertical retort which is maintained at 1000°F. Shale oil which was driven from the rock was coked and then fractionated. The middle distillate fraction was hydrotreated and desulfurized in two stages. The major process steps employed are shown schematically in Figure 2. The refining of this batch of shale oil has been reported in greater detail elsewhere (5).

Tar Sands Derived Fuel

Bitumen obtained from the Athabasca (Canadian) deposits was mined and refined by Great Canadian Oil Sands, Ltd. (GCOS). Mined tar sands are treated with basic hot water and the bitumen was isolated by froth flotation. The crude bitumen was coked (900-1000°F) and the distillates fractionated. The straight run middle distillate from coking was hydrotreated (\sim 1500 psig H₂; 700-750°F). The hydro-treated middle distillate, known as Unifined Kerosene (herein designated "Tar Sands") is usually used for blending stock. The major process steps employed are shown schematically in Figure 3. Details of the processing of Canadian tar sands have been reported elsewhere (6).

Petroleum Derived Fuels

The petroleum derived fuels used in this work were typical JP-5 grade fuels which passed all Navy specifications for JP-5 grade fuels and were typical of the fuels used at the Naval Air Propulsion Test Center. The history and details of refining of these fuels were not available.

Fuel Properties

The physical properties of all fuels used in this study were determined according to Navy specification MIL-T-5624J, using ASTM standard methods. Heats of combustion, freeze points, flash points, smoke points, viscosities, as well as *n*-alkane composition for these fuels are reported in reference (1). Complete tabulations of physical properties for all fuels used in this study have been reported (3, 4, 7, 8).

Results and Discussion

FMR Analysis

The aromatic fraction of each fuel was isolated by column chromatography over activated silica gel. The aromatic fractions, which were cleanly separated from the fuel saturates, were combined and the solvent removed under reduced pressure on a rotary evaporator. The aromatic concentrate was diluted approximately 1:3 (vol:vol) with spectrograde CCl₄ and the 60 MHz FMR spectrum recorded. The FMR spectrum of a typical JP-5 grade fuel aromatic fraction is shown in Figure 4. The areas under the peaks which correspond to structurally distinct protons were determined and the data analyzed according to the method of Clutter and co-workers (9). The results of this analysis describe the fuel aromatic fraction in terms of the "average molecule." The calculated parameters which are presented in Table I are defined below:

Average Molecular Parameter

<u>Symbol</u>	<u>Definition</u>
# CA	Average number aromatic carbons per average molecule
# naphthene	Average number naphthene (tetralin) rings per average molecule
MW	Average molecular weight
# alkyl gps	Average number alkyl substituents per average molecule
n	Average number carbons per alkyl substituent
% mono	Average percent monocyclic aromatics in sample

TABLE I

AVERAGE MOLECULAR PARAMETERS OF JP-5 GRADE
FUEL AROMATICS FROM PMR DATA

Fuel	# CA	# NAPHTHENE	Parameters [Ⓐ]			% MONO	FORMULA
			MW	# ALKYL GPS	n		
Sun 1	6.65±0.05	0.75±0.05	179.7±2.8	3.05±0.05	2.25±0.15	84.3±2.0	C _{13.5} H _{17.4}
Sun 2	6.4±0.0	0.65±0.05	177.9±3.6	3.15±0.05	2.20±0.1	89.8±0.9	C _{13.4} H _{17.8}
Aged Sun 1	6.5±0.1	0.7±0.0	175.9±2.4	3.1±0.0	2.15±0.05	86.8±2.4	C _{13.3} H _{17.1}
Aged Sun 2	6.6±0.2	0.6±0.0	174.0±0.5	3.25±0.05	2.05±0.05	86.7±3.3	C _{13.1} H _{16.9}
Sun 5	6.5±0.2	0.45±0.05	156.5±1.3	2.7±0.1	1.95±0.05	87.7±4.2	C _{11.8} H _{14.9}
Sol. Extr.	6.55±0.05	0.70±0.0	191.5±6.3	3.25±0.05	2.40±0.1	87.0±1.5	C _{14.3} H _{19.4}
Paraho [Ⓛ]	6.8±0.3	0.35±0.5	172.5±4.1	2.95±0.05	2.05±0.05	80.0±6.5	C _{13.0} H _{16.8}
Tar Sands	6.45±0.05	0.35±0.05	165.9±2.9	3.0±0.2	2.0±0.0	87.6±1.3	C _{12.5} H _{16.3}
Petroleum-1	7.1±0.2	0.4±0.0	172.1±3.9	2.85±0.05	2.1±0.2	74.6±3.7	C _{13.0} H _{16.6}
Petroleum-2 [Ⓢ]	7.3	0.3	171.1	2.9	1.9	68.4	C _{12.9} H _{15.9}

[Ⓐ] Calculated from 60 MHz PMR spectrum according to reference (9). Average parameters ± average deviation of two runs shown, unless specified otherwise.

[Ⓛ] Average of three runs.

[Ⓢ] Average of one run.

In a separate set of experiments, some coal derived fuels were subjected to mild but prolonged heating (110°F; 6 months) to ascertain storage stability. The aromatic fractions of the Sun 1 and Sun 2 fuels, so treated, were isolated and subjected to FMR analysis in an effort to observe changes in composition upon storage. The results of analysis of the aromatic fractions of these fuels ("aged Sun 1," "aged Sun 2") are also reported in Table I.

Before a detailed analysis of the results in Table I is made, a discussion of sources of error in the data is necessary. There are a number of potential sources of error: incomplete resolution of the aromatic fractions from other fuel components; loss of low boilers during concentration of the column chromatography fractions; incorrect estimation of the average parameters caused by using a narrow cut aromatic fraction. Column chromatography over activated silica gel is a well known technique which has been widely used for separation of fuel components (10). However, it has recently been called to our attention that *n*-paraffins, particularly in higher boiling fractions, can tail into the aromatics fractions during chromatography over silica gel (11). The data in Table I indicates that such processes are not detectable by FMR if they are occurring at all. For instance, the Paraho fuel, which is almost 40% *n*-paraffins (1), shows a low value for *n* (average number of carbons per substituent). If appreciable quantities of paraffins were tailing into the aromatic fractions during the chromatographic separation, this parameter would be much higher. It would not be required to have a large concentration of *n*-hexadecane, for instance, in the separated aromatics in order to observe a large increase in *n*. Furthermore, the values for *n* found for all fuels vary only slightly from run to run (approximately 5%). We would expect a larger variation for the *n* parameter if incomplete separation were occurring.

Loss of low boiling aromatic components during concentration of the individual fractions was also of concern to us. However, the data in Table I indicate that this process is unimportant. Loss of low boilers would result in a higher "apparent" concentration of naphthalenes. The % mono data in Table I shows little variation between runs for most fuels.

Lastly, the method of Clutter and co-workers (9) may incorrectly estimate some average parameters if narrow cut fuels are used (12). Qualitative analysis by glpc of some of the aromatic fractions on a 10' X 1/8" OV-225 column indicates the presence of at least 60 distinct peaks which are not resolved (implying presence of related structural isomers). We therefore feel the calculated parameters in Table I correctly reflect the composition of the aromatic fractions. A complete discussion of the advantages of the Clutter method, compared to others available, has been given elsewhere (9).

In another control experiment, the molecular weights calculated from FMR data (Table I) were compared to those determined by vapor phase osmometry (VPO) (13) and by mass spectroscopy (MS) (14). A comparison of the molecular weights determined by the three methods is presented in Table II below.

TABLE II
COMPARISONS OF MOLECULAR WEIGHTS OF AROMATIC FRACTIONS

<u>Sample</u>	<u>Molecular Weight</u>		
	<u>VPO</u>	<u>MS</u>	<u>FMR</u>
Sun 1	194	179	176
Sol. Extr.	240	206	198
Sun 5	175	-	158
Paraho	189	171	176
	195	-	168
Petrol. JP-5	195	-	176

The VPO molecular weights indicate that the PMR method correctly reveals changes in molecular weights between samples. The mass spectrometric molecular weights correspond very closely to those obtained by PMR. These data imply that the PMR method generates accurate molecular weights for these aromatic fractions. By analogy, the other parameters listed in Table I are at least as accurate as the molecular weight.

The data in Table I suggest a fairly clear picture of the nature of the aromatic fractions of these fuels. The average molecular weight of Sun 1 and Sun 2 (new and aged), Paraho, Tar Sands, and both petroleum fuels, Pet-1 and Pet-2, is 174.5 (Table I). Only two fuels, Sol. Extr. and Sun 5, had molecular weights which differed markedly from this average. The former fuel had the highest distillation end point ($>287^{\circ}\text{C}$) of all fuels, while the latter fuel had the lowest distillation end point (261°C). Most fuels had between 6.5 and 7 aromatic carbons, approximately 3 alkyl groups and 2 carbons per alkyl group in their average aromatic molecule. This similarity in the nature of the aromatic fractions is noteworthy since the fuels examined were derived from starting materials which are chemically, as well as geologically, different.

While the aromatic fractions of these fuels are similar in overall features, there are important differences. For instance, the widest variation in the value of any parameter was observed for # naphthene. It must be recognized that for tetralin (1,2,3,4 - tetrahydronaphthalene), there is one (1.0) naphthene ring per molecule. In Table I, the # naphthene, of the aromatic fractions, varies from 0.75 and 0.7 (Sun 1 and Sol. Extr.) to 0.3 (Pet-2). This fundamental difference in the aromatic fractions might account for differences in the viscosities of the whole fuels (17,18). There are also variations in n, # CA, and # alkyl gp between these fuels. For instance, one might have a priori assumed that the Sun 1 and Sun 2 fuels would exhibit a high # CA due to the polycondensed aromatic nature of coals (15). However, the # CA is higher for both petroleum derived fuels used than for any of the other non-petroleum derived fuels. This is also reflected in the % mono values. The % mono is lowest for the petroleum derived fuels, which implies more naphthalenes in the petroleum fuels than in the other fuels.

This apparent anomaly, that the coal derived fuels contain less dicyclic aromatics, can be made understandable if we consider the naphthene content of these aromatic fractions. The naphthenes present in these aromatic fractions are of the tetralin-indane type. Clearly, these naphthenes are derived from the parent dicyclic aromatic by hydrogenation. The aromatic protons of these naphthenes contribute to the area of monocyclic aromatics (7.05 - 6.6 ppm; Figure 4), while the # naphthene is calculated from the integrated area under the protons β to the aromatic ring of tetralin or indane (1.9 - 1.65 ppm; Figure 4). Since vigorous hydrotreatment will convert naphthalenes to tetralins, we should ideally compare % mono (or # CA) between fuels which have undergone equivalent processing. This process data was not available for the petroleum derived fuels. Instead, we can compare the total amount of dicyclics (naphthalenes + tetralins-indanes) between fuels.

The percent of dicyclic compounds in these fractions can be calculated to a first approximation in the following manner:

$$\% \text{ Dicyclics} = (\% \text{ mono}) (\# \text{ naphthene}) + (100 - \% \text{ mono}) \quad 1)$$

If the results in Table I gave a value of 1.0 for # naphthene, then each aromatic molecule would contain a tetralin or indane type ring. Hence, values less than 1.0 for # naphthene indicate the fraction of the total number of aromatic molecules which are of the tetralin-indane type. For instance, in the case of the Sun 1 fuel, 75% of the molecules are tetralins or indanes (i.e., # naphthene = 0.75). Since the aromatic protons of these naphthenes are counted as "benzenes," we must correct the % mono figure as shown in equation 1). The last term on the right hand

side of equation 1) is the % naphthalenes in the sample. By working through this equation, we find that 78.9% of the aromatic molecules in the Sun 1 fuel are dicyclic ($84.3 \times (0.75) + (100-84.3)$). Similarly, 68.5% of the aromatic molecules are dicyclic in the Sun 2 fuel. However, the % dicyclic aromatic molecules for the Pet-1 and Pet-2 fuels was found to be 55.2 and 52.1, respectively. Hence, the coal derived fuels have significantly more dicyclic (condensed) ring structures than the petroleum derived fuels. As expected, the coal derived fuels contained less naphthalenes than the petroleum derived fuels, because of the vigorous hydrotreatment to which they were subjected.

In addition to correctly predicting the order of molecular weights (Table II), the FMR method detects changes in other parameters which are consistent with changes in fuel properties. For instance, Sun 1 and Sun 5 were fuels produced from a Western Kentucky coal via an identical sequence of process steps but the distillation end point of Sun 1 was 279.5°C, while the distillation end point of the Sun 5 was 261°C. The lower distillation end point of the Sun 5 fuel is clearly reflected in the properties of the Sun 5 aromatics: lower values for n, MW, # alkyl gp compared with those values for Sun 1.

While large changes in fuel aromatics are clearly detectable by the FMR method employed, we could not detect changes in the aromatic fractions after a storage stability test (Table I). Under the static, oxygen deficient conditions of the storage test, aromatic hydroperoxide which forms would not decompose rapidly. The aromatic hydroperoxides would be separated from unoxidized compounds upon silica gel chromatography (16). The most oxygen labile aromatics would therefore be removed from the remainder of the aromatic "pool." There are small and irregular changes in the average parameters of aged Sun 1 and Sun 2. These changes are probably insignificant, although a statistical analysis was not performed. The latter conclusion is consistent with the observation that no gums or sediment were observed in the aged Sun 1 and aged Sun 2 fuels and furthermore, that the thermal stability of both aged fuels was unchanged.

Correlation of Average Parameters with Fuel Properties

The correlation of fuel properties with compositional data has been an active area of research for some time (19-21). Our interest in this area was not to develop a set of equations from which one can calculate a specific fuel physical property from compositional data (21), but rather to attempt to explain some of the sub-specification properties of these alternate fuels. Some properties which were of concern to us were the smoke point, viscosity and freeze point (1).

In general, fuel properties were plotted against n, # CA, # alkyl gps, # naphthene. Each individual parameter, combinations of parameters (i.e., # CA/n X # alkyl gp) and parameters which can be calculated from the data in Table I, such as wt. % H (aromatics) and approximate diameter of the average aromatic molecule, were plotted against the fuel property of interest. When straight line relationships were observed, least squares regression analysis was used to calculate the coefficient of correlation, r. It should be emphasized that baseline data for a representative sampling of petroleum JP-5 grade fuels has not yet been obtained. Selected fuel property-FMR parameter correlations, which are typical of our results, are illustrated below.

It has been shown that fuel smoke point is controlled by the aromatic content (vol. %) of the fuel (1). This correlation, as well as others (19, 22), suggest that some property of fuel aromatics controls combustion characteristics. However, we could find no correlation between fuel smoke point and any property of fuel aromatics. Two examples, which are typical, are shown in Figures 5 and 6.

Fuel viscosity is a fundamental property which directly controls atomization in combustors and affects fuel control equipment. It is known that viscosity of liquid mixtures can often be represented by a simple additivity law (25). In addition, the viscosity of cycloparaffins, as well as tetralins and indanes, can differ widely from the viscosity of the parent aromatic (17, 18). It was therefore somewhat surprising that the fuel viscosity was found to correlate so closely with the "diameter" of the average aromatic molecule (Figure 7). The diameter of the average aromatic molecule was estimated as follows:

$$\text{Diameter (A)} = \text{Fr. mono} (2.8) + \text{Fr. DI} (4.9) + n(0.89) (\# \text{ alkyl gp}) \quad (2)$$

where Fr. mono = Fraction monocyclic rings
Fr. DI = Fraction dicyclic rings, including tetralins (from equation 1))

In these JP-5 grade fuels, we may be dealing with a special phenomenon. When lube oil fractions are hydrotreated, the viscosity of the oil decreases (17). However, the graph in Figure 7 implies that the viscosities of the aromatics and the tetralins and cycloparaffins derived therefrom are similar. This view is supported by the negligible change in fuel viscosity upon vigorous hydrotreatment of the Sun 1 and Sun 2 fuels (3), which resulted in nearly complete dearomatization.

Dimitroff and co-workers (16, 17) have shown fuel freezing to be a complex process with *n*-alkanes playing an important role, but with all fuel components interacting during freezing. Hazlett and co-workers (1) determined that fuel freeze point is related to the concentration of *n*-hexadecane but not the total *n*-alkane concentration for these alternate fuels. It can be shown (26) that fuel freeze point probably does not follow a simple additivity rule. In Figure 8, a plot of fuel freeze point against the diameter of the average aromatic molecule is shown. The good correlation degrades markedly when the volume % aromatics (in each fuel) is accounted for (Figure 9). Hence, fuel freeze point seems to depend more strongly on the size rather than the quantity of aromatics present in fuel. One possible explanation for this behavior is that the larger aromatics cause an ordering of non-aromatic fuel components in a way similar to the ordering of water by dissolved soaps. As shown in Figure 8, the Paraho fuel (2.45% *n*-hexadecane) does not correlate well but the urea extracted (1) Paraho fuel (0.17% *n*-hexadecane) does fall near the line. Work is continuing on a variety of petroleum derived JP-5 grade kerosene in order to establish baseline data.

Acknowledgement

The authors would like to acknowledge the cooperation of the Gulf Oil Corporation for providing a computer program to calculate average parameters from PMR data and Dr. L. Petrakis for helpful discussions.

Fig. 1
PROCESSING SCHEMATIC FOR SUN COAL DERIVED FUELS

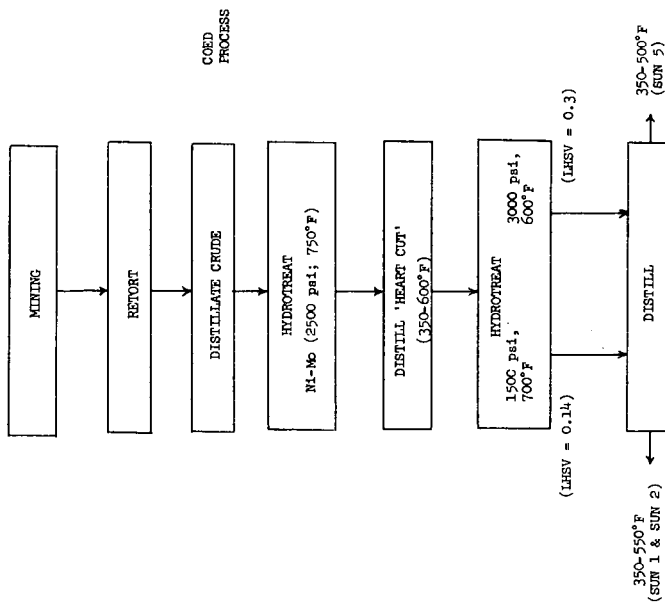


Fig. 2
PROCESSING SCHEMATIC FOR PARAHO FUEL

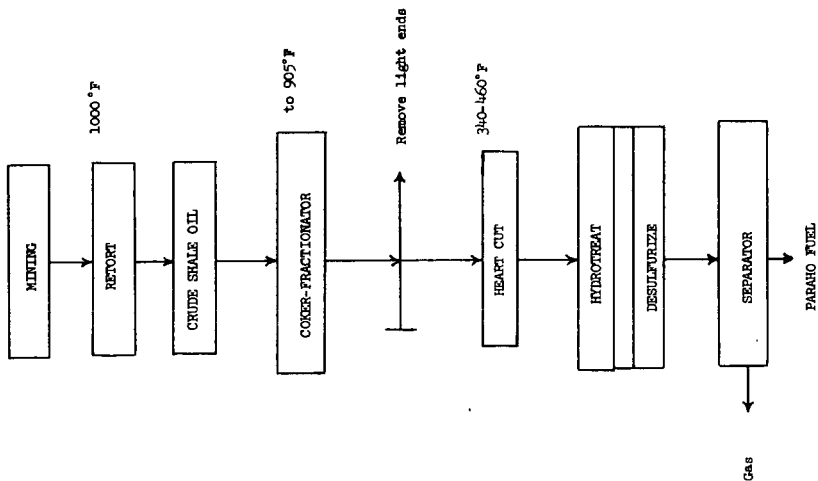


Fig. 3
PROCESSING SCHEMATIC FOR TAR SANDS FUEL
("UNIFIED KEROSENE")

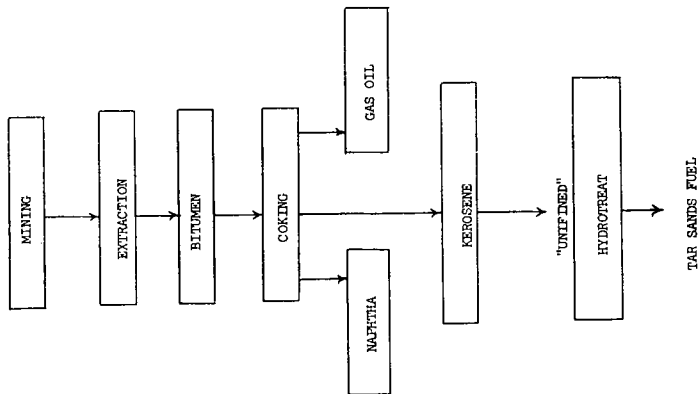


Fig. 4

60 MHz PMR Spectrum of Kerosene Aromatic Fraction

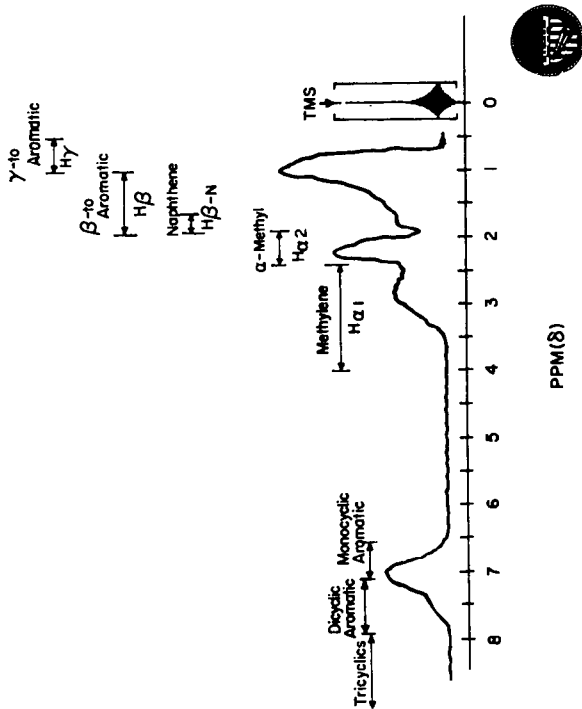


Fig. 1

PROCESSING SCHEMATIC FOR SUN COAL DERIVED FUELS

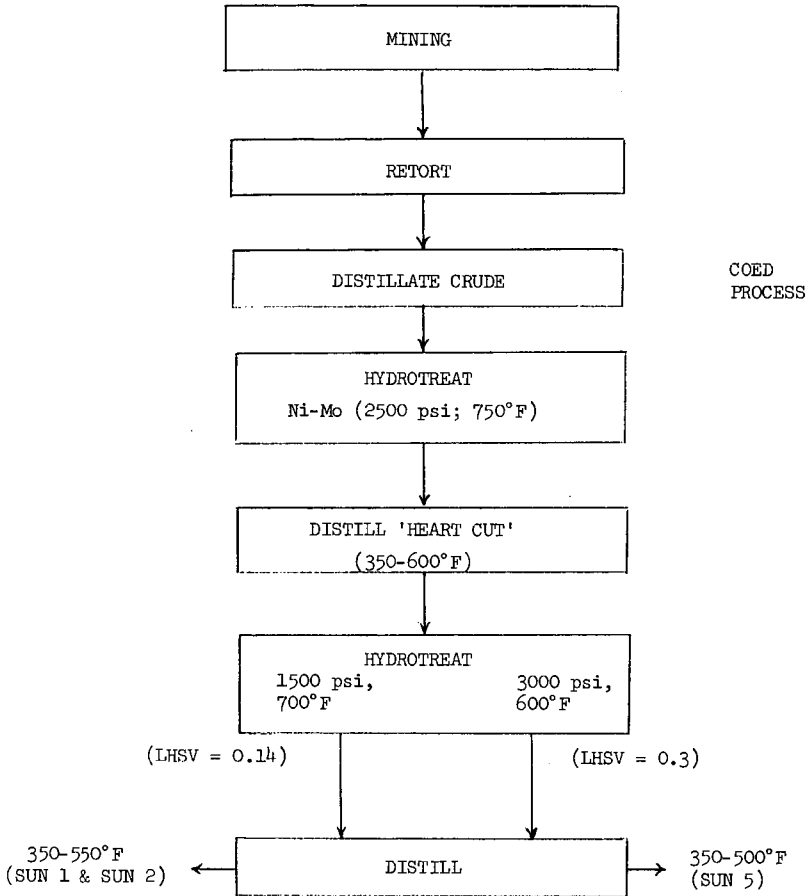


Fig. 2
PROCESSING SCHEMATIC FOR PARAHO FUEL

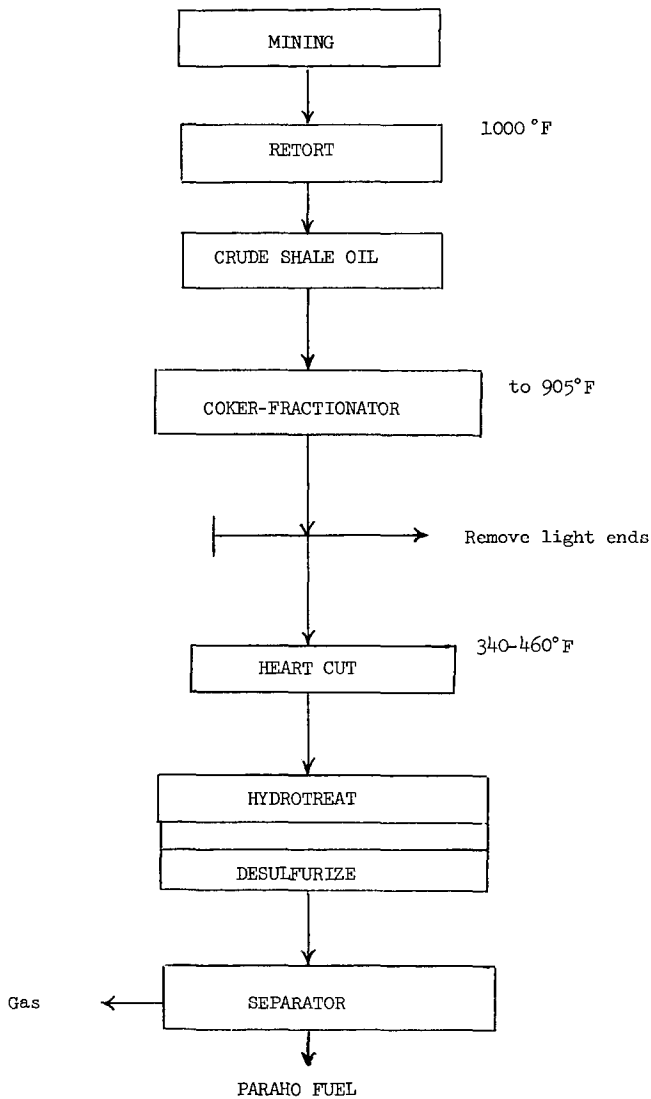


Fig. 3

PROCESSING SCHEMATIC FOR TAR SANDS FUEL
("UNREFINED KEROSENE")

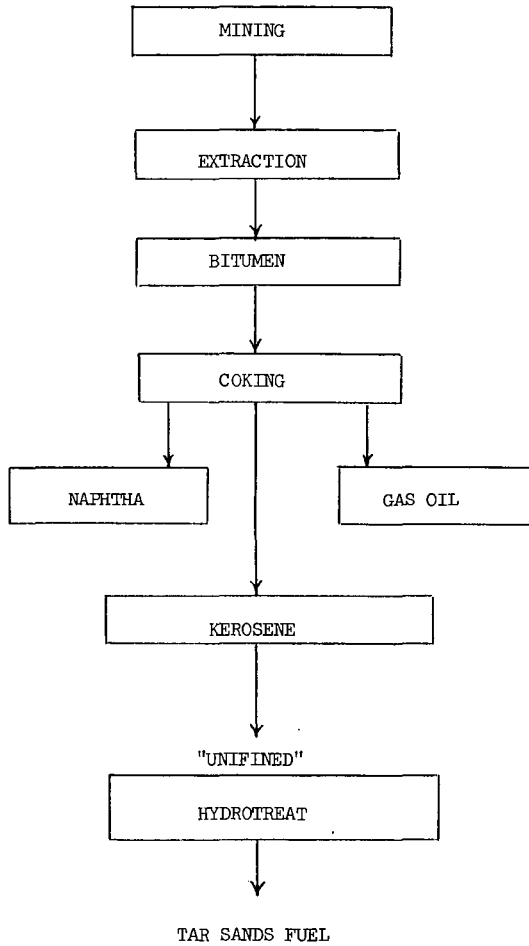


Fig. 4

60 MHz PMR Spectrum of Kerosene Aromatic Fraction

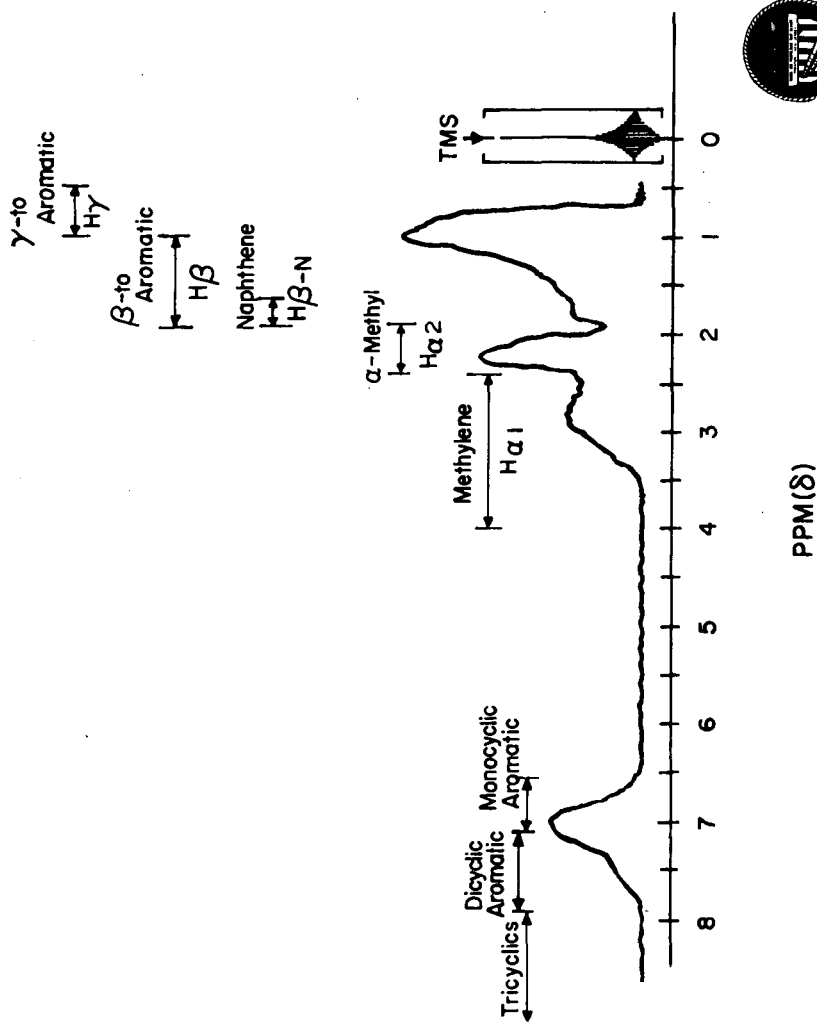


Fig. 5
FUEL SMOKE POINT VS. AROMATICITY

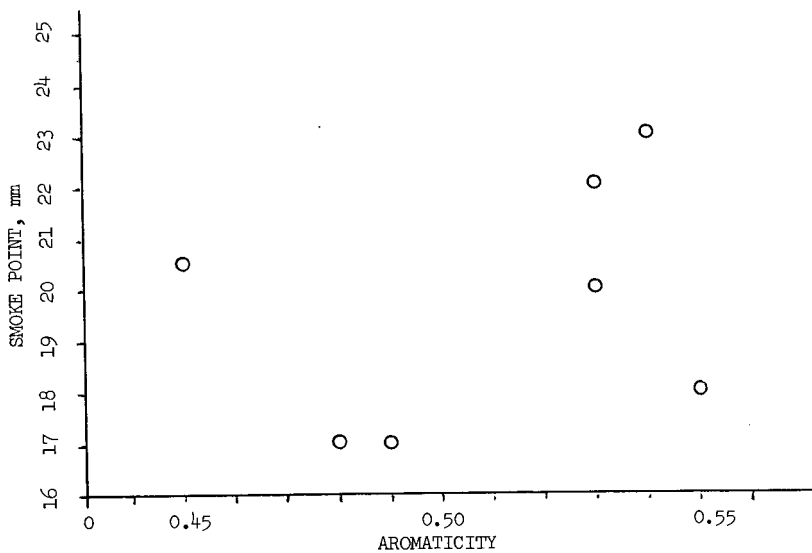


Fig. 6
FUEL SMOKE POINT VS. $\text{Wt \% H}_{(\text{AROM.})} \times \text{Vol \% AROMATICS}$

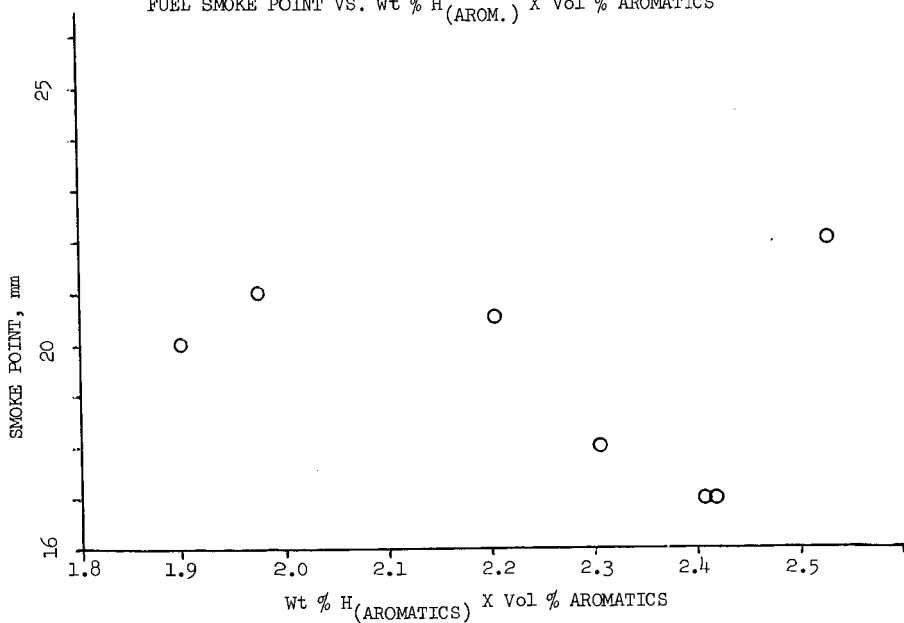


Fig. 7

FUEL KINEMATIC VISCOSITY (-30°F) VS. DIAMETER OF AVERAGE AROMATIC MOLECULE

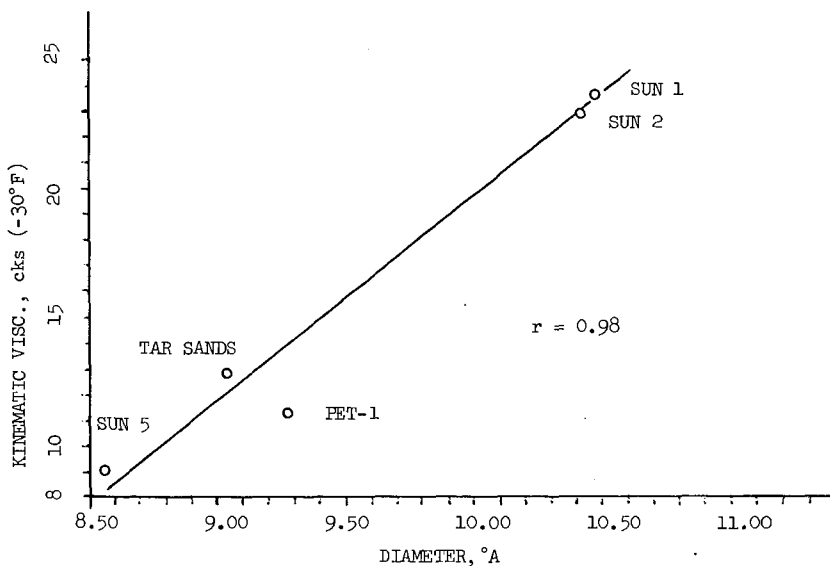


Fig. 8

FUEL FREEZE POINT VS. DIAMETER OF AVERAGE AROMATIC MOLECULE

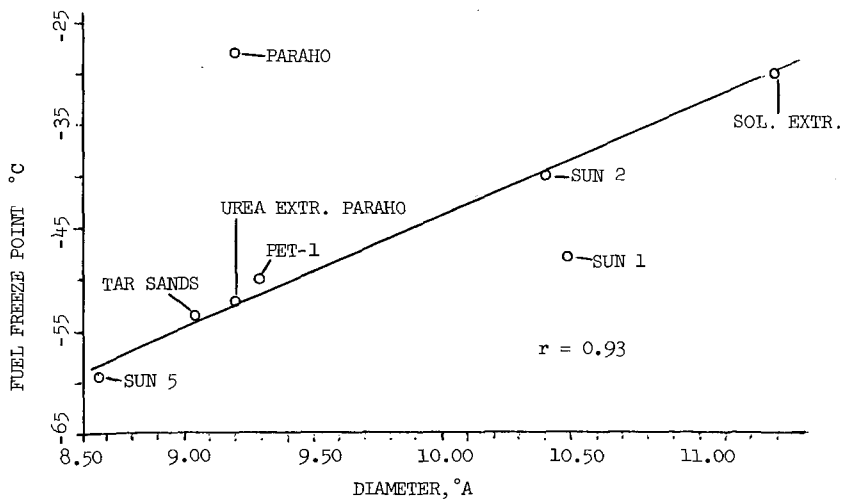
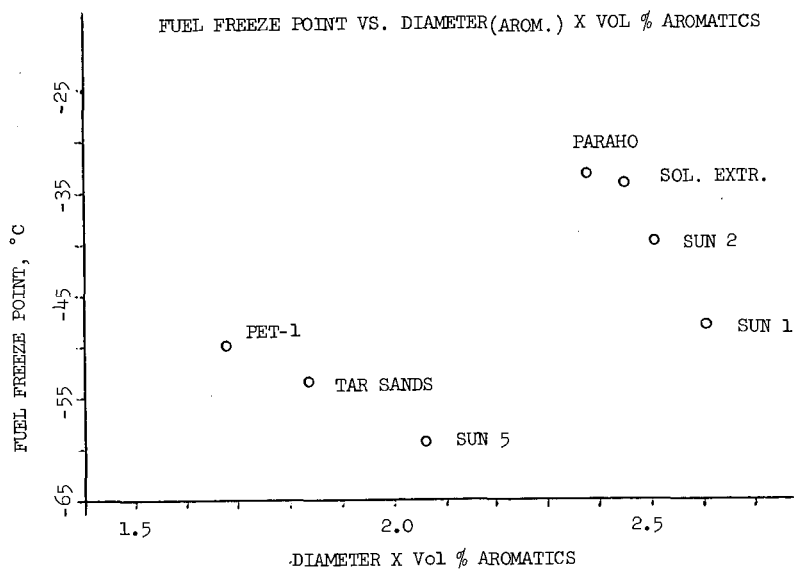


Fig. 9



References

- (1) R. N. Hazlett, J. M. Hall and J. Solash, 172nd ACS Meeting, Div. of Fuel Chemistry, this symposium.
- (2) COED is an acronym for Char Oil Energy Development. The FMC Corporation, Princeton, NJ, developers of this process, kindly supplied the Navy with samples of crude oil. For further details concerning the COED process, see M. I. Greene, L. J. Scotti and J. F. Jones, 167th ACS Meeting, Div. of Fuel Chemistry, Los Angeles, April 1974.
- (3) F. S. Eisen, "Preparation of Gas Turbine Engine Fuel from Synthetic Crude Oil Derived from Coal," by Sun Oil Co. for the Office of Naval Research, NTIS No. AD/A007923, 6 February 1975.
- (4) J. Solash, Naval Air Propulsion Test Center, Letter Report, in preparation.
- (5) H. Bartick, K. Kunchal, D. Switzer, R. Bowen and R. Edwards, "The Production and Refining of Crude Shale Oil into Military Fuels, Final Report," submitted to the Office of Naval Research, August 1975.
- (6) E. D. Innes and J. V. D. Fear, 7th World Petroleum Congress, Vol. 3, Elsevier, Essex, England (1967), p. 633.
- (7) J. Solash, C. J. Nowack and R. J. Delfosse, Naval Air Propulsion Test Center, Formal Report No. NAPTC-PE-82, in press.
- (8) C. J. Nowack, Naval Air Propulsion Test Center, Letter Report No. NAPTC-LR-75-29, of 23 June 1975.
- (9) D. R. Clutter, L. Petrakis, R. L. Stenger, Jr., and R. K. Jensen, Anal. Chem., 44, 1395 (1972).
- (10) D. L. Camin and A. J. Raymond, J. Chrom. Sci., 11, 625 (1973).
- (11) Private communication from Dr. F. Newman.
- (12) Private communication from Dr. L. Petrakis.
- (13) VPO molecular weights determined by Galbraith Laboratories, Inc., Knoxville, TN.
- (14) Mass spectrometric molecular weights determined by Gulf Analytical Services, Div. Gulf Research and Development Co., Pittsburgh, PA.
- (15) I. G. C. Dryden, in Chemistry of Coal Utilization, Supplementary Volume, Edited by H. H. Lowry, John Wiley and Sons, New York (1963), p. 232.
- (16) B. D. Boss, R. N. Hazlett and R. L. Shepard, Anal. Chem., 45, 2388 (1973).
- (17) J. A. Dixon, 5th World Petroleum Congress, Sect. V (No. 16), Elsevier, Essex, England (1959), p. 205.
- (18) J. A. Dixon and S. G. Clark, III, J. Chem. Eng. Data, 4, 94 (1959).
- (19) P. Desikan and A. V. Venkatesh, Petrol. Hydrocarbons, 1 (4), 450 (1967); in Chem. Abstr., 66, 117640n (1967).
- (20) R. P. Walsh and J. V. Mortimer, Speech at the Informal ASTM Symposium on Use of Analytical Data, ASTM D-2 Meeting, Dallas, December 1970.

References (continued)

- (21) C. R. Martel, Air Force APL, Wright-Patterson Air Force Base, Tech. Report No. AFAPL-TR-74-122 (March 1975).
- (22) M. Smith, Aviation Fuels, G. T. Foulis and Co., Ltd., Henly-on-Thames, England, 1970, p. 85.
- (23) E. Dimitroff, J. T. Gray, N. T. Meckel and R. D. Quillian, Jr., 7th World Petroleum Congress, Individ. Paper No. 47, Mexico City, 1967.
- (24) E. Dimitroff and H. E. Dietzmann, 158th National Meeting of the American Chemical Society, Div. of Petroleum Chemistry, New York City, September 1969.
- (25) A. Bondi, Physical Properties of Molecular Crystals, Liquids and Glasses, John Wiley and Sons, New York (1968).
- (26) The 95 vol % distilled temperature of these fuels roughly describes fuel composition. A plot of T (95 vol %) correlates well with fuel viscosity ($r = 0.98$) but not with fuel freeze point ($r = 0.7$).

FLAMMABILITY, IGNITION AND ELECTROSTATIC PROPERTIES OF NAVY FUELS
DERIVED FROM COAL, TAR SANDS AND SHALE OIL

W. A. Affens, J. T. Leonard, G. W. McLaren and R. N. Hazlett

Naval Research Laboratory
Washington, D. C. 20375

INTRODUCTION

As part of the coordinated synthetic fuels research and development program of the Navy and other departments of the Department of Defense, National Aeronautic and Space Administration, Energy Research and Development Administration, Maritime Administration, and the Department of the Interior, the Naval Research Laboratory is investigating the flammability and related properties of JP-5 jet fuel derived from sources other than petroleum. NRL has also made a related study on ship propulsion fuels derived from coal, and these studies will be included in the last section of this paper.

Seven samples of turbine fuels from alternate sources were examined in this study, five from coal and one each from tar sands and shale oil. These materials were selected because they had been processed to have properties close to that of JP-5, the Navy's primary jet aircraft fuel. All five coal products were prepared by the Char Oil Energy Development (COED) process, followed by distillation and hydrogenation. The preparation and properties of coal-derived jet fuels are described in a Sun Oil Company report (1). Shale crude oil, made by the Paraho retort process, was converted to jet fuel (and other military fuels) by delayed coking, distillation, and hydrogenation (2). The tar sands fuel was produced by the Great Canadian Oil Sands Company (3). More details concerning the preparation of these fuels will be given in another paper of this Symposium (4). Two conventional JP-5 fuel samples (from petroleum) were included in the study for comparison. All of the JP-5 samples were supposed to meet the requirements of the military specifications of jet fuel (5), but some were not met.

FLAMMABILITY AND IGNITION PROPERTIES OF JP-5 JET FUELS FROM ALTERNATE SOURCES

This portion of the paper is concerned with the flammability and related properties of alternate jet fuels. Additional properties were also investigated and are reported in two other papers of this Symposium (4,6).

Flammability and Ignition Properties - Three flammability properties were included in this study: flash point, flammability index, and autoignition temperature. Flash points were determined by the Pensky-Martens Closed-Cup (PMCC) (7), Tag Closed-Cup (Tag) (8), or Seta Closed-Cup (Setaflash) flash point method (9). Flammability indices at several temperatures were determined by the NRL flame ionization detector method (10,11), and minimum autoignition temperatures (AIT) by ASTM D-2155 (12). Only the PMCC flash point determination is a specification requirement (60°C minimum), although the flammability index at 51.7°C is related to the "Explosive-ness" requirement of the specification (5). The flash point and flammability index determinations are important since they are a measure of the tendency of a liquid fuel to form a flammable mixture with air at a given temperature. The significance of autoignition temperature is that it is a measure of the likelihood that spontaneous or autoignition might occur if the fuel contacts a hot surface, such as by leakage onto a steam pipe.

Results - Flammability index, flash point, and autoignition data are shown in Tables I - III. It is seen that the first three fuels in Table I (tar sands, shale oil, and COED 5) did not meet the 60°C minimum flash point (PMCC) requirement of the specification (5). On the other hand, the other coal samples had PMCC flash points

which are considerably above that of the specification requirement. As is usually the case for fuels in the JP-5 flash point range, the Tag flash points are lower (average = 2°) than those obtained by PMCC. Both the flash point and flammability index data for the petroleum JP-5 samples fell within the range found for the alternate fuel samples.

Flammability Index - Flammability index (E) is defined as the ratio of the vapor concentration in air (C, %v/v) to that at the lower flammability limit (L, %v/v), so that $E = C/L$. Flammability index may be expressed as a decimal or as percent. If E is less than 1 (100%), the vapor-air mixture is nonflammable, and if E is equal to or greater than unity, the mixture is flammable (10). In the case of liquids, the flammability index refers to the vapor-air mixture which is in equilibrium with the liquid at a given temperature. The flammability indices of all the fuels were determined at several temperatures, and are plotted in Figure 1. The flammability indices at 51.7°C (125°F) are shown in Table I. Flammability index, which is a vapor pressure function, has been shown to vary exponentially with temperature for hydrocarbons and their mixtures according to the following relationship (11):

$$\text{Log } E = m/(T^{\circ}\text{C} + 230) + k \quad 1)$$

where T is temperature (°C), and m and k are constants. As is shown in Figure 1, a plot of Log E vs reciprocal temperature is linear with slope m, and intercept k. Slopes and intercepts are included in the table.

If we let E = 100% in Equation 1, and solve for T, a value is obtained (T_E) which is related to flash point. T_E is that temperature at which the concentration of the vapor in equilibrium with the liquid fuel is equal to that at the lower flammability limit. T_E may also be obtained graphically by noting the temperatures at which the curves intersect the horizontal line at %E = 100%. In Figure 1, the small triangles are actual flash points (Tag) and it is seen that they lie close to the intersection points. A comparison of T_E and Tag flash points are shown in the table. The slopes (m) and intercepts (k), as in the case of flammability index, are dependent on fuel composition. In general, the slopes (negative) of the alternate fuel samples (1554 to 1906) are lower than that of the petroleum samples (1917 and 1994). Similarly, the intercepts (5.46 to 6.14) are lower than that of the petroleum fuels (6.65 and 6.84), so that it can be concluded that there are differences in composition between the alternate fuels and that of the petroleum fuel. Previous unpublished NRL work with six conventional JP-5 fuels gave a range of 1917 to 2076 (average = 1987) for slopes, and 6.65 to 7.19 (average = 6.88) for the intercepts.

Effect of Fuel System Icing Inhibitor Additive on Flash Point - Ethylene glycol monomethyl ether (EGME) is presently used as a fuel system icing inhibitor additive in JP-5 (5). It has been shown that at use concentrations (0.1 to 0.15%), EGME additive lowers the flash point of JP-5 3 to 4°C (13). This effect complicates the burden on refiners in meeting the minimum flash point requirement of the specification. The question of whether this problem might also exist with JP-5 from alternate sources was also investigated and results are shown in Table II. A pure hydrocarbon is also included in the table for comparison. It will be seen in the table that the flash point depression at 0.15% EGME ranges from 2 to 5°C with the greatest effects occurring at the higher flash points. From this data, we conclude that the problem of flash point depression by EGME for petroleum fuels also exists for the fuels from alternate sources.

Autoignition Temperatures - Autoignition temperatures (AIT) for the JP-5 fuels are shown in Table III. The AIT data by the standard ASTM method (12) are shown under "hot flames" in the table. These temperatures represent the lowest temperatures at which visible ignition occurs in the standard 200-ml ASTM flask without the aid of an external ignition source. Observations were made in total darkness and with the aid of a thermocouple-recorder arrangement for monitoring the internal

gas temperature inside of the flask. Cool flame ignitions were observed in the case of four of the coal samples, and one of the petroleum samples. It will be noted that the cool flame ignitions occurred at lower temperatures than that of the hot flame ignitions. From the point of view of safety, it is desirable to be able to determine a true minimum AIT. Since cool flames are precursors of hot flame ignitions, either type of ignition should be considered as a "positive" ignition. The differences in the table range from 4 to 14°C. If we pay attention to the lower values in all cases (cool flame or hot flame), the AIT values for the alternate fuel samples range from 241 to 247°C and these values are in the same range as that of the petroleum fuel samples.

Conclusions - The tar sands, shale oil, and one of the coal samples had flash points which were below that of the 60°C specification requirement. The remaining fuels from coal had flash points which were higher than specification requirements and also higher than those of the usual run of petroleum JP-5.

Flammability indices and flammability-temperature relationships of the alternate fuels were also measured, and found to differ somewhat from that of the petroleum fuels. Autoignition temperatures of the alternate fuels were similar to that of petroleum derived fuels.

In general, the flammability properties of the JP-5 from alternate sources were not significantly different from that of JP-5 from petroleum. If the alternate fuels were refined to more closely agree with the flash point requirement, the other observed differences would probably be diminished.

ELECTROSTATIC PROPERTIES OF JP-5 JET FUELS FROM ALTERNATE SOURCES

Although neither electrical conductivity nor charging tendency are part of the present specifications for turbine fuels, both properties are useful in predicting whether an electrostatic ignition hazard exists in handling such products. Therefore these properties were measured on the alternate fuels to determine if these fuels posed a lesser or greater hazard than their petroleum-derived counterparts.

Determination of Electrostatic Properties - Electrical conductivity was determined by the ASTM method (14) and charging tendency with the EXXON Mini-Static Tester (15). The latter method measures the amount of electrical charge generated by flowing a fuel sample through a paper filter. Since the two methods were used to evaluate samples taken in a recent survey of jet fuels from ten commercial airports and three military bases (16), the results of the present study can be directly related to actual field experience.

Results and Conclusions - The electrical conductivity and charging tendency of the JP-5 samples derived from coal, tar sands and shale are summarized in Table IV. Conductivity is expressed in terms of picosiemens/meter (pS/m) and charging tendency as the density of charge in the fuel in microcoulombs/meter³ ($\mu\text{C/m}^3$). The results of the present study are compared with the data obtained for various turbine fuels (Jet A, JP-4 and JP-5) in Figures 2 and 3. The data show that, with the exception of the JP-5 from shale oil, the conductivity and charging tendency of the alternate fuels are well within the ranges of the petroleum-derived Jet A samples but somewhat lower than the values obtained for the petroleum-derived JP-4 fuels. Since the total number of JP-5 samples in the fuel conductivity survey was quite small (18 samples from only one Naval Air Station vs 338 samples of Jet A from ten airports), it is better perhaps to restrict the comparison of the present data to the survey data for Jet A.

The JP-5 derived from shale oil was an exception. This fuel was an off-specification product containing a sediment which clogged the filter of the charging tendency apparatus making it impossible to obtain a charge density measurement. After this sample was filtered through a 0.45 μ Millipore filter, a charge density of 7035

$\mu\text{C}/\text{m}^3$ was obtained, a value somewhat above the maximum observed in the study on petroleum derived jet fuels. However, in this case, the high charge density is of no concern since the conductivity of the JP-5 fuel derived from shale oil was sufficiently high (215 pS/m) that most of the charge generated in the filter decays in less than one second and hence does not constitute a hazard. In view of the rather low conductivities and charging tendencies exhibited by the other alternate fuels, no greater electrostatic hazard is envisioned in the handling of these products than their petroleum derived counterparts.

FLAMMABILITY AND IGNITION PROPERTIES OF SHIP PROPULSION FUELS DERIVED FROM COAL

The Navy has also been exploring the feasibility of burning fuel oil derived from coal in ships' propulsion systems (17). One fuel for this purpose was prepared from Illinois No. 6 coal by the COED process at FMC Corporation, Princeton, New Jersey under a contract with the Office of Coal Research, Department of the Interior (17). The crude COED product possessed a wide boiling range and, hence, a low flash point, 14°C . Therefore this product was distilled to remove the light fractions (17) and raise the flash point above 60°C , the minimum acceptable for ship propulsion fuel (18-20).

Results and Conclusions - The flammability and ignition properties of the processed COED fuel (SP-4) are compared in Table V with the properties of three petroleum derived fuels. These latter fuels include the current Navy ship propulsion fuel, Diesel Fuel Marine (DFM), and two obsolete types, Navy Distillate (ND) and Navy Special Fuel Oil (NSFO). The flash point of the COED fuel is slightly lower than that of the petroleum fuels and the flammability index is seen to be near the average of the three petroleum fuels. The autoignition temperature was somewhat higher than that of the three petroleum fuels.

A plot of flammability index vs reciprocal temperature for the processed COED fuel along with similar plots for typical petroleum derived ship fuels are shown in Figure 4. As in the case of the JP-5 data (Figure 1), the graphs are linear and intersect the horizontal $E = 100\%$ line relatively close to the flash point temperature.

The single sample of processed COED ship propulsion fuel (SP-4) which was investigated is not necessarily representative of synthetic fuel derived from coal. However, the data on this sample indicate that coal derived fuels will be satisfactory for ship propulsion use, at least from the viewpoint of flammability hazards.

SUMMARY AND CONCLUSIONS

The flammability, ignition, and electrostatic properties of JP-5 jet fuel from alternate sources and a ship propulsion fuel derived from coal were investigated. Flash points, flammability indices, autoignition temperatures, electrical conductivities and electrostatic charging tendencies were measured. In general, the properties of the alternate fuels were not significantly different from similar fuels derived from petroleum. These differences could probably be diminished by altering the production process and by observing care in meeting specification requirements.

ACKNOWLEDGMENT

This research was supported in part by the Naval Air Systems Command and in part by the Naval Sea Systems Command.

LITERATURE CITED

- (1) F. S. Eisen, "Preparation of Gas Turbine Engine Fuel From Synthetic Crude Oil Derived From Coal-Phase II Final Report," Sun Oil Co. report on U. S. Navy Contract N00140-74-C-0568, Feb. 6, 1975.
- (2) Applied Systems Corp., "The Production and Refining of 10,000 Barrels of Crude Shale Oil into Military Fuels," report on U. S. Navy Contract N00014-75-C-0055, June, 1975.
- (3) C. J. Nowack, "Development of Alternate Sources of JP-5 Fuel, Endurance and Emission Tests of a T63-A-5A Engine Using a Tar Sands Derived JP-5," Naval Air Propulsion Test Center, report NAPTC-LR-75-29, 23 June 1975.
- (4) J. Solash and R. T. Taylor, This Symposium
- (5) MIL-T-5624, Military Specification, Turbine Fuel, Aviation, Grades JP-4 and JP-5, 30 October 1973
- (6) R. N. Hazlett, J. M. Hall and J. Solash, This Symposium
- (7) Amer. Soc. for Testing and Materials, "Flash Point by Pensky-Martens Closed Tester," ASTM D93-72 (1972).
- (8) Amer. Soc. for Testing and Materials, "Flash Point by Tag Closed Tester," ASTM D56-70 (1972).
- (9) Amer. Soc. for Testing and Materials, "Flash Point of Aviation Turbine Fuels by SETAFASH Closed Tester", ASTM D3243-73 (1973).
- (10) W. A. Affens, H. W. Carhart and G. W. McLaren, "Determination of Flammability Index of Hydrocarbon Fuels by Means of a Hydrogen Flame Ionization Detector", Preprints, General Papers, Division of Petroleum Chemistry, Amer. Chem. Soc., 19, No. 1, 36-42 (Feb. 1974).
- (11) W. A. Affens, H. W. Carhart and G. W. McLaren, "Relationship Between Flammability Index and Temperature, and Flash Point of Liquid Hydrocarbon Fuels", Preprints, General Papers, Division of Petroleum Chemistry, Amer. Chem. Soc., 20, No. 1, 30-34 (Feb. 1975).
- (12) Amer. Soc. for Testing and Materials, "Autoignition Temperature of Liquid Petroleum Products", ASTM D2155-66 (1969).
- (13) W. A. Affens and G. W. McLaren, "The Effect of Icing Inhibitor and Copper Passivator Additives on the Flammability Properties of Hydrocarbon Fuels", NRL Memorandum Report 2477, Naval Research Laboratory, August 1972.
- (14) Amer. Soc. for Testing and Materials, "D. C. Electrical Conductivity of Hydrocarbon Fuels", ASTM D 3114-72 (1972).
- (15) D. A. Young, "Mini-Static Test Procedure", EXXON Research and Engineering Co., Linden, N.J., June 1972
- (16) Coordinating Research Council, "A Survey of Electrical Conductivity and Charging Tendency Characteristics of Aircraft Turbine Fuels", CRC Report No. 478, New York, N.Y., April 1975

LITERATURE CITED (Continued)

- (17) Naval Ship Engineering Center, Philadelphia Division, "Processing of Synthetic Fuel Drived from Coal", NAVSECPHILADIV Project A-1599, Ser. 1236, Final Report, September 24, 1973.
- (18) MIL-F-859E, Military Specification, Fuel Oil Burner, September 22, 1965.
- (19) MIL-F-24397, Military Specification, Fuel, Navy Distillate, July 2, 1969
- (20) MIL-F-16884G, Military Specification, Fuel Oil, Diesel, Marine, March 7, 1973.

Table I - Flammability Index vs Temperature and Flash Point
for JP-5 From Alternate Sources

Source	Flam. Index at 51.7°C (%)	Slope ^a (°m)	Intercept ^a (k)	T _E (°C) ^b	Flash Point (°C)	
					Tag ^c	PMCC ^d
Tar sands	91.0	1554	5.48	54	55	57
Shale oil	87.8	1559	5.46	56	57	58
COED 5	86.0	1710	5.97	56	58	59
COED 3	31.5	-	-	-	76	77
COED 4	30.2	1828	5.97	76	76	78
COED 1	22.8	-	-	-	78	79
COED 2	21.9	1906	6.14	81	79	83
Petroleum 1	56.0	1994	6.84	62	61	62
Petroleum 2	62.0	1917	6.65	58	61	65

a - $\log E = m/(T^{\circ}\text{C} + 230) + k$.

b - $T_E(^{\circ}\text{C}) = -m/k - 230$.

c - ASTM D-56.

d - ASTM D-93

Table II - Effect of EGME* Icing Inhibitor Additive on Flash
Points of JP-5 From Alternate Sources

Source	Flash Point (°C) *					Flash Point Depression (0.15% EGME) (°C)
	%EGME					
	0	0.10	0.15	0.30	0.50%	
Tar Sands	55	54	53	--	49	2
Shale Oil	57	-	54	53	-	3
COED 5	58	-	55	53	-	3
COED 3	76	73	71	--	62	5
COED 4	76	72	71	--	64	5
COED 1	78	74	73	--	63	5
COED 2	79	76	74	--	65	5
Petroleum 2	61	58	57	--	52	4
n-Undecane	66	63	62	--	56	4
EGME	41					

*Ethylene glycol monomethyl ether

* Tag Closed Cup, ASTM D-56

Table III - Autoignition Temperatures of JP-5 from Alternate Sources

SOURCE	Autoignition Temperature (°C)		
	Hot Flame*	Cool Flame*	Difference
Shale oil	241	-	-
Tar sands	248	-	-
COED 4	248	-	-
COED 1	252	248	4
COED 3	253	243	10
COED 5	253	249	4
COED 2	254	245	9
Petroleum 1	243	-	-
Petroleum 2	254	240	14

*ASTM D-2155

* "Spike" in temperature-time trace and/or an observed cool flame.

Table IV - Electrostatic Properties of JP-5 Fuels from Alternate Sources

SOURCE	Conductivity, ps/m	Charging Tendency, $\mu\text{C}/\text{m}^3$
Tar sands	0.271	170
COED 1	8.49	1274
COED 2	0.964	418
COED 3	0.371	575
COED 4	0.288	584
COED 5	4.55	2705
Shale oil, as received	246	(*)
Shale oil, filtered thru 0.45 μ millipore	215	7035

*Fuel contained a sediment which clogged the filter of the charging tendency apparatus.

Table V - Average Flammability and Ignition Properties of Ship Propulsion Fuels

Fuel	Flash Point (°C)*	Flammability Index (E %)*	Autoignition Temperature (°C)
Diesel Fuel, Marine (DFM)	79	36	240
Navy Distillate (ND) *	79	41	238
Navy Special Fuel Oil* (NSFO)	85	30	259
Processed COED Fuel (SP-4)	73	35	266

*Pensky-Martens closed cup.

* %E at 51.7° C

*Single sample.

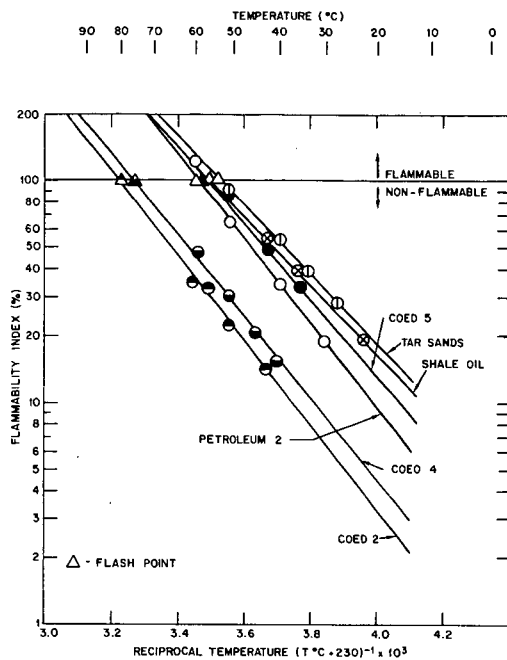


Figure 1. Flammability Index vs Temperature for Jet Fuels

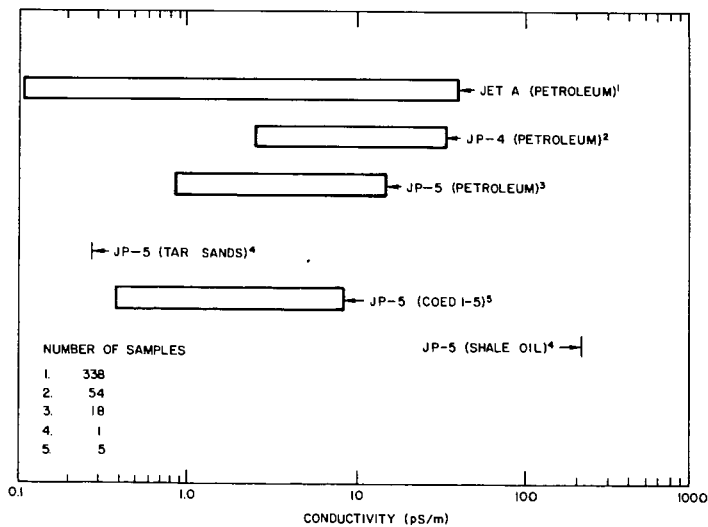


Figure 2. Ranges of Electrical Conductivities of Jet Fuels

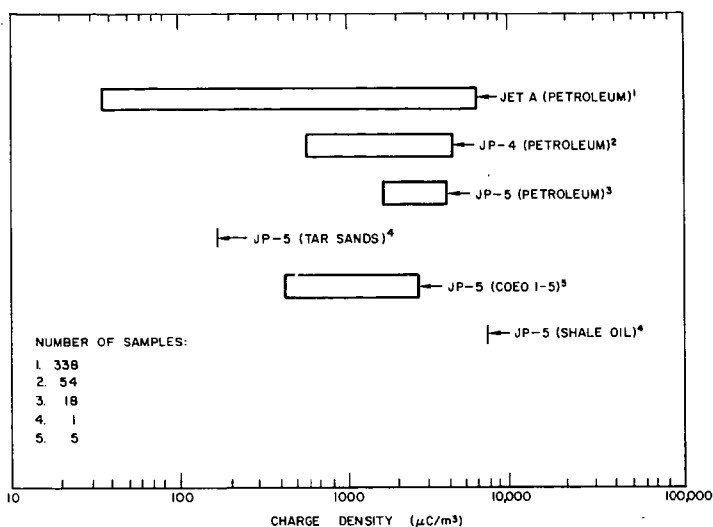


Figure 3 Ranges of Electrostatic Charge Densities of Jet Fuels

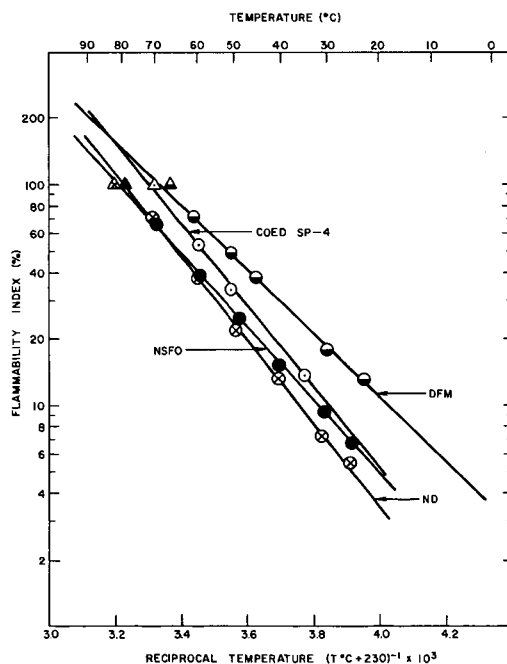


Figure 4 Flammability Index vs Temperature for Ship Propulsion Fuels

CHEMICAL CHARACTERIZATION OF SHALE OIL AND RELATED FUELS

by Peter W. Jones, Robert J. Jakobsen, Paul E. Strup,
and Anthony P. Graffeo

Battelle, Columbus Laboratories, Columbus, Ohio 43201

INTRODUCTION

In view of the recent activity directed towards the production of fuel oils as a substitute for natural petroleum products, there has arisen a need for chemical characterization of these materials. Chemical characterization of new fuels is important not only in order to provide an understanding of their chemical and physical properties, but also to provide preliminary data from which their potential environmental impact may be judged.

The results reported here represent a preliminary analytical survey of the organic constituents of shale oil, synthoil, and Prudhoe Bay crude oil, as a prelude to the comprehensive analytical intercomparison which will be reported subsequently. The analytical techniques employed in this study are liquid chromatography (LC), Fourier transform infrared spectroscopy (FTIR), and gas chromatographic-mass spectrometry (GC-MS). The analytical procedures used are similar to those described in a recent EPA publication⁽¹⁾ "Technical Manual for Analysis of Organic Materials in Process Streams", with regard to Level I analysis.

EXPERIMENTAL AND RESULTS

Liquid chromatography was carried out using 25 x 250 mm columns packed with 80 g of >200 mesh silica gel, which had been activated at 200 C for over 24 hours. The columns were pre-eluted with 200-ml methanol, 200-ml methylene chloride, and finally 200-ml 60/80 petroleum ether. Approximately 2.0 g of shale oil, synthoil, and Prudhoe Bay crude oil were separately dissolved in 25-ml 60/80 petroleum ether, and any insoluble residue was removed by centrifuging. Each oil was separately eluted on a silica gel column, using the following elution profile:

<u>Fraction</u>	<u>Eluent</u>
1	200-ml petroleum ether
2	200-ml 20% methylene chloride in petroleum ether
3	200-ml 20% methylene chloride in petroleum ether
4	400-ml 20% methylene chloride in petroleum ether
5	400-ml methylene chloride
6	400-ml 10% methanol in methylene chloride
7	400-ml methanol

Following elution and reduction in volume of each of the fractions by Kuderna-Danish evaporation, 1% of each fraction was used to determine the weight of material in each fraction after complete evaporation of the solvent by this procedure. Thus, the weight of material present in each fraction was calculated to be as follows:

Weight of Material (g) in Each LC Fraction

								Petroleum Ether Insoluble	Original Sample
	1	2	3	4	5	6	7		
Shale Oil	0.50	0.37	0.12	0.06	0.19	0.50	0.10	0.06	2.00
Prudhoe Bay	0.81	0.43	0.11	0.04	0.06	0.07	0.02	0.08	2.01
Synthoil	0.13	0.46	0.21	0.04	0.15	0.18	0.06	0.81	2.02

Previous knowledge of the type of organic compounds which are typically observed in the fractions of this LC separation scheme permits the following introductory observations.

- (1) The hydrocarbon content of shale oil is somewhat similar to Prudhoe Bay Crude, with slightly lower aliphatic content. There are substantially larger quantities of highly polar materials in shale oil.
- (2) Synthoil contains far less aliphatic hydrocarbons than either shale oil or Prudhoe Bay crude; its hydrocarbon content being largely aromatic. It contains less polar materials than shale oil, but more than Prudhoe Bay crude oil.

FTIR analysis of a thin film of material from each fraction was subsequently carried out; the results are summarized below (shale oil = SH, synthoil = SY, and Prudhoe Bay crude oil = PR).

Fraction 1

Fractions from all three oils contained saturated aliphatic hydrocarbons; shale oil showed some evidence of olefins. The degree of branching of the hydrocarbon chains is given by

$$\text{CH}_3/\text{CH}_2 \quad \text{SH} > \text{PR} > \text{SY}.$$

Fraction 2

Fractions from all three oils were largely saturated aliphatic hydrocarbons, with some evidence for aromatic hydrocarbons. GC-MS analysis subsequently showed that the aromatic compounds present were alkyl benzenes and alkyl naphthalenes in all cases. Again shale oil was shown to contain the most highly branched hydrocarbons, as shown by the CH_3/CH_2 ratio

$$\text{CH}_3/\text{CH}_2 \quad \text{SH} \gg \text{PR} > \text{SY}.$$

Synthoil contains substantially more aromatic hydrocarbons than either shale oil or Prudhoe Bay crude oil

$$\text{Aromaticity} \quad \text{SY} \gg \text{SH} \approx \text{PR}.$$

Fraction 3

Shale oil and Prudhoe Bay crude exhibited considerable saturated hydrocarbon chain, with some aromatics. Synthoil showed evidence of large amounts of aromatic compounds. Prudhoe Bay crude oil showed evidence of aldehydes or ketones, while shale oil additionally showed small evidence of hydroxy compounds. The degree of hydrocarbon chain branching and aromaticity are given by

$$\begin{array}{ll} \text{CH}_3/\text{CH}_2 & \text{SH} > \text{PR} \gg \text{SY} \\ \text{Aromaticity} & \text{SY} \gg \text{PR} > \text{SH}. \end{array}$$

Fraction 3 was additionally subject to GC-MS analysis in all cases, and the distribution of polynuclear aromatic hydrocarbons (PAH) in each oil was established (see later).

Fraction 4

All three oils showed evidence for hydroxy and carbonyl compounds, in addition to strong indications of both aliphatic and aromatic hydrocarbons. Shale oil and Prudhoe Bay crude both showed considerably less aromatic content than synthoil, which in turn showed far less evidence of branched hydrocarbon chains. Shale oil showed substantially more hydroxy and carbonyl compounds than the other oils.

CH ₃ /CH ₂	PR > SH >> SY
Aromaticity	SY >>> PR > SH
OH	SH >> PR > SY
C=O	SH >> PR > SY

Fraction 5

Shale oil and Prudhoe Bay crude both contain considerable saturated aliphatic hydrocarbons and some aromatic hydrocarbons; both contain traces of hydroxy compounds and larger amounts of carbonyl compounds. In addition to all of the foregoing, synthoil contains considerable quantities of aromatic hydrocarbons, and most probably amines and acid salts.

Aromatics	SY >>> PR > SH
CH ₃ /CH ₂	SH ≈ PR > SY
C=O	SH ≈ PR >> SY
OH	SY >> SH > PR.

Fraction 6

All three oils showed evidence for saturated hydrocarbons, but only synthoil showing significant aromaticity. Phenols and carbonyl compounds were evident in each oil but synthoil showed additional evidence for acid salts and sulfonates. The FTIR analysis of each fraction may be summarized as follows:

Aromaticity	SY >>> PR ≈ SH
CH ₃ /CH ₂	SY >> PR > SH
OH	PR > SY > SH
C=O	SH >> PR >> SY.

Fraction 7

In addition to saturated aliphatic hydrocarbons in all oils, there was evidence for phenols and carbonyl compounds in each fraction. Synthoil additionally showed evidence of moderate sulfonate content, while amine and amine salts were evident in shale oil. The analyses may be summarized

CH ₃ /CH ₂	PR > SH > SY
OH	SY > PR > SH
C=O	PR ≈ SH > SY.

Summary of FTIR Analyses

The FTIR analysis of each LC fraction of shale oil, synthoil permits some general observations to be made regarding these fuels. Synthoil is by far the most aromatic in character and shale oil exhibits the greatest extent of branching in the aliphatic side chains. Shale oil contains the greatest proportion of carbonyl compounds, with synthoil containing the least. Each of the oils contains phenols, and to a lesser extent amino compounds, in similar amounts to each other.

These general findings may be briefly summarized as follows:

Aromatic Content of Fraction

Fraction	
2	SY >> PR ≈ SH
3	SY >>> PR > SH
4	SY >>> PR > SH
5	SY >>> PR > SH
6	SY >>> PR ≈ SH.

CH₃/CH₂ Ratio by Fraction

Fraction	
1	SH > PR > SY
2	SH >> PR > SY
3	SH > PR >> SY
4	PR > SH >> SY
5	SH = PR > SY
6	SY >> PR > SY
7	PR > SH > SY

OH or NH Content by Fraction

Fraction	
3	SH -- --
4	SH >> PR > SY
5	SY >> SH > PR
6	PR > SY > SH
7	SY > PR > SH

C=O Content by Fraction

Fraction	
3	SH = PR
4	SH >> PR > SY
5	SH = PR >> SY
6	SH >> PR >> SY
7	SH = PR > SY

Polycyclic Aromatic Hydrocarbon (PAH)

Analysis by GC-MS

Fraction 3 in all cases was shown to contain PAH compounds with molecular weight distribution between 150 and 400. Quantitative measurements were made on a large number of methyl isomers using the ion current integration technique⁽²⁾, but due to the unavailability of sufficient standard reference materials the ionization efficiencies of the methyl isomers were assumed to be equal to the parent PAH compound in every case. Separation was achieved using a 6' 1 percent OV-101 column, programmed from 100 to 340 C at 4-1 C min⁻¹. Mass spectra were obtained using a Finnigan 3200 quadrupole mass spectrometer with a chemical ionization source. Data handling was accomplished with a Digital PDP8 mini-computer.

In absolute terms, synthoil was estimated to contain at least 10 times more PAH than either shale oil or Prudhoe Bay crude oil, by measurement of the species reported in Table 1.

PAH Content SY > PR = SH

The relative differences in the distribution of methyl isomers of several PAH compounds are shown in Table 1. Shale oil exhibits a very distinctive pattern among all of the PAH methyl isomers observed, in that the maximum abundance usually occurs for the five or six methyl compound. Prudhoe Bay crude oil is somewhat similar to shale oil, and generally exhibits a maximum abundance of the methyl isomers at the four methyl compound on the average. Synthoil on the other hand shows a much lower tendency to contain a high proportion of very highly methylated species; the average most abundant methyl PAH in this fuel being the dimethyl compound, or smaller. This methyl isomer distribution is undoubtedly useful in fingerprinting different types of oil. However, the potential environmental impact of few methyl groups or many is not clear. While it is true that the addition of one or two methyl groups to a PAH nucleus tends to make the resultant molecule more

hazardous from a health standpoint, the addition of a large number of methyl groups could potentially be desirable from the standpoint of a reduced health risk and possibly increased biodegradability and photooxidation in the environment.(2)

REFERENCES

- (1) "Technical Manual for Analysis of Organic Materials in Process Streams", P. W. Jones, A. P. Graffeo, R. Detrick, P. A. Clarke, and R. J. Jakobsen, EPA Publication No. 600/2-76-072.
- (2) Polynuclear Aromatic Hydrocarbons: Chemistry, Metabolism, and Carcinogenesis, R. I. Freudenthal and P. W. Jones, Editors, Raven Press (New York) 1976.

TABLE 1. RELATIVE DISTRIBUTION OF PAH METHYL ISOMERS IN SHALE OIL (SH),
SYNTHOIL (SY), AND PRUDHOE BAY CRUDE OIL (PR)

Methyl Groups		0	1	2	3	4	5	6	7	8	9	10
Anthracenes/ Phenanthrenes	SH	1.00	1.82	2.38	3.00	2.41	2.92	3.06	2.22	1.70	1.18	1.77
	SY	1.00	1.11	2.21	2.04	1.71	1.04	0.56	0.29	0.13	0.04	0.02
	PR	1.00	1.98	1.47	0.75	0.92	0.10	0.39	0.14	0.01	0.04	0.02
Pyrenes/ Fluoranthenes/ Benzfluorenes	SH	1.00	3.08	4.08	5.86	5.42	9.92	13.9	12.5	11.2	11.9	--
	SY	1.00	0.57	0.28	0.51	0.39	0.30	0.17	0.10	0.06	0.03	--
	PR	1.00	3.89	4.86	9.06	--	7.72	4.19	2.75	1.89	--	--
Benzanthracenes/ Chrysenes	SH	1.00	1.47	2.39	7.07	8.92	9.03	9.08	7.44	7.25	6.15	5.46
	SY	1.00	3.24	2.64	2.27	2.18	1.49	1.13	0.60	0.24	0.04	--
	PR	1.00	1.57	3.68	4.14	3.38	3.11	2.68	1.57	--	--	--
Cholanthrenes	SH	1.00	2.46	3.35	4.41	4.54	4.57	3.50	3.30	1.98	1.76	0.70
	SY	1.00	0.95	1.24	1.20	1.15	0.71	0.37	0.17	0.03	--	--
	PR	1.00	2.82	4.05	4.23	5.05	3.73	1.59	0.82	--	--	--
Benzpyrenes/ Benzfluoranthenes/ Perylenes	SH	1.00	1.77	2.96	3.54	7.27	5.73	6.35	5.27	4.58	3.46	2.58
	SY	1.00	2.25	2.86	3.30	5.50	4.29	2.64	0.86	0.23	--	--
	PR	1.00	3.93	8.61	7.54	20.1	17.83	11.66	5.66	--	--	--
Indenopyrenes/ Benz(ghi)perylene	SH	1.00	1.50	2.21	--	2.10	--	2.11	--	2.13	2.04	1.79
	SY	1.00	0.90	0.53	0.62	0.72	0.34	--	--	--	--	--
	PR	1.00	3.78	2.33	--	1.73	1.16	--	--	--	--	--

TABLE 1. (Continued)

Methyl Groups		0	1	2	3	4	5	6	7	8	9	10
Dibenzanthracenes/ Picones	SH	1.00	4.60	--	6.44	6.67	6.69	--	6.60	--	6.16	5.04
	SY	1.00	2.51	3.89	3.46	2.77	1.06	0.49	--	--	--	--
	PR	1.00	1.42	2.36	5.69	3.61	2.35	0.47	--	--	--	--

FRACTIONATION OF SOLUBLE EXTRACTS OBTAINED FROM KEROGEN THERMAL
DEGRADATION WITH CO AND H₂O

Shuang-Ling Chong, J. J. Cummins, and W. E. Robinson

U.S. Energy Research and Development Administration
Laramie Energy Research Center, Laramie, Wyoming 82071

INTRODUCTION

Various techniques (1, 2, 3)¹ have been developed for the conversion of oil-shale kerogen to usable products. Each technique of conversion produces a different product with different characteristics. The thermal degradation of oil-shale kerogen in the presence of carbon monoxide and water has been studied at the Laramie Energy Research Center (4, 5). It was shown from this study that more kerogen is converted to a benzene-methanol soluble extract at temperatures below 500° C than is converted to oil by dry retorting. Because this reaction appears to have some potential advantages (5) over other conversion methods, it is desirable to investigate the soluble extracts obtained from this reaction.

This study was conducted to determine the types of compounds present in the soluble extracts that represent as much as 90 percent of the kerogen in Green River oil shale. This was accomplished by separating the soluble extracts into acid, base, neutral nitrogen, *n*-alkane, branched plus cyclic, aromatic, and cyclohexane-insoluble fractions by the established method. The method was used to compare the amount of each fraction produced under various reaction conditions where the temperature was varied from 300° to 450° C and the time was varied from 0.25 to 6 hours at charged CO pressure of 1,000 psig.

Because most of the extracts showed very little solubility in *n*-pentane, the previous separation method used for the natural bitumen in this laboratory (6 - 8) was not applicable and another technique had to be used. The modified method incorporated the uses of ion exchange resins first suggested by Munday and Eaves (9) and some of the techniques developed by Jewell (10) to remove the acid, base, and neutral nitrogen fractions. The hydrocarbon fractions were separated into *n*-alkane, branched plus cyclic alkane, and aromatic fractions by using molecular sieves as described by O'Connor and others (11) and silica-gel chromatography.

The soluble extracts obtained from each of the time-temperature tests were fractionated by the separation techniques. Because of the similarity of the data, only a limited number of these separations will be discussed in this report. For evaluation and comparison of the soluble extracts obtained by thermal degradation of kerogen in the presence of CO and H₂O with other oil-shale degradation products, three shale oils (1, 2, 3) obtained by different conversion methods were fractionated by the same separation technique. The component distribution of the soluble extracts will be discussed relative to the shale oils.

¹ Underlined numbers in parentheses refer to items in the list of references at the end of this report

It was found that below 375° C the fraction amounts of the soluble extracts were significantly different from those obtained from the three shale oils and that the temperature or the time of reaction had little effect upon the amount of each fraction. At 400° and 450° C, the fraction amounts of the soluble extracts changed with increase in temperature and at 450° C the soluble extracts resembled to some degree the shale oils.

EXPERIMENTAL

Materials

IRA-904 anion resin², A-15 cation resin (Rohm and Haas Company) and ferric chloride supported on clay were prepared and extracted similar to the procedures described by Jewell (10).

Silica gel (grade 12, 28-200 mesh, Davison Chemical Co.) was activated at 200° C for 24 hours and 5A molecular sieve (Matheson, Coleman, and Bell) was activated at 250° C for 24 hours.

N-pentane (99 percent, Phillips Petroleum) and 1,2 dichloroethane (reagent grade, Eastman Chemical Co.) were purified by flash distillation and by percolation through activated silica gel. Benzene, chloroform, methanol (reagent grade, J. T. Baker), and cyclohexane (99.5 percent, Phillips Petroleum) were flash distilled. The isopropylamine (reagent grade, J. T. Baker) and acetic acid (reagent grade, Eastman Chemical Co.) were used as received. Isooctane (99 percent, Phillips Petroleum) was purified by percolation through an activated 5A molecular sieve.

Samples of Soluble Extracts

The soluble extracts were obtained from the thermal conversion of Green River oil-shale kerogen in the presence of carbon monoxide and water as described by Cummins, et al. (4). The oil-shale samples were heated at temperatures from 300° to 450° C for 0.25 to 6 hours at charged CO pressure of 1,000 psig. The soluble extracts were obtained by treating the products of the CO-H₂O reaction in benzene and methanol.

Fractionation Procedure

The fractionation scheme is shown in detail in figure 1 and is essentially the same as the one used by D. M. Jewell, et al. (10). Since the soluble extracts obtained from CO-H₂O reaction with kerogen were generally polar, it was necessary to use cyclohexane rather than *n*-pentane as a solvent and to use a circulating system for all acid and base fractions to be removed from the extracts by IRA-904 anion resin and A-15 cation resin. The solution containing the acid and base components to be removed was circulated continuously over the resin bed for 24 hours by a pumping system. Excellent recoveries of acid and base fractions from the resins were obtained. Ferric chloride-Attapulpus clay was used to separate the acid and base-free fraction into hydrocarbon and neutral nitrogen fractions. The hydrocarbon fraction was then separated into *n*-alkane, branched plus cyclic alkane, and aromatic fractions by using silica-gel chromatography and molecular sieves.

² Reference to specific trade names or manufacturers does not imply endorsement by the Energy Research and Development Administration.

All fractions obtained were freed of solvent and then dried under reduced pressure at 60° C and weighed. By using the various fractionation techniques the average recovery of the soluble extract amounted to more than 90 percent. All data shown was normalized to 100 percent.

Cyclohexane-insoluble fraction

Approximately 2 g of the benzene-methanol soluble extract was heated and stirred with 200 ml of cyclohexane at 80° C for 1 hour. After cooling to room temperature, the mixture was filtered. The cyclohexane-insoluble fraction was washed with fresh cyclohexane until the solvent became clear.

Acid fraction

The cyclohexane-soluble fraction was redissolved in cyclohexane and slowly pumped through the anion resin for 24 hours. A ratio of 7 parts of resin to 1 part of sample was used. The acid-free fraction was transferred to a flask and the resin was washed with fresh cyclohexane.

The total acid fraction was recovered from the resin by 2 percent of acetic acid in benzene with Soxhlet extraction for 24 hours.

Base fraction

The technique and the amount of resin used to remove the base fraction from the acid-free fraction were the same as for the removal of the acid fraction. The base fraction was recovered from A-15 cation resin by 8 percent isopropylamine in benzene and methanol with Soxhlet extraction for 24 hours.

Neutral nitrogen and hydrocarbon fractions

Five parts of IRA-904 anion resin to 1 part sample were packed into a column and 7 parts of ferric chloride-Attapulgus clay mixture to 1 part sample were packed on the top of the resin with a glass wool plug in between the two materials. The acid- and base-free fraction was dissolved in pentane and then percolated slowly downward through the column. The hydrocarbon fraction was obtained by pentane elution and the neutral nitrogen fraction was desorbed from the column by elution with 1,2 dichloroethane.

Alkane and aromatic fractions

Two hundred g of activated silica gel to 1 g of hydrocarbon fraction were packed into a column and the hydrocarbon fraction dissolved in pentane was charged to the column. The alkane fraction was obtained by elution with pentane. Chloroform was used to deactivate the column and the aromatic fraction was removed by elution with methanol.

Branched plus cyclic alkane and n-alkane fractions

The alkane fraction obtained from the silica-gel column was dissolved in isooctane (100 ml for 0.2 g of sample) and 20 parts of 5A molecular sieves to 1 part sample were added to the solution. The solution was refluxed for 24 hours then filtered. The branched plus cyclic alkane fraction was obtained by drying the filtrate of this solution.

The molecular sieves were extracted with benzene and methanol for 24 hours in order to remove any traces of polar materials. The *n*-alkane fraction was recovered from the molecular sieves by decomposing the sieves with HF in benzene. Gas chromatograms of the *n*-alkane fractions of the selected samples were obtained.

Gas Chromatography

All gas chromatographic results were obtained on a Hewlett-Packard Model 700 gas chromatograph equipped with a thermoconductivity detector using a 50 ft SE-30 SCOT column programmed from 100° to 275° C at 5°/min with a helium flow of 5 cc/min.

RESULTS AND DISCUSSION

The weight percents of kerogen converted and the elemental analyses of the soluble extracts for 1 hour reaction time at various temperatures are shown in table 1. From these data it appears that the soluble extracts prepared at

TABLE 1. - Weight percent of kerogen converted and elemental analyses of the soluble extracts

Temp., °C	Time, hrs	Kerogen converted, weight-percent	Weight-percent of total					H/C ratio
			C	H	N	S	O	
300	1	26.2	83.4	10.8	1.3	0.7	3.8	1.6
325	1	29.9	82.6	11.0	1.3	0.9	4.2	1.6
350	1	31.3	81.1	10.9	1.2	0.5	6.3	1.6
375	1	46.8	83.6	11.3	1.5	0.5	3.1	1.6
400	1	76.9	82.1	11.1	1.7	0.3	4.8	1.6
425	1	93.9	83.3	11.5	1.4	0.4	3.4	1.7
450	1	97.9	83.4	10.5	2.7	0.5	2.9	1.5

¹ Oxygen was determined by difference.

different temperatures do not differ significantly in elemental contents. The weight percent of kerogen converted varied from 26.2 to 97.9 as temperatures increased from 300° to 450° C.

Effect of temperature

Seven soluble extracts obtained at 300°, 325°, 350°, 375°, 400°, 425°, and 450° C for 1 hour reaction time were fractionated to determine the effect of reaction temperature upon the composition of each extract. These results are shown in figure 2. Below 375° C the compositions of each extract remain fairly constant. Apparently the acid and the base fractions are fairly stable at this temperature range and do not undergo drastic changes. The polar materials which are the sum of acid, base, and neutral nitrogen fractions represent about 65 percent of the soluble extract. Above 375° C, the relative amounts of acid fractions decrease rapidly whereas the relative amounts of base and hydrocarbon fractions increase. This suggests that the acid fractions consist of bifunctional groups that presumably decarboxylate to give additional bases and hydrocarbons at higher temperatures. The concentrations of neutral nitrogen fractions remain about 1 to 2 percent and apparently are not affected by temperature.

Figure 3 shows the distribution of the *n*-alkane, the branched plus cyclic alkane, and the aromatic fractions. The increase in concentration in each fraction shows that more thermal degradation of the higher-molecular-weight kerogen to the lower-molecular-weight hydrocarbons occurs at high temperatures. The relative distribution of the various hydrocarbon components remains fairly constant showing that they are formed at approximately the same rate.

Effect of reaction time

The relationship of fraction amounts of the soluble extracts to reaction time at 300° C is shown in figure 4. It is obvious that the component distribution does not change appreciably with time of heating at 300° C and the amount of each fraction is independent of the time of heating.

The fraction amounts of the soluble extracts prepared at 450° C shown in figure 5 are almost time independent. This figure is broken into two sections for clarity. There is a slight decrease of cyclohexane-insoluble fractions and a slight increase of hydrocarbon fractions. This is probably due to the fact that as the reaction time increases at 450° C, the cyclohexane-insoluble fractions, presumably with high-molecular-weight, start to degrade to hydrocarbons. These changes are not drastic. It can be observed that the relative amounts of the fractions of the soluble extracts are not affected significantly by reaction time at 450° C.

Comparison with shale oils

Because there is some indication that the CO-H₂O reaction with oil shale may have some advantages as a process reaction over other methods of thermal degradation, it is desirable to compare the soluble extracts obtained by the CO-H₂O reaction with shale oils. This comparison is shown in table 2. The soluble

TABLE 2. - Comparison between the soluble extracts from CO-H₂O reaction and shale oils

Sample	Weight-percent of total				
	Acid fractions	Base fractions	Neutral nitrogen fractions	Hydrocarbons	Cyclohexane-insoluble fractions
Soluble extract at 300° C ¹	54.4	12.6	1.4	18.8	12.8
Soluble extract at 375° C ¹	50.3	12.6	1.5	17.7	17.9
Soluble extract at 450° C ¹	24.5	23.2	1.3	38.4	12.6
In situ shale oil (Rock Springs)	16.9	14.4	0.7	58.4	9.6
Gas combustion shale oil	19.9	26.3	2.1	44.6	7.1
150-ton retort shale oil	13.5	20.5	2.1	55.7	8.2

¹ At 1 hr reaction time.

extracts from the 300° to 375° C tests were very polar and contained only about 20 percent hydrocarbons. As the temperature increased above 375° C, more hydrocarbons were produced, presumably because of more thermal cracking. At 450° C the hydrocarbon fractions represented 38.4 percent of the total extract which approximated the amount of hydrocarbons in the three shale oils chosen for this comparison. In general, the three shale oils (in situ shale oil from Site 4, Rock Springs; gas combustion shale oil, and 150-ton retort shale oil) are less polar and contain more hydrocarbons than the soluble extracts from the 300° to 375° C, CO-H₂O reaction of kerogen. This suggests that the latter products have been subjected to less thermal cracking and less destructive degradation. The soluble extract obtained at 450° C contains higher percentage of hydrocarbon fractions somewhat similar to the gas combustion shale oil and should be a suitable feedstock for further hydrocracking techniques.

Distribution of *n*-alkane fractions of the extracts and natural bitumen

The carbon-number distribution of the *n*-alkanes is a good indicator of the thermal history of the organic material in Green River oil shale. The natural bitumen and low-temperature thermal degradation products show odd-even predominance (OEP) (12) of the carbon numbers in the C₂₅ to C₃₁ range. Extensive thermal degradation causes a rearrangement of carbon numbers with a drastic decrease in the odd-even predominance for the *n*-alkanes.

Figure 6 shows the *n*-alkane distribution of the soluble extracts obtained at 300°, 350°, 400°, and 450° C for 1 hour reaction time and the *n*-alkane distribution of the benzene-soluble bitumen from a Mahogany zone oil-shale sample (13). The change in distribution from 300° to 450° C indicates that temperature has a strong effect on the carbon-number distribution of *n*-alkanes. At 300° C the *n*-alkane distribution appears to be more like that of natural bitumen where the OEP of the carbon number reaches four in the C₂₉ to C₃₁ area. The *n*-alkane distribution obtained at 300° C may be partly accounted for by the presence of the natural bitumen in the raw oil-shale samples used for the tests. At 450° C the distribution of *n*-alkanes becomes more envelope shaped which is the typical distribution for thermally degraded products. The OEP is about one indicating that there is little or no odd-even predominance. This shows that the soluble extracts prepared at 300° and 350° C for 1 hour have not been subjected to drastic thermal alteration and should be suitable products for constitutional study. Undoubtedly they contain many of the basic structures present in the original kerogen.

CONCLUSION

High recoveries of the various fractions show that this modified separation method works well with the high-molecular-weight and polar extracts from the CO-H₂O reaction of kerogen. The *n*-alkane distribution of the soluble extracts prepared below 350° C shows that the soluble extracts have not been subjected to drastic thermal degradation and will be suitable samples for compositional study. As temperature increases above 375° C, the relative amounts of acid fractions decrease but the base and hydrocarbon fractions increase. This indicates that the increases in the amounts of base and hydrocarbon fractions result from decomposition of the acid fraction above 375° C. The reaction time has no effect on the relative amount of each fraction at constant temperature from 300° to 450° C for 0.25 to 6 hrs, with the exception of hydrocarbons at the highest temperatures where a minor increase in amount is noted.

Increase in temperature of the CO-H₂O reaction from 300° to 450° C results in a change of the relative amount of each fraction. As temperature of the CO-H₂O reaction is increased to 450° C, the soluble extract obtained becomes more like a shale oil and should be a suitable feedstock for further hydrocracking techniques.

REFERENCES

1. Burwell, E. L., H. C. Carpenter, and H. W. Sohns. *Experimental In Situ Retorting of Oil Shale at Rock Springs, Wyo.* BuMines TPR 16, 1969, 8 pp.
2. Dannenberg, R. O., and A. Matzick. *Bureau of Mines Gas-Combustion Retort for Oil Shale, A Study of the Effects of Process Variables.* BuMines RI 5545, 1960, 73 pp.
3. Harak, A. E., L. Dockter, and H. C. Carpenter. *Some Results from the Operation of a 150-ton Oil-Shale Retort.* BuMines TPR 30, 1971, 14 pp.
4. Robinson, W. E., and J. J. Cummins. *An Oil-Shale Conversion Process Using Carbon Monoxide and Water.* E.R.D.A. TPR 75/1, 1975, 14 pp.
5. Cummins, J. J., and W. E. Robinson. *Thermal Conversion of Oil-Shale Kerogen in the Presence of Carbon Monoxide and Water.* This Symposium.
6. Robinson, W. E., and J. J. Cummins. *Composition of Low-Temperature Thermal Extracts from Colorado Oil Shale.* J. of Chem. and Eng. Data, v. 5, 1960, p. 74.
7. Anders, D. E., and W. E. Robinson. *Cycloalkane Constituents of the Bitumen from Green River Shale.* *Geochim. Cosmochim. Acta*, v. 35, 1971, p. 661.
8. Anders, D. E., F. G. Doolittle, and W. E. Robinson. *Polar Constituents Isolated from Green River Oil Shale.* *Geochim. Cosmochim. Acta*, v. 39, 1975, p. 1423.
9. Munday, W. A., and A. Eaves. *Analytical Applications for Ion Exchange Resins in the Petroleum Industry.* *World Petrol. Cong. Proc.* 5th N. Y., Sect. V., Paper 9, 1959, p. 103.
10. Jewell, D. M., J. H. Weber, J. W. Bunger, H. Plancher, and D. R. Latham. *Ion Exchange, Coordination and Adsorption Chromatographic Separation of Heavy End Petroleum Distillates.* *Anal. Chem.*, v. 44, 1972, p. 1391.
11. O'Conner, J. G., F. H. Burow, and M. S. Norris. *Determination of Normal Paraffins in C₂₀ to C₃₂ Paraffin Waxes by Molecular Sieve Adsorption.* *Anal. Chem.* v. 34, 1962, p. 382.
12. Scalan, R. S., and J. E. Smith. *An Improved Measure of the Odd-Even Predominance in the Normal Alkanes of Sediment Extracts and Petroleum.* *Geochim. Cosmochim. Acta*, v. 34, 1970, p. 611.
13. Cummins, J. J., and W. E. Robinson. *Normal and Isoprenoid Hydrocarbons Isolated from Oil-Shale Bitumen.* *J. Chem. Eng. Data*, v. 9, 1964, p. 304.

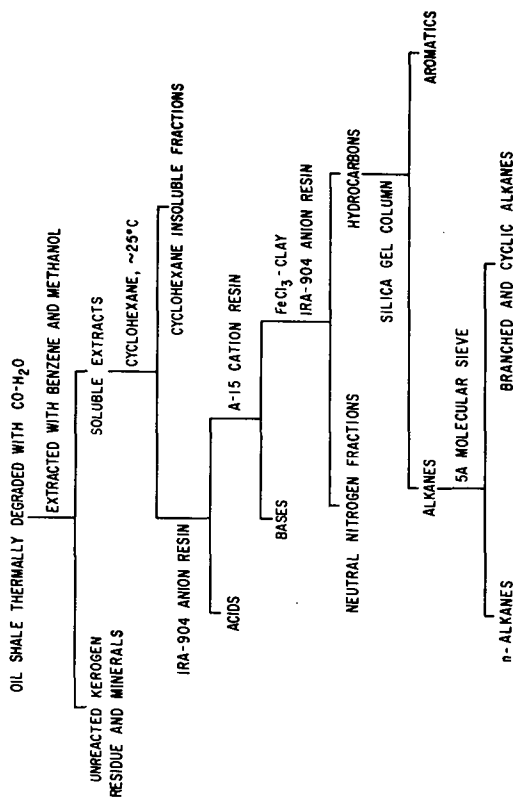


FIGURE 1.- FRACTIONATION SCHEME FOR THE SOLUBLE EXTRACTS FROM
CO-H₂O REACTION.

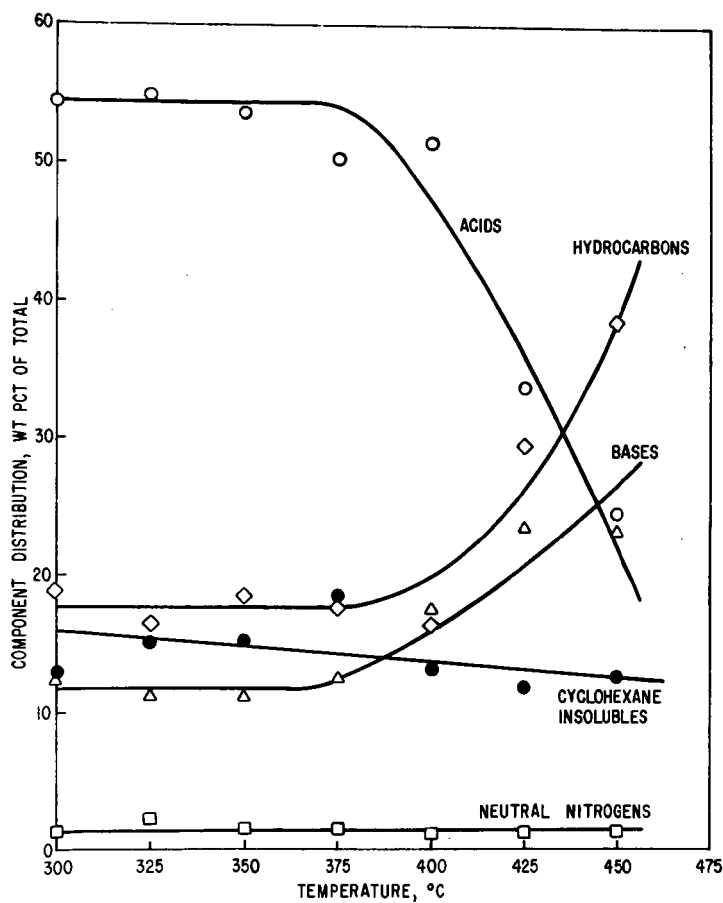


FIGURE 2.-RELATIONSHIP OF FRACTION AMOUNTS TO TEMPERATURE FOR ONE HOUR REACTION TIME.

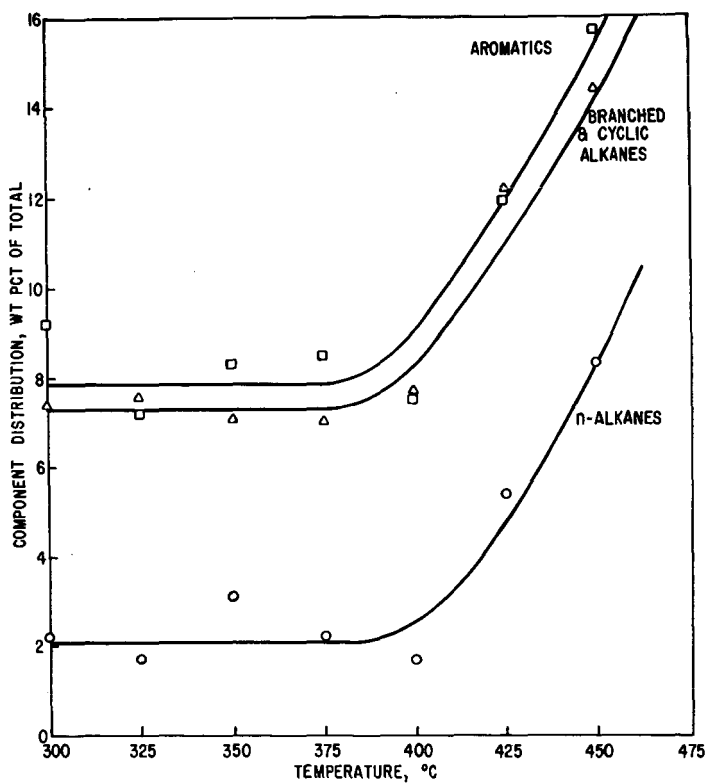


FIGURE 3.-RELATIONSHIP OF HYDROCARBONS TO TEMPERATURE
FOR ONE HOUR REACTION TIME.

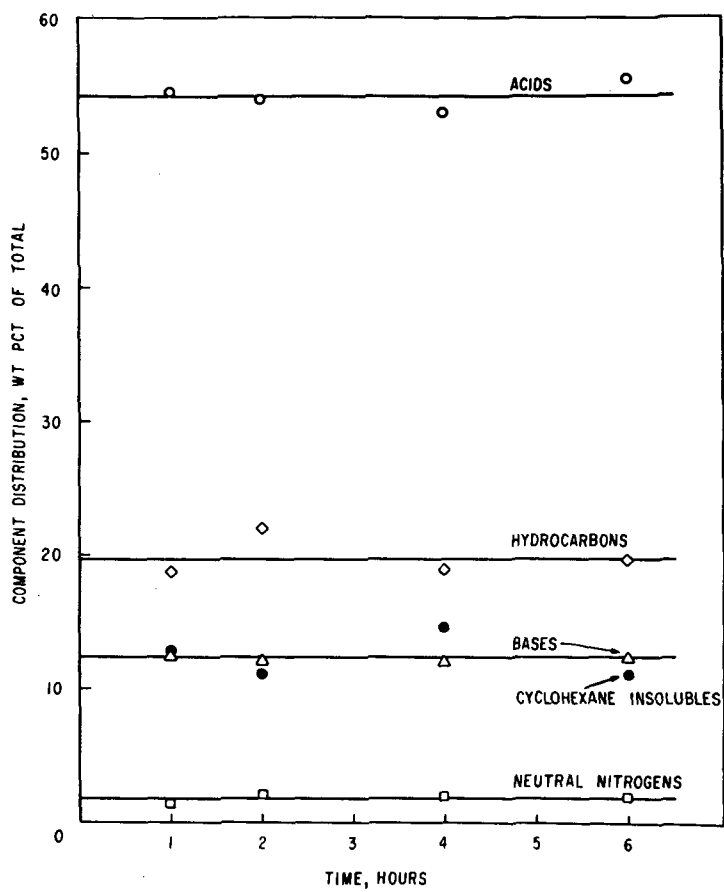


FIGURE 4.-RELATIONSHIP OF FRACTION AMOUNTS TO REACTION TIME AT 300°C.

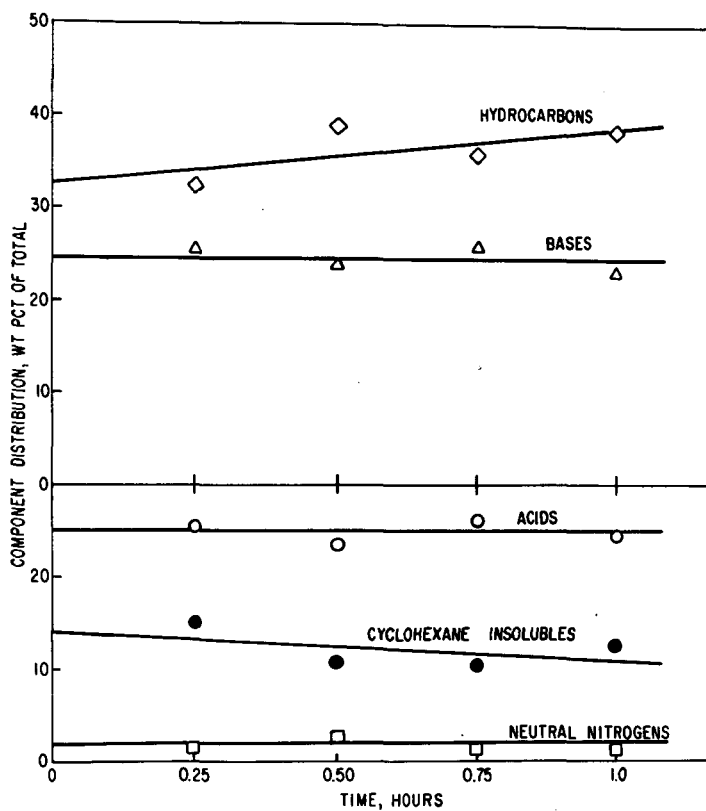


FIGURE 5.- RELATIONSHIP OF FRACTION AMOUNTS TO REACTION TIME AT 450 °C.

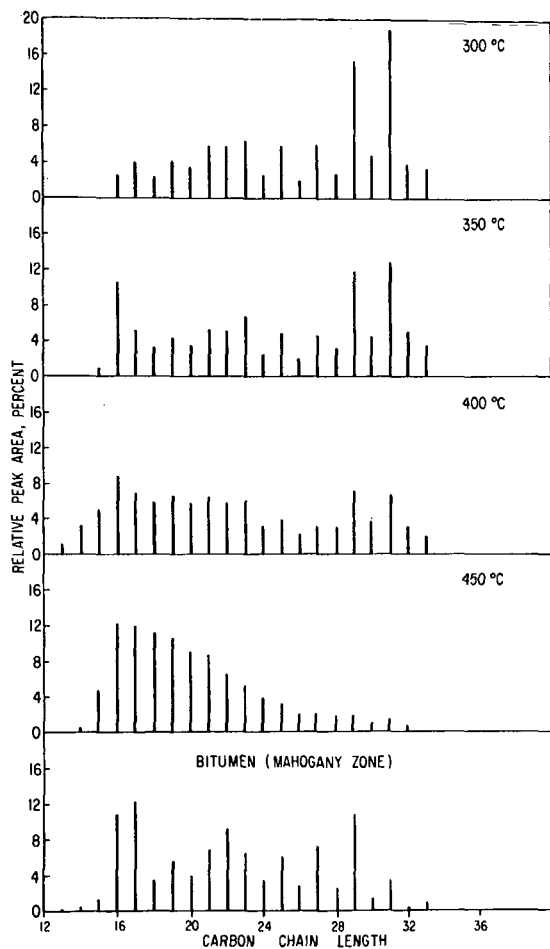


FIGURE 6.-DISTRIBUTION OF n-ALKANE FRACTIONS OF THE EXTRACTS AND NATURAL BITUMEN.

PYROLYSIS OF UTAH TAR SANDS--PRODUCTS AND KINETICS

R. V. Barbour, S. M. Dorrence, T. L. Vollmer, and J. D. Harris

Laramie Energy Research Center
Energy Research and Development Administration
P. O. Box 3395, University Station
Laramie, Wyo. 82070

INTRODUCTION

Bitumen-impregnated sandstone, or tar sand, represents an enormous world hydrocarbon source, estimated at over one trillion barrels of oil in place. Although the vast majority of this resource is found in the deposits of western Canada and eastern Venezuela, sizeable portions, currently estimated at 30 billion barrels, reside in the continental U.S.; most of this is located in the state of Utah. A small percentage of this world resource is recoverable by known or projected surface mining methods. The bulk can be recovered only by the development of effective and economical in situ recovery methods which allow the recovery of oil values from in-place deposits without the need of extensive mining operations.

Many methods have been proposed for the in situ recovery of unaltered and/or modified bitumen from tar sand deposits (1). Of these, in situ thermal methods possess many attractive features over other proposed in situ recovery methods. In general, thermal recovery refers to the process of in-place heating of the tar sand, usually through combustion of a portion of the tar sand bitumen, allowing recovery of bitumen as a now-mobile tar or as a cracked bitumen product. It is this process of in-place thermal cracking that is of particular interest to us and which prompted this study of the pyrolytic behavior of tar sands as a part of the Laramie Energy Research Center's overall effort in the development of in situ tar sand recovery technology.

Studies of the thermal cracking of petroleum materials have been extensive (2); however, studies directed at the thermal cracking of tar sand bitumen have been only sparsely reported (3). Most of these latter studies investigated the cracking properties of bitumen after it had been separated from the accompanying sand. Conclusions drawn from pyrolysis studies of separated bitumen may not be valid when applied to pyrolysis of bitumen that remains in contact with mineral material as in the natural state. Rather, one would expect to find differences in the product yields and observed kinetics from pyrolysis of neat bitumen vs pyrolysis of bitumen-sand because of such system differences as thermal conductivity, product escape paths, surface area to bulk volume ratios, and mineral catalysis.

This paper reports a laboratory study of the thermal cracking behavior of four Utah tar sands and a Canadian tar sand in which no prior separation of bitumen from the mineral material has taken place. This thermal cracking behavior has been investigated in terms of the products formed, i.e., liquid products, gaseous products, and char. The kinetics of the overall pyrolysis reaction has been suggested.

EXPERIMENTAL

Tar Sand Samples

Representative samples of the parent tar sand material listed below were frozen in liquid nitrogen and crushed to pass a 14-mesh (U.S. series No. 16) screen. This sized material was used in all pyrolysis experiments.

Northwest Asphalt Ridge tar sand from a core of the 295- to 305-ft zone at NW1/4 NE1/4 SE1/4 sec. 23, T. 4 S., R. 20 E., Uintah Co., Utah;

P.R. Spring tar sand outcrop material from NE sec. 32, T. 15-1/2 S., R. 23 E., Uintah Co., Utah;

Tar Sand Triangle tar sand from a core of the 1180- to 1200-ft zone at SW1/4 SE1/4, sec. 22, T. 30 S., R. 16 E., Wayne Co., Utah;

Sunnyside tar sand from a core of the 421- to 438-ft zone at NE1/4 SW1/4, sec. 31, T. 13 S., R. 15 E., Carbon Co., Utah;

Athabasca tar sand from a pit-run sample supplied by the Great Canadian Oil Sands Co., Alberta, Canada.

Pyrolysis Experiments

Product Collection Experiments. - Pyrolysis experiments were performed using a horizontal tube furnace, equipped with an electronic temperature controller, to heat a 250-mm section of pyrex pyrolysis tube (20-mm i.d.) containing charges of 140 to 170 g of tar sand. Heat-up rates were such that the desired temperatures (500, 750, and 1000°F) were reached within 15 min. All experiments were conducted under a nitrogen atmosphere flowing at 0.5 l/min (uncorr.) corresponding to a flux rate of 230 scf/ft²/hr. The nitrogen was preheated to approximate final furnace temperature. Major liquid products were collected in two receivers; the first was an air condenser, the second was an ice-cooled trap. In all runs the majority of products were collected at the air condenser; only trace amounts of very light products were collected in the ice trap. All oil products were combined, sealed, and stored under nitrogen at 5°F for later analysis. Gas samples were collected in 100-ml gas sampling bottles downstream of the ice trap.

Product Analysis. - Oil products were analyzed for elemental composition, specific gravity (60°F/60°F), and Ramsbottom carbon residue. Oil products were analyzed for saturates, aromatics, polar aromatics, and asphaltenes (SAPA analysis). This involves deasphalting with n-pentane and chromatography of the resulting maltenes on a water-jacketed column containing 200 g of grade 62 silica gel (Grace) made up in n-pentane (loading ratio 100:1); successive elution with n-pentane, benzene, and benzene/methanol (9:1) separated the maltenes into saturate, aromatic, and polar aromatic fractions, respectively. Simulated distillation analyses of the oil products were obtained by the internal standard method of Poulson, et al. (4). Gas analyses were obtained using a CEC-21-620 mass spectrometer.

Kinetic Experiments

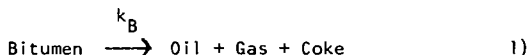
Kinetic data were obtained using the same tube furnace with its preheated, inert sweep-gas arrangement (flow rate 0.2 l/min, uncorr., flux rate 92 scf/ft²/hr); however, the pyrolysis tube was modified to allow the ready insertion and removal of small ceramic combustion boats containing the tar sand samples. Prior to a run, the furnace temperature was adjusted to the desired temperature, using a thermocouple contained within a boat filled with 6.5 g of clean sand. Once thermally established, the furnace showed a maximum drift of + 2°F over a 3-hr period. Runs were performed by inserting into the hot zone of the pyrolysis tube an accurately weighed sample of approximately 6.5 g of tar sand contained in a ceramic boat. The boat was placed in the hot zone for the desired time period, drawn to the cold end of the tube, and cooled for 2 min under a nitrogen atmosphere. The boat was then removed, rapidly cooled in powdered dry ice, and stored in a dessicator. Upon returning to ambient temperature, the boat was weighed to record the total volatile loss and placed in a glass extraction thimble containing

a fine fritted disc overlaid with a glass-fiber pad. The thimble was weighed and extracted exhaustively with hot benzene/ethanol, 3/1, in a modified Soxhlet extractor (5). After extraction, the thimble and boat were dried in vacuo at 175°F and reweighed; the difference in initial and final weights was taken as the weight of extractable bitumen remaining on the tar sand.

RESULTS AND DISCUSSION

Pyrolysis Products

Although the chemical processes occurring in tar sands bitumen at elevated temperatures are most likely numerous and complex, the overall conversion can be viewed simply as given in Equation 1:



that is, that bitumen upon heating is converted into three products; oil, gas, and coke. To be useful, this view requires a definition of terms. Bitumen is the total native organic portion of tar sand that is soluble in boiling benzene/ethanol; oil is the sum of all liquid products, condensable at 0°C, that volatilizes from the heated tar sand material; gas is the total volatile product, not condensable at 0°C, that is evolved from the heated tar sand; and coke is the benzene/ethanol-insoluble, nonvolatile carbonaceous material remaining on the sand after bitumen decomposition. Implicit in this definition is the realization that native bitumen may contain material defined as oil and gas before pyrolysis.

Pyrolysis experiments were performed on the four Utah and one Canadian tar sands at 500, 750, and 1000°F under a flowing, inert atmosphere. Analyses of starting bitumens, oil recovery, and routine product inspections of the pyrolysis oils are given in Table 1. Several general trends are apparent in these data. Oil recovery increased with increasing temperature, although the majority of this increase occurred as the temperature was increased through the lower pyrolysis temperatures, i.e., 500 to 750°F. At temperatures from 750 to 1000°F, oil recoveries increased only moderately with the increased temperature. Oil recoveries represent actual oil product collected and do not account for the possible loss of oil due to mist formation. Coke-forming character of the bitumens generally followed their Ramsbottom carbon residue values except for the P.R. Spring sample which showed a very low coking value. Coke values at 500°F are not reported, as the pyrolysis was very incomplete at this temperature leaving large quantities of extractable bitumen and essentially no coke. Elemental analyses of the produced oils indicated that pyrolysis caused little change in the C/H ratio while affecting a reduction in nitrogen and sulfur content. As compared to the parent bitumen, specific gravities of the produced oils decreased throughout the pyrolysis temperature range while Ramsbottom carbon residue values dropped on all produced oils. Pour points of the produced oils were low for the 500°F pyrolysis and increased for the 750 and 1000°F oils. Pour points for the Asphalt Ridge 750 and 1000°F pyrolysis oils were unusually high, perhaps reflecting the presence of heavy hydrocarbons in these oils as further evidenced by their waxy appearance.

The produced oils and the starting bitumens were analyzed by silica gel chromatography to determine their major compositional fractions. They were deasphalted with n-pentane and the resulting maltenes chromatographed on silica gel to give saturates, aromatics, and polar aromatics fractions. The results of this chromatographic analysis (SAPA) are given in Table 2. All produced oils contained a substantially higher saturates content than the parent bitumen and essentially no asphaltenes. As the pyrolysis temperature is increased there is a clear shift in the SAPA fractions toward the more polar constituents. At lower temperatures, the polar constituents, both native and cracked products, probably lack sufficient

volatility to escape the bitumen, and remain behind to be further cracked until they are sufficiently volatile to escape. As the pyrolysis temperature is increased, these polar materials are capable of vaporizing from the bitumen in a molecular state retaining their polar character.

Simulated distillation analysis of the tar sand bitumens and of the produced pyrolysis oils from these bitumens is given in Table 3. The data are reported as the weight percent of the sample distilling within 100° ranges from 300° to 1000°F. Material distilling above 1000°F is classified as residuum. Because the sample oils were analyzed in benzene solution, this analysis did not allow accurate determination of materials distilling between 0° and 300°F; however, qualitative inspection of the corresponding GC traces indicated that the quantity of material distilling in this range is small, estimated to be 0 to 2 wt percent.

Although minor differences may be observed among the distilling range characteristics of the various produced oils reported in Table 3, more significant are the similarities. All tar sands, regardless of pyrolysis temperature, produced only small amounts, usually 10 percent or less of oil boiling under 500°F. However, the distillation curves for all produced oils showed the same trend toward higher proportions of the product distilling at higher temperatures as the pyrolysis temperature increased. An important observation can be made considering the distillation data and the oil recovery data (Table 3 and Table 1). At a pyrolysis temperature of 750°F, oil recovery is high, approaching that attainable at 1000°F, while the distillation character of the 750°F product oil indicates this material is considerably lighter than that produced at 1000°F. That is, a lower boiling product oil can be generated at the lower pyrolysis temperature with a moderate reduction in oil recovery or increase in coke formation.

Results of the analyses of the gases produced during the pyrolysis are given in Table 4. Although it was not possible in these experiments to obtain an accurate material balance on the gases produced, due to misting of the oil, incomplete bitumen conversion, and dilution with inert gas, the reported values represent the composition of the gas (nitrogen-free) averaged over the entire pyrolysis. The produced gas was predominantly composed of hydrogen and methane, with C₂ and C₄ hydrocarbons being next most abundant. Also produced were small quantities of other gases such as carbon dioxide, carbon monoxide, carbonyl sulfide, and hydrocarbons above C₅. Production of hydrogen sulfide was high for Athabasca tar sands, which contains high-sulfur bitumen, but low for Tar Sand Triangle tar sands, which also contains high-sulfur bitumen. This difference suggests that the sulfur in these tar sands is incorporated into chemically different species, thereby significantly affecting the production of hydrogen sulfide from the two bitumens.

Pyrolysis Kinetics

The overall reaction depicted in Equation 1 defines the pyrolysis process as one involving the conversion of bitumen (reactants) to oil, gas, and coke (products) by the application of heat to a tar sand. Many chemical and physical processes contribute to this conversion and to the observed loss of bitumen, each process being governed by its own concentration and rate dependencies. The overall rate constant, k_b , describing this process is therefore a net rate constant, being the summation of all contributing processes. Although the pyrolysis is complex, two basic steps encompass the net conversion: 1) cracking of low-volatility organics to yield products of higher volatility and coke and 2) vaporization of the native and produced oils allowing their escape from the bitumen-sand matrix. It is not possible from the present study to separate these steps to study their kinetics independently thereby obtaining true rate data in the fundamental sense. Rather our approach has been to study the rate of loss of bitumen in a process sense

where the determined rate data reflect not only cracking and product volatilization rates, but also other contributing experimental variables such as bitumen film thickness, sample porosity, inert atmosphere sweep rates, and others.

Analysis of our data to determine reaction order indicated that the best straight-line fit was obtained by application of a first-order treatment to the loss of bitumen as a function of time. The first-order rate equation expressing this relation is given in Equation 2 (6, 7):

$$k_B = \frac{1}{t} \ln [a_0/(a_0-x)] \quad 2)$$

where: t = reaction time

a_0 = initial quantity of bitumen

x = quantity of bitumen disappearing in time (t)

Figure 1 is the plot of data obtained for the pyrolysis of the Asphalt Ridge tar sand at four temperatures plotting time (t) vs $\ln [a_0/(a_0-x)]$. These plots show that temperatures of 800, 900, and 1000°F produce good straight lines after the initial heat-up period, whereas the 700°F run resulted in a nonlinear plot throughout the entire time span. Analysis of the data for pyrolysis of the other tar sand samples gave plots of very similar character to Figure 1 with only minor differences in line position at the specific pyrolysis temperatures.

Rate constants, k_B , for each of these pyrolyses were determined from the slope of plots of Equation 2, using the best fitting linear regression line. Statistical coefficients of determination for these regression lines were 0.96-0.99 for the 800, 900, and 1000°F runs, indicating a good to excellent straight line fit, while that for the 700°F runs were 0.90 to 0.92, indicating nonlinearity and/or significant curvature in the data points.

The rate constants calculated for the five tar sands are given in Table 5. The pyrolysis rates increased by a factor of about 200 as pyrolysis temperatures increased from 700° to 1000°F. Bitumen half-life values, $t_{1/2}$, were calculated from the observed rate constants and are given in Table 5. These $t_{1/2}$ values ranged from 5800 to 8500 sec at 700°F to 37 to 63 sec at 1000°F.

An Arrhenius (6) plot ($1/T$ vs $\ln k_B$) for the P. R. Spring tar sand pyrolysis is shown in Figure 2. Similar plots for the other four sets of rate constants allowed the calculation of apparent Arrhenius activation energies, given in Table 5, for the pyrolysis of each tar sand. Straight line correlations were obtained for each Arrhenius plot, with coefficients of determination of 0.94 to 0.99. The apparent Arrhenius activation energies for the pyrolysis of the five tar sands were nearly equal, which suggests that the pyrolysis steps contributing to the rate-determining process are similar in each case; and although the rate constants at a given temperature vary from tar sand to tar sand, the effect of an increase in temperature on the reaction rate is the same in each.

SUMMARY

The general pyrolytic behavior of the Utah tar sands is remarkably similar deposit to deposit and follows the trends in pyrolysis characteristics of the Athabasca tar sands. Common to all tar sands investigated is the production by pyrolysis of an upgraded oil, relative to the native bitumen, in terms of elemental composition, SAPA composition, distillate content, carbon residue, and specific

gravity. The rate constants for bitumen pyrolysis, measured as the rate of loss of extractable bitumen, were found to be first order in bitumen and to range from $1 \times 10^{-4} \text{ sec}^{-1}$ at 700°F to $200 \times 10^{-4} \text{ sec}^{-1}$ at 1000°F . Each tar sand pyrolysis exhibited an apparent Arrhenius activation energy in the range of 33 to 35 kcal, suggesting a similarity between the tar sands in their principle pyrolysis processes.

REFERENCES

1. F. W. Camp, "The Tar Sands of Alberta, Canada," 2nd ed., Cameron Engineers, Denver, Colo., 1974.
2. S. W. Martin and L. E. Wills in "Advances in Petroleum Chemistry and Refining," Vol. 2, K. A. Kobe and J. J. McKetta, Ed., Interscience Publishers, Inc., New York, 1959.
3. J. G. Speight, Fuel, 49, 134 (1970).
4. R. E. Poulson, H. B. Jensen, J. J. Duvall, F. L. Harris, and J. R. Morandi, Proc., "Analysis Instrumentation," 10, Instrument Society of America, 193 (1972).
5. H. Plancher, E. L. Green, and J. C. Petersen, Proc. Assoc. Asphalt Paving Technol., 45 (1976).
6. K. J. Laidler, "Chemical Kinetics," 2nd ed., Chap. 1-3, McGraw-Hill Book Co., New York, 1965.
7. E. A. Moelwyn-Hughes, "Physical Chemistry," 2nd ed., Pergamon Press, New York, 1961, pp. 1114-1128.

TABLE 1. - Analysis of tar sand bitumens and pyrolysis oils

Tar sand	Pyrolysis temp, °F	Oil recovery, wt. % of starting bitumen		C	H	N	S	C/H	Ramsbottom carbon	Specific gravity, 60/60	Pour points, °F
		wt. % of bitumen	Coke formed, wt. % of bitumen								
Asphalt Ridge	Bitumen			86.74	13.04	1.06	0.77	0.55	7.76	0.963	95
	500	17	--	86.26	12.08	0.31	0.41	0.59	nil	0.923	-40
	750	72	7	85.88	11.98	0.56	0.36	0.60	nil	0.906	115
P.R. Spring	1000	86	7	85.96	11.86	0.76	0.40	0.60	0.90	0.932	160
	Bitumen			86.51	10.77	1.31	0.56	0.67	12.49	1.006	115
	500	19	--	86.34	11.75	0.33	0.46	0.61	nil	0.936	-5
Tar Sand Triangle	750	75	4	86.05	11.68	0.87	0.41	0.61	1.12	0.952	40
	1000	84	2	85.39	11.20	0.96	0.54	0.63	3.78	0.953	40
Sunnyside	Bitumen			84.62	10.41	0.55	4.49	0.68	20.26	1.020	95
	500	20	--	85.13	12.04	0.06	2.55	0.59	0.85	0.951	5
	750	45	26	85.63	11.65	0.15	2.82	0.61	1.40	0.935	30
Athabasca	1000	56	25	85.85	10.97	0.25	3.09	0.65	3.38	0.953	25
	Bitumen			84.05	11.58	0.95	0.44	0.60	15.17	0.980	115
	500	14	--	86.72	12.19	0.29	0.32	0.59	nil	0.931	-30
Athabasca	750	55	16	86.65	12.05	0.71	0.18	0.60	1.94	0.958	15
	1000	68	12	86.67	11.94	0.66	0.31	0.60	3.46	0.964	60
Athabasca	Bitumen			81.66	11.23	0.44	4.71	0.61	12.63	1.006	70
	500	23	--	84.67	11.68	0.06	2.28	0.60	1.60	0.919	-50
	750	59	12	84.18	11.21	0.14	3.09	0.63	1.81	0.927	-15
Athabasca	1000	75	12	84.12	11.09	0.20	3.48	0.63	3.38	0.945	-15

TABLE 2. - SAPA analysis of tar sand bitumens and pyrolysis oils

Tar sand	Pyrolysis temp, °F	Saturates, wt. %	Aromatics, wt. %	Polar aromatics, wt. %	Asphaltenes, wt. %
Asphalt Ridge	Bitumen	48	18	27	6
	500	90	6	4	0
	750	84	11	6	0
	1000	77	13	9	1
P.R. Spring	Bitumen	29	25	35	11
	500	82	8	10	0
	750	74	16	12	0
	1000	65	18	13	1
Tar Sand Triangle	Bitumen	42	22	10	26
	500	87	10	3	0
	750	91	7	2	0
	1000	70	25	5	0
Sunnyside	Bitumen	40	15	25	20
	500	83	7	10	0
	750	73	16	11	0
	1000	65	22	13	1
Athabasca	Bitumen	43	25	14	17
	500	95	3	2	0
	750	91	4	2	0
	1000	84	10	6	0

TABLE 3. - Simulated distillation analysis of tar sand bitumens and pyrolysis oils

Tar sand	Pyrolysis temp, °F	Wt. percent distillable in the range: °F									
		300-400	400-500	500-600	600-700	700-800	800-900	900-1000	Resid.		
Asphalt Ridge	Bitumen	<1	2	3	4	6	12	16	56		
	500	3	10	18	22	27	17	1	2		
	750	2	6	9	11	15	24	22	11		
P.R. Spring	1000	4	7	9	10	13	19	19	19		
	Bitumen	<1	1	3	5	6	9	9	67		
	500	2	12	23	30	22	7	1	2		
Tar Sand Triangle	750	2	6	9	12	17	23	20	12		
	1000	2	5	8	12	14	18	14	27		
	Bitumen	<1	1	5	8	9	10	8	60		
Sunnyside	500	<1	5	16	22	24	23	8	2		
	750	2	5	13	17	20	20	13	9		
	1000	3	4	11	14	17	18	15	18		
Athabasca	Bitumen	<1	<1	3	5	6	10	7	68		
	500	1	8	20	31	21	13	2	4		
	750	2	6	9	14	18	27	17	7		
Athabasca	1000	3	5	7	12	15	22	16	20		
	Bitumen	<1	2	5	8	10	10	10	55		
	500	7	10	17	31	27	3	1	4		
Athabasca	750	4	8	19	23	25	13	2	6		
	1000	6	8	12	17	17	17	11	12		

TABLE 4. - Gas analysis

Tar sand	Pyrolysis	Composition, wt. %, nitrogen-free ^{a/}							
	temp., °F	H ₂	CH ₄	C ₂	C ₃	C ₄	C ₅	H ₂ S	Other
Asphalt Ridge	500	36	15	18	2	1	0	0	28
	750	25	25	9	6	18	3	7	7
	1000	30	21	8	6	12	6	6	11
P.R. Spring	500	25	13	13	4	2	0	27	16
	750	27	24	9	6	14	6	2	12
	1000	28	30	8	4	6	4	1	19
Tar Sand Triangle	500	5	38	24	7	0	0	0	26
	750	11	23	14	10	21	10	9	2
	1000	26	47	12	3	5	1	3	3
Sunnyside	500	30	23	21	0	0	0	0	26
	750	36	25	13	6	16	1	1	2
	1000	56	31	4	1	4	1	0	3
Athabasca	500	19	8	14	1	1	0	14	43
	750	10	22	12	9	13	8	21	5
	1000	19	36	11	8	7	4	12	3

^{a/} Nitrogen averaged 90 to 99% of total gas

TABLE 5. - Rate constants and apparent Arrhenius activation energies
for tar sand pyrolysis

Tar sand	Pyrolysis temp., °F	$k_B \times 10^4, \text{sec}^{-1}$	$t_{1/2}, \text{sec}$	Apparent E_a, kcal	Arrhenius constant
Asphalt	700	0.81	8500		
Ridge	800	4.5	1500	33	16.5
	900	89	78		
	1000	110	63		
P.R. Spring	700	1.1	6300	33	16.5
	800	6.7	1000		
	900	64	110		
	1000	180	38		
Tar Sand	700	1.2	5800	33	16.5
Triangle	800	7.2	960		
	900	52	130		
	1000	150	46		
Sunnyside	700	0.88	7800	35	17.9
	800	5.1	1400		
	900	99	70		
	1000	160	43		
Athabasca	700	1.1	6300	33	16.4
	800	7.1	970		
	900	59	120		
	1000	190	37		

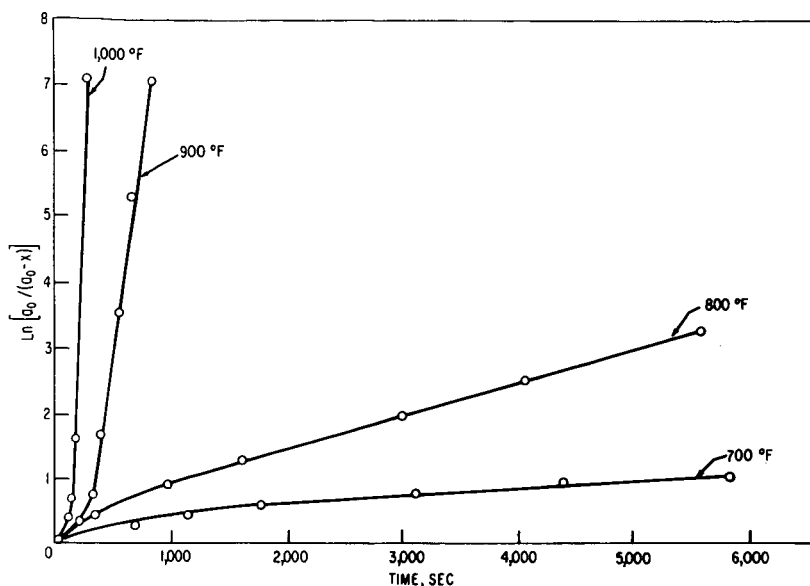


FIGURE 1.- FIRST-ORDER KINETIC PLOT FOR ASPHALT RIDGE TAR SAND PYROLYSIS.

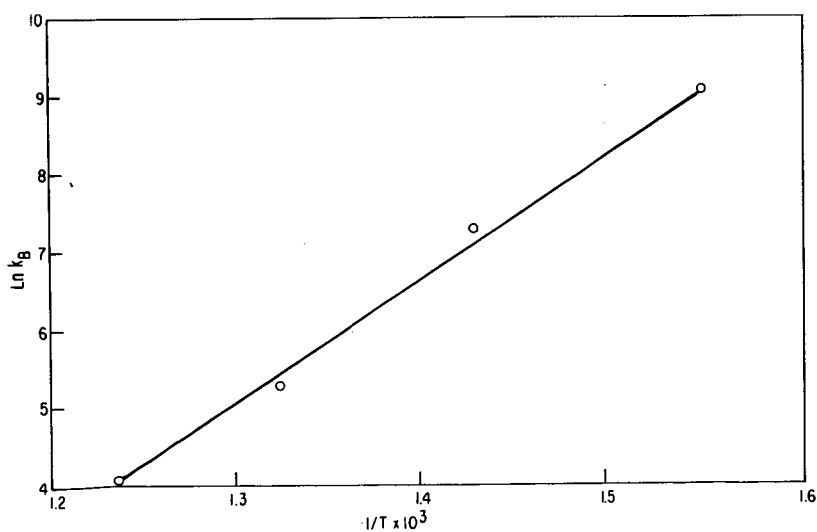


FIGURE 2.- ARRHENIUS PLOT FOR P.R. SPRING TAR SAND PYROLYSIS.

STUDIES OF SOLUBLE ORGANICS IN SIMULATED IN SITU OIL-SHALE RETORT WATER
BY ELECTRON IMPACT AND CHEMICAL IONIZATION FROM A COMBINED GAS CHROMATOGRAPH-
MASS SPECTROMETER SYSTEM

C. S. Wen and T. F. Yen

University of Southern California
Los Angeles, California 90007

J. B. Knight

Finnigan Corporation
Sunnyvale, California 94086

R. E. Poulson
E.R.D.A., Laramie Energy Research Center
Laramie, Wyoming 82070

INTRODUCTION

Research on the development of in-situ oil shale processes has recently accelerated into a nation-wide program. This technique of in-place underground retorting of oil shale deposits virtually eliminates the environmental problems posed by the conventional mining of oil shale and the disposal of resulting spent materials. However, the in-situ process also presents a serious disposal problem, namely the co-production of vast amounts of process water along with the oil shale.

The composition and properties of the retort water produced usually depends upon the technique and operating conditions employed in the retorting process as well as the location and nature of the oil shale. Generally, the retort water is loaded with considerable quantities of soluble organic and inorganic materials. The presence of carboxylic acids (from acetic to caprylic acid) has been noted earlier by Cook (1) in TOSCO oil shale retort water; but, the presence of phenols in retort water from the Green River Oil Shales has been doubted for several years (2). In addition to these acidic organic compounds, substituted benzenes and nitrogen bases are present since these too, exist abundantly in shale oils (3,4). Untreated retort water effluents contain varying quantities of organics which could seriously impair the quality of ground water. This would pose a health hazard to humans due to the presence of certain phenolic and toxic components in the retort water.

A number of processes have been suggested for retort water treatment. The objective of this work is aimed not at a discussion of the purification of organic components present in retort water; but rather to provide an identification of the organic compounds found in the benzene soluble fraction of retort water, including carboxylic acids, phenols, nitrogen bases, and substituted benzenes, from gas chromatography-mass spectrometry (GC-MS) data.

EXPERIMENTAL

A. Sampling and Extraction Procedures

The retort water samples formed from Green River Oil Shale of either the Utah or Colorado region were all collected from the Laramie 10-ton simulated in-situ retorting process. A homogeneous representative sample of retort water was obtained by filtration through a Nalge 0.2 micron filter unit for removal of oily particulate prior to sampling. To avoid biological and physical degradative effects, all samples were kept under refrigeration. A 200 ml aliquot of retort water was taken and poured into a 500 ml lyophilizing container. This was then allowed to freeze-dry at a low temperature. The extraction method chosen was Soxhlet extraction using benzene as the solvent over an 8-10 hour period. The extracts were then adjusted to the desired concentration for GC-MS injection by evaporating the benzene solvent with a purified

nitrogen stream. A portion of the extract was methylated by BF_3 esterification in methanol, followed by subsequent extraction of the ester by heptane for analysis.

B. Gas Chromatograph-Mass Spectrometer Analysis

Gas chromatography is often employed in the analysis of complex mixtures of organic compounds. Through gas chromatography, it is possible to separate an organic mixture into its various fractions on the basis of volatility. Each fraction will be composed of constituents having similar boiling points, with the lower boiling compounds being vaporized and recorded by the detector before the higher boiling components. The advantages of the gas chromatograph lie in its speed and convenience of operation as well as the relatively few instruments required as basic apparatus, its high degree of sensitivity in determining the composition of the gas effluent, and its capability of producing both qualitative and quantitative data.

When a mass spectrometer is attached to a gas chromatograph, even more specific results are obtained. The combination of a gas chromatograph with a mass spectrometer (with the aid of a computer) allows the detection of two or more components belonging to a single gas chromatograph peak. GC-MS works on the principle of either chemical or electron impact ionization of organic compounds. Chemical ionization (CI)-mass spectrometry involves a much milder ionization process than electron impact (EI) and thus improves the chances of detecting molecular ions for labile compounds. The mass spectral data of an unknown compound can be compared against reference EI or CI spectra to aid in the identification of the unknown compound. However, EI mass spectrometry cannot be used alone since some molecular ions (M^+) produce weak signals and therefore go undetected. This is especially true of some alcohols, amines, ethers, esters, and other labile molecules. The absence of these molecular ions makes the interpretation of unknown mass spectra extremely difficult if not impossible.

C. Conditions

1. Column: 3/8 OV-17 on 80/100 mesh Gas Chrom Q, 6 ft x 2 mm ID
2. Column temp: 60-250°C programmed at 8°/min
3. Carrier Gas: Helium (methane) at a flow of 18 cc/min
4. Injection temp: 250°C
5. Ion source pressure: 1.0×10^{-5} torr (1.0 torr)
6. Electron energy: 70 eV (120 eV)
7. Filament current: 500 microamps
8. Ion source temp: 180°C
9. Scan speed: 2.5 sec
10. Mass Range: 34-350 (60-350)
11. GC-MS Interface temp: 260°C

(The CI conditions, when different from EI, are in parenthesis.)

The GC-MS interface for EI analysis was a single stage glass jet separator. For CI analysis, the GC column was connected directly to MS ion source via an isolation valve. The mass spectrometer used was a Finnigan Model 3300 interfaced to a Finnigan Model 9500 gas chromatograph. Data collection and output was done using a Finnigan Model 6000 GC-MS data system.

RESULTS AND DISCUSSION

The examination of the methylated benzene-soluble fraction shows that the normal carboxylic acids do exist in retort water; however, these carboxylic acids represent only the minor portion in the methylated fraction. As shown in Figure 1, there are two series of these acids presented. One has carbon numbers below C_{11} (undecanoic acid) which could come directly from the pyrolysis of retorting. Another series have carbon numbers above C_{16} (palmitic acid) which has been found in the original oil shale sediment (5). The even normal carboxylic acids are dominant in this series. However, the C_{12} to C_{15} acids are entirely absent. An example of the search for methyl palmitate (C_{16}) is shown in Figure 2 in which a weak peak of m/e 270 in EI (electron impact) spectrum can be enlarged and identified certainly by the chemical ionization (CI) mass spectrometer.

Phenols from shale oil have been identified by various investigators (3,6), but their presence in the Green River retort water was doubtful (2). Figure 3a represents the gas chromatographic peak of m/e 94. It was confirmed by the mass spectrum of the odd-electron $66(M-CO)^+$ peak accompanied by $65(M-CHO)^+$ to recognize the phenol functionality (7) in the retort water (Figure 3b). Additionally, cresols have also been found in retort waters. The mass spectrum of the methylated fraction also indicate a trace amount of long-chain alkanes. Their presence is not surprising since they exist abundantly in shale oils.

Compounds of the C_nH_{2n-6} substituted benzene series consist of xylenes (C_8H_{10}) and ethyltoluene (C_9H_{12}). The most prominent M-15 ion peak in the spectra of these two types of compounds indicates a methyl substituent with the benzene ring. In addition to the above substituted benzene series, biphenyl ($C_{12}H_{10}$) has also been identified in the benzene soluble fraction of retort water. Figure 4 represents the identification of the parent molecular ion peak M^+ 154 and the isolated GC peak of biphenyl.

Two types of oxygen-containing nitrogenous compounds, $C_nH_{2n-5}NO_2$ and $C_nH_{2n-3}NO_2$, have been identified from benzene extracts of retort waters. Recently, in a comprehensive study on polar constituents of Green River oil shale by Anders et al. (8), $C_nH_{2n-5}NO_2$ has been listed among the identified nitrogen compounds. Figure 5 represents the mass spectrum and possible structures of this compound ($C_7H_9NO_2$). The experimental mass of the fragment ions appearing at nominal masses 53, 67, 81, 96, 106, 110, 111, 121, 124, and M^+ 139 all correspond closely to that reported by Anders et al. (8) in which M-15, M-18, M-28, and M-29 fragment ions indicate a loss of CH_3 , H_2O , CO, and CHO from the parent structure. The mass spectrum of other oxygenated nitrogen compounds, $C_5H_7NO_2$ (n-methylsuccinimide), are shown in Figure 6. These two compounds could be derived partly from the oxidation products after cleaving the amide C-C bond to the C=O group in the original kerogen matrix, and partly from the dehydration of dicarboxylic acids with amines. The organic sulfur compound has also been searched by the chemical ionization mass spectrometer in which the major representative falls into a M+1, mass number of 128. However, not enough information is available to speculate about this sulfur compound.

The above preliminary report constitutes the initial investigation of the organic components in retort waters. The major results of the investigation can be summarized as follows:

1. There are two series of long-chain normal carboxylic acids existing in retort waters which could come partly from the pyrolysis of retorting, and partly from the original oil shale sediment.
2. Phenolic compounds have been found in the retort water which may be formed from the thermal decomposition under retorting conditions.
3. Long-chain normal alkanes and substituted benzenes were identified in retort waters, since they exist abundantly in shale oils.
4. Spectral analysis of nitrogen compounds showed that two types of oxygenated nitrogen components (maleimides and succinimide) can be identified from the benzene extract of retort waters. Maleimides have been found in the polar fraction of Green River oil shale (8). The amide oxidation as well as the dehydration between dicarboxylic acids and amides will all cause the formation of these two nitrogen compounds.

Further experiments to characterize and isolate retort water into acid, base, and neutral fractions are in progress. The present method of the combination of electron impact and chemical ionization MS in conjunction with GC offers the inherent advantages for the analysis of the vast number of organic components in retort waters.

ACKNOWLEDGEMENT

The work described here was sponsored by E.R.D.A. E(29-2)3619, to whom the authors wish to express their appreciation.

REFERENCES

1. Cook, E. W., Organic Acid in Process Water from Green River Oil Shale, Chem. and Ind., May 1971, p. 485.
2. Jackson, L. P., Poulson, R. E., Spedding, T. J., Phillips, T. E., and Jensen, H. B., Characteristics and Possible Roles of Various Waters Significant to In-Situ Oil Shale Processing, Quarterly Colorado School of Mines, 1976, p. 105.
3. Thorne, H. M. and Ball, J. S., The Composition of Shale Oils, in The Chemistry of Petroleum Hydrocarbons, (Brooks, B. T., Boord, C. E., Kurtz, S. S. Jr., and Schmerling, L. eds), Reinhold Pub. Co., New York, 1954, v. 1, Ch. 5.
4. Poulson, R. E., Nitrogen and Sulfur in Raw and Refined Shale Oils, Div. of Fuel Chem., ACS, 20(2), 183, 1975.
5. Burlingame, A. L. and Simoneit, B. R., Isoprenoid Fatty Acids Isolated from the Kerogen Matter of the Green River Formation (Eocene), Sci., 160, 531, 1968.
6. Bureau of Mines, Synthetic Liquid Fuel, Annual Rep. of the Secretary of the Interior for 1952, Part II, Oil from Oil Shale, RI 4943, 1953.
7. McLafferty, F. W., Interpretation of Mass Spectra, 2nd Ed., W. A. Benjamin, Inc., London, 1973, p. 118.
8. Anders, D. E., Doolittle, F. G., and Robinson, W. E., Polar Constituents Isolated from Green River Oil Shale, Geochem. et Cosmochim. Acta, 39, 1423, 1975.

Fig. 1.

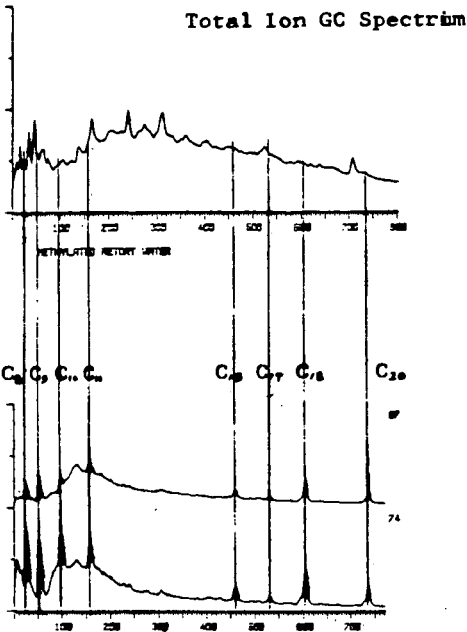


Fig. 2 METHYLATED RETORT WATER SAMPLE BY EI

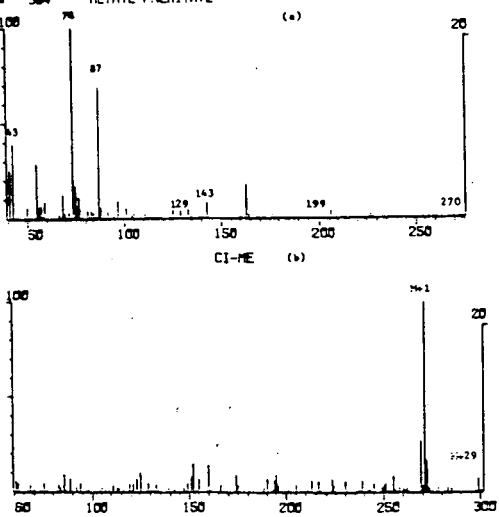


Fig. 3... RETORT WATER ELECTRON IMPACT
M/E94

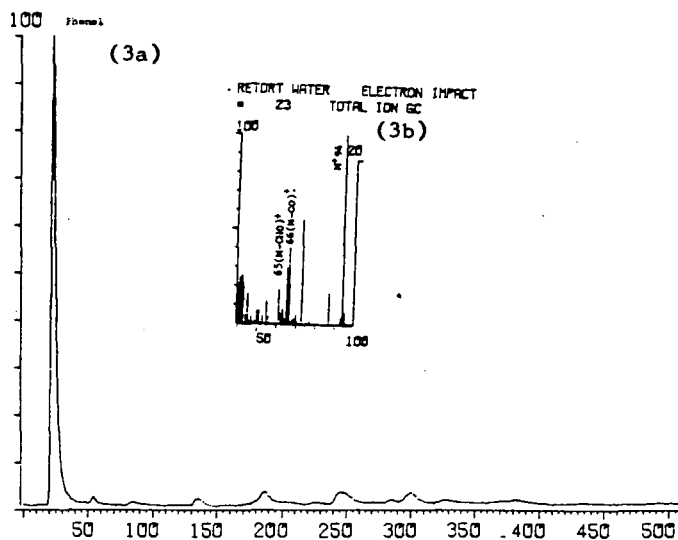
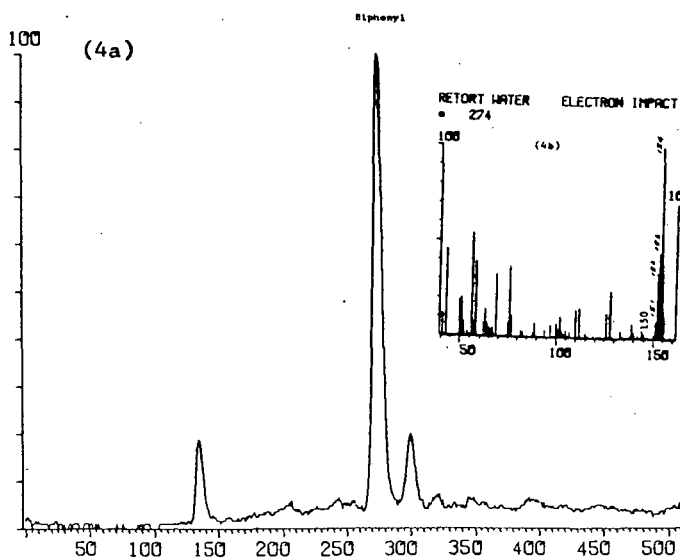
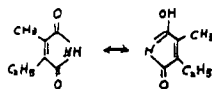


Fig. 4. RETORT WATER ELECTRON IMPACT
M/E 154



CN1C(=O)CCC1=O